ROLE OF CHEMERIN, A NOVEL ADIPOCHEMOKINE, IN THE HUMAN MICROVASCULAR ENDOTHELIAL CELL (HMEC)-1 LINE

Jaspreet Kaur
BSc (Hons)

PhD in Medical Sciences

A thesis submitted in partial fulfilment of the requirements for the degree of Doctor of Philosophy in Medical Sciences

Division of Metabolic and Vascular Health
Warwick Medical School
The University of Warwick
01.05.2012

To my Parents

Table of Contents

Acknowledgements

First of all, I would like to record my profound gratitude to my supervisor, Dr Harpal Randeva, for his valuable support and guidance; and I am also thankful to Dr Jing Chen for his helpful suggestions throughout this study. I have also benefited by advice and guidance from many other scientists within the organisation as well as fellow researchers.

I am very much thankful to The General Charities of the City of Coventry for providing me with financial support throughout the duration of this project. I am also grateful to both Warwick Medical School and Medical Research Fund organisations for giving me a highly competitive Postgraduate Research Scholarship Award, and a consumable money award respectively.

Where would I be without my family? My parents deserve special mention for their non-dispensable support. My father, Jaspal Singh, in the first place, is the person who steered my life through in the past few years and deserves a special mention. My mother, Daljit Kaur, is the one who sincerely raised me with her caring and gentle love. My siblings, Harpreet Kaur and Vivek Singh – thanks for being supportive and caring siblings.

Finally, I would like to thank everybody who was important to the successful realisation of this thesis, as well as expressing my sincere apology that I could not mention personally one-by-one.

Declaration

I declare that this thesis was composed by my own self, and the work reported in this thesis is my own except where explicitly stated otherwise in the text (Refer to appendix 15, page number 287 for a list of experiments and methods that were carried out by other researchers, however, are part of this thesis).

This work has not been submitted for any other degree or professional qualification except as specified, however, some of the data obtained during the course of this project has already been submitted for publishing (see publications).

All the sources accessed during the preparation of this thesis are referenced appropriately.

Jaspreet Kaur

……**.....**

List of Publications

KAUR, J., ADYA, R., & RANDEVA, H. S. (2011) Chemerin induced endothelial cell adhesion molecules expression – involvement of Nuclear Factor – kappa B pathway. *Atherosclerosis,* (in revision).

KAUR, J., ADYA, R., TAN, B. K., CHEN, J., & RANDEVA, H. S. (2010) Identification of chemerin receptor (ChemR23) in human endothelial cells: chemerin-induced endothelial angiogenesis. *Biochem Biophys Res Commun,* 391 (4), 1762-68.

Other publications

TAN, B. K., CHEN, J., FARHATULLAH, S., ADYA, R., **KAUR, J.,** HEUTLING, D., LANDOWSKI, K. C., O'HARE, J. P., LEHNERT, H., & RANDEVA, H. S. (2009) Insulin and metformin regulate circulating and adipose tissue chemerin. *Diabetes,* 58 (9), 1971-77.

Posters and Presentations

1. Abstracts and Posters

a) Postgraduate Annual Poster Competition 2009, The University of Warwick, UK – Abstract and Poster.

Role of a novel chemokine, chemerin in Human Microvascular Endothelial Cell (HMEC)-1 line.

b) Warwick Medical School Annual Symposium 2010, The University of Warwick, UK – Abstract and Poster.

Role of a novel chemokine, chemerin in Human Microvascular Endothelial Cell (HMEC)-1 line.

c) Heart, UK 2011 - Abstract only.

Pro-angiogenic chemerin behaviour in Human Microvascular Endothelial Cell (HMEC)-1 line.

d) The Endocrine Society, ENDO 2011, Boston, USA – Abstract and Poster.

The inflammatory and angiogenic properties of chemerin: implications for the metabolic syndrome.

f) Human Metabolic Research Unit (HMRU) Annual Conference 2011, University of Warwick, UK – Abstract and Poster.

The inflammatory and angiogenic properties of chemerin: implications for the metabolic syndrome.

2. Oral Presentations

a) British Endocrine Society (BES) 2009, Harrogate, UK.

Insulin increases, and metformin decreases chemerin expression – Polycystic Ovary Syndrome (PCOS) as a paradigm.

b) Warwick Medical School Annual Symposium 2011, The University of Warwick, UK.

Chemerin in endothelial cell biology – inflammatory and angiogenic properties.

3. Conferences

a) British Endocrine Society (BES) 2009, Harrogate, UK.

b) The Annual Warwick Medical Day Symposium 2011, Warwick Medical School, UK.

c) The Endocrine Society, ENDO 2011, Boston, MA, USA.

d) Human Metabolic Research Unit (HMRU) Annual Conference 2011, The University of Warwick, UK.

Summary

Chemerin is a newly identified adipokine and exerts its functional effects by binding to its natural GPCR, known as CMKLR1. Chemerin is highly expressed in the adipose tissue and in lower levels in other body tissues; and is known to play an important role in adipocyte differentiation and metabolism. Chemerin circulates at the normal physiological concentrations of approximately 3-4nM in humans, and circulating chemerin levels positively correlate with various facets of metabolic abnormalities; such as insulin resistance, type 2 diabetes, high triglycerides, hypertension, and associated risks of development of diseases of cardiovascular system. Endothelial Cells (ECs) line the vasculature of the entire circulatory system and form a direct contact with the bloodstream. In this project, the role of chemerin in EC biology was proposed, and was studied in terms of activation of important signalling Mitogen-activated Protein Kinases (MAPKs) including Extracellular signal-regulated Kinase (ERK) 1/2, ERK5, p38, Stress-activated Protein Kinase/c-Jun NH2-terminal Kinase (SAPK/JNK); and Akt/Protein Kinase B (PKB) and Adenosine Monophosphate Protein Kinase (AMPK)-α in a time- and concentration-dependent manners. These signalling kinases regulate the activity of different transcription factors which then regulate the expression of different genes. Chemerin increased the expression of Hypoxia-inducible Factor (HIF)-1α, a hypoxia-inducible transcription factor which is known to regulate the Vascular Endothelial Growth Factor (VEGF) gene expression. Interestingly, VEGF165, the most potent angiogenic isoform of VEGF protein expression was down-regulated by chemerin in a concentration-dependent manner; whereas, chemerin upregulated the protein expression of VEGF165b, an opposite anti-angiogenic counterpart of VEGF165. Chemerin mediated EC proliferation, migration and capillary tube formation; which are the key processes implicated in the process of normal and pathological angiogenesis. Chemerin altered the protein expression levels of Cell Adhesion Molecules (CAMs) including E-selectin, ICAM-1 and VCAM-1 – increased the activity of Nuclear Factor (NF)–kappa (κ) B pathway – and encouraged Endothelial-Monocyte cell adhesion in a concentration-dependent manner. Nitric Oxide (NO), not only keeps the vascular health in check by downregulating the expression levels of adhesion molecules, but also acts as a potent vasodilator. Endothelial Nitric Oxide Synthase (eNOS), an enzyme constitutively expressed in the endothelial cells regulates the production of NO in the endothelium. Chemerin increased eNOS activity by causing eNOS phosphorylation at Ser1177, and dephosphorylating at Thr495 phosphorylation sites. Chemerin increased the protein expression of non-constitutively expressed enzyme, inducible Nitric Oxide Synthase (iNOS), which is mainly induced during injury or inflammation and is known to produce 100- to 1000-times more NO compared to that of eNOS. However, interestingly, chemerin failed to show any significant changes in the amounts of combined nitrite and nitrate (NOx) levels in HMEC-1 cells; whereas, nitrite ($NO2^{-}$) levels were decreased in a concentration-dependent manner.

Abbreviations

AC	Adenylase Cyclase
AT	Adipose Tissue
ATP	Adenosine Triphosphate
BAT	Brown Adipose Tissue
bp	Base pairs
BCA	Bicinchoninic Acid
BSA	Bovine Serum Albumin
cAMP	Cyclic Adenosine Monophosphate
cDNA	Complementary Deoxyribonucleic Acid
cGMP	Cyclic Guanosine Monophosphate
CCRL2	Chemokine (C-C motif) Receptor-like 2
CMKLR1	Chemokine like Receptor 1
dH_2O	Distilled Water
DNase	Deoxyribonuclease
DNA	Deoxyribonucleic Acid
ECL	Enhanced Chemiluminescence
EDTA	Ethylenediamine Tetra-acetate
ERK	Extracellular signal Regulated Kinases
FCS	Fetal Calf Serum
F/S	Filtered Sterilised
g	Gram
GAPDH	Glyceraldehyde-3-Phosphate Dehydrogenase
GDP	Guanosine Diphosphate
GPCR	G Protein-Coupled Receptors
GPR1	G Protein Receptor 1
GTP	Guanosine Triphosphate

HBSS	Hank’s Balanced Salt Solution
HEK293	Human Embryonic Kidney Cells 293
HMEC-1	Human Microvascular Endothelial Cells-1
HRP	Horse-radish Peroxide
HUVECs	Human Umbilical Vein Endothelial Cells
IL-1β	Interleukin-1 beta
IP3	Inositol 1, 4, 5 triphosphate
IU	International Units
kDa	Kilodaltons
M	Molar
mA	Milliampere
MAPK	Mitogen Activated Protein Kinase
mg	Milligram
mL	Millilitre
mM	Millimolar
mm	Millimetre
min	Minute
mRNA	Messenger Ribonucleic Acid
MWt	Molecular Weight
myrPKAi	Myristoylated Protein Kinase A inhibitor
NADH	Nicotinamide Adenine Dinucleotide (reduced form)
NCBI	National Centre for Biotechnology Information
NF-κB	Nuclear Factor Kappa B
ng	Nanogram
nM	Nanomolar
NO	Nitric Oxide
PAGE	Polyacrylamide Gel Electrophoresis

PBS	Phosphate Buffer Saline
PCR	Polymerase Chain Reaction
PI3-K	Phosphatidylinositol-3 OH Kinase
PKA	Protein Kinase A
PKC	Protein Kinase C
pM	Picomolar
PMA	Phorbol-12-myristater-13-acetate
PVDF	Polyvinylidene Fluoride
RNA	Ribonucleic Acid
RT-PCR	Reverse Transcriptase Polymerase Chain Reaction
RT	Room Temperature
SDS	Sodium Dodecyl Sulphate
Secs	Seconds
SEM	Standards Errors of Mean
Ser	Serine
TBE	Tris Buffered EDTA
TBS	Tris Buffered Saline
TBS-T	Tris Buffered Saline-0.1% Tween-20
TEMED	N, N, N^1, N^1-Tetramethylethylenediamine
Tris	Tris (hydroxymethyl) aminomethane
Thr	Threonine
Tyr	Tyrosine
UV	Ultraviolet
V	Volts
v/v	Volume per volume ratio
VAT	Visceral Adipose Tissue
WAT	White Adipose Tissue

w/v	Weight per volume ratio
µg	Microgram
µM	Micromolar
µL	Microlitre
µmol/L	Micromole per Litre

List of Figures

List of Tables

Table of Contents

Chapter 1 Introduction and Background

Chapter 2 Research Methods

Future Work

Appendices

Bibliography

1.1 Vascular Endothelium

1.1.1 Normal Vascular Endothelium

1.1.1a Origin, structure and functions of endothelial cells

In 1973, Endothelial Cells (ECs) were cultured for the very first time by Jaffe and colleagues which lead to the revolution in the field of EC biology (Jaffe et al., 1973a). ECs are a single epithelial-like cells that line the innermost layer of all blood vessels in the circulatory system, forming a direct contact with flowing bloodstream, and modulating various biological systems in the blood (Baldi et al., 2000). Adult vascular endothelium weighs approximately 1000*g* and comprises of $1.6x10^{13}$ cells with a surface area between 1-7m^2. ECs participate in five primary physiological functions in the body; (1) the most basic and important feature of ECs is the capacity to maintain blood in its fluid state by preventing blood clot formation (Arnout et al., 2006) (2) ECs control the exchange of fluids and other macromolecules between the blood and the tissues mainly at the capillary level (Minshall and Malik, 2006), (3) ECs control blood flow at the arterial and arteriolar level of circulation (Busse and Fleming, 2006), (4) a fourth important physiological function of the ECs is stopping the inflammatory responses (Ley and Reutershan, 2006) and, finally (5) ECs participate in maintaining control of body's immune system (Choi et al., 2004). In normo-physiological states, ECs remain in a dormant state, retain an anti-thrombotic surface, and maintain the normal vascular homeostasis.

1.1.2 Diseased Vascular Endothelium

Abnormal EC functioning is coined as 'Endothelial Dysfunction (ED)' and is defined as the failure of ECs to perform normal functions which may be due EC injury or death. In clinical scenario, ED is defined as the failure of ECs to respond to increased blood flow by releasing excessive amounts of endothelium Nitric Oxide (NO) and causing local vasodilation (Giannotti and Landmesser 2007).

1.1.2a Endothelial cell activation, injury and inflammation

EC activation is characterised as a new EC function that benefits the host; e.g., role of ECs in controlling the inflammatory responses at different levels which are important in innate and adaptive immunity of the body.

1.1.2b Vascular disease - EC angiogenesis

The mesodermal precursor cells, which are formed by the differentiation of angioblast from the early vascular plexus, subsequently form primitive blood vessels, and the process is characterised as vasculogenesis (Folkman and Shing, 1992b). The cardiovascular (CV) system is the very first functional organ system that develops in the vertebrate embryo, and acts as a nutrient supply as well as a waste removal system, promoting embryonic growth and differentiation. Later in adult life, it serves as a nutrient and waste pipeline and also as a primary communicatory system between all distant organs and body tissues. ECs then arrange in a single layer and line the innermost layer of all blood vessels. More ECs are generated after the primary vascular plexus, which then form new capillaries from the pre-existing vessels by sprouting or splitting from their original vessel, and the process is termed as angiogenesis. Angiogenesis is an essential process in the normal growth; and under normo-physiological conditions, angiogenesis mainly occurs in wound healing

and tissue repair processes. Angiogenesis is also implicated in disease states such as cancers, diabetic retinopathy, as well as in inflammatory diseases such as rheumatoid arthritis. Process of angiogenesis involves the degradation of Extracellular Matrix (ECM) by matrix degrading enzymes such as Matrix Metalloproteinases (MMPs), followed by EC migration, proliferation and formation of tube-like structures. Vascular Endothelial Growth Factor (VEGF) is the most common endothelial-specific growth and chemotactic factor and is widely studied as an angiogenesis-activating factor (Keswani et al., 2011).

Vascular Endothelial Growth Factor and Angiogenesis

Vascular Endothelial Growth Factor (VEGF) was initially identified as a Vascular Permeability Factor (VPF) (Senger et al., 1983), and was isolated as a soluble heparin-binding heterodimeric glycoprotein (Ferrara and Henzel, 1989, Zhang et al., 2011). A number of other proteins that share structural similarities with VEGF are grouped together in a VEGF family, including VEGF-A (commonly known as VEGF), VEGF-B, VEGF-C, VEGF-D, VEGF-E isoforms and Placental Growth Factor (PIGF) (Nittoh et al., 1997b). Alternative splicing of human VEGF gene results in the formation of pro-angiogenic, and opposite anti-angiogenic counterparts, latter been grouped together in VEGFxxxb family (xxx representing the number of amino acids) (Appendix 5, Fig. 5.1a, page number 248) (Craine et al., 1995). The pro-angiogenic VEGF isoforms include VEGF121, VEGF165, VEGF189 and VEGF206, each having 121, 165, 189 and 206 amino acids (Ohuchi et al., 1997c) - VEGF145 and VEGF183 are other two less frequently produced isoforms of VEGF (Neufeld et al., 1999). VEGF165 (commonly represented as VEGF) is a secreted protein and is the most predominant and biologically active isoform of VEGF, and is known to share properties with that of native VEGF protein (Hirasawa et al., 1997b).

VEGF165 is the principal isoform that is known to play important role in normal and pathological angiogenesis (Ferrara and Davis-Smyth, 1997), as well as in vasculogenesis (Folkman and D'Amore, 1996). New vessel formation and growth are highly complex and co-ordinated processes involving the activation of a number of different receptors by external stimuli (Ferrara, 2000, Carmeliet, 2000). In addition to its mitogenic actions, VEGF165 also stimulates fluid and protein extravasation from blood vessels (Dvorak et al., 1995a), mediates calcium influx (Brock et al., 1991, Seymour et al., 1996), and is known to release NO in primary HUVECs cells (van der Zee et al., 1997, Ahmed et al., 1997).

Vascular Endothelial Growth Factor Receptors and Angiogenesis

VEGFR1 (fms-like tyrosine kinase, Flt-1), VEGFR2 [Kinase insert-domain containing receptor, KDR (in humans) and fetal liver kinase (flk)-1 (in mouse)] and VEGFR3 (Flt-4) are three different tyrosine kinase receptors that are stimulated upon VEGF binding. Both VEGFR1 and VEGFR2 are co-expressed on EC surfaces (Ferrara and Davis-Smyth, 1997), whereas, VEGFR3 is mainly expressed on the lymphatic endothelium and in tumour blood vessels during neovascularisation (Nakamura et al., 1997). VEGF binds both VEGFR1 and VEGFR2 receptors, however, VEGFR2 is the main signalling receptor implicated in VEGF-dependent angiogenesis (Waltenberger et al., 1994). Upon stimulation, VEGFR2 becomes activated (Nittoh et al., 1997b) and autophosphorylates at multiple phosphorylation sites (Dougher-Vermazen et al., 1994). Carboxy terminal of VEGFR2 receptor contains different Serine (Ser) and Tyrosine (Tyr) phosphorylation sites which are crucial for VEGFR2 phosphorylation and functions (Nguyen et al., 1993a, Nguyen et al., 1992, Folkman and Shing, 1992a). Different tyrosine phosphorylation sites include Tyr1175, 1214, and 1223, and are essential for VEGFR2 activity and

functions. VEGFR2 phosphorylation at Tyr1214 is essential for complete autophosphorylation of VEGFR2 receptor (Koch et al., 1995); and receptor phosphorylation at Tyr1175 is crucial, as mice carrying Tyr-to-Phe substitution at position 1173 (corresponds to Tyr1175 in human VEGR2) are reported to die at the embryonic stage due to lack of vasculogenesis or angiogenesis (Palframan et al., 2001). VEGFR2 phosphorylation at Tyr1175 results in the recruitment of p85 and Phosphoinositide-3-Kinase (PI3K) (Weidner et al., 1992), and activates downstream signalling pathways such as Protein Kinase C pathway (PKC) (Takahashi et al., 2001). Signalling via VEGFR2 receptor is essential for the VEGF-stimulated proliferation, chemotaxis, sprouting and survival of cultured ECs *in vitro,* as well as angiogenesis *in vivo* (Okamoto et al., 1997). Other VEGF isoforms, such as VEGF-B binds to VEGFR1 and is known to play a role in extracellular matrix degradation, cell adhesion, and migration; both VEGF-C and VEGF-D bind VEGFR2 and VEGFR3 receptors, and primarily affect the development of the lymphatic vasculature via VEGFR3 activation (Sakata et al., 1997). VEGF-E is implicated in mediating angiogenesis via VEGFR2 signalling, however, not through VEGFR1 (Nittoh et al., 1997b).

Hypoxia Inducible Factor -1 and Angiogenesis

Hypoxia Inducible Factor (HIF)-1 is a heterodimeric transcription factor, composed of an alpha (α), and a beta (β) subunit. HIF-1α is induced by altered oxygen levels, whereas, HIF-1β is expressed in an oxygen-independent manner. Under normoxic conditions, HIF-1α is rapidly degraded by ubiquitin-proteasome system and is rarely detectable; however, in hypoxic conditions, HIF-1α expression increases due to decreased ubiquitination and degradation, which then regulates the expression of different genes including VEGF (Shimaoka et al., 2001). HIF-1α activates and regulates the VEGF gene transcription by binding to the Hypoxia Response Element (HRE) in the gene promoter region (Laughner et al., 2001). A number of other factors such as cytokines, growth factors, and oxidative stresses are also known to modulate HIF-1α transcriptional activity.

Matrix Metalloproteinases and Angiogenesis

Matrix Metalloproteinases (MMPs), also known as matrixins are the enzymes that are involved in the degradation of extracellular matrix, a process vital for normal growth, development and morphogenesis. So far, twenty three different types of MMP have been characterised, which are further divided into secreted MMPs and Membrane-Type MMPs (MT-MMPs). Both secreted MMPs, MMP-2 and -9, have been intensively implicated in the process of angiogenesis (van Hinsbergh et al., 2006). Upon stimulation, these MMPs become activated and are regulated at transcriptional, translational and zymogen stages (Ohuchi et al., 1997a); and their activities are inhibited by Tissue Inhibitors of Metalloproteinases (TIMPs).

1.1.2c Vascular disease – vascular inflammation

Cell Adhesion Molecules and Vascular Inflammation

The endothelial Cell Adhesion Molecules (CAMs) are the molecules expressed on the surface of EC and maintain vessel homeostasis, wound healing, coagulation, inflammation, immune responses and related diseases such as atherosclerosis and angiogenesis. CAMs are grouped together into four main families; the integrins, the immunoglobulins, the selectins and the cadherins. E-selectin is one of the selectin molecules and is absent in normal tissues, however, is expressed in the endothelium of post-capillary venues in inflammatory states, such as rheumatoid arthritis. E-selectins are involved in leukocyte adhesion to the vessel wall, as well as known to play a role in angiogenesis (Koch et al., 1995). The specific antibodies directed against E-selectin protein inhibit the tube formation *in vitro* (Nguyen et al., 1993b). The Intracellular Cell Adhesion Molecule (ICAM)-1 and Vascular Cell Adhesion Molecule (VCAM)-1 are the adhesion molecules of immunoglobulin superfamily, and are involved in cell-cell adhesion and leukocyte transmigration. ICAM-1 is constitutively expressed on the EC surfaces and immune cells. There are five different isoforms of ICAM (ICAM-1, 2, 3, 4 and 5) which all bind leukocyte integrins. Resting endothelium does not bind leukocytes, however, when activated by inflammatory cytokines or external stimuli, protein expression levels of adhesion molecules is increased. CAMs facilitate the entry of leukocytes into inflamed tissues, promoting angiogenesis and neovascularisation, which constitute as the key processes implicated in the initiation and progression of inflammatory diseases such as rheumatoid arthritis, tumour growth, and wound repair (Folkman and Shing, 1992a). These molecules are shed from the EC surfaces and circulate freely in the bloodstream, for example soluble forms of E-selectin (sE-selectin) and VCAM-

(sVCAM-1) are known to induce HUVEC and microvascular ECs chemotaxis *in vitro* and *in vivo* (Koch et al., 1995).

Monocyte Chemoattractant Protein-1 and Vascular Inflammation

Monocyte Chemoattractant Protein (MCP)-1 is a chemoattractant protein that acts as a major recruitment protein across ECs, resulting in chemo attraction and infiltration of circulating monocytes across the endothelial- and epithelial-cell barrier (Randolph and Furie, 1995). In *in vivo* models, MCP-1 is also reported to mediate monocyte infiltration to High Endothelial Venules (HEV)-draining lymph nodes of inflamed skin (Palframan et al., 2001).

Nuclear Factor-kappa B Signalling Pathway and Vascular Inflammation

Nuclear Factor (NF)-κB signalling pathway is widely implicated in the pathogenesis of inflammatory diseases such as atherosclerosis (de Winther et al., 2005). There are five different transcription factors which are grouped together in NF-κB group of transcription factors and include c-Rel, relB, p65 (relA), p105/p50, and p100/p52. The protein inhibitors of NF-κB, denoted as IκBs, keep the NF-κB dimers in an inactive state. Upon stimulation by pro-inflammatory stimuli, the IκB Kinase (IKK) phosphorylates IκB proteins on specific Serine residues, which cause ubiquitination and consecutive proteasomal degradation of the dimer complex. The NF-κB dimers get released and accumulate in the nucleus, which upon stimulation get activated and are implicated in regulating the expression of different pro-inflammatory cytokines, adhesion molecules including VCAM-1, ICAM-1 and E-selectin and other chemokines such as MCP-1 (de Winther et al., 2005). Activated NF-κB in ECs is also known to encourage endothelial-monocyte cell adhesion (Hajra et al., 2000).

1.1.2d Vascular Disease – endothelium nitric oxide

Endothelial Nitric Oxide Synthase and NO Production

Endothelial Nitric Oxide Synthase (eNOS) is one of the three Nitric Oxide Synthases (NOSs) enzymes which were initially characterised in 1989 (Palmer and Moncada, 1989). The three different isoforms of NOSs are; neuronal Nitric Oxide Synthase (nNOS), inducible Nitric Oxide Synthase (iNOS) and endothelial Nitric Oxide Synthase (eNOS) and were all cloned and purified between 1991 and 1994. These NOSs were named after the type of tissue they were first identified in, and are also denoted as type I or NOS-I or NOS-1 (nNOS), type II or NOS-II or NOS-2 (iNOS) and type III or NOS-III or NOS-3 (eNOS). These NOSs have also been differentiated on the basis of their constitutive – nNOS and eNOS, and inducible – iNOS expression; as well as on their calcium-dependence – eNOS and nNOS, and -independence – iNOS.

Initially identified in 1989, eNOS was cloned in 1992 (Janssens et al., 1992, Marsden et al., 1992). eNOS is phosphorylated and dephosphorylated on a number of different sites, however, eNOS phosphorylation at Ser1177, and dephosphorylation at Thr495 are the two significant sites that primarily regulate the activity of eNOS (Dimmeler et al., 1999, Fleming et al., 2001). Additionally, eNOS phosphorylation at Ser116 and Ser617 is also reported to regulate the enzyme activity and functions (Bauer et al., 2003, Boo et al., 2003). Over-expression of eNOS reduces blood pressure and plays an important role in blood pressure regulation (Ohashi et al., 1998). Calmodulin (CaM) is another protein that interacts with eNOS (Bredt and Snyder, 1990), and is required for the activity of all three

different NOSs by increasing the rate of electron transfer from Nicotinamide Adenine Dinucleotide Phosphate-hydroxylase (NADPH) to the reductase domain.

In 1987, Palmer and colleagues demonstrated the release of NO from the vascular endothelium for the very first time (Palmer et al., 1987) and characterised L-arginine as a substrate molecule for NO synthesis (Palmer et al., 1988). Initially, NO was characterised as a Endothelium-Derived Relaxing Factor (EDRF) by Furchgott and Zawadzki (Furchgott and Zawadzki, 1980). NO generated by the vascular endothelium is a major regulator of vascular homeostasis, and altered NO levels are implicated in the development of a number of diseases of the vascular system. NO also acts as an inhibitor of platelet aggregation and retains the anti-thrombotic properties of endothelium (Radomski et al., 1987). NO modulates leukocyte adhesion to the vascular wall and is also implicated in the down-regulation of expression of CAMs such as P-selectin (Davenpeck et al., 1994), E-selectin (De Caterina et al., 1995), VCAM-1 (Khan et al., 1996) and ICAM-1 (Biffl et al., 1996). NO is also suggested to play an important role in maintaining vascular integrity, as the absence of eNOS enzyme, which is implicated in NO production, results in increased fluid and protein flux (Kubes, 1995). NO increases vascular permeability by increasing VEGF protein expression, which then activates eNOS in a NO-dependent manner (Feng et al., 1999). eNOS-derived NO is reported to be involved in EC angiogenesis (Jenkins et al., 1995, Kroll and Waltenberger, 1998, Ziche and Morbidelli, 2000), as well as in capillary tube organisation (Papapetropoulos et al., 1997). VEGF, the most potent angiogenic factor increases the NO production via up-regulating eNOS activity (van der Zee et al., 1997, Hood et al., 1998), which then mediates the migratory and proliferatory actions of VEGF (Papapetropoulos et al., 1997, Pribylova et al., 1995). Shear stress of blood flow on the EC surface is the

most important activator of eNOS that results in the activation of a number of pathways; especially PI3K pathway which activates Akt1 at Ser473 phosphorylation site, which then phosphorylates eNOS at Ser1177 (Ayajiki et al., 1996, Go et al., 1998, Dimmeler et al., 1999, Fulton et al., 1999), finally leading to NO production which is also known to promote angiogenesis (Liu et al., 2002). Angiogenesis induced via pathways independent of VEGF are also known to be modulated by angiogenic properties of NO (Ziche et al., 1994, Leibovich et al., 1994, Vodovotz et al., 1999).

Caveolae and NO Production

Caveolae are small cell-surface invagination of approximately 50 to 100nm (Yamada, 1955, Rothberg et al., 1992), and are characterised as 'Ω-shaped' structures in the cell membrane. Caveolin-1 is highly expressed in ECs and constitutes the largest amount in the caveolae (Lisanti et al., 1994). eNOS enzyme is reported to be localised in a caveolae, and interacts with caveolin-1 and caveolin-3 – the coat proteins of a caveolae – via a caveolin-binding motif in the eNOS (Garcia-Cardena et al., 1996). In resting ECs, both caveolin-1 and caveolin-3 are reported to bind to eNOS, and this interaction inhibits the activity of eNOS enzyme, hence, interfering with NO production (Bucci et al., 2000). Caveolae are also known to increase vascular permeability, as VEGF treatments are reported to induce caveolae clustering, and results in the formation of vesiculovacuolar organelles (VVOc) (Vasile et al., 1999); whereas, prolonged VEGF treatments resulted in the formation of fenestrae (Chen et al., 2002). Caveolin-1 is also reported to inhibit the activity of eNOS which may further contribute to the regulation of vascular permeability. These findings suggest an important role for caveolin-1 in cell-to-cell interactions, and also with extracellular matrix and many other different proteins (Wary et al., 1998).

Calcium/Calmodulin binding to eNOS competitively disrupts the eNOS-caveolin-1 binding, and dissociates eNOS from caveolin-1 protein, hence, increasing the activity of eNOS enzyme. Caveolin-1 also plays an important role in the process of angiogenesis; as caveolin-1 protein expression is reported to be down-regulated during EC proliferation, however, is markedly increased during EC differentiation and vessel formation (Liu et al., 2002).

Heat Shock Protein 90 and NO Production

Heat Shock Proteins (HSPs) are ubiquitously expressed proteins and are essential for maintaining cellular homeostasis, and are known to trigger various cellular responses after exposure to external stress stimuli. There are different classes of HSPs, however, HSP90 is the most important signalling HSP and is a key organiser of several cytoplasmic complexes. Five different isoforms of HSP90 have been identified, however, HSP90α and HSP90β are the major cytosolic isoforms. Both HSP90 isoforms share approximately 85% sequence homology, contain an ATP-binding domain in NH_2-terminal region, a dimerised COOH-terminal, and a highly charged mid-domain which encourages substrate-protein interactions (Hainzl et al., 2009, Csermely et al., 1998). Both these isoforms are known to regulate eNOS enzyme activity, NO and superoxide production (Cortes-Gonzalez et al.).

1.2 Chemerin, a Novel Adipochemokine

1.2.1 Discovery of Chemerin

Chemerin was initially identified as a product encoded by Tazarotene-induced Gene (TIG)-2 in psoriatic skin lesions. TIG-2, also known as Retinoic Acid Receptor Responder 2 (RARRES2), is a cDNA product of 830 base pairs and encodes 164 amino acids long protein (Nagpal et al., 1997). Later in 2003, Meder and colleagues defined TIG-2 as a natural ligand to a previously known orphan G Protein-Coupled Receptor (GPCR), known as Chemokine-like Receptor 1 (CMKLR1) (previously denoted as ChemerinR and ChemR23) (Samson et al., 1998, Meder et al., 2003). In the same year, Wittamer and colleagues characterised chemerin as a natural ligand to CMKLR1 receptor (Wittamer et al., 2003). Throughout this thesis text, human chemerin receptor is represented as CMKLR1.

1.2.2 Chemerin Synthesis and Structure

1.2.2a Chemerin synthesis

Chemerin is translated as a 163 amino acid long pre-proprotein, called pre-prochemerin. Following the removal of 20 amino acid long NH_2-terminal signal sequence, pre-prochemerin gets secreted as a 143 amino acid long peptide, and is named as prochemerin (Wittamer et al., 2003, Meder et al., 2003). Prochemerin is of low biological activity and undergoes extracellular COOH-terminal processing by a number of serine and cysteine proteases of the inflammatory, coagulation and fibrinolytic cascades - plasmin and carboxypeptidases are also reported to convert inactive chemerin peptides into active chemerin fragments (Wittamer et al., 2003, Zabel et al., 2005a, Meder et al., 2003, Zabel et al., 2008, Zabel et al., 2006a, Zabel et al., 2005b). Chemerin circulates at the normal physiological concentration of 3nM in humans and 4nM in mice.

1.2.2b Chemerin structure

Unlike other chemokines, chemerin has a disordered NH_2-terminus, three β-pleated sheets, and a COOH-terminal α-helix (Zabel et al., 2006b). However, both NH_2-terminal domain and COOH-terminal peptide possess chemotactic properties involving GPCR binding and activation (Das et al., 2000). Prochemerin shares structural similarities with cathelicidins, cystatins and other related proteins such as kininogen (a bradykinin precursor). Similar to chemerin, these proteins are also synthesised as pro-proteins, and undergo COOH-terminal cleavage to generate bioactive peptides (Kolligs et al., 2000). Secreted prochemerin protein is of low biological activity and shows poor CMKLR1 receptor binding and activation. Prochemerin is further cleaved at the COOH-terminal end which results in the formation of a number of active and inactive chemerin fragments with different affinities for CMKLR1 receptor.

1.2.3 Proteolytic Processing of Chemerin and Chemerin-derived Peptides

1.2.3a Proteolytic processing of chemerin

A number of different serine proteases and enzymes of inflammatory and coagulation cascades are reported to be involved in the proteolytic processing of prochemerin at the COOH-terminal end. Serine protease, cathepsin G converts prochemerin (21-163) into chemerin (21-156) after the removal of seven amino acid residues from the COOH-terminal end. Elastases remove six, eight or eleven amino acids from the precursor molecule, prochemerin, resulting in the formation of chemerin (21-157), (21-155) and (21-152) respectively. Plasmin-mediated cleavage forms chemerin (21-158), and tryptase cleaves native prochemerin into two different chemerin fragments; chemerin (21-158) and chemerin (21-155). These chemerin fragments further act as substrates to a number of different enzymes; for example,

inactive chemerin (21-158) further undergoes second cleavage by carboxypeptidases N and B (CPN and CPB) resulting in the formation of chemerin (21-157), the most active chemerin fragment (Du et al., 2009). In addition, neutrophil-derived enzymes, proteinase 3 and mast cell chymases (Guillabert et al., 2008), – and Angiotensin-Converting Enzyme (ACE) (John et al., 2007) also convert various different active or inactive chemerin fragments into shorter, less active or inactive chemerin fragments such as (21-155), chemerin (21-154) and chemerin (21-155) respectively (Fig. 1.2.3a.1, page number 16). Urokinase Plasminogen Activator (uPA) and tissue Plasminogen Activator (tPA), which are known to convert inactive plasminogen into plasmin, are also reported to convert inactive prochemerin into active chemerin fragments (Du et al., 2009). These different chemerin fragments circulate in the blood, and chemerin fragments isolated from a number of different body fluids and tissues are of different lengths compared to its precursor prochemerin; for example, chemerin purified from hemofiltrate lacks nine amino acids in the COOH-terminal region, and serum-derived chemerin lacks only eight amino acid residues (Zabel et al., 2005a, Guillabert et al., 2008). Chemerin isolated from ovarian cancer ascitic fluid lacks only six amino acids from COOH-terminal end (Wittamer et al., 2003). Chemerin lacking six COOH-terminal amino acids, chemerin (21-157), is the most abundant and active chemerin fragment present in the bloodstream.

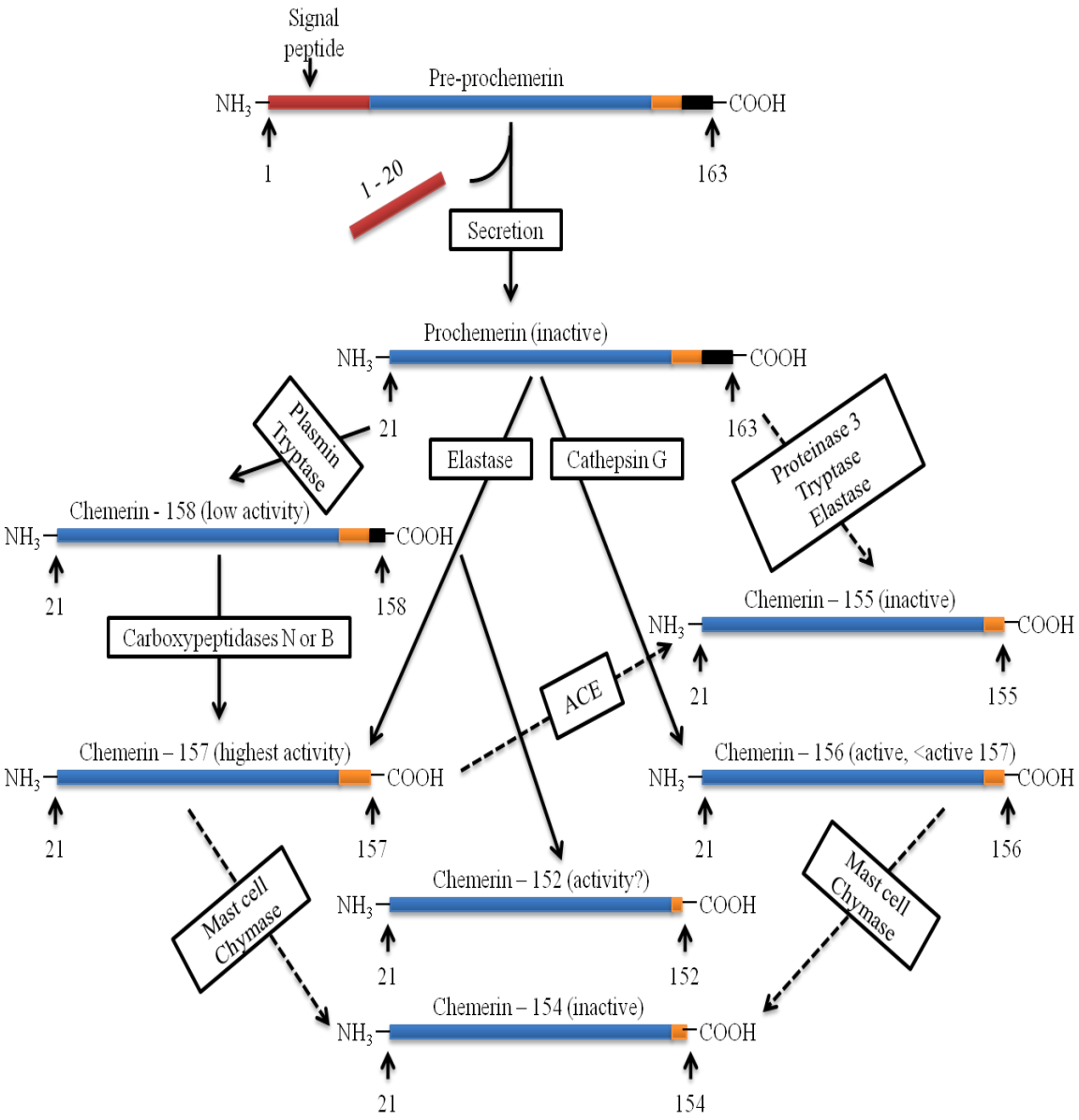

Figure 1.2.3a.1a Proteolytic processing of prochemerin into different chemerin fragments

This figure shows the proteolytic processing of pre-prochemerin (1-163) into mature prochemerin (21-163) after the removal of N-terminal signal peptide. Cathepsin G removes seven amino acids from C-terminal end, resulting in the formation of chemerin (21-156); elastase forming chemerin (21-157) after the removal of six amino acids, chemerin (21-155) after removing eight amino acids, and chemerin (21-152) after the removal of eleven amino acids. Plasmin removes five amino acids and forms chemerin (21-158), and tryptase cleaves five and eight amino acids resulting in the formation of chemerin (21-158) and chemerin (21-155) respectively. Prochemerin undergoes multiple cleavages, such as trypsate cleavage forming less active chemerin (21-158) which then undergoes further cleavage by CPN or CPB resulting in chemerin (21-157) formation. Active chemerin (21-156) and chemerin (21-157) peptides are prone to undergo further cleavages resulting in the formation of inactive chemerin fragments. Solid arrows represent activation pathways; broken arrows represent inactivation pathways. Adapted from (Kukkonen et al., 1996a).

1.2.3b Chemerin-derived peptides and their functions

Chemerin (21-157) and chemerin (21-156) are potent chemoattractants in comparison to their precursor protein, prochemerin (Zabel et al., 2005a, Wittamer et al., 2005), however, chemerin (21-157) is the most active and abundant form of biologically active chemerin. Chemerin (21-158), which is formed by plasmin and trypsate-mediated cleavage, is of low biological activity and undergoes further cleavage by CPN and CPB resulting in the formation of most active chemerin (21-157) peptide (Du et al., 2009). Active chemerin fragments are further cleaved into less active or inactive chemerin fragments; Chemerin (21-155) is a less active peptide, whereas, chemerin (21-154) is an inactive fragment (Guillabert et al., 2008), and biological activity of chemerin (21-152) remains unknown. Wittamer and colleagues (2004) found that the chemerin peptides obtained after the removal of amino acids from the NH_2-terminus region show very poor CMKLR1 binding affinity, in comparison to other shorter chemerin fragments derived from COOH-terminal end. Chemerin (149-157) [Y^{149}FPGQFAFS^{157}] is the shortest COOH-terminal-derived nine amino acid long fragment, termed as a Nona-peptide or a nonamer, and is reported to retain most of the activity of full length active chemerin (21-157) fragment (Wittamer et al., 2004). In addition, mouse nonamer or a Nona-peptide [L^{148}FPGQFAFS^{156}] is also reported to show similar properties (Luangsay et al., 2009). Cash and colleagues (2008) described that mouse chemerin-derived chemerin-15 peptide [A^{140}GEDPHGYFLPGQFA^{154}] possess anti-inflammatory properties *in vitro* as well as in mouse models of peritonitis (Cash et al., 2008).

1.2.4 Chemerin Expression

Chemerin is primarily expressed in a number of tissues including liver, white adipose tissue, lungs, pituitary gland; and in lower levels in skin, adrenal glands, pancreas and kidneys (Wittamer et al., 2003). Prochemerin mRNA transcripts are also present in various epithelial cells (Luangsay et al., 2009), ECs (Du et al., 2009, Kaur et al., 2010), fibroblasts (Vermi et al., 2005), chondrocytes and platelets (Aksela et al., 1996a). Under normal physiological conditions, inactive prochemerin circulates at a relatively higher concentrations in plasma compared to serum concentrations. Adipose tissue (Kukkonen et al., 1996a) and liver (Eriksson et al., 1996) are reported to be the major sources of prochemerin secretion in the body. Du et al. (2009) reported that chemerin is also stored in platelet granules and is released upon platelet activation by different platelet activating factors (Du et al., 2009).

1.2.5 Functions of Chemerin

Chemerin is reported to play a number of different functions in the body and is mainly implicated in adipogenesis and adipocyte metabolism (Roh et al., 2007, Goralski et al., 2007), known to exhibit pro- and anti-inflammatory properties, and in angiogenesis (Bozaoglu et al., 2010).

1.2.5a Chemerin in adipogenesis and adipocyte metabolism

Both chemerin and its natural receptor, CMKLR1 are expressed in adipocytes, however, CMKLR1 is also highly expressed in stromal vascular cells. Adipose tissue acts as a major source of chemerin secretion (Goralski et al., 2007, Bozaoglu et al., 2007, Roh et al., 2007). In 2007, Bozaoglu and colleagues reported for the first time that chemerin expression was higher in *Psammomys obesus,* which is an animal model of obesity and type 2 diabetes (T2D), compared with normoglycemic lean

model. In 3T3L1 adipocytes, chemerin expression is reported to increase during differentiation into mature adipocytes; whereas, in comparison, CMKLR1 expression down-regulates. Both chemerin and CMKLR1 receptor knockdown is reported to rresult in malfunctioning of normal mature adipocytes due to alteration in the expression levels of specific genes that help in maintaining glucose and lipid homeostasis. Muruganandan and colleagues (2011) showed that during Bone marrow Mesenchymal Stem Cell (BMSC) differentiation into adipocytes, chemerin expression levels increase and positively correlate with Peroxisome Proliferator-Activated Receptor (PPAR)–γ, which is the most important regulator of adipogenesis (Eriksson et al., 1996). Inflammatory cytokines such as TNF-α and IL-1β are reported to increase chemerin synthesis and secretion in 3T3-L1 adipocytes, human primary adipocytes, and in mouse adipocytes *in vivo* (Uibo et al., 1996) via acting through pathways involving the activation of NF-κB pathway, and by phosphorylating Extracellular signal-regulated Kinase (ERK) 1/2 (Kukkonen et al., 1996d). Chemerin expression in adipocytes was also reported to be induced by Free Fatty Acids (FFAs), through the activation of transcription factor Sterol Regulatory Element-Binding Proteins 2 (SREBP2) (Joukov et al., 1996). In obese states, circulating chemerin levels positively correlate with Body-Mass-Index (BMI), Waste-to-Hip (WHR) ratio, glucose levels, hypertension and circulating triglycerides (Bozaoglu et al., 2007), which all are well-documented risk factors associated with development of insulin resistance as a result of abnormal glucose uptake in muscles, and storage in adipose tissue; ultimately resulting in the pathogenesis of Cardiovascular Diseases (CVDs) such as, Atherosclerosis Cardiovascular Diseases (ASCVD) (Fig. 1.2.5a, page number 21).

1.2.5b Pro- and/or anti-inflammatory chemerin behaviour

As CMKLR1 is selectively present on the cells of the immune system, chemerin binding to CMKLR1 stimulates the receptor and promotes chemotaxis of all leukocyte cell populations expressing CMKLR1 receptor (Wittamer et al., 2004, Luangsay et al., 2009, Vermi et al., 2005, Aksela et al., 1996a). Recently, Hart and Greaves (2010) reported that chemerin promotes macrophage adhesion to the extracellular matrix protein fibronectin, and VCAM-1 as well as encourages the clustering of Very Late Antigen (VLA)-4 and -5 integrins (Hart and Greaves, 2010).

1.2.5c Chemerin in EC angiogenesis

Chemerin promotes EC angiogenesis by mediating EC migration, proliferation and capillary tube formation in Human Microvascular Endothelial Cell (HMEC)-1 line. Chemerin increased the activity of matrix degrading enzymes, such as Matrix Metalloproteinases (MMP)-2 and -9, thereby, promoting angiogenesis (Kaur et al., 2010, Bozaoglu et al., 2010).

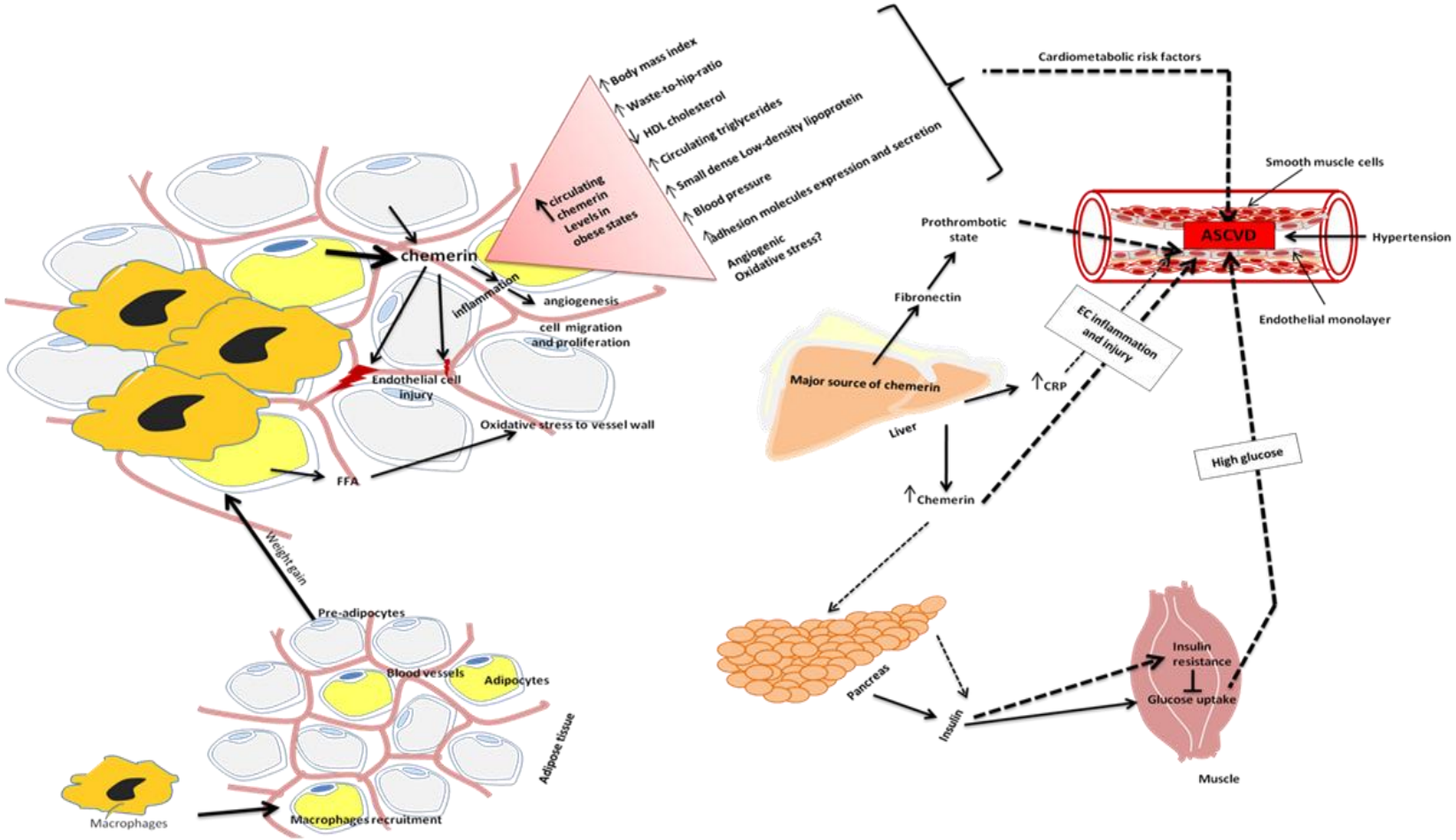

Figure 1.2.5a Relationship of chemerin with various metabolic risk factors and implications for the cardiometabolic syndrome

This figure shows that with increased adiposity, chemerin secretion is increased and positively correlates with body-mass-index, Waste-to-hip ratio, low HDL-C, high LDL-C and increased blood pressure. Chemerin secretion positively affects the inflammatory protein, CRP in the bloodstream which is an acute inflammatory protein and is used as a hallmark of inflammatory disease. Chemerin results in insulin resistance which then inhibits glucose uptake in muscle tissues resulting in increased circulating glucose levels and the development of ASCVDs.

1.3 Chemerin Receptors

1.3.1 Chemokine-like Receptor 1, a Natural GPCR Chemerin Receptor

Chemerin binds to its natural GTP Protein-Coupled Receptor (GPCR) known as Chemokine-like Receptor 1 (CMKLR1) (previously denoted as chemerinR and ChemR23 in humans) (Samson et al., 1998, Wittamer et al., 2003). Chemerin receptor is presented as CMKLR1 throughout the text of this thesis.

1.3.1a Cloning of CMKLR1 gene and structure

In 1996, the human CMKLR1 gene was first cloned using Polymerase Chain Reaction (PCR) with degenerate oligonucleotides based on conserved region in the third and sixth transmembrane domain of the 7-transmembrane (7-TM) G protein linked somatostatin receptor subtypes 1-4 (Gantz et al., 1996). This gene encoded a putative 371 amino acid 7-TM receptor, and was found to share 40% nucleotide sequence similarity to somatostatin receptors 1-4. Later in 1998, Samson and colleagues cloned an identical gene known as ChemR23 (Samson et al., 1998), that is now denoted as CMKLR1, and is located on human chromosome 12q.24.1 (Murphy et al., 2000). Structurally, CMKLR1 is more closely related to chemoattractant receptors such as anaphylatoxin C3a and C5a receptors rather than to the members of other chemokine receptors such as CC- or CXC- (Samson et al., 1998). The murine orthologue of the human CMKLR1 (mCMKLR1) gene, known as DEZ, and is reported to share 80.3% sequence homology with CMKLR1 (Methner et al., 1997).

1.3.1b CMKLR1 receptor expression and functions

CMKLR1 is expressed in haemopoitic tissues such as thymus, bone marrow, spleen, fetal liver and lymphoid organs, and in lower levels in a number of other body tissues (Wittamer et al., 2003). Wittamer and colleagues reported that CMKLR1 is also present in blood monocytes, monocyte-derived human macrophages and immature Dendritic Cells (iDCs), and in low levels in un-stimulated $CD4^+$ T lymphocytes and Polymorphonuclear (PMN) cells (Wittamer et al., 2003, Arita et al., 2007), and in ECs (Kaur et al., 2010). As CMKLR1 is primarily expressed on the cells of the immune system, upon chemerin binding, CMKLR1 directs the migration of dendritic cells to the lymphoid organs and inflamed tissues (Vermi et al., 2005). Additionally, Resolvin E1 (RvE1), an eicosapentaenoic acid-derived lipid is also known to bind CMKLR1 and exerts anti-inflammatory effects (Arita et al., 2007). CMKLR1 also acts as a co-receptor for immunodeficiency viruses including Simian Immunodeficiency Virus (SIV) (Samson et al., 1998) and Human Immunodeficiency Virus (HIV)-1 (Martensson et al., 2006).

1.3.2 G-Protein Receptor 1

G-Protein Receptor 1 **(**GPR1) is another GPCR receptor to which chemerin binds with an affinity similar to that of CMKLR1, however, showing relatively poor intracellular cell signalling in G protein-mediated pathways (Fig. 1.3.1a, page number 26). Barnea and colleagues (2008) identified chemerin as a ligand to GPR1 while developing an assay to identify ligands for orphan receptor GPR1. Upon chemerin binding, GPR1 internalises weakly compared to CMKLR1, and shows weak calcium mobilisation and ERK1/2 MAPK activity in cell lines expressing GPR1. GPR1 is characterised as a decoy receptor for chemerin, and chemerin-

induced functional responses are still unknown. GPR1 is expressed in the central nervous system, adipose tissue and in the skeletal muscles (Barnea et al., 2008).

1.3.3 Chemokine (C-C motif) Receptor-like 2

In 2008, Zabel and colleagues identified Chemokine (C-C motif) Receptor-like 2 (CCRL2) as another orphan GPCR to which chemerin binds (Zabel et al., 2008). Human CCRL2 was first cloned and identified in Polymorphonuclear (PMN) cDNA library in 1998 (Qunibi et al., 2004), and is located on 3p21 chromosome alongwith other chemokine receptors (Meyer, 2004b). Human CCRL2 is also denoted as CKRX, HCR or CRAM and is represented as L-CCR in mice. CCRL2 is a functional chemokine receptor and shares 40% sequence homology with other chemokine receptors; CCR1, CCR2, CCR3 and CCR5. Human CCRL2 is expressed in majority of human hematopoietic cells including monocytes, macrophages, DCs, neutrophils, T cells, natural killer cells, mast cells and $CD34^+$ bone marrow precursors (Kukkonen et al., 1996b, Herlidou et al., 2004, Meyer, 2004b, Meyer et al., 2004). Well-known inflammation mediating agents including Lipopolysaccaride (LPS) and TNF-α are reported to increase CCRL2 receptor expression (Meyer, 2004b, Meyer, 2004a). CCRL2 binds to a number of chemokines including CCL2, CCL5, CCL7 and CCL8 (Enkvist et al., 1996) and CCL19 (Kukkonen et al., 1996c). CCRL2 is also activated by agonists such as MCP-1, -2 and -3, RANTES, and by 'joint fluid' taken from rheumatoid arthritis patients (Meyer et al., 2004, Meyer, 2004c, Sakurai et al., 2005). Comparatively, chemerin NH_2-terminal binds CCRL2 receptor instead of COOH-terminal, and is reported not to mediate any intracellular signalling pathways. The CCRL2 receptor only acts as a sponge or decoy receptor (Cash et al., 2008), facilitating the presentation and also increasing the COOH-terminal chemerin availability to the other neighbouring cells expressing CMKLR1 (Zabel et al., 2008)

(Fig. 1.3.1a, page number 26). CCRL2 receptor lacks –DRY– motif, a motif involved in GPCR coupling, at the cytosolic end of transmembrane segment 3. In 2010, Otero and colleagues showed that CCRL2 knockout mice were protected against ovalbumin-induced airway inflammation, and showed normal recruitment of circulating DCs to the lungs, however, defective trafficking of antigen-loaded lung DCs to mediastinal lymph nodes (Kukk et al., 1996a). It is still unclear whether this defective DC function is due to CCRL2 acting as a silent receptor; or more interestingly, due to NH_2-terminal chemerin binding to CCRL2, and presenting COOH-terminal to nearby cells (Fig. 1.3.1a, page number 26), thereby, increasing the local availability of bioactive chemerin to functional chemerin receptor, CMKLR1.

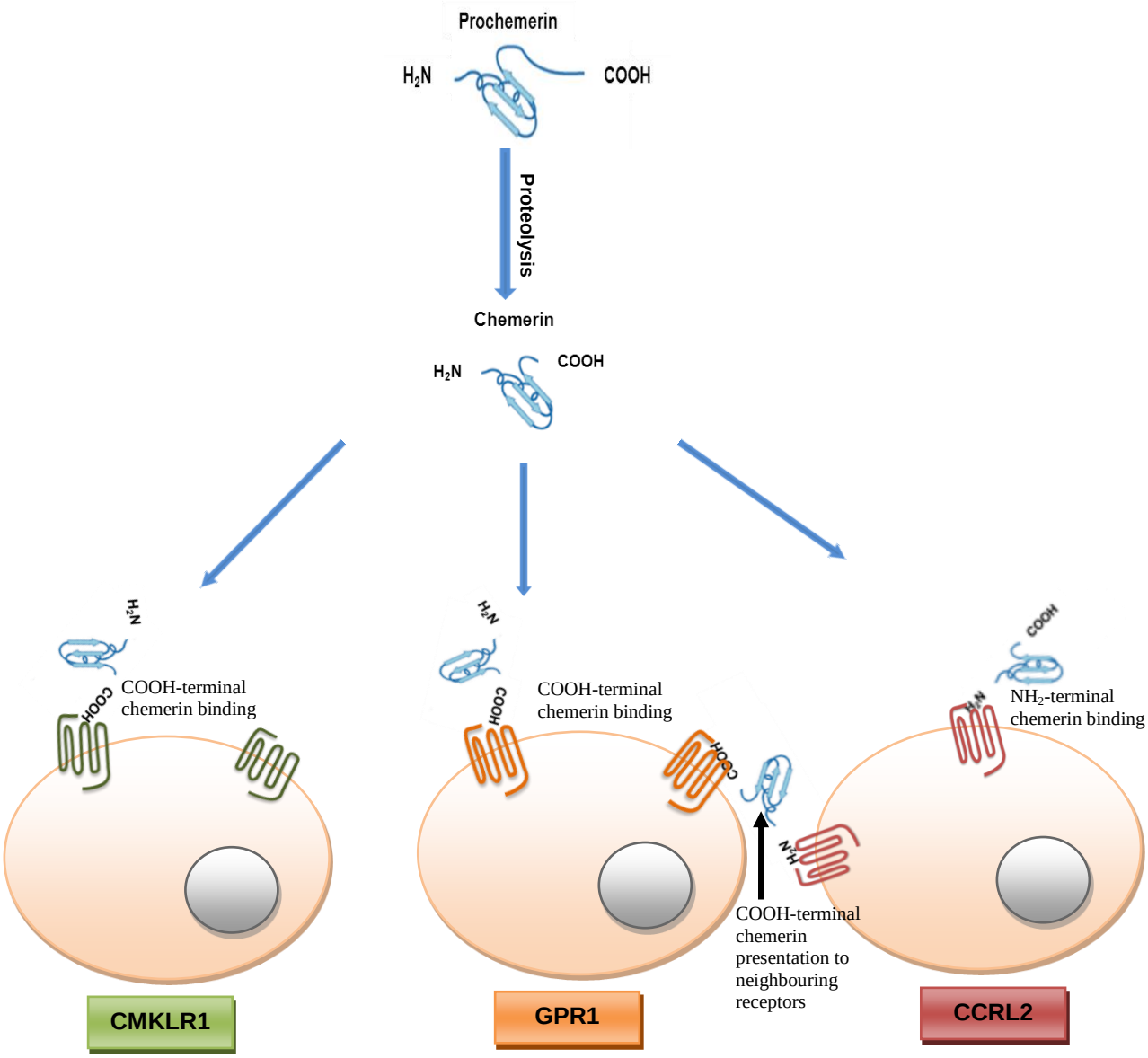

- High-affinity chemerin binding to CMKLR1
- Efficient intracellular signals
- Receptor internalisation

- High-affinity chemerin binding to GPR1
- Weak intracellular signals
- Receptor internalisation

- High-affinity chemerin binding to CCRL2
- No intracellular signals
- No receptor internalisation
- Presentation of COOH-terminal chemerin to other GPCRs on the neighbouring cells – 'sponge' effect

Figure 1.3.1a Chemerin binding to its receptor; CMKLR1, GPR1 and CCRL2

This figure shows chemerin binding to its natural receptor, CMKLR1, as well as to other two orphan GPCR receptors, GPR1 and CCRL2; and the events triggered upon ligand binding. Chemerin binding to CMKLR1 results in strong signalling and internalisation, resulting in final functional outcome; whereas, chemerin binding to GPR1 causes receptor internalisation, however, functions are poorly understood. N-terminal chemerin binds CCRL2 receptor, which acts as decoy receptor and presents C-terminal chemerin to neighbouring functional receptors. Adapted from (Wong et al., 2011).

1.4 G Protein-Coupled Receptors

1.4.1 G Protein Coupled Receptors and G Proteins

1.4.1a G protein-coupled receptors and families

The G Protein-coupled Receptors (GPCRs) family is the largest family of proteins in the human genome (Ponticos et al., 1998). There are 720-800 human GPCRs accounting for 2% of human genome (Fredriksson et al., 2003). These receptor genes are further classified into three main families on the basis of sequence similarities – as A, B and C or 1, 2 and 3 respectively (Garthwaite et al., 1989). GPCR family A is the largest group, and consists of rhodopsin-like receptors and contains the opsins, olfactory GPCRs, small molecule/peptide hormone, and glycoprotein hormone GPCRs. The ligand binding site for class A GPCRs is located within the 7-TM bundle. Family B is a relatively small GPCRs containing family and comprises of ~25 GPCRs for gastrointestinal peptide hormones (e.g., secretin), corticotrophin-releasing hormone, calcitonin and parathyroid hormone. Family C has 17 GPCRs for mGluR, the γ-aminobutyric acid type B ($GABA_B$), calcium-sensing receptors (CaR) as well as some taste receptors (Pierce et al., 2002). An additional Frizzled-Smoothened (F/S) receptor-like class contains 11 GPCRs. The GPCRs with specific ligands are classified as natural GPCRs, and receptors with no ligands are known as orphan receptors. GPCRs are complex receptors and are compartmentalised into three different components; (1) a 7-TM receptor loop with an extracellular ligand-binding NH_2-terminal and an intracellular functional COOH-terminal, (2) a heterotrimeric G proteins including alpha (α), beta (β) and gamma (γ)-subunits, and (3) an effector. Upon ligand binding, activated receptor interacts with heterotrimeric G proteins, and activates a number of different downstream signalling cascades (Fig. 1.4.1a, page number 29).

1.4.1b G Proteins, receptor activation and effectors

The heterotrimeric G proteins consist of an α-subunit and a βγ-complex. The α-subunit is divided into four major different classes that include Gαs (stimulatory), Gαi/o (inhibitory), $G\alpha_{q/11}$ and $G\alpha_{12/13}$, which are further sub-divided into three, eight, four and two subtypes respectively. The β-subunit has five different subtypes, and γ-subunit has twelve different subtypes (Rees et al., 1989). In the absence of an external stimuli, GDP-bound α-subunit and the βγ-complex are associated together. Upon receptor activation, the heterotrimeric G protein complex undergoes an activation-inactivation cycle and involves: (1) exchange of GDP for GTP on the G protein α-subunit, (2) dissociation of GTP-bound α-subunit from the receptor as well as from the βγ-complex which both separately modulate the activity of a number of different enzymes and effectors within the cell and finally, (3) the hydrolysis of GTP by the GTPase enzyme which results in the formation of GDP-bound α-subunit that re-associates with the βγ-complex making receptor inactive (Palmer and Moncada, 1989). In general, G proteins are referred by their α-subunits; Gs heterotrimeric complex contains Gαs, Gq for Gαq, and Gi contains Gαi. Gαs is stimulatory α-subunit that stimulates effector adenylase cyclase (AC), Gαi inhibits the stimulation of AC, and Gαq complex results in the activation of phospholipase C (Pierce et al., 2002). Prolonged GPCR stimulation results in receptor de-sensitisation or down-regulation leading to decreased G protein activity and intracellular signalling (Houvenaeghel et al., 2006) (Fig. 1.4.1a, page number 29).

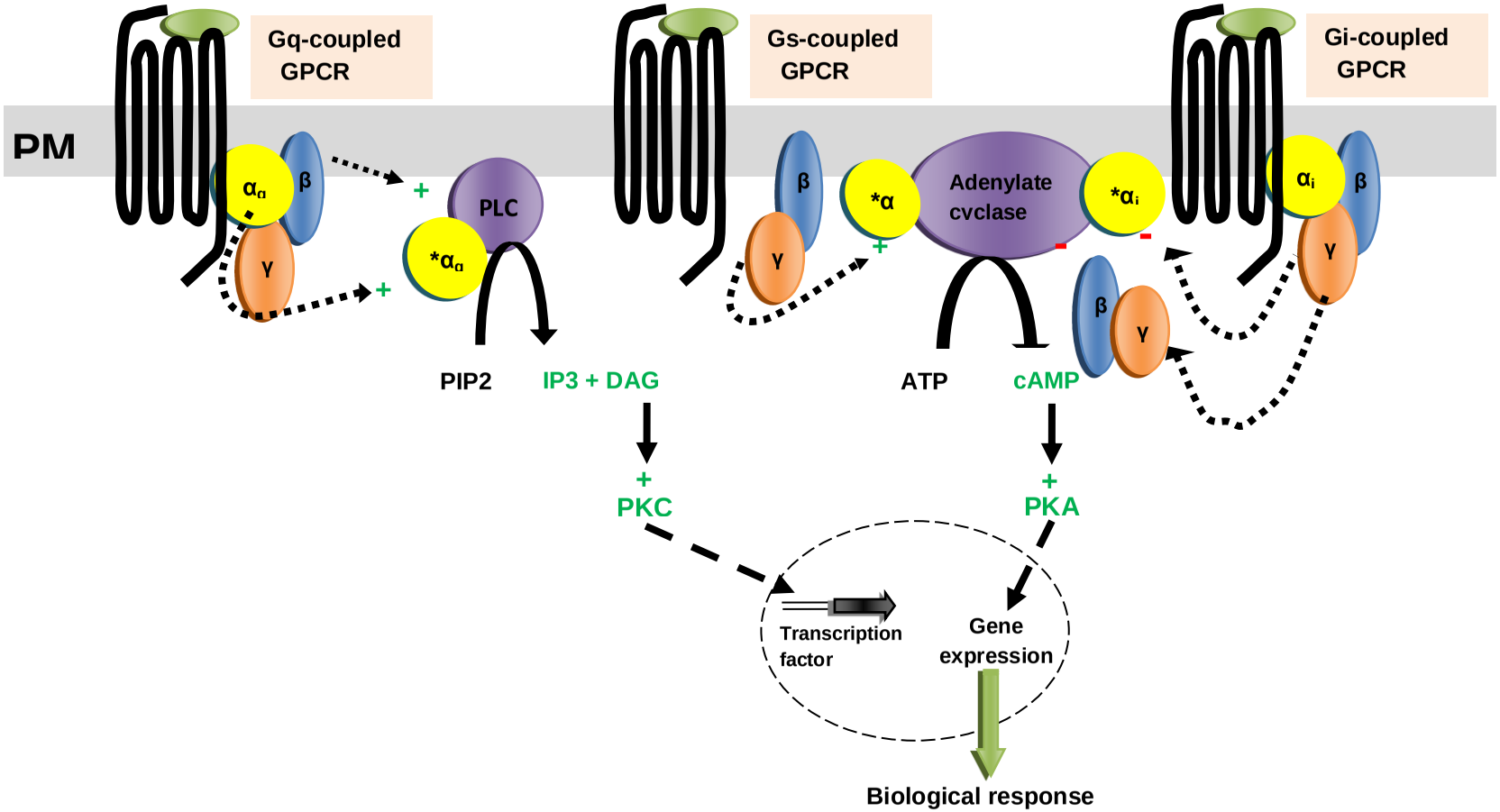

Figure 1.4.1a Classical GPCR signalling and involvement of Gq, Gs and Gi proteins

This figure shows the involvement of different G proteins in mediating different downstream signalling pathways leading to biological outcomes. Ligand binding to GPCR results in the exchange of G protein-bound GDP to GTP. The heterotrimeric G proteins dissociate from the GPCR loop and become activated, both activated α (denoted as *α) and βγ dimer; are capable of signalling forward through the activation or inhibition of effectors . Adapted from (Jacoby et al., 2006).

1.5 Mitogen-Activated Protein Kinases

Mammalian Mitogen-Activated Protein Kinases (MAPKs) are activated by a number of stimuli including hormones (insulin), growth factors [Platelet Derived Growth Factor (PDGF) and Epidermal Growth Factors (EGF)], and inflammatory cytokines (TNF)-α, and various other environmental stresses such as osmotic shock, radiations and ischaemic injury. These stimuli bind to a number of different receptors expressed on the cell membranes and activate different MAPKs which further co-ordinate diverse cellular activities like mRNA expression, cell cycle machinery, cell metabolism, motility, survival, apoptosis and differentiation. There are six different distinct groups of mammalian MAPKs: Extracellular Regulated Kinases (ERK1/2), Jun NH_2-terminal Kinases (JNK1/2/3), p38 (α/β/γ/δ), ERK7/8, ERK3/4 and ERK5. Each MAPK is a member of separate module and is regulated by a wide variety of external stimuli. In general, the 'core signalling module' consists of three sequentially acting kinases that include (1) MAPK, (2) MAPK kinase (MAPKK), and (3) MAPK Kinase Kinase (MAPKKK) (Fig. 1.5.1a, page number 35). The MAPKKKs, also known as MAP3Ks or MEKKs, are Serine (Ser)/Threonine (Thr) kinases that are activated via phosphorylation, and/or their interaction with G proteins of Ras/Rho family in response to external stimuli. Activation of MAP3Ks further results in the activation of MAPKK by phosphorylating Serine (Ser)/ threonine (Thr) residues, causing Thr/Tyrosine (Tyr) phosphorylation of MAPKs which further have transcription factors as their primary substrates and regulate the activity of a number of different genes and proteins, ultimately determining the biological response. 7-TM or GPCR are known to activate each of the different families of MAPKs via both Gα- and βγ-dependent mechanisms resulting in the phosphorylation of different MAPK via activation of a particular receptor (Fig. 1.5.1a, page number 35).

1.5.1 Extracellular Regulated Kinases 1/2 MAPKs

Extracellular Regulated Kinases 1/2 (ERK1/2) MAPKs are the most widely studied mammalian MAPKs and are activated by a number of extracellular and intracellular stimuli including GPCR ligands, cytokines, osmotic stress, and various different growth factors (Fig. 1.5.1a, page number 35) (Lewis et al., 1998). Both these ERK1 and ERK2 MAPKs isoforms share 83% sequence homology and are expressed in varying levels in different tissues. ERK1/2 MAPKs activation or signalling is initiated by cell membrane Receptor Tyrosine Kinases (RTKs) or GPCRs (Goldsmith and Dhanasekaran, 2007). ERK1/2 MAPKs play crucial role in cell proliferation by controlling both cell growth, and cell cycle progression and require persistent ERK1/2 activation (Aksela et al., 1996b). In addition to cell proliferation, ERK1/2 MAPKs are also known to play an important role in angiogenesis, cell migration, invasion and metastasis (Vapalahti et al., 1996), as well as in mesoderm formation (Yao et al., 2003). Interestingly, Bhat and colleagues reported that although ERK1/2 MAPKs play important role in cell survival, however, they are also known to induce cell death (Bhat and Zhang, 1999). A number of studies showed that ERK2 and MEK1 isoforms are essential for embryonic development compared to that of ERK1 and MEK2; as mice lacking ERK2 or MEK1 isoforms showed defective placenta development, whereas, ERK1- or MEK2-deficient mice showed normal growth (Giroux et al., 1999, Belanger et al., 2003).

1.5.2 Extracellular Regulated Kinase 5 MAPK

Extracellular Regulated Kinase 5 (ERK5), also known as Big MAP Kinase-1 (BMK1) is a stress-activated MAPK, and was identified as a 90kDa MAPK. ERK5 MAPK is activated by a number of external stimuli such as oxidants, osmotic stress, and inflammatory cytokines (Abe et al., 1996) (Fig. 1.5.1a, page number 35). Similar to that of ERK1/2 MAPK, ERK5 MAPK is implicated in the regulation of cell proliferation (Kato et al., 1998). A decade ago, ERK5 MAPK has was reported to play an important role in cardiovascular development, and mice lacking ERK5 MAPK died due to lack of angiogenesis in the embryonic and extra-embryonic tissues (Sohn et al., 2002). Endothelial-specific ERK5 knockout mice are reported to show cardiovascular defects (Hayashi et al., 2004), however, no defects were seen in cardiomyocyte-specific ERK5 knockout model; suggesting that ERK5 is one of the important MAPK in ECs (Hayashi and Lee, 2004).

1.5.3 p38 MAPKs

p38 MAPKs constitute a second stress-activated MAPK group and were first isolated as a 38kDa protein. There are four different splice variants of the p38 family including p38α, p38β (Jiang et al., 1996), p38γ (Li et al., 1996) and p38δ (Jiang et al., 1997); and among these p38α is the most extensively studied MAPK. p38 MAPKs are activated by different external stress stimuli, inflammatory cytokines and various different growth factors such as interleukins, insulin-like analogues, and fibroblast growth factors (Freshney et al., 1994) (Fig. 1.5.1, page number 35). A number of GPCR agonists such as TGF-β are also documented to activate p38 MAPKs and are known to mediate cellular functions such as chemotaxis, adherence, immune responses, and especially the role of p38 MAPKs in apoptosis is widely studied (Dong et al., 2002, Merritt et al., 2000). Upon activation, p38 MAPKs phosphorylate several different cellular targets, for example transcription factors and other proteins such as phospholipase A2 and microtubule-associated protein Tau. The p38 MAPKs are implicated in various different biological responses such as cell cycle arrest (Takenaka et al., 1998), apoptosis and cancers (Olson and Hallahan, 2004, Bradham and McClay, 2006), abnormal embryo development and differentiation (Allen et al., 2000) and angiogenesis (Mudgett et al., 2000). The p38 MAPKs are known to play critical role in immune functions including production of inflammatory cytokines such as IL-1β, TNF-α and IL-6, induction of iNOS, and other adhesion molecules including VCAM-1(Pietersma et al., 1997).

1.5.4 Stress-Activated Protein Kinase/Jun-amino-terminal Kinase

The Stress-Activated Protein Kinase/Jun-amino-terminal Kinases (SAPK/JNKs) are a group of MAPKs that are activated by exposure of cells to environmental stresses such as radiations, growth factors, and inflammatory cytokines (Semenzato et al., 2012, Hattori et al., 2011) (Fig. 1.5.1, page number 35). JNKs consist of 10 isoforms coded by three SAPK genes, SAPKα, - β and - γ (JNK-2, -3 and -1, respectively): JNK1 (4 isoforms), JNK2 (4 isoforms), and JNK3 (2 isoforms). SAPK/JNKs are implicated in a number of cellular functions such as cell proliferation and differentiation, cell apoptosis, and interestingly, also in cell protection (Zhang et al., 2012). JNKs are known to activate different substrates depending upon the type of stimuli involved and the 'type' of cells, hence showing different and opposite functional effects (Fogar et al., 2011, Rechel et al., 2011). SAPK/JNK/c-Jun interactions are also reported to play a central role in obesity related insulin resistance (Nittoh et al., 1997a) by interfering with insulin signalling which may serve as a possible link between Non-alcoholic Fatty Liver Disease (NAFLD) and Coronary Artery Disease (CAD) (Semenza, 2011).

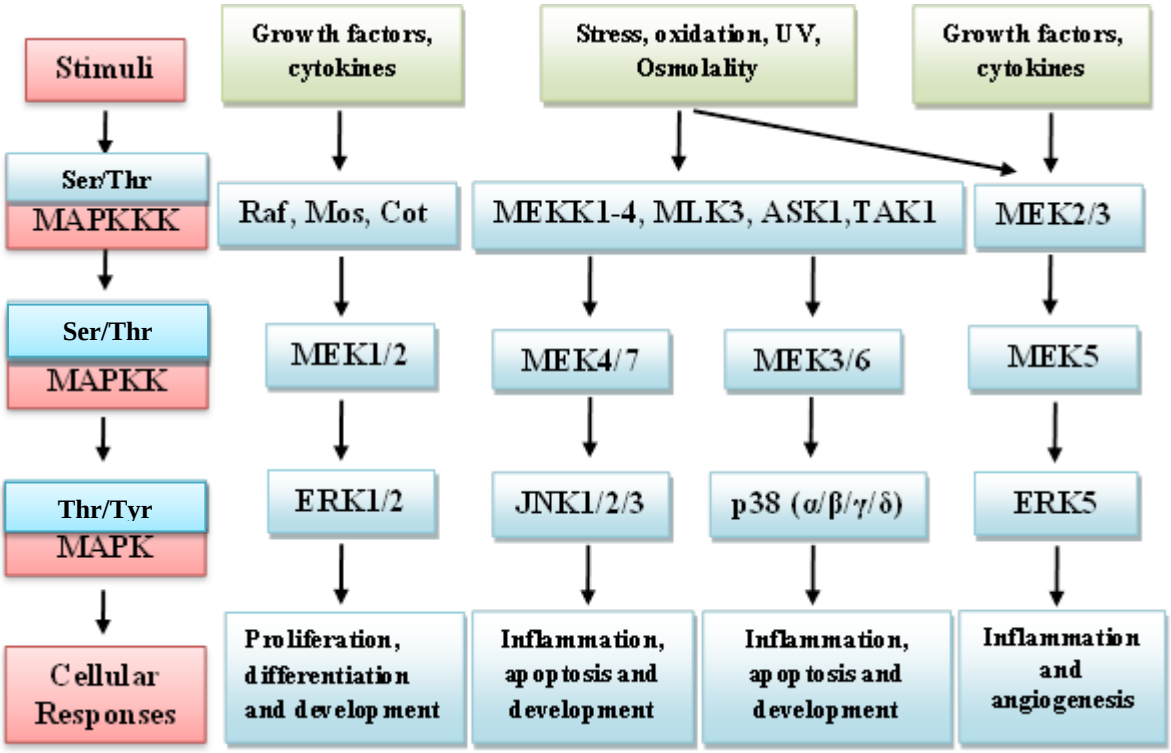

Figure 1.5.1a The MAPK module signalling cascade

A MAPKK Kinase Kinase (MAPKKK) is phosphorylated and, in turn phosphorylates a MAPK Kinase (MAPKK), which leads to the phosphorylation of a MAPK. The MAPKKKs, also known as MAP3Ks or MEKKs, are Serine (Ser)/Threonine (Thr) kinases that are activated via phosphorylation, and/or their interaction with G proteins of Ras/Rho family in response to external stimuli. Activation of MAP3Ks further results in the activation of MAPKK by phosphorylating Serine (Ser)/ threonine (Thr) residues, causing Thr/Tyrosine (Tyr) phosphorylation of MAPKs. An activated MAPK is then shuttled into the nucleus where it targets its specific substrates, such as transcription factors which ultimately lead to gene transcription and cell proliferation. Activation of ERK1/2 MAPK is important in cell proliferation, differentiation and development. p38 and JNK1/2/3 MAPK are important in the processes of inflammation, apoptosis and development. ERK5 MAPK plays an important role in inflammation and angiogenesis. Adapted from (Krishna and Narang, 2008).

1.6 Akt/PKB Kinases

Akt kinases are implicated in mediating a variety of essential cell functions such as cell proliferation, metabolism, transcription and the process of angiogenesis. Akt/PKB kinases are activated immediately upon ligand stimulation by various different growth factors and phosphorylate multiple substrates controlling various different short- and long-term cellular processes both at transcriptional and translational level (Baekkevold et al., 2001). There are three different Akt isoforms; Akt1 (de Winther et al., 2005), Akt2 (Ranu et al., 2000) and Akt3 (Hajra et al., 2000); Akt1 being the most predominant isoform of Akt in the ECs (Majumder et al., 2000). Akt is activated by phosphatidylinositol-3-phosphates (PIP3), the products of PI3K activity. Akt1 plays a prominent role in VEGF-induced responses, whereas the expression of Akt2 and Akt3 remains unchanged in $Akt^{-/-}$ mice. Recently, activation of PI3K pathway has been widely established as the main signal transduction pathway employed by VEGFR2 to stimulate EC survival and proliferation. Various *in vivo* and *ex vivo* experiments have showed that activation of PI3K by VEGFR2 receptor activation promotes EC survival, proliferation and angiogenesis, and manipulations of this pathway results in the inhibition of cell proliferation and angiogenesis (Semenza et al., 2001, Folkman, 1992, Ryan et al., 1992). It is also known that PI3K regulates angiogenesis by regulating expression of Tie-2 receptors (Folkman and Ingber, 1992).

1.7 5` Adenosine Monophosphate-activated Protein Kinase

5` Adenosine Monophosphate-activated Protein Kinase (AMPK) is a heterotrimeric enzyme which is made up of an alpha (α), a catalytic unit; beta and gamma (β and γ) the two regulatory units. AMPK is known to play an important role as a metabolic sensor or 'fuel gauge' and is activated by change in the AMP/ATP ratio (Luo and Semenza, 2011). In ATP-deprived hypoxic conditions, AMPK regulates HIF-1α mRNA expression at transcription level which then induces VEGF mRNA expression under hypoxic condition, a key pro-angiogenic molecule (Hirasawa et al., 1997a). During AMPK phosphorylation, the AMPK γ-subunit undergoes conformational change, and exposes the Thr172 active site on the AMPKα subunit. AMPK activation *in vivo* improves blood glucose uptake, fatty acid and protein metabolism. In contrast, a very recent study published by Becker and colleagues (2010) reported that chemerin induced insulin resistance in mice skeletal muscles by reducing insulin-stimulated increase in Akt/PKB and AMPKα phosphorylation (Becker et al., 2010). Ernst et al (2010) found that acute recombinant chemerin administration in *ob/ob* and *db/db* mice resulted in glucose intolerance by lowering serum insulin levels, and showed no effect on glucose tolerance in wild-type mice fed on chow diet (Ernst and Sinal, 2010). Interestingly, chemerin significantly decreased liver glucose uptake in *db/db* mice in comparison to that of skeletal muscles (Kukkonen et al., 1996a). Also, Sell and colleagues demonstrated similar findings that chemerin impaired insulin signalling and glucose uptake in skeletal muscle cells *in vitro* (Sell et al., 2009).

1.8 Hypothesis

Globally, obesity and associated abnormalities such as insulin resistance, type 2 diabetes and related cardiovascular complications are increasingly becoming a major concern. Adipose tissue, in addition to storing fat, also acts as a major endocrine organ and secretes a number of hormones or molecules into the bloodstream which are collectively termed as 'adipokines' or 'adipocytokines'. Altered secretion levels of these adipokines in obese states are implicated in a number of abnormalities such as inflammation, insulin resistance, type 2 diabetes and related cardiovascular complications. Chemerin is a newly identified adipocytokine, and adipose tissue acts as a major source of chemerin expression and secretion in the body. In obese states, circulating chemerin levels positively correlate with various facets of metabolic syndrome including insulin resistance, type 2 diabetes, hypertension and circulating triglycerides – these states are associated with EC injury, which is an initial hallmark of EC inflammation, disease initiation and progression such as atherosclerosis. In obesity related diseased states, endothelial cell injury and endothelial dysfunction is the initial trigger for the development of diseases of the cardiovascular system – and as previously mentioned – ED is defined as the failure of ECs to respond to increased blood flow by releasing excessive amounts of endothelium Nitric Oxide (NO) and causing local vasodilation. Chemerin circulating levels positively correlate with hypertension and NO plays an important role as a vasodilator, hence we hypothesised that chemerin interferes with the activity of eNOS enzyme – the endothelial specific enzyme which regulates the production of NO in the vascular endothelium, finally resulting in disturbed NO production, hence, leading to abnormal vessel wall functions such as increased cell adhesion molecules, dysregulated angiogenesis and promoting inflammation.

Chemerin, most commonly known for its cytokine like functions and is heavily implicated in the process of inflammation. Altered adhesion molecules expression and impaired NO production in the endothelium are well documented promoters of angiogenesis; hence, we also sought to elucidate the role of chemerin (21-157) in endothelial cell migration, proliferation and capillary tube formation.

Therefore, in nutshell, we tested the hypothesis that whether chemerin (21-157):

- down-regulates the activity of eNOS enzyme, resulting in
- decreased NO production, causing
- increased endothelial cell adhesion molecule expression, and finally promoting
- endothelial cell angiogenesis, based on the initial presumption that CMKLR1 receptor is expressed in the endothelial cells.

Hereby, the specific aims of this project were to study the role of human recombinant chemerin (21-157) in EC functioning with specific aims to explore the role (s) of chemerin (21-157) in; (1) EC angiogenesis in terms of EC proliferation, migration and capillary tube formation, (2) mediating inflammation in the vasculature by altering the levels of endothelium specific Cell Adhesion Molecules, Nuclear Factor – kappa (κ) B pathway and endothelial-monocyte cell adhesion, and finally (3) the endothelial-specific eNOS enzyme activity and the specific protein kinase signalling pathways involved in regulating the activity of this enzyme.

2.1 Materials

- List of buffer solutions and cell media – appendix number 1.1, page number 233.
- DNA and protein markers – appendix number 1.2, page number 234.
- List of chemicals and reagents – appendix number 1.3, page numbers 235-6.
- Inhibitors – appendix number 1.4, page number 237.
- Lab apparatus and glass- and plastic-ware – appendix number 1.5, page number 238.
- Lab equipment – appendix number 1.6, page number 239.
- Specialised Assay Kits – appendix number 1.7, page number 240.
- Antibodies – appendix number 1.8, page numbers 241-2.

2.2 Research Methods

2.2.1 Tissue Culture Methods

2.2.1a Cell culture materials and growth conditions

Tissue culture flasks (T25, T75 and 175cm^2), multi-well plates (6, 12, 24 and 96 wells) and petri dishes were purchased from BD Falcon™ glassware. High purity polystyrene coated tissue culture flasks with canted-neck were used, which provide a state suitable for the cell attachment to flask surface (Aubier et al., 2006). Cells were incubated in Sanyo CO_2 incubator with optimal conditions comprising of 37^{o}C temperature, 5% carbon dioxide (CO_2) environment at 95% relative humidity. Humidity in the incubators prevents evaporation and condensation from the tissue culture flasks and plates. CO_2 maintains the cultures at optimal pH (6.9-7.4) by favouring bicarbonate-CO_2 buffering system. CO_2 levels must be maintained as excessive CO_2 proves to be toxic and may alter cell metabolism (Min et al., 1996). Temperature is another variable which must be kept constant at 37^{o}C as minor fluctuations of one or two degrees on either side may cause slower cell growth when temperature falls, and cell death at high temperatures.

2.2.1b Primary Human Umbilical Vein endothelial Cells (HUVECs)

Primary Human Umbilical Vein Endothelial Cells (HUVECs) were isolated from umbilical veins as described originally (Jaffe et al., 1973b). Dr Raghu Adya (a post-doc in Dr Randeva's lab) performed HUVEC cell isolation from umbilical cords.

The entire procedures were carried out in a dedicated sterilised environment and all the cell media and solutions were pre-warmed at 37^{o}C. The umbilical cords were obtained from mothers giving birth at maternity unit at University Hospital Coventry and Warwickshire (UHCW) (Coventry, UK). Ethical committee's approval

and patients' informed consent was obtained. Cords with blood clots, signs of damage, needle pricks and also those from infected parturient women (positive for HBV or HIV) were not considered suitable for experimental purposes and were discarded. Umbilical cord was severed from the placenta soon after the baby was delivered, clamped at both ends, stored in a sealed polythene bag and transported to the laboratory. Cord was processed immediately after the arrival. The clamp was removed from one end of the cord and PBS was used to wash away any blood. A sterile glass cannula was inserted into the umbilical vein and secured in place using a plastic tie. Clamp was removed from the other end, and another PBS wash was performed to get rid of any remaining traces of blood. In order to remove any air bubbles trapped inside the vein, Phosphate Buffer Solution (PBS) was flushed through the cord a couple of times. Once cleaned, cord was clamped at one end and was filled with 1mg/ml collagenase solution in PBS, and second clamp was replaced at the other end. Cord was then wrapped in an aluminium foil and placed in a humidified incubator at 37^{o}C for 15 minutes. Prolonged exposure to collagenase enzyme causes digestion of basement membrane and also disrupts underlying structures (Jaffe et al., 1973b). The cord was gently massaged to release the cells, and the collagenase solution containing detached cells was emptied out into a sterile falcon tube. Pre-warmed Medium 199 (M199; Invitrogen, Paisley, UK) was run through the cord, and the run-through was collected in the same tube. Cells collected were centrifuged at 1,500rpm for 15 minutes, supernatant was carefully discarded, and replaced with fresh 5ml cell medium. The contents were transferred to T25cm^2 tissue culture flask, and incubated in a humidified incubator at 37^{o}C for a maximum of 5 minutes to encourage cell attachment to flask surface. Cell medium was then replaced with fresh new cell medium to remove any unattached or dead cells from

the flask. The cells were trypsinised with 0.5ml of trypsin/EDTA solution (Media Preparation Laboratory, Department of Life Sciences, The University of Warwick, UK) and incubated at 37^{o}C for 3 minutes to release cells from the flask surface. 10ml of cell medium was added to the flask to inhibit further actions of trypsin solution, and the contents were decanted into a new falcon tube and centrifuged at 1,000rpm for 5 minutes. Cell supernatants were aspirated out, and remaining cell residue was re-suspended in a fresh cell medium containing 10% Fetal Calf Serum (FCS; Sigma Aldrich, Dorset, UK), and transferred to a T75cm^2 flask and replaced back in a humidified incubator at 37^{o}C at 5% CO_2 environment.

Growth, maintenance and subculturing of HUVECs

HUVECs were cultured in M199 medium supplemented with 10% FCS 100IU/ml penicillin (Sigma Aldrich, Dorset, UK), 100µg/ml streptomycin (Sigma Aldrich, Dorset, UK), 30µg/ml Endothelial Cell Growth Supplement (ECGS; BD Biosciences, Bedford, MA, UK) and 10µg/ml heparin (Aventis Pharma, Milan, Italy) in a humidified incubator at 37^{o}C at 5% CO_2 environment.

Cells were monitored on a regular basis for confluence and morphology using inverted phase microscope. When 80-90% confluence was reached, cells were either sub-cultured into culture plates for stimulation or split into new multiple culture flasks to allow further cell growth. Cells between passage numbers three and five were used for experiments. HUVEC cells were only used for the preliminary identification of chemerin receptors, and were not used for any other experiments included in this thesis.

2.2.1c Human Macrovascular Endothelial Cells - EA.hy926 Cell Line

Human macrovascular endothelial cell line, EA.hy926, was established in 1983 by fusing human umbilical vein endothelial cells with permanent human alveolar adenocarcinoma cell line A549 (Edgell et al., 1983). EA.hy926 cell line was kindly provided by Dr C. J. Edgell (Universities of North Carolina School of Medicine, USA).

Growth, maintenance and subculturing of EA.hy926 cell line

EA.hy926 cell line was cultured in Dulbecco's Modified Eagle Medium (DMEM; Invitrogen, Paisley, UK) supplemented with 10% FCS, 100IU/ml penicillin, and 100μg/ml streptomycin.

Cells were monitored and examined on a regular basis for confluence and morphology using inverted phase microscope. Once cells reached 80-90% confluence, cells were either sub-cultured into plates for stimulation or split into new multiple culture flasks to encourage more cell growth. Cells between passage numbers three and fifteen were used for stimulating with chemicals of interest. EA.hy926 cells were cultured to identify the presence of chemerin and its receptors, and like HUVECs, were not used for any other experiments included in this thesis.

2.2.1d Human Microvascular Endothelial Cell-1 (HMEC)-1 Cell Line

Human Microvascular Endothelial Cell (HMEC)-1 line is the first immortalised human microvascular EC line that is known to retain most of the characteristics of normal human microvascular ECs. HMEC-1 cell line is the most widely used microvascular endothelial cell line, as it is easy to grow, and is three to seven times more denser in growth compared to regular microvascular endothelial cells and remains viable up to passage number 95 (Ades et al., 1992). HMEC-1 cell line was obtained from the Centre for Disease Control (CDC; Atlanta, Georgia, USA).

Growth, maintenance and subculturing of HMEC-1 cell line

HMEC-1 were cultured in MCDB medium (Sigma-Aldrich, Dorset, UK) supplemented with 10% FCS, 100IU/ml penicillin, 100µg/ml streptomycin, 5ml of 200mM L-glutamine (Media Preparation Laboratory, Department of Life Sciences, The University of Warwick, UK), 2µM hydrocortisone (Sigma-Aldrich, Dorset, UK) and 10ng/ml Epidermal Growth Factor (EGF; Invitrogen, Paisley, UK) (Carter et al., 2003) for every 500ml of medium at 37^{o}C at 5% CO_2 environment.

Medium was stored at 4^{o}C, and was incubated at 37^{o}C for 30 minutes prior to use. ECs were grown to approximately 80-90% confluence before sub-culturing, and split twice weekly. The medium was removed and the cells were washed with PBS twice to remove any traces of serum as it contains excess of proteins that deactivate the actions of trypsin and glycoproteins such as fibronectin. To release cells from the flask surface, approximately 3ml of 1x trypsin/EDTA solution was added to the flask and incubated for 3 minutes. Trypsin which is a proteolytic enzyme, aids the release of cells from the flask surface by breaking down the extracellular matrix, and EDTA chelates any remaining divalent cations. After 3 minutes, 5ml of fresh incubation

medium was added to the flask to inactivate the actions of trypsin. The cell suspension was then transferred to a tube and centrifuged for 3 minutes at 1,000rpm. The cell supernatants were discarded under sterile conditions in the tissue culture hood, and cell pellets were re-suspended in 10ml fresh incubation medium.

Cells were monitored on a regular basis for confluence and morphology using inverted phase microscope. Cells at 80-90% confluence were either sub-cultured into culture plates for stimulation or split into new multiple culture flasks to allow further growth. Cells between passages number ten and twenty five were used for stimulating with chemicals of interest for all experiments included in this thesis. Throughout this thesis, all the work was carried out in HMEC-1 cells, unless otherwise stated.

2.2.1e Culturing HEK293T cell line

The HEK293T cells were cultured in Dulbecco's Modified Eagle Medium (DMEM; Invitrogen, Paisley, UK) containing 10% FCS, 1% penicillin, and 100μg/ml streptomycin in a humidified incubator at 37^{o}C at 5% CO_2 environment. HEK293T cells were sub-cultured regularly to avoid over-confluence. After aspirating out the cell medium, cells were washed using pre-warmed PBS, and incubated in 3 ml of trypsin/EDTA for 3 minutes. 5ml of fresh medium was added to the cells and the contents were transferred into a universal container. Cells were centrifuged at 1,000 rpm for 5 minutes and supernatant were discarded. Remaining cell residues were re-suspended into 5ml of fresh medium and added to flask containing 10ml of cell growth medium.

2.2.1f Cell count using haemocytometer

Haemocytometer, also known as Neubauer Chamber, was used to calculate the number of cells in different cell suspensions. A haemocytometer is made up of a thick glass slide with four different counting chambers that allow the determination of number of cells per unit volume of a suspension.

Preparing haemocytometer and cell count

Prior to use, the haemocytometer glass slide and coverslip were thoroughly cleaned using 70% ethanol and counting chamber was set up under the microscope. The haemocytometer glass slide is typically engraved with a nine square counting grid, each square having dimensions of $1mm^2$ and is further divided into 16 or 25 smaller squares. After trypsinising the cells, fresh cell medium was added to the cells to make a cell suspension. 50µl of resulting volume was mixed with equal volumes of Trypan Blue solution (Invitrogen, Paisley, UK). Trypan Blue is a dye which penetrates the cell membrane of dead cells, staining the dead cells blue, hence providing an estimation of number of dead cells in a cell suspension. 20µl of the resultant cell suspension was added to the haemocytometer and cells were counted in four 1 mm^2 areas and average cell number was counted. Cells in the left-hand side and top of the grid markings were included whilst those in the right-hand and bottom markings were excluded from the total count.

The total number of viable cells in a suspension were calculated as below:

Viable cells = Total cell volume x 2 x average number of counted cells x 10^4

Total cell volume = in ml
2 = Trypan Blue dilution factor
Average cell number = total number of cells counted/4

2.2.1g Cell storage and revival

Cells can be stored for longer periods in a freezing medium containing a cryoprotectant such as Dimethylsulphoxide (DMSO; Sigma Aldrich, Dorset, UK) which protects cells from disruption by preventing build-up of electrolytes during the freezing process (Lovelock and Bishop, 1959). Both EA.hy926 and HMEC-1 cell lines were grown up to 80-90% confluence in 175cm^2 tissue culture flasks in 25ml of growth medium. Cells were removed from the sides of the flask as described previously for each cell line using trypsin/EDTA solution. The density of viable cells was determined using a haemocytometer as described previously (Refer to section 2.2.1f). Cell suspension containing 5x10^6 cells was transferred into a sterile 15ml centrifuge tube and was centrifuged at 1,000rpm at RT for 2 minutes. The cell supernatants were discarded under sterile conditions and remaining cell residues were re-suspended in 5ml of freezing medium containing 50% v/v FCS, 40% v/v growth media and 10% v/v DMSO and mixed thoroughly. 1ml of resultant cell mixture was transferred into previously labelled 1.5ml cryotubes, placed in a Freezing container (Nalgene® Mr Frosty, Sigma-Aldrich, UK), and allowed to freeze in a -70^{o}C freezer overnight for 2 days. The cryotubes were then transferred to a liquid nitrogen container for storage. To revive the cells from frozen stock, a cryotube vial of cells from liquid nitrogen was removed and placed immediately on dry ice for transport. The cells were thawed quickly by placing the cryotube in a water bath at 37^{o}C, and the contents were transferred to a 25cm^2 culture flask containing 5ml of respective growth medium. After overnight incubation, the cell medium was replaced with fresh cell medium, and the cells were cultured for another 24 hours prior to transferring the contents into T75cm^2 flask for routine cell cultures.

2.3 Molecular Biology Techniques

2.3.1 Total Ribonucleic Acid Extraction and Complementary Deoxyribonucleic Acid (cDNA) Synthesis

Total Ribonucleic Acid (RNA) was extracted from endothelial cells using Qiagen RNeasy Lipid Tissue Mini Kit according to manufacturers' guidelines (Qiagen, Crawley, UK). Extracted RNA was quantified, and checked for purity using NanoDrop spectrophotometer (Labtech International, Ringmer, UK). RNA concentrations were normalised and was reverse transcribed into cDNA using Moloney Murine Leukaemia Virus (M-MuLV) reverse transcriptase (Fermentas, York, UK) and random hexamers (Promega, Southampton, UK) as primers.

2.3.2 Real Time Quantitative Polymerase Chain Reaction (RT-PCR)

Quantitative PCR was performed on a Roche Light Cycler^{TM} system (Roche Molecular Biochemicals, Mannheim, Germany). PCR reactions were carried out in a reaction mixture containing 5µl reaction buffer (Fermentas, York, UK), 2.0mM $MgCl_2$ (Biogene, Kimbolton, UK), 1µl of each forward and reverse primer (10 µg/µl), 2.5µl of cDNA and 0.5µl of Light Cycler Master SYBR Green 1 (Roche, Manheim, Germany). PCR reactions were carried out as follows; denaturation at 94^{o}C for 1 min, then 40 cycles at 94^{o}C for 30 seconds (sec), 60^{o}C for 45 sec, and 72^{o}C for 30 sec, followed by a 7 minutes extension step at 72^{o}C. As a negative control for all reactions, preparations lacking RNA or reverse transcriptase were used.

2.3.3 Agarose Gel Electrophoresis

Agarose gel electrophoresis is the most commonly known method for separating DNA products. 1 or 2% agarose gel in 1x Tris-Borate-EDTA (TBE; Media Preparation Laboratory, Department of Life Sciences, The University of Warwick, UK) was used to separate and visualise DNA bands. 1-2g agarose gel was weighed and dissolved in 1x TBE, heated in a microwave for 1 minute, and cooled at RT by gentle mixing on a magnetic stirrer. 1µl of 10mg/ml Ethidium Bromide (EB; Sigma Aldrich, Dorset, UK) was added to the gel. The gel was poured into the tank gently to avoid any air bubble formation, and well combs were carefully placed in the gel to make wells for sample loading. Gel was allowed to set for 30 minutes (preferably 1 hour) at RT. 15µl of sample volume was mixed with 2µl of agarose gel loading buffer (Fermentas, UK) and allowed to run at 70V for 45 minutes.

2.3.4 DNA Sequence Analysis

The PCR products from all samples were visualised using UV illuminator. PCR product bands were excised and isolated to purify DNA using QIAquick Gel Extraction Kit (QIAGEN, Crawley, UK). PCR products were sequenced in an automated DNA sequencer (Molecular Biology Lab, Department of Life Sciences, University of Warwick, UK), and the sequence data was analysed using Basic Local Alignment Search Tool (BLAST) from the National Centre for Biotechnology Information, in order to confirm the authenticity of the products.

2.3.5 Clone and Sequence Analysis

2.3.5a Making competent Escherichia coli cells for transformation

I observed and assisted Dr Jing Chen (Senior Research Fellow in Dr Randeva's lab) in making competent *Escherichia coli* cells for transformation.

1. A sterile wire was dipped with DH5α *Escherichia coli* cells from a glycerol stock, and streaked on a Liquid Broth (LB) plate containing no antibiotics and incubated overnight at 37^{o}C.

2. After overnight incubation, an isolated single colony was picked and suspended in a sterile flask containing liquid LB and incubated overnight in a shaking incubator at 250-300 rpm at 37^{o}C.

3. Using sterilised conditions, the neck of universal tube was sterilised by slightly exposing to flame. 125µl of overnight culture of *Escherichia coli* was added to the 20ml LB in the tube. The universal container was incubated in a shaking incubator at 250-300 rpm at 37^{o}C for 2-3 hours.

4. The optical density was measured using a Spectrophotometer at 600nm wavelength. The cells were then centrifuged at 300rpm for 10 minutes at 4^{o}C and cell supernatants were discarded carefully.

5. 10ml of 100mM ice cold calcium chloride was added to cell residues obtained from above step. The pellets were re-suspended by shaking and kept on ice for 40 minutes, centrifuged at 3,000rpm for 10 minutes at 4^{o}C, and kept in a refrigerator prior to performing transformations.

2.3.5b Transformation into bacterial cells

The reactions from 2.3.5a were added to 200µl of competent cells and kept on ice for 30 minutes, temperature shocked at 42^{o}C for 40 seconds, and placed back on ice for further 30 minutes. 800µl of LB was added to cells and incubated at 250rpm at 37^{o}C for 1 hour in a shaking incubator. The cells were then spread onto a plate with LB-medium and ampicillin and incubated overnight at 37^{o}C.

2.3.5c Purification and sequence analysis of recombinant DNA

After overnight incubation of agar plates of transformed bacteria, single colony was picked using a sterile toothpick and added into a tube with 100ml of selective medium. Tube was incubated in a shaking incubator at 250rpm for 16 hours at 37^{o}C. The recombinant pcDNA3.1 was extracted using QIAprep maxiprep kit (QIAGEN, Crawley, UK).

1. After incubation, the broth culture were transferred to 50ml falcon tubes and centrifuged at 3,300 *g* for 25 minutes and supernatants were discarded carefully.

2. Remaining residues were homogeneously re-suspended in 10ml of buffer P2. The mixture was mixed vigorously by inverting 4-6 times and incubated at RT for 5 minutes.

3. 10ml of buffer P3 was added and mixed vigorously inverting 4-6 times, and incubated at RT for 20 minutes and contents were centrifuged at 13,000rpm for 10 minutes.

4. To allow DNA binding, a QIAGEN-tip was equilibrated by adding 10ml buffer QBT and column was allowed to empty by gravity flow.

5. Cell supernatants from step 3 were applied to the QIAGEN-tip and allowed to enter the resin by gravity flow.

6. Once the QIAGEN-tip column emptied out, 30ml of QC solution was allowed to move through the QIAGEN-tip by gravity flow. The column was wasted out twice.

7. DNA bound to QIAGEN-tip column was eluted using 15ml of buffer QF and flow-through was collected in a conical glass container.

8. Eluted DNA was precipitated out by adding 10ml of isopropanol at RT and centrifuged at 15,000*g* for 30 minutes at 4^{o}C.

9. Supernatants were carefully removed and residual DNA pellets were washed using 10ml of 70% ethanol. The mixture was centrifuged at 15,000*g* for 10 minutes and supernatants were discarded.

10. The remaining DNA pallets were air-dried for 5 minutes, re-suspended in 400µl distilled water, and DNA concentration was determined using Nanodrop at A260/280 nm.

The DNA was submitted to Molecular Biology Services for DNA sequencing.

2.3.6 Transfections

A number of transfection methods are used for transferring nucleic acids into mammalian cells yielding a large quantity of a single protein for studying the regulation and function of a specific genes of interest. Lipofectamine reagent was used to carry out transfections both in HMEC-1 and HEK293T.CMKLR1 cell lines.

Transient transfection of clones using Lipofectamine reagent

Lipid-mediated transfections involved the incorporation of DNA into mammalian cells, by way of liposome vesicles, positively charged lipid and negatively charged DNA bind to the cell and are internalised by endocytosis (Gross et al., 2005).

2.3.6a Transient transfections in HMEC-1 cell line

HMEC-1 cells were transiently transfected with dominant-negative G-proteins.

Transient transfections of dominant-negative G proteins in HMEC-1 cell line

HMEC-1 cells were plated in 6-well culture plates and were transfected with dominant-negative G proteins. Cells were transfected with empty pcDNA3.1, pcDNA3.1 (+)-Gα1, pcDNA3.1 (+)-Gα2, pcDNA3.1 (+)-Gαs, pcDNA3.1 (+)-Gq11 using Lipofectamine (Invitrogen, Paisley, UK) and Opti-MEM® medium (Invitrogen, Paisley, UK). 4µg of each plasmid DNA was added to 250µl of Opti-MEM® medium (Solution 1). 10µl of Lipofectamine reagent per reaction was mixed with 250µl of Opti-MEM® medium (Solution 2). Both solution 1 and 2 were mixed together and allowed to stand at RT for 30 minutes before adding the transfecting mix into the HMEC-1 cells. After 24 hours of incubation, cell medium containing transfection reagent mix was replaced with fresh pre-warmed MCDB medium containing 10% FCS and cells were further incubated for another 48 hours. Different chemerin (21-

157) treatments were performed in G protein-transfected HMEC-1 cells (data not included).

Transient transfection of NF-κB-Luc plasmid in HMEC-1 cell line

Dr Raghu Adya carried out transient transfections of NF-κB-Luc plasmid in HMEC-1 cell line.

The pcDNA3.1-NF-κB-Luc was transfected into HMEC-1 using Lipofectamine reagent. HMEC-1 cells were trypsinised and plated in 12-well culture plates at a final cell density of $3x10^5$ cells/well. Cells were transfected using a *cis*-reporter plasmid containing luciferase reporter gene linked to five repeats of NF-κB binding sites (pcDNA3.1-NF-κB-Luc; Stratagene, La Jolla, CA). For each sample transfection, 5µl of pcDNA3.1-NF-κB-Luc [0.35µg/µl] was added to 125µl of Opti-MEM® medium in an eppendorf tube (Solution 1). Solution 2 was prepared in a separate eppendorf tube by adding 5µl of Lipofectamine and 125µl of Opti-MEM® medium. Both solution 1 and solution 2 were mixed and allowed to stand at RT for 15 minutes. 250µl of the resultant solution was added to each well and incubated for 12 hours in a humidified incubator at 37^oC at 5% CO_2 environment. Opti-MEM® medium was added to some wells which served as transfected control wells. A control plasmid with a luciferase gene insert was also transfected and used as a control in measuring luciferase activity. Following 12 hours incubation, the cell medium was replaced with MCDB medium containing 10% FCS and further incubated for 12 hours. Cells were treated with different chemerin (21-157) concentrations [0-10nM] and TNF-α [10ng/ml] for a maximum of 24 hours. Following cell treatments, cell lysates were collected and luminescence was measured using a dual luciferase reporter assay system (Luminometer, Promega, UK). For achieving HMEC-1 cell line stably expressing NF-κB-Luc, HMEC-1 cells

were transfected with pcDNA3.1-NF-κB-Luc in MCDB cell medium containing Geneticin (G)-418 sulphate (G418) [0.5mg/ml] (Invitrogen, Paisley, UK). The non-transfected cells were killed within 5 days. A number of selected colonies were cultured for a total of 8 weeks in cell medium containing G-418. A number of clones were selected to measure NF-κB activation and luciferase activity as described above and cells were stored in liquid nitrogen as described previously (Section 2.2.1g, page number 48).

2.3.6b Stable and transient transfections in HEK293T cells

Both stable and transient transfections were performed in HEK293T cells.

Stable CMKLR1 transfections in HEK293T Cell Line

Dr Jing Chen carried out stable transfections of pcDNA3.1-CMKLR1 in HEK293T cell line.

In order to generate HEK293T cells stably expressing CMKLR1 receptor (HEK293T.CMKLR1), pcDNA3.1-CMKLR1 was transfected into HEK293T cells in DMEM cell medium containing G418 [0.5mg/ml] (Invitrogen, Paisley, UK) and was replaced every three days. The non-transfected cells were killed within 5 days. After 2 weeks, the colonies were selected and isolated by using cloning rings, and then each colony was grown DMEM cell medium containing G418. Finally, a single cell from a resistant colony was transferred into a 96-well plate and cultured in G418 containing DMEM medium for further 8 weeks.

Transient transfections of dominant-negative G proteins in stably transfected HEK293T cells

HEK293T cells were plated in 6-well plates and were transfected with dominant-negative G proteins. Cells were transfected with empty pcDNA3.1, pcDNA3.1 (+)-Gα1, pcDNA3.1 (+)-Gα2, pcDNA3.1 (+)-Gαs, pcDNA3.1 (+)-Gq11 using Lipofectamine reagent and Opti-MEM® medium. Different chemerin (21-157) treatments were performed in G protein-transfected HEK293T.CMKLR1 cells (data not included).

2.3.7 Sodium Do-decyl Sulphate Polyacrylamide Gel Electrophoresis

Sodium Do-decyl Sulphate Polyacrylamide Gel Electrophoresis (SDS-PAGE) is the most commonly used technique for separating proteins.

Sample preparation

Samples for SDS-PAGE analysis were prepared from all different cell types. After treating the cells with different chemicals of interest, cells were washed with ice-cold PBS twice and were lysed in 1x Radioimmunoprecipitation Assay (RIPA) buffer (100mM Tris pH 7.4, 300mM NaCl, 20mM sodium pyrophosphate, 2mM EDTA, 200µM β-glycophosphate, 2% sodium vanadate, 1% Nonidet P40, 0.2% sodium deoxycholate, 0.2% sodium dodecyl sulphate) containing 2µl of protease inhibitor cocktail, 1µl of Phenylmethylsulfonyl Fluoride (PMSF) and 1µl of sodium orthovanadate solution. 120µl of 1x RIPA was added to each well of a 6-well plate, incubated on ice for 2-3 minutes, and cell lysates were collected in eppendorf tubes and replaced back on ice. Samples were centrifuged at 8,000rpm for 5 minutes and protein concentrations were determined using BCA protein quantification method (Refer to section 2.4.1). Cell lysates were mixed with 1x Laemmli buffer [(120 mM Tris-HCl, pH 6.8, 4% SDS, 20% glycerol, β-mercaptoethanol and 0.01%

bromophenol blue (1:1 w/v)] and boiled in the water bath at 95^{o}C for 5-6 minutes to denature the proteins. Samples were centrifuged at 4,000 rpm for 5 minutes at 4^{o}C and stored at -80^{o}C until analyses.

Preparing SDS-PAGE gels

The polyacrylamide gels of different percentages were prepared. Resolving gel was prepared by adding protogel [30% Acrylamide: Bisacrylamide (37.5:1) (GENEFLOW Limited, UK)], resolving gel (GENEFLOW Limited, UK), deionised water, 10% Ammonium Persulphate (APS) (Sigma Aldrich, Dorset, UK) and *N, N, N', N'*- tetramethyl-ethylenediamine (TEMED) (Sigma Aldrich, Dorset, UK) in a universal container and mixed gently. The mixture was poured between the gel casts leaving sufficient space for the stacking gel and allowed to polymerise at RT for 15-20 minutes. The stacking gel was prepared by adding protogel, stacking gel, deionised water, APS and TEMED in a universal container, mixed gently, and the mixture was subsequently applied on top of the pre-set resolving gel. The comb was placed in the stacking gel to allow well formation and was allowed to stand at RT for 20 minutes. The gels were placed in the gel holder tank and sufficient 1x protein gel running buffer (10g SDS, 30g Tris and 144g Glycine per litre solution) was added.

Protein electrophoresis and detection

Ten to thirty micrograms of protein sample was loaded in the gel wells, and was electrophoresed at a constant current of 40mA for approximately 60-120 minutes. Following electrophoresis, the proteins were transferred onto activated Polyvinylidene Fluoride (PVDF) membranes (Millipore, UK) at 100V for 60 minutes. The PVDF membranes were activated by placing the membranes in methanol for 20 sec, washed in water for 3 minutes and placed in transfer buffer for 5 minutes. After the transfer (transfer buffer - 100ml of 10x Tris/Glycine (30g Tris

and 144g Glycine per litre solution), 200ml of methanol, and 700 ml dH_2O to make a total volume of 1L), the membranes were blocked using 5% Bovine Serum Albumin (BSA) prepared in 1% TBS (24.2g Tris and 80g NaCl per litre solution) /0.1% (v/v) Tween-20 (TBS-T) (represented as '5% BSA solution' in this thesis text throughout) for 1 hour at RT. Membranes were incubated with specific primary antibodies constituted in 5% BSA solution at 4^oC with gentle shaking overnight. Following overnight incubation, the primary antibodies were removed by washing with TBS-T solution every 15 minutes for four times. Membranes were incubated with corresponding secondary Horseradish-Peroxide (HRP)-labelled detection antibodies diluted in 5% BSA solution for 1 hour at RT. Membranes were washed for another 1 hour using TBS-T solution every 15 minutes. A final 15 minutes membrane wash was performed in TBS only solution to remove any traces of Tween, which may interfere with chemiluminescence. The labelled antibody complexes were detected using Enhanced Chemiluminescence Plus detection reagent [ECL; GE Healthcare, Little Chalfont, UK] according to manufacturer's instructions. Membranes were stored at 4^oC in TBS solution for further stripping and re-probing.

Stripping and Re-probing Membranes

Membranes were stripped and re-probed with loading controls. The membranes were placed in 30ml stripping buffer (120ml of 10% SDS, 37.5ml of 1M Tris-HCl pH 6.8, 4.7ml β-mercaptoethanol and dH_2O for a total volume of 600ml solution) in clear plastic containers and incubated in a shaking water bath at 50^oC for 30 minutes. After incubation, membranes were washed with TBS-T solution twice, each 15 minutes at RT. The membranes were blocked with 5% BSA solution for 1 hour at RT and were incubated with specific antibodies overnight at 4^oC with gentle shaking. Following overnight incubation, the primary antibodies were removed and

the membranes were washed four times with TBS-T solution for 15 minutes each. Membranes were incubated with corresponding HRP-labelled secondary detection antibodies prepared in 5% BSA solution for 1 hour at RT and washed with TBS-T solution for 1 hour every 15 minutes. A 15 minutes TBS only membrane wash was performed in to remove any traces of Tween. Antibody complexes were detected using ECL Plus detection reagent according to manufacturer's instructions. The band densities were measured using a scanning densitometer coupled to scanning software Scion Image™ (Scion Corporation, Maryland, USA).

2.3.8 Immunostaining

Immunostaining method was employed for studying specific cellular or tissue constituents. Sterilised coverslips were placed inside the wells of a 6-well plate and covered in poly-L-lysine [10µg/ml] solution (Sigma Aldrich, Dorset, UK) for 1 hour. Following incubation, poly-L-lysine solution was aspirated out and HMEC-1 cells were trypsinised and cultured on coverslips for 24 hours. After 24 hours the cell medium was removed and wells were gently washed with PBS twice. 2% formaldehyde was added to the wells and incubated for 30 minutes at RT and washed with PBS immediately after the incubation for 5 minutes. 3% BSA solution prepared in PBS containing 0.01% Triton X-100 was added to the wells for blocking for 1 hour at RT. Cells were incubated with mouse anti-CMKLR1 antibody [(1:400); Santa Cruz, MA, USA] constituted in PBS containing 0.01% Triton X-100 overnight at 4^{o}C. After overnight incubation, cells were washed with PBS containing 0.01% Triton X-100 for three times every 10 minutes. A detection antibody Alexa 680 conjugated anti-mouse IgG in PBS containing 0.01% Triton X-100 [(1:400); Cell Signalling, Beverly, MA, USA] added to the wells and incubated in the dark for 2 hours. The cells were washed three times for every 10 minutes with PBS containing

0.01% Triton X-100. A glycerol drop containing 4´, 6-Diamidino-2-phenylindole hydrochloride (Sigma-Aldrich, Dorset, UK) was placed on a slide, and cells covered coverslip was attached to the slide with a drop of DAPI and mounted with nail varnish. Cells were mounted in VECTASHIELD mounting medium with DAPI (Vector Laboratories, Inc. Orton Southgate, Peterborough, UK) on microscope slides. Cells were observed under an oil immersion objective lens using a Leica model DMRE laser-scanning confocal microscope (Milton Keynes, UK).

2.3.9 Gelatin Zymography

I only observed Dr Raghu Adya carrying out Gelatin zymography procedure.

Gelatin zymography was used to measure the gelatinolytic activities of secreted MMP-2 and MMP-9 in endothelial cell supernatants. Under non-reducing conditions, 10µl of culture supernatants were mixed with 10µl zymography sample buffer and were resolved using 10% SDS-PAGE containing 1mg/ml of gelatin (Sigma, St. Louis, USA). The gels were electrophoresed at 4^{o}C and gels were washed twice for 30 minutes with denaturation buffer (2.5% Triton X-100) at RT, and incubated overnight in the incubation buffer (50mM Tris-HCl pH 7.5, 200mM NaCl, 10mM CaCl2, 1µM ZnCl2) at 37^{o}C. Characterization of MMP activity was determined by inhibition with EDTA (10mM). Following day, gels were stained for 1 hour (0.25% Coomassie brilliant blue R-250 in 45% methanol, 10% acetic acid), and de-stained in the same buffer without Coomassie (Media Preparation Laboratory, Department of Life Sciences, The University of Warwick, UK). White bands against a blue background were observed following de-staining which indicated gelatinolytic activities of the expressed MMPs. Gel Pro image analysis (Gel Pro 4.5, Media Cybernetics, USA)] was used to measure the intensities and fold increase was calculated.

2.4 Specialised Assays

2.4.1 Bis-Chorionic Acid Protein Quantification Assay

Bis-chorionic Acid (BCA) protein quantification assay was used to determine protein concentrations in cell lysates from different cell lines (Rampazzo et al., 2012) (Sigma Aldrich, Dorset, UK). Following cell treatments with different chemicals, cells were lysed in 1x RIPA and centrifuged at 8,000 rpm for 5 minutes. 5µl of each cell supernatant or standard was added to 96 well plate and a 195µl of a mixture of BCA solution, CuSO4 and PBS was added to each well (4µl CuSO4, 5µl PBS and 200µl of BCA solution per sample). The plate was incubated for 20 minutes at 37^{o}C and the absorbance was measured using a plate reader (Multiskan Ascent 96/384 Plate Reader) at 570nm.

2.4.2 CellTiter 96® AQueous One Solution Cell Proliferation Assay

HMEC-1 cell proliferation was determined using CellTiter 96 AQ_{ueous} One Solution Cell Proliferation Assay (MTS) kit (Promega, UK). This assay is a based on the colorimetric method for determining the number of viable cells in cell proliferation or cytotoxicity assays. HMEC-1 cells were trypsinised and cultured in 96-well plate (provided in the kit) at the cell density of $2.5x10^5$ cells/well for 24 hours in a humidified incubator at 37^oC at 5% CO_2 environment. Cells were serum-starved in MCDB medium containing 1% FCS overnight and treated with different chemerin (21-157) concentrations [0-30nM] for a maximum of 24 hours. After 24 hours, the cell medium was replaced with 100µl of fresh MCDB medium containing 1% FCS, and 20µl MTS reagent was added to each well and incubated for 1 hour in a humidified incubator at 37^oC at 5% CO_2 environment. The absorbance was recorded at 490 nm using an ELISA plate reader (EL800, Bio-Tek Instruments, Inc., Winooski, VT, USA). The percentage increase in absorbance was calculated against untreated cells.

2.4.3 Wound-healing Cell Motility Assay

Dr Raghu Adya carried out wound-healing cell motility assay.

HMEC-1 cells were trypsinised and were plated in 6-well plates at the final cell density of $1x10^5$ cells/ml in MCDB cell medium containing 10% FCS and incubated overnight. In 75-80% confluent cells, a single scratch wound was created using a sterile p10 micropipette tip, and markings were created to serve as reference points in order to eliminate any possible variation caused by the difference in the width of the scratches. Cell medium was replaced with MCDB medium containing 1% FCS and incubated overnight. Cells were treated with different human recombinant chemerin (21-157) concentrations [0-30nM] (R and D systems, Abingdon, UK) and

incubated for a maximum of 24 hours. VEGF [0.5µM] (Sigma Aldrich, Dorset, UK) was used as a positive control. Images were captured using phase contrast microscopy. The distance between the two sides of the scratch was analysed quantitatively by using Image Pro-plus software (Media Cybernetics, Bethesda, MD).

2.4.4 *In vitro* Cell Invasion Assay

Dr Raghu Adya carried out *in vitro* cell invasion assay.

HMEC-1 cell invasion was studied using BD BioCoat™ Matrigel™ Invasion Chamber assay (BD Biosciences, San Jose, CA, USA). This assay is useful in studying the cell invasion of malignant and normal cells. BD BioCoat Matrigel Invasion Chambers consist of a BD Falcon™ TC Companion Plate with Falcon Cell Culture Inserts with an 8 micron pore size PET membrane with a thin layer of MATRIGEL Basement Membrane Matrix, latter acting as a reconstituted basement membrane *in vitro.* Before performing the experiments, equal number of Matrigel Culture Inserts and Control Culture Inserts were rehydrated using pre-warmed MCDB medium for 2 hours in a humidified tissue culture incubator at 37^{o}C at 5% CO_2 environment. After incubation, the cell medium was carefully removed without disturbing the layer of Matrigel™ Matrix on the surface. HMEC-1 cells were trypsinised and the cell suspension containing approximately $3x10^4$ cells/ml was prepared. 750µl of 1%FCS containing MCDB medium treated with different chemerin (21-157) concentrations [0-30nM] was added to the BD Falcon™ TC Companion Plate. The rehydrated Culture Inserts were transferred to the wells containing the chemoattractant, and 250µl of HMEC-1 cell suspension was added. The BD BioCoat Matrigel Invasion Chambers were incubated for 24 hours in a humidified incubator at 37^{o}C at 5% CO_2 environment. After incubations, the non-invading cells were scrubbed off using a cotton-tipped swab into the Culture Inserts

by applying firm pressure and swirling gently over the membrane surface. The cells invaded through the Matrigel™ Matrix were labelled with 4µg/ml Calcein-AM (BD Biosciences) for 90 minutes. Fluorescence of migrated cells was read at 494/517nm (excitation/emission) using a fluorescence plate reader.

2.4.5 Endothelial Cell Capillary Tube Formation Assay

I observed and assisted Dr Raghu Adya in carrying out endothelial cell capillary tube formation assay for generating data presented on page number 136 (Fig. 4.3.11a), and carried out this assay myself for capillary tube formation experiment using chemerin (149-157) (Fig. 8.6a, page number 232).

Capillary tube formation in HMEC-1 cells was determined using Growth Factor Reduced Matrigel™ Matrix (BD Biosciences, San Jose, CA, USA). Matrix Matrigel is obtained from soluble basement membrane extract of the Engelbreth-Holm-Swarm (EHS) tumour which polymerises at the RT and forms a reconstituted basement membrane (Kleinman et al., 1986). Under sterilised conditions, Matrix Matrigel was thawed overnight at $4^{o}C$, and was diluted in MCDB medium containing 1% FCS. 200µl of Matrix Matrigel was added to pre-cooled 24-well culture plates and allowed to polymerise for 30 minutes in a humidified incubator at $37^{o}C$ at 5% CO2 environment. HMEC-1 cells were trypsinised and a final cell suspension containing $2x10^{4}$ cells/well was prepared in MCDB medium containing 10% FCS. 300µl of the resultant cell suspension was added to Matrigel-coated plates and incubated for 2 hours in a humidified incubator at $37^{o}C$ at 5% CO2 environment. Post-incubation, cell medium was carefully removed from the wells avoiding any damage to the coated gel, and was replaced with cell medium containing 1% FCS and incubated for 4 hours. Endothelial cells were treated with or without chemerin (21-157) [0-30 nM] or VEGF [0.5µM] for a maximum of 24 hours. Capillary-like

cell structures were captured with a digital microscope camera system (Olympus, Tokyo, Japan) Image-Pro Plus software was used to quantify tube formation; the tube lengths in 3-4 randomly selected fields in each of the wells were measured both for treated and untreated groups.

2.4.6 Endothelial Cell Apoptosis Assay

Endothelial cell apoptosis assay was studied using Cellular DNA Fragmentation ELISA kit (Roche diagnostics, UK). HMEC-1 cells were trypsinised and plated in 96-well plate at the cell density of $1x10^3$ cells/ml and incubated overnight. Cells were labelled with anti-BrdU solution (solution 7) at the final concentration of 10µM and incubated overnight. Cells were treated with different chemerin (21-157) concentrations [0-30nM] for 24 hours. After incubation, cell supernatants were carefully removed and 200µl of 1x incubation solution (solution 5) was added to each well and incubated for 30 minutes at RT. Cells were centrifuged at 250g for 10 minutes and 100µl of lysed cell supernatants were transferred to previously anti-DNA antibody coated microplates. To coat the microplates, 100µl of anti-DNA antibody 1x coating solution was added to each well and incubated overnight at 4^oC. On the following day, coating solution was aspirated out from the wells, and 200µl of 1x blocking solution (solution 5) was added to each well, covered with adhesive plate and incubated for 30 minutes at RT. Blocking solution was removed from the wells and plate was washed using 300µl 1x wash solution (solution 4).

After transferring the lysed cells into the microplate, plate was covered and incubated for 90 minutes at RT. After incubation, the wells were emptied out by inverting the plate and tapping on a layer of absorbent papers. The wells were washed three times using 300µl of wash solution. After the last wash, 200µl of wash solution was added to each well and plate was placed in a microwave for 5 minutes to irradiate at 500W. A beaker containing 500ml of water was also placed in the microwave to prevent dehydration. The plate was placed in -20^{o}C freezer for 10 minutes for cooling and the contents were aspirated out. 100µl of anti-BrdU-POD conjugate solution (solution 6) was added to each well. The plate was covered using an adhesive plate cover and incubated for further 90 minutes at RT. The plates were washed three times using 300µl of wash solution. 100µl of substrate solution was added to each well and plate was covered in foil and incubated on a shaker for 5 minutes. 25µl of stop solution (solution 8) was added to each well and incubated for 10 minutes on a shaker. The absorbance was recorded at 450nm within 5 minutes of adding the stop solution using a colorimetric plate reader.

2.4.7 NF-κB Luciferase Activity Assay

Dr Raghu Adya carried out NF-κB Luciferase Activity Assay.

For each sample transfection, 5µl of pcDNA3.1-NF-κB-Luc [0.35µg/µl] was added to 125µl of Opti-MEM® medium in an eppendorf tube (Solution 1). Solution 2 was prepared in a separate eppendorf tube by adding 5µl of Lipofectamine and 125µl of Opti-MEM® medium. Both solution 1 and solution 2 were mixed and allowed to stand at RT for 15 minutes. 250µl of the resultant solution was added to each well and incubated for 12 hours in a humidified incubator at 37^{o}C at 5% CO_2 environment. Opti-MEM® medium was added to some wells which served as un-transfected control wells. A control plasmid, TK-plasmid, with a luciferase gene insert was also transfected and used as a control in measuring luciferase activity. Following 12 hours incubation, the cell medium was replaced with MCDB medium containing 10% FCS and further incubated for 12 hours. Cells were treated with different chemerin (21-157) concentrations [0-10nM] and TNF-α [10ng/ml] for a maximum of 24 hours. Following cell treatments, cell lysates were collected and luminescence was measured using a dual luciferase reporter assay system (Luminometer, Promega, UK).

2.4.8 Endothelial-Monocyte Cell Adhesion Assay

Dr Raghu Adya carried out endothelial-monocyte cell adhesion assay.

Endothelial-Monocyte cell adhesion assay was performed using BD BioCoat Endothelial Cell Adhesion Assay kit (BD Biosciences, San Jose, CA, USA). THP-1 monocytes, a human acute monocytic leukaemia cell line, were labelled with 2.5µM Calcein AM. The cells were mixed gently by inverting and the cell suspension was incubated at 37^{o}C for 30 minutes. An excess of Calcein from the cells was removed by repeated washing with PBS. The Calcein labelled cell suspension was prepared to a final concentration of $2x10^{6}$ cells/ml. Alongside, HMEC-1 cells were also trypsinised and a cell suspension containing $1.5x10^{6}$ cells/ml in a specific cell medium was prepared. 100µl of HMEC-1 cell suspension was added to each 96-well tissue culture plate (included in the kit) and incubated for 2-3 hours to allow attachment of cells to the plate surface. Post incubation, cell medium was aspirated out and 100µl of Cycloheximide solution was added to the control wells, and 100µl of fresh 10% FCS MCDB cell medium in rest of the wells. Endothelial cells were activated by adding 10µl of TNF-α [20ng/ml] (Calbiochem, UK) to respective wells and cells were stimulated with chemerin (21-157) [0-10nM] with and without inhibitors and incubated for 2-6 hours. 75µl of medium was aspirated out from the plate wells and were gently washed using 200µl of Assay Buffer solution. After the last wash, fresh 50µl of Assay Buffer solution was added to each well. 100µl of Calcein AM labelled THP-1 monocytes (~50,000 to 200,000 cells) were added to each well and incubated at 37^{o}C for 30 minutes. Approximately, 120µl solution was removed from the plate wells and two 200µl cell washes were performed using Assay Buffer solution. An additional wash was performed to remove any remaining unbound cells in order to eliminate non-specific binding. 100µl of Assay Buffer was

added to each well and the plate reading was performed using a fluorescent plate reader with an excitation/emission filter at 485/530nm.

2.4.9 Quantification of sE-selectin, sICAM-1, sVCAM-1 and sPAI-1 in EC Supernatants

Adhesion molecules (sE-selectin, sICAM-1 and VCAM-1) and sPAI-1 levels were quantified using multiplex assay kit (Millipore, UK). This kit allows simultaneous quantification of various different analytes in combination. Before using, pre-wet the microtitre plate by adding 200µl of 1x wash solution to each well, cover the plate using adhesive film and incubate for 10 minutes on a plate shaker at RT. Wash buffer was removed by vacuum and by placing the plate on a blotting paper to remove excess of wash buffer. 25µl of assay buffer was added to 0 standard and the sample wells. 25µl of each standard or control solution was added to each well, followed by 25µl of matrix solution and 25µl of each sample solution was added to the wells. 25µl of Mixed Beads were added to each well, sealed with adhesive plate cover, wrapped in aluminium foil and incubated overnight at 2-8^{o}C with shaking. After overnight incubation, the contents were removed by vacuuming the plate and washed twice using 300µl/well 1x wash buffer. The wash solution was removed using vacuum filtration and excess by placing the plate on an absorbent paper. 25µl of detection antibody cocktail was added to each well, sealed and covered the plate with aluminium foil and incubated with shaking for 2 hours at RT. Following the incubation, 25µl of Streptavidin-Phycoerythrin detection antibody was added to each well, sealed and covered in aluminium foil and incubated for 30 minutes at RT on a shaking incubator. After incubation, contents were gently removed by vacuuming and plate was washed two times using 300µl of 1x wash buffer, removing the wash buffer using vacuum filtration and excess by placing the

plate on an absorbent paper or tissue. 100µl of Sheath Fluid was added to each well, sealed and covered in aluminium foil and incubated for 5 minutes on a shaker. Plate was run on Luminex® 100 instrument and 50 beads per bead set in 50µl of sample were read.

2.4.10 Assessment of Nitrites and Nitrates in Endothelial Cell Lysates and Supernatants

Nitrates and nitrites were measured using Griess reagent assay. This assay is the most commonly used method for indirect measurement of Nitric Oxide (NO) (Miranda et al., 2001) and was used to determine the nitrite only, and combined amount of nitrite and nitrates (NOx) in cell culture lysates and supernatants. HMEC-1 cells were plated in 6-well plates in MCDB cell medium containing 10% FCS and were serum starved in the same medium before performing different chemerin (21-157) treatments. Cell medium was removed and cells were washed with pre-warmed PBS twice. 1ml of PBS was added to the wells and different chemerin (21-157) treatments were performed for 15 minutes. Cell supernatants were collected in pre-labelled eppendorf tubes for NOx and nitrite analyses. 500µl of dH_2O was added to the wells, cells were lysed and collected for both NOx and nitrite analysis. Both cell supernatants and lysates were centrifuged at 8,000rpm for 5 minutes and stored at 4^oC until analysis. 100mM sodium nitrite stock solution was prepared by adding 1.725g of sodium nitrite (Sigma Aldrich, Dorset, UK) in 250ml of PBS and dH_2O; and 100mM sodium nitrate (Sigma Aldrich, Dorset, UK) standard solution was prepared by adding 2.125g sodium nitrate in 250ml of PBS and dH_2O. Vanadium chloride (Sigma Aldrich, Dorset, UK) was prepared by adding 400mg in 50ml 1M HCL solution (Sigma Aldrich, Dorset, UK). N-(1-Naphthyl) ethylenediamine dihydrochloride (NEDD) (Sigma Aldrich, Dorset, UK) was prepared by dissolving

0.1g in 100ml dH_2O. Sulphanilamide (SULF) (Sigma Aldrich, Dorset, UK) was prepared by adding 2g in 100ml 5% 1M HCL solution. Standard solutions for both sodium nitrite and nitrate was serially diluted from 800µM to 0.75µM. For NOx assessment, 100µl of each standard or sample (both cell lysates and supernatants) solution was added to each well in a 96-well plate. 100µl of Vanadium chloride solution was added to each standard or sample followed by 100µl of Griess reagent mix (50µl of NEDD + 50µl SULF) and the plates were incubated for 45 minutes. The absorbance was recorded at 550nm. For nitrite only analysis, 300µl of a standard or sample (both cell lysates and supernatants) solution was added to pre-labelled 1.5 ml eppendorf tubes. Equal volume of Griess reagent mix (150µl of NEDD + 150µl SULF) was added to the standard or sample and mixed thoroughly. 300µl of each standard or sample was transferred to 96-well plate and incubated for 10 minutes. The absorbance was recorded at 550nm.

2.5 Statistics and Software Used

Western blotting protein band intensities were determined using Scion Image™ densitometer (Scion Corporation, Maryland, USA). All results were normalised as a ratio of expression of specific proteins to β-actin loading control, or as a ratio of phosphorylated protein to total protein; and results were expressed as a fold increase relative to basal. The results were expressed as mean ± Standard Errors of Mean (SEM) of three independent experiments. Single-factor one-way Analysis of variance (ANOVA) (non-parametric) was performed for each treatment and results were reported to be significant when $p < 0.05$.

3.1 Introduction

The initial aims of this project were to; (1) identify and confirm the presence of chemerin gene and protein expression in human microvascular (HMEC-1) and macrovascular (EA.hy926) EC lines, (2) identify and confirm the presence of chemerin receptor, CMKLR1 at gene and protein levels in HMEC-1, EA.hy926 cell lines as well as in primary HUVEC cells, and finally, (3) study the role of known inflammatory cytokines such as Tumour Necrosis Factor (TNF)-alpha (α), Interleukin (IL)-6 and IL-1β in CMKLR1 receptor regulation in HMEC-1 cell line.

Chemerin, as mentioned previously, is a product of TIG-2 gene [also known as Retinoic Acid Receptor Responder 2 (RARRES2)] and is synthesised as a 164 amino acids long protein, known as prochemerin (Meder et al., 2003, Zabel et al., 2006b). Prochemerin undergoes C-terminus cleavage to form various active and inactive chemerin fragments at the sites of inflammation (Fig. 1.2.3a.1, page number 16). Chemerin (21-157) is the most active and abundant circulating chemerin form in the human body. Chemerin binds to its natural GPCR, CMKLR1, which is primarily expressed on the cells of the immune system. In addition, chemerin also acts as a ligand to two other orphan GPCRs, CCRL2 (Zabel et al., 2008) and GPR1 (Zabel et al., 2008, Barnea et al., 2008). Chemerin is expressed in a number of body tissues including liver, white and brown adipose tissue, heart and placenta (Bozaoglu et al., 2007), and plays an important role in various immunological and metabolic functions (Goralski et al., 2007, Wittamer et al., 2003). CMKLR1 is mainly expressed in the cells of immune system and in lower levels in a number of other body tissues including lungs, heart and adipose tissue (Goralski et al., 2007, Roh et al., 2007). First of all, the main aim of this project was to identify the presence of chemerin and its receptors in both microvascular and macrovascular EC lines.

Endothelial cells form a protective barrier between the circulating blood and the surrounding organs. Microvascular (HMEC-1) and macrovascular (EA.hy926) EC lines, as well as primary HUVECs cells were cultured to study gene and protein expressions of chemerin and its receptors. In addition, CMKLR1 receptor expression regulation by known inflammatory mediators such as Tumour Necrosis Factor (TNF)-α, Interleukin (IL)-6 and IL-1β was determined in HMEC-1 cell line.

3.2 Materials and Methods

HMEC-1 and EA.hy926 cells were cultured in 6-well plates in MCDB and DMEM cell media respectively. Primary HUVECs were cultured in M199 medium. Cells were plated in 6-well plates in specific cell media and were serum starved. Cells were lysed in RNA lysis solution or protein lysis solution (1x RIPA) for RNA isolation and protein sample preparations. RNA was isolated using GenElute™ Mammalian Total RNA Miniprep Kit (Qiagen, Crawley, UK), and RNA concentrations were quantified using NanoDrop spectrophotometer (Labtech International, Ringmer, UK). RNA concentrations were normalised and were reverse transcribed into cDNA using Reverse-Transcription Polymerase Chain Reaction (RT-PCR). Using specific gene primers (Table 3.2.1b), PCR reactions were carried out using different PCR components (Table 3.2.1a). For human chemerin gene, the following PCR conditions were used: 95^{o}C for 1 minute; 95^{o}C for 45sec, 55^{o}C for 30sec, 72^{o}C for 1 minute in a total of 40 cycles with a final extension step at 72^{o}C for 10 minute. For all three different human chemerin receptors, CMKLR1, CCRL2 and GPR1, 45 cycles were performed under similar conditions. PCR products were separated using agarose gel electrophoresis, were excised from the agarose gel and DNA was isolated and purified. DNA samples for each gene were sequence analysed at the Molecular Biology Laboratories at The University of Warwick (Coventry, UK). The cellular protein expressions of chemerin, CMKLR1, CCRL2 and GPR1 were detected using SDS-PAGE (Chapter 2, section 2.3.7, page numbers 57-60) using different percentages of polyacrylamide gels to separate different proteins (Table 3.2.1b).

Table 3.2.1a

The chemical components of PCR reactions used per sample

Chemical components	Concentrations	Volume used per reaction
10x PCR buffer	1x	5µl
$MgCl_2$	1.5mM	1.5µl
Taq polymerase	0.5 U/µl	2µl
10 dNTP	0.2mM	1µl
R and F primers	100ng/ml	1µl
cDNA	200ng	2µl
H_2O	n/a	37.5µl

Table 3.2.1b

The sense (forward) and anti-sense (reverse) primer sequences for human chemerin, CMKLR1, CCRL2, GPR1 and β-actin genes

Gene	Forward primer	Reverse primer
Chemerin	AGA CAA GCT GCC GAA GA CG	TGG AGA AGG CGA ACT TCC AA
CMKLR1	CAA CCT GGC AGT GGC AGA TT	AGC AGG AAG ACG CTG GTG AA
CCRL2	GCT GGC ACC AGA GGA TGA AT	GTC CAG GAC ACC GAT CAC AA
GPR1	TCA GGC ACC ATG TTC TGA CT	AGG ATG CTT CGC TTC TTC AC
β-actin	AAG AGA GGC ATC CTC ACC CT	TAC ATG GCT GGG GTC TTG AA

Table 3.2.1c

The molecular weights of proteins and gel percentages used for SDS-PAGE analysis

Protein name	Molecular weight (kDa)	Percentage gels used
Chemerin	16	15
CCRL2	40	12
CMKLR1	42	12
GPR1	60	10

3.3 Data Presentation and Analyses

3.3.1 Identification of Human Chemerin mRNA Expression in HMEC-1 Cell Line

HMEC-1 cells were cultured in 6-well plates in MCDB medium containing 10% FCS, and were serum starved overnight in cell medium containing 1% FCS. Cells were lysed in RNA lysis solution and RNA was isolated. mRNA was reverse transcribed into cDNA using specific primers (Table 3.2.1a). Conventional PCR was carried out to identify the presence of human chemerin mRNA expression in ECs. Chemerin PCR products were separated and visualised as a 252bp product by agarose gel electrophoresis (Fig. 3.3.1a). DNA product was purified and sequenced for sequence authenticity. BLAST search confirmed chemerin gene sequence.

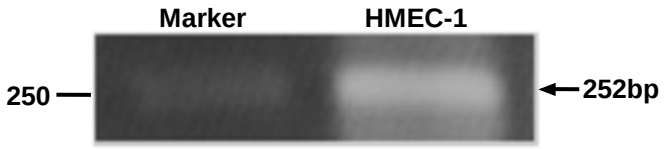

Figure 3.3.1a Human chemerin mRNA expression identification in HMEC-1 cell line

HMEC-1 cells were cultured in 6-well plates in MCDB medium. Cells were lysed using RNA lysis solution and RNA was isolated and quantified using NanoDrop spectrophotometer (Labtech International, Ringmer, UK). PCR analysis identified human chemerin gene as a 252bp DNA product. The PCR products were resolved on 1% agarose gel, purified and sequenced to confirm the authenticity of the product. Three independent experiments were performed and identical results were obtained. GeneRuler^{TM} 1kb DNA ladder was used as a marker.

3.3.2 Chemerin Protein Expression in HMEC-1 and EA.hy926 Cell Lines

HMEC-1 and EA.hy926 cells were cultured in 6-well plates in specific cell media containing 10% FCS and were serum starved overnight in respective cell media containing 1% FCS. Cells were lysed in 1x RIPA buffer and protein lysates were separated using SDS-PAGE. Chemerin protein was identified as a 16kDa product in both HMEC-1 and EA.hy926 cell lines (Fig. 3.3.2a).

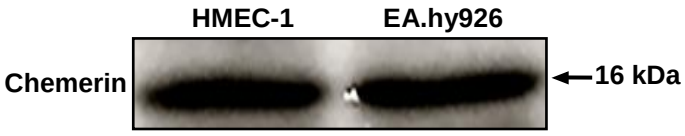

Figure 3.3.2a Chemerin protein expression in HMEC-1 and EA.hy926 cell line

Both HMEC-1 and EA.hy926 cells were lysed in 1x RIPA buffer and amount of proteins were quantified using BCA method. Samples were prepared by mixing equal volumes of cell lysates with 1x Laemmili buffer solution, and the proteins were separated using 15% polyacrylamide gels, and transferred to PVDF membranes at 100V for 1 hour. Membranes were incubated with goat anti-chemerin antibody [(1:1000); R and D systems, UK] overnight at 4^{o}C. After removing the primary antibody complexes, membranes were incubated with HRP-conjugated rabbit anti-goat antibody [(1:2000); Dako, Ely, UK] for 1 hour at RT. Protein complexes were visualised using ECL plus detection reagent on X-ray films. The corresponding bands for chemerin were detected as a 16kDa product.

3.3.3 Identification of Human CMKLR1, CCRL2 and GPR1 mRNA Expression in ECs

HMEC-1, EA.hy926 cell lines and primary HUVEC cells were cultured in 6-well plates in specific cell media containing 10% FCS and were serum starved overnight in respective cell media containing 1% FCS. The cells were lysed, RNA was isolated and reverse transcribed into cDNA. Using specific primers for all three different receptors and other PCR components (Table 3.2.1a), conventional PCR was performed to identify the presence of chemerin receptors in ECs. Human CMKLR1 gene was identified as a 153bp DNA product in HMEC-1, EA.hy926 and HUVEC cells (Fig. 3.3.3a). Both human CCRL2 and GPR1 mRNA expression was also identified in HMEC-1 cell line (Fig. 3.3.3b), EA.hy926 cell line (Fig. 3.3.3c), as well as in primary HUVEC cells (Fig. 3.3.3d). DNA products were separated using 2% agarose gel and were visualised using UV illuminator. All three receptor PCR products were purified and sequenced for sequence authenticity. BLAST search confirmed the gene sequences for all three receptors.

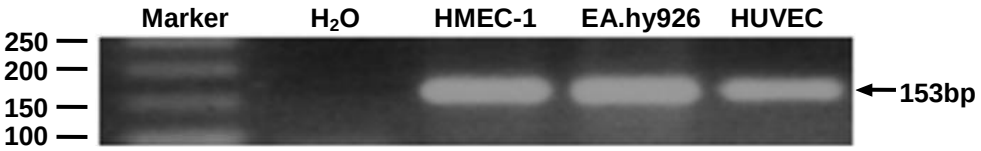

Figure 3.3.3a Human CMKLR1 receptor identification in HMEC-1 and EA.hy926 cell lines and in primary HUVEC cells

HMEC-1, EA.hy926 cell lines and primary HUVEC cells were cultured in specific cell media. Cells were lysed using RNA lysis solution and RNA was isolated and quantified using NanoDrop spectrophotometer (Labtech International, Ringmer, UK). PCR analysis identified human CMKLR1 as a 153bp DNA product in all three different EC types. The PCR products were resolved on 2% agarose gel, purified and sequenced to confirm the authenticity of the products. Three independent experiments were performed and identical results were obtained. GeneRuler^{TM} 50bp DNA ladder was used as a marker.

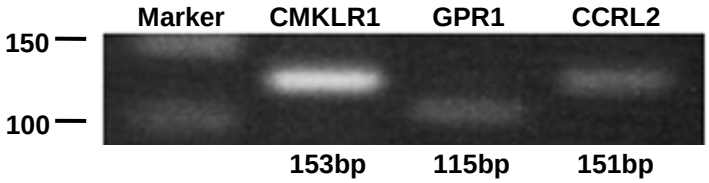

Figure 3.3.3b Human CMKLR1, GPR1 and CCRL2 mRNA expression in HMEC-1 cell line

HMEC-1 cells were cultured in specific cell medium. Cells were lysed using RNA lysis solution and RNA was isolated and quantified using NanoDrop spectrophotometer (Labtech International, Ringmer, UK). Specific primers identified human CMKLR1, GPR1 and CCRL2 as a 153bp, 115bp and 151bp DNA products in HMEC-1 cell line respectively. The PCR products were resolved on 2% agarose gel, purified and sequenced to confirm the authenticity of the products. Three independent experiments were performed and identical results were obtained. GeneRuler^{TM} 50bp DNA ladder was used as a marker.

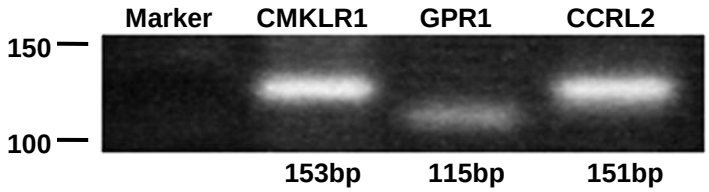

Figure 3.3.3c Human CMKLR1, GPR1 and CCRL2 mRNA expression in EA.hy926 cell line

EA.hy926 cells were cultured in specific cell medium. Cells were lysed using RNA lysis solution and RNA was isolated and quantified using NanoDrop spectrophotometer (Labtech International, Ringmer, UK). Specific primers identified human CMKLR1, GPR1 and CCRL2 as a 153bp, 115bp and 151bp DNA products in EA.hy926 cell line respectively. The PCR products were resolved on 2% agarose gel, purified and sequenced to confirm the authenticity of the products. Three independent experiments were performed and identical results were obtained. GeneRuler^{TM} 50bp DNA ladder was used as a marker.

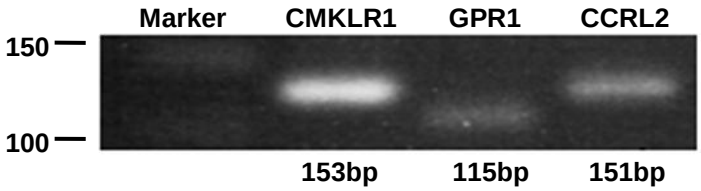

Figure 3.3.3d Human CMKLR1, GPR1 and CCRL2 mRNA expression levels in primary HUVEC cells

Primary HUVEC cells were cultured in specific cell medium. Cells were lysed using RNA lysis solution and RNA was isolated and quantified using NanoDrop spectrophotometer (Labtech International, Ringmer, UK). Specific primers identified human CMKLR1, GPR1 and CCRL2 as a 153bp, 115bp and 151bp DNA products in HUVEC cells respectively. The PCR products were resolved on 2% agarose gel, purified and sequenced to confirm the authenticity of the products. Three independent experiments were performed and identical results were obtained. GeneRuler^{TM} 50bp DNA ladder was used as a marker.

3.3.4 CMKLR1 Receptor Sequence Analysis

DNA was isolated and purified from CMKLR1 PCR products separated by agarose gel electrophoresis. DNA was sequence analysed to confirm the authenticity of the product. The sequence analysis for CMKLR1 receptor using Basic Local Alignment Search Tool (BLAST) confirmed the authenticity of the product (Fig. 3.3.4a).

NM_001142345.1 Homo sapiens chemokine-like receptor 1 (CMKLR1)

Gene ID: 1240 CMKLR1

Score = 171 bits (92), Expect = 4e-42

Identities = 93/94 (99%), Gaps 0/94 (0%)

Strand = Plus/Plus

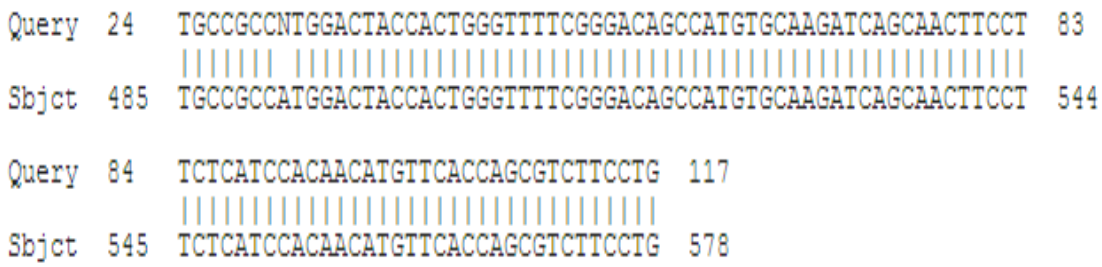

Figure 3.3.4a Part of human CMKLR1 sequence analysis

Subject sequence is obtained from NM_001142345.1 (BLAST Nucleic Acid Database), and the Query sequence is cloned from CMKLR1.

3.3.5 Identification of CMKLR1, GPR1 and CCRL2 Protein Expression in HMEC-1, EA.hy926 Cell Lines and Primary HUVEC Cells

HMEC-1, EA.hy926 cell lines and primary HUVEC cells were cultured in 6-well plates in specific cell media containing 10% FCS and were serum starved overnight in respective cell media containing 1% FCS. Cells were lysed in 1x RIPA buffer and protein lysates were separated using SDS-PAGE. CMKLR1 protein was detected both in HMEC-1 and EA.hy926 cell lines as well as in primary HUVEC cells as a 42kDa product (Fig. 3.3.5a). Both orphan chemerin GPCRs, CCRL2 and GPR1 were identified as 40kDa and 60kDa protein products in HMEC-1 and EA.hy926 cell lines (Fig. 3.3.5b).

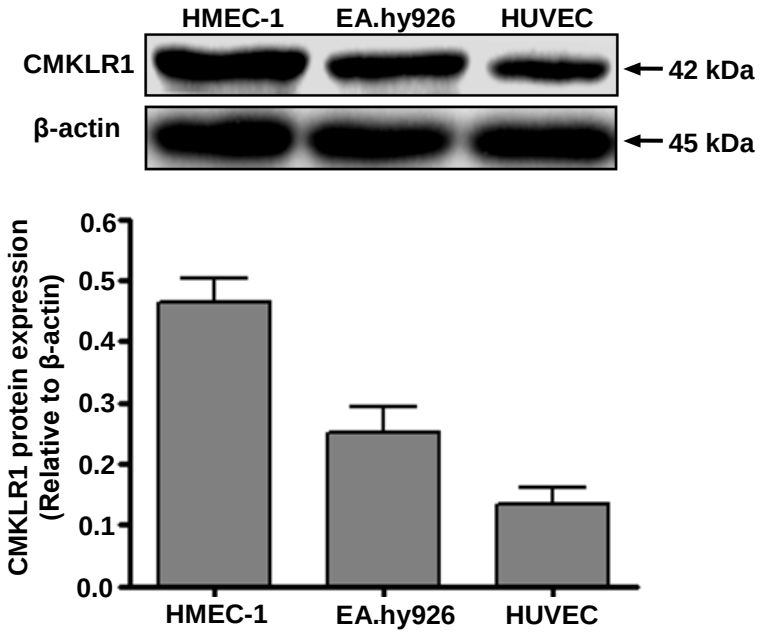

Figure 3.3.5a CMKLR1 protein expression in HMEC-1 and EA.hy926 cell lines and in primary HUVEC cells

Both HMEC-1 and EA.hy926 cell lines, and primary HUVEC cells were cultured in 6-well plates and lysed in a cell lysis solution (1x RIPA). For sample preparations, equal volumes of cell lysates were mixed with 1x Laemmli buffer, and the proteins were separated using 15% polyacrylamide gels and transferred to PVDF membranes at 100V for 1 hour. Membranes were incubated with mouse anti-CMKLR1 antibody [(1:500); Santa Cruz, USA] overnight at 4^{o}C. After removing the primary antibody complexes, membranes were incubated with HRP-conjugated anti-mouse antibody [(1:1500); Sigma, UK] for 1 hour at RT. Protein complexes were visualised using ECL plus detection reagent on X-ray films. Membranes were re-probed with rabbit β-actin antibody [(1:1500); Cell signalling, Beverly, MA, USA] and used as a loading control. The corresponding bands for CMKLR1 and β-actin were detected as 42kDa and 45kDa products. The band intensities were measured using Scion Image™ densitometer (Scion Corporation, Maryland, USA).

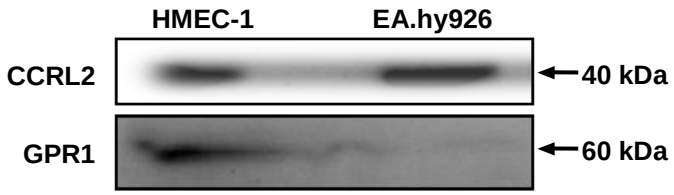

Figure 3.3.5b Chemerin orphan receptors, CCRL2 and GPR1 protein expressions in HMEC-1 and EA.hy926 cell lines

Both HMEC-1 and EA.hy926 cell lines were cultured in 6-well plates and lysed in a cell lysis solution (1x RIPA). For sample preparations, equal volumes of cell lysates were mixed with 1x Laemmli buffer, and the proteins were separated using 12% (CCRL2) and 10% (GPR1) polyacrylamide gels and transferred to PVDF membranes at 100V for 1 hour. Membranes were incubated with rabbit anti-CCRL2 antibody [(1:1000); Abcam, Cambridge, UK] and mouse anti-GPR1 [(1:1000); Santa Cruz, California, USA] overnight at 4^{o}C. After removing the primary antibody complexes, membranes were incubated with HRP-conjugated anti-rabbit antibody [(1:2000); Dako, Ely, UK] and anti-mouse antibody [(1:1500); Sigma, UK] for CCRL2 and GPR1 for 1 hour at RT respectively. Protein complexes were visualised using ECL plus detection reagent on X-ray films. The corresponding bands for CCRL2 and GPR1 were detected as 40kDa and 60kDa products.

3.3.6 Known Inflammatory Mediators; Tumour Necrosis Factor (TNF)-α, Interleukin (IL)-6 and IL-1β Increased CMKLR1 Receptor Protein Expression in HMEC-1 Cell Line

HMEC-1 cells were cultured in 6-well plates in MCDB medium containing 10% FCS and were serum starved overnight in cell medium containing 1% FCS before performing different treatments. HMEC-1 cells were treated with different concentrations of TNF-α [0-20ng/ml], IL-1β [0-100ng/ml] and IL-6 [0-100ng/ml] for 12 and 24 hours. Cells were lysed in 1x RIPA buffer and protein lysates were separated using SDS-PAGE. TNF-α significantly upregulated CMKLR1 receptor protein expression in HMEC-1 cell line in a concentration-dependent manner ($p < 0.001$) both at 12 (Fig. 3.3.6a) and 24 hours (Fig. 3.3.6b). IL-6 upregulated CMKLR1 receptor expression significantly at [100ng/ml] after 12 (Fig. 3.3.6c) and 24 hours of incubation ($p < 0.001$) (Fig. 3.3.6d). IL-1β significantly upregulated CMKLR1 receptor expression in HMEC-1 cells in a concentration-dependent manner at 12 hours ($p < 0.001$) (Fig. 3.3.6e) and 24 hours (Fig. 3.3.6f).

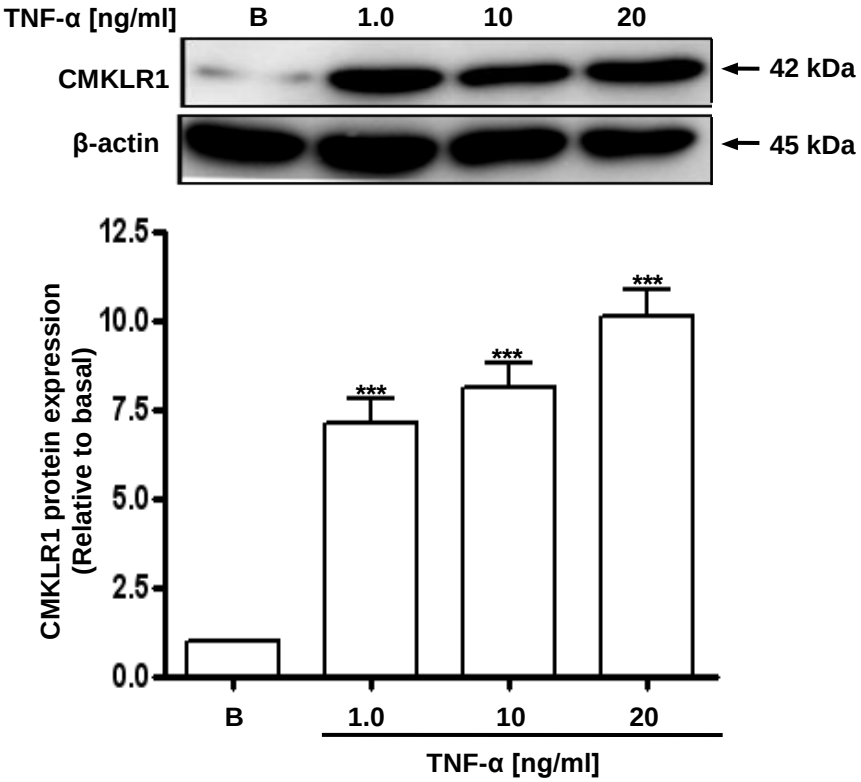

Figure 3.3.6a TNF-α increased CMKLR1 receptor protein expression in HMEC-1 cell line after 12 hours

HMEC-1 cells were treated with different TNF-α concentrations [0-20 ng/ml] for 12 hours. Following cell lysis and sample preparations, protein lysates were separated using 12% polyacrylamide gels and transferred to PVDF membranes at 100V for 1 hour. Membranes were incubated with mouse anti-CMKLR1 antibody [(1:500); Santa Cruz, USA] overnight at 4^{o}C. After removing the primary antibody complexes, membranes were incubated with HRP-conjugated anti-mouse antibody [(1:1500); Sigma, UK] for 1 hour at RT. Protein complexes were visualised using ECL plus detection reagent on X-ray films. Membranes were re-probed with rabbit β-actin antibody [(1:1500); Cell signalling, Beverly, MA, USA] and used as a loading control. The corresponding bands for CMKLR1 and β-actin were detected as 42kDa and 45kDa products. The band intensities were measured using Scion Image™ densitometer (Scion Corporation, Maryland, USA). The data are presented as mean ± SEM of three independent experiments in duplicates ***$p < 0.001$ and **$p < 0.01$ compared to basal.

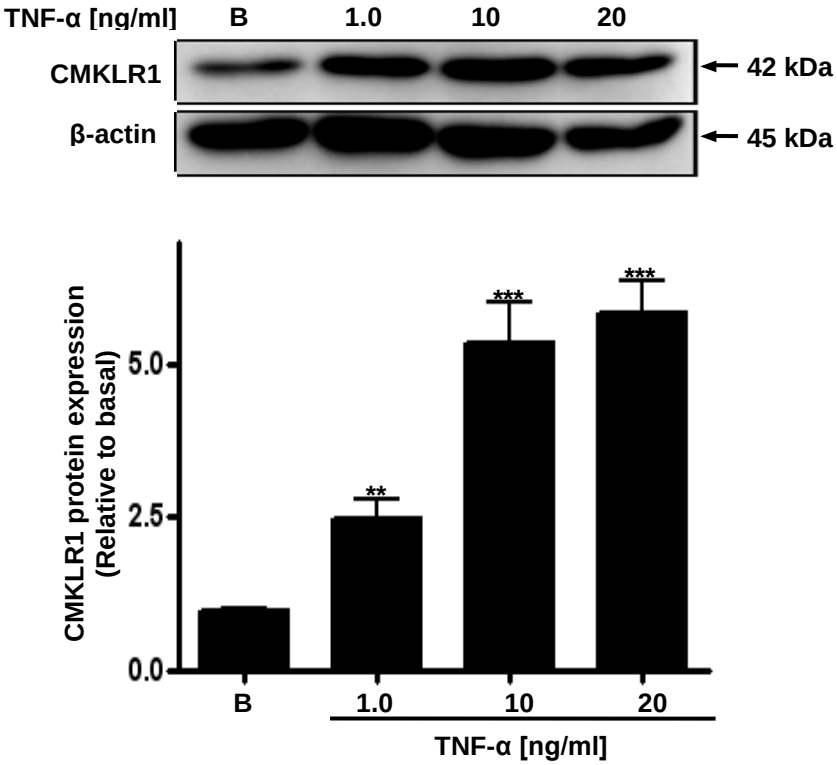

Figure 3.3.6b TNF-α increased CMKLR1 receptor protein expression in HMEC-1 cell line after 24 hours

HMEC-1 cells were treated with different TNF-α concentrations [0-20 ng/ml] for 12 and 24 hours. Following cell lysis and sample preparations, protein lysates were separated using 12% polyacrylamide gels and transferred to PVDF membranes at 100V for 1 hour. Membranes were incubated with mouse anti-CMKLR1 antibody [(1:500); Santa Cruz, USA] overnight at 4^{o}C. After removing the primary antibody complexes, membranes were incubated with HRP-conjugated anti-mouse antibody [(1:1500); Sigma, UK] for 1 hour at RT. Protein complexes were visualised using ECL plus detection reagent on X-ray films. Membranes were re-probed with rabbit β-actin antibody [(1:1500); Cell signalling, Beverly, MA, USA] and used as a loading control. The corresponding bands for CMKLR1 and β-actin were detected as 42kDa and 45kDa products. The band intensities were measured using Scion Image™ densitometer (Scion Corporation, Maryland, USA). The data are presented as mean ± SEM of three independent experiments in duplicates ***$p < 0.001$ and **$p < 0.01$ compared to basal.

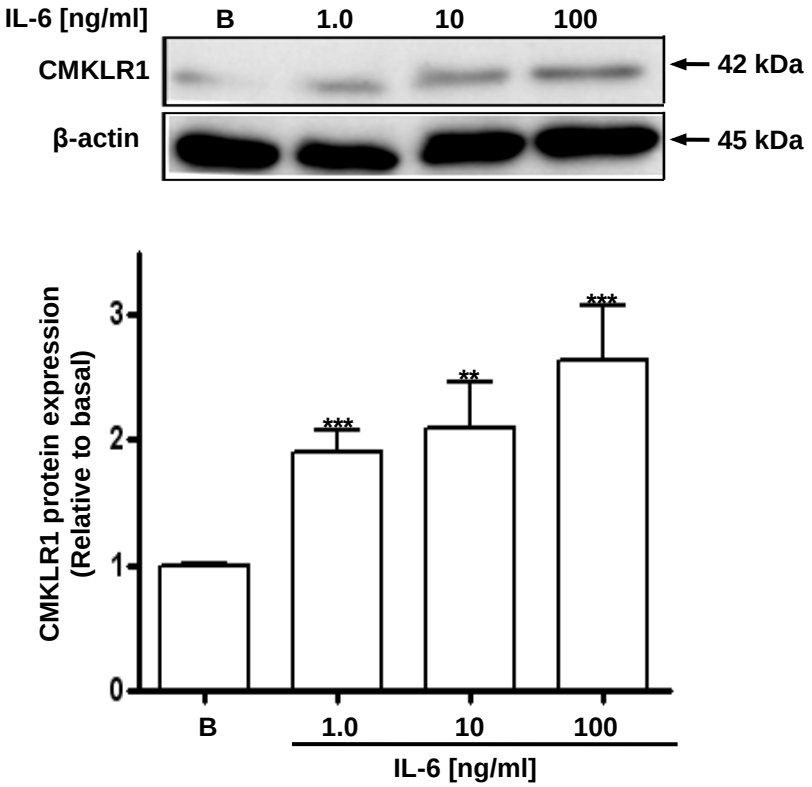

Figure 3.3.6c IL-6 increased CMKLR1 receptor protein expression in HMEC-1 cell line after 12 hours

HMEC-1 cells were treated with different IL-6 concentrations [0-100 ng/ml] for 12 hours. Following cell lysis and sample preparations, protein lysates were separated using 12% polyacrylamide gels and transferred to PVDF membranes at 100V for 1 hour. Membranes were incubated with mouse anti-CMKLR1 antibody [(1:500); Santa Cruz, USA] overnight at 4^{o}C. After removing the primary antibody complexes, membranes were incubated with HRP-conjugated anti-mouse antibody [(1:1500); Sigma, UK] for 1 hour at RT. Protein complexes were visualised using ECL plus detection reagent on X-ray films. Membranes were re-probed with rabbit β-actin antibody [(1:1500); Cell signalling, Beverly, MA, USA] and used as a loading control. The corresponding bands for CMKLR1 and β-actin were detected as 42kDa and 45kDa products. The band intensities were measured using Scion Image™ densitometer (Scion Corporation, Maryland, USA). The data are presented as mean ± SEM of three independent experiments in duplicates ***$p < 0.001$ compared to basal.

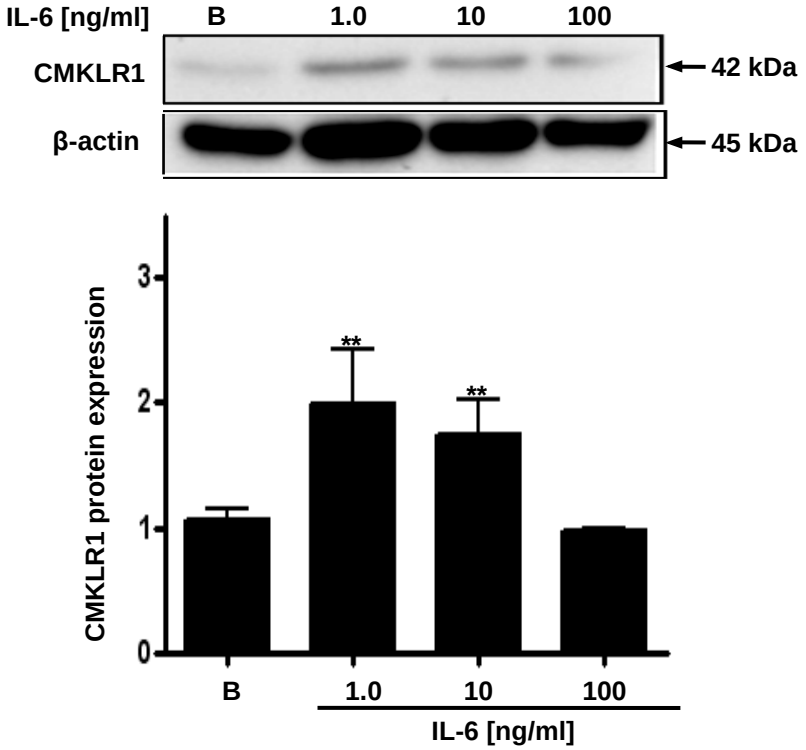

Figure 3.3.6d IL-6 increased CMKLR1 receptor protein expression in HMEC-1 cell line after 24 hours

HMEC-1 cells were treated with different IL-6 concentrations [0-100 ng/ml] for 24 hours. Following cell lysis and sample preparations, protein lysates were separated using 12% polyacrylamide gels and transferred to PVDF membranes at 100V for 1 hour. Membranes were incubated with mouse anti-CMKLR1 antibody [(1:500); Santa Cruz, USA] overnight at 4^{o}C. After removing the primary antibody complexes, membranes were incubated with HRP-conjugated anti-mouse antibody [(1:1500); Sigma, UK] for 1 hour at RT. Protein complexes were visualised using ECL plus detection reagent on X-ray films. Membranes were re-probed with rabbit β-actin antibody [(1:1500); Cell signalling, Beverly, MA, USA] and used as a loading control. The corresponding bands for CMKLR1 and β-actin were detected as 42kDa and 45kDa products. The band intensities were measured using Scion Image™ densitometer (Scion Corporation, Maryland, USA). The data are presented as mean ± SEM of three independent experiments in duplicates ***$p < 0.001$ compared to basal.

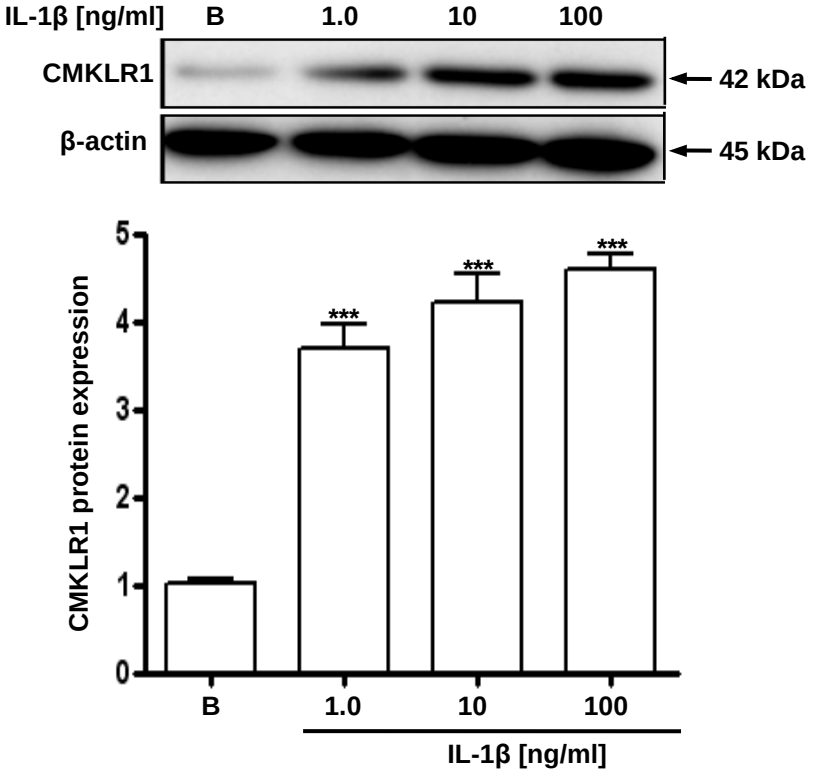

Figure 3.3.6e IL-1β increased CMKLR1 receptor protein expression in HMEC-1 cell line after 12 hours

HMEC-1 cells were treated with different IL-1β concentrations [0-100 ng/ml] for 12 hours. Following cell lysis and sample preparations, protein lysates were separated using 12% polyacrylamide gels and transferred to PVDF membranes at 100V for 1 hour. Membranes were incubated with mouse anti-CMKLR1 antibody [(1:500); Santa Cruz, USA] overnight at 4^{o}C. After removing the primary antibody complexes, membranes were incubated with HRP-conjugated anti-mouse antibody [(1:1500); Sigma, UK] for 1 hour at RT. Protein complexes were visualised using ECL plus detection reagent on X-ray films. Membranes were re-probed with rabbit β-actin antibody [(1:1500); Cell signalling, Beverly, MA, USA] and used as a loading control. The corresponding bands for CMKLR1 and β-actin were detected as 42kDa and 45kDa products. The band intensities were measured using Scion Image™ densitometer (Scion Corporation, Maryland, USA). The data are presented as mean ± SEM of three independent experiments in duplicates ***$p < 0.001$ and **$p < 0.01$ compared to basal.

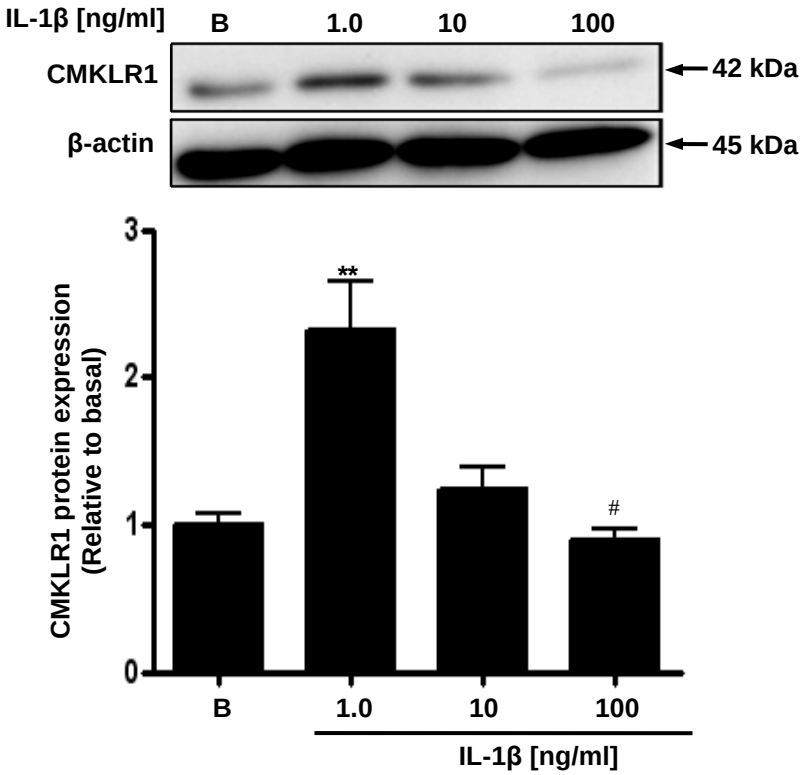

Figure 3.3.6f IL-1β increased CMKLR1 receptor protein expression in HMEC-1 cell line after 24 hours

HMEC-1 cells were treated with different IL-1β concentrations [0-100 ng/ml] for 24 hours. Following cell lysis and sample preparations, protein lysates were separated using 12% polyacrylamide gels and transferred to PVDF membranes at 100V for 1 hour. Membranes were incubated with mouse anti-CMKLR1 antibody [(1:500); Santa Cruz, USA] overnight at 4^{o}C. After removing the primary antibody complexes, membranes were incubated with HRP-conjugated anti-mouse antibody [(1:1500); Sigma, UK] for 1 hour at RT. Protein complexes were visualised using ECL plus detection reagent on X-ray films. Membranes were re-probed with rabbit β-actin antibody [(1:1500); Cell signalling, Beverly, MA, USA] and used as a loading control. The corresponding bands for CMKLR1 and β-actin were detected as 42kDa and 45kDa products. The band intensities were measured using Scion Image™ densitometer (Scion Corporation, Maryland, USA). The data are presented as mean ± SEM of three independent experiments in duplicates ***$p < 0.001$ and **$p < 0.01$ compared to basal.

3.4 Summary of Results

In these preliminary set of experiments, human chemerin gene and protein expression levels were identified in both human microvascular and macrovascular EC lines. All three different chemerin receptors – CMKLR1, CCRL2 and GPR1 receptors were also identified and confirmed in human EC lines both at gene and protein levels. PCR analysis identified chemerin gene as a 252bp product in HMEC-1 cell line (Fig. 3.3.1a). Chemerin proteins levels were detected in both HMEC-1 and EA.hy926 cell lines as a 16kDa product (Fig. 3.3.2a).

PCR analysis identified CMKLR1 gene in all three different types of ECs as a 153bp product (Fig. 3.3.3a), and the product authenticity was confirmed using BLAST search (Fig. 3.3.4a). In addition to CMKLR1, two other chemerin orphan GPCRs, CCRL2 and GPR1 gene levels were also identified and confirmed in HMEC-1 (Fig. 3.3.3b), EA.hy926 (Fig. 3.3.3c) cell lines and in primary HUVEC cells (Fig. 3.3.3d). Western blotting confirmed the protein expression levels of both CCRL2 and GPR1 receptors in both microvascular and macrovascular ECs (Fig. 3.3.5b). Throughout the rest of this project, only HMEC-1 cell line was used to perform different experiments, unless otherwise stated. Microvascular ECs line most of the vascularised organs in the human body alongwith macrovascular ECs. Both these cell types possess different functional, morphogenetic, and functional characteristics (Dye et al., 2004), and are known to secrete varied range of vasoactive substances. Different cell types are also known to respond differently to a variety of external stimuli, which are likely to affect the activities and functionality of different proteins in the cell, alter the transcriptional regulation of various different transcription factors, hence regulating the expression of different genes, and finally altering the overall biological responses.

4.1 Introduction

The specific aims of this part of the project were to explore the role (s) of chemerin (21-157) in; (1) the phosphorylation of important signalling kinases including Extracellular Kinases (ERK) 1/2 Mitogen-activated Protein Kinases (MAPK), ERK5 MAPK, p38 MAPK and Akt/PKB kinases, (2) the protein expression of Vascular Endothelial Growth Factor 165 (VEGF165), a potent angiogenic molecule; and of VEGF165b, an anti-angiogenic VEGF isoform, (3) the transcriptional regulation of Hypoxia Inducible Factor (HIF)-1α, a transcription factor that regulates VEGF165 protein expression and secretion, (4) the phosphorylation of Vascular Endothelial Growth Factor Receptor (VEGFR) 2, the main signalling receptor for VEGF-mediated angiogenesis, (5) the activity of extracellular matrix degrading enzymes such as Matrix Metalloproteinase (MMP)-2 and -9, and finally (6) inducing biological responses such as EC proliferation, migration and capillary tube formation in HMEC-1 cell line.

Angiogenesis is the process of formation of new capillaries from pre-existing blood vessels, and is necessary during wound healing and tissue regeneration. In normo-physiological states, angiogenesis is a tightly-controlled process regulated by a fine balance between pro- and anti-angiogenic factors (Rangasamy et al., 2011, Klagsbrun and D'Amore, 1991). ERK1/2, ERK5 and p38 MAPK are important MAPKs which are activated by a number of different stimuli (Fig. 1.5.1a, page number 34). Various different cytokines and adipokine are known to activate these MAPKs and are implicated in various different cellular responses; for example ERK1/2 and ERK5 MAPK are important in cell proliferation (Zhang and Liu, 2002), whereas, p38 and SAPK/JNK MAPKs are known to mediate cell apoptosis (Xia et al., 1995, Henkart, 1996).

Akt/PKB kinase is an important kinase implicated in EC survival via VEGF/Akt/PI3K pathway and is known to regulate the expression of VEGF165, the most potent isoform of VEGF; which is specifically expressed in the endothelium and is implicated in EC angiogenesis, vasodilation and microvascular permeability (Semenza et al., 2011, Senger et al., 1983, Dvorak et al., 1995a). VEGF gene undergoes alternative splicing and results in the formation of anti-angiogenic isoforms of VEGF, which are collectively grouped in VEGFxxxb family – xxx representing the number of amino acids (Appendix 5, Fig. 5.1a, page number 248). VEGF165b is the most abundant anti-angiogenic, and opposite counterpart of VEGF165 which is reported to exert anti-angiogenic functions (Craine et al., 1995). Different VEGF isoforms bind and signal via two different Receptor Tyrosine Kinases (RTKs), VEGFR1 and VEGFR2. Upon ligand stimulation, both receptors dime rise and undergo trans-autophosphorylation, however, VEGFR2 is the main functional receptor for VEGF-dependent angiogenesis and vascular permeability (Okamoto et al., 1997). Under hypoxic conditions, Hypoxia Inducible Factor (HIF)-1, a heterodimer transcription factor composed of an α and a β subunit, regulates the expression and secretion of VEGF protein (Shimaoka et al., 2001). VEGF induces the expression of matrix degrading enzymes such as MMP-2 and -9, which further promote EC proliferation, migration and capillary tube formation (Hagemann et al., 2004).

4.2 Materials and Methods Used

The cellular protein expression and phosphorylation were determined using SDS-PAGE (Chapter 2, section 2.3.7, page numbers 57-60) using different percentage polyacrylamide gels for separating different proteins (Table 4.2.1a). The gelatinolytic activity of secreted MMP-2 and -9 in EC culture supernatants was studied using gelatin zymography (Chapter 2, section 2.3.9, page numbers 61). Endothelial cell proliferation was determined using CellTiter® 96 AQueous One Solution cell proliferation assay (MTS) (Chapter 2, section 2.4.2, page number 63). EC migration was studied by using both Wound-healing Cell Motility Assay (Chapter 2, section 2.4.3, page numbers 63-4), and also by using i*n vitro* Cell Invasion Assay (Chapter 2, section 2.4.4, page numbers 64-5). Chemerin (21-157) and EC capillary tube formation was studied using Growth Factor Reduced Matrigel (Chapter 2, section 2.4.5, page number 65-6). EC death was studied using Cellular DNA Fragmentation ELISA kit (Chapter 2, section 2.4.6, page numbers 66).

Table 4.2.1a

The molecular weights of different proteins and gel percentages used for SDS-PAGE analysis

Protein	Molecular weight (kDa)	Percentage gels used
Akt/PKB Kinase	60	10
ERK1/2 MAPK	44/42	12
ERK5 MAPK	110	8
HIF-1α	93	10
MMP-2 and -9	68 and 88	10
p38 MPAK	38	12
VEGFR2	230	6
VEGF165	45	12
VEGF165b	22	15

4.3 Data Presentation and Analyses

4.3.1 Chemerin (21-157) Lead to ERK1/2 MAPK Phosphorylation in a Time- and Concentration-dependent manner in HMEC-1 Cell Line

HMEC-1 cells were cultured in 6-well plates in MCDB cell medium containing 10% FCS, and were serum starved in the same medium containing 1% FCS overnight before performing different treatments. To study time-dependent ERK1/2 MAPK phosphorylation, HMEC-1 cells were treated with [0.1nM] chemerin (21-157) at different time-points for a maximum of 30 minutes. For concentration-dependent ERK1/2 MAPK phosphorylation, HMEC-1 cells were treated with different chemerin (21-157) [0-30nM] concentrations for 5 minute. Cells were lysed in 1x RIPA buffer and protein lysates were separated using SDS-PAGE. Chemerin (21-157) increased ERK1/2 (Thr202/Tyr204) MAPK phosphorylation in a time-dependent manner with a significant increase at 5 minutes ($p < 0.001$) compared to basal and decreasing at 30 minutes (Fig. 4.3.1a). Chemerin (21-157) at [0.1nM] significantly increased phosphorylation of ERK1/2 (Thr202/Tyr204) MAPK ($p < 0.001$), and decreasing at 1, 10 and 30nM concentrations compared to basal (Fig. 4.3.1b).

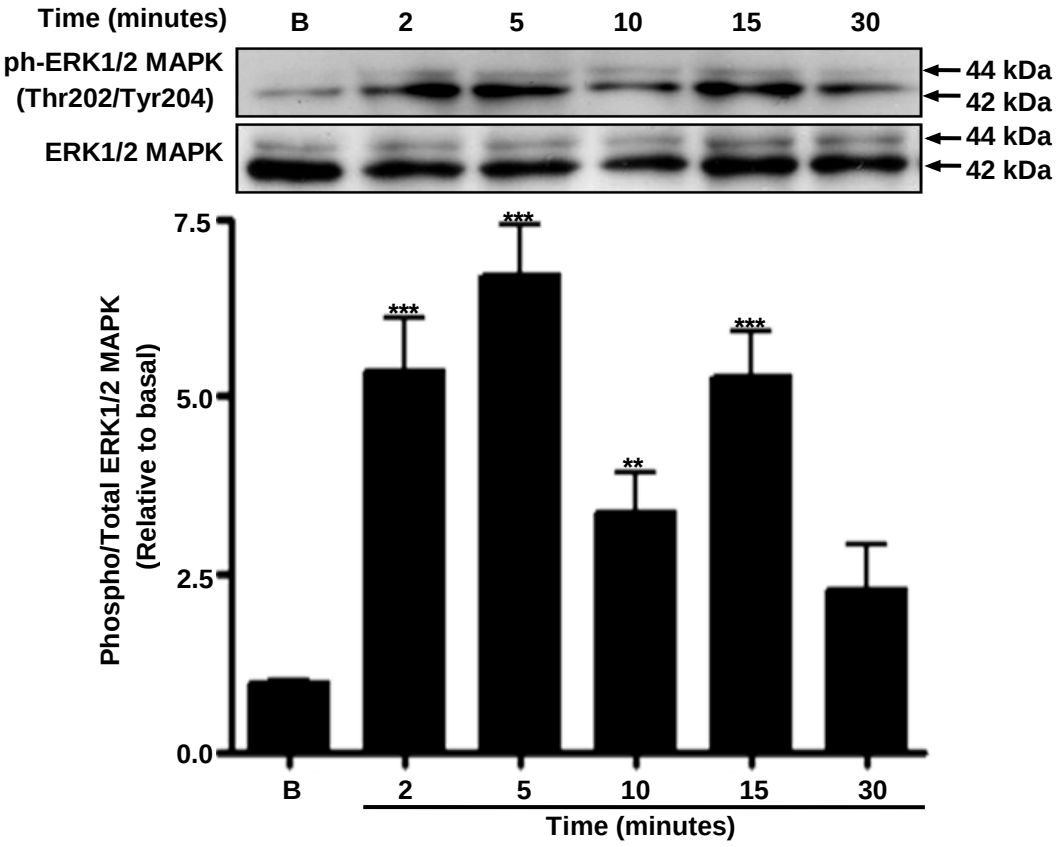

Figure 4.3.1a Chemerin (21-157) lead to ERK1/2 MAPK phosphorylation in a time-dependent manner in HMEC-1 cell line

HMEC-1 cells were treated with [0.1nM] chemerin (21-157) for 0-30 minutes. Following cell lysis and sample preparations, the proteins were separated using 12% polyacrylamide gels, and transferred to PVDF membranes at 100V for 1 hour. Membranes were incubated with specific phospho-ERK1/2 (Thr202/Tyr204) antibody [(1:1500); Cell signalling, Beverly, MA, USA] overnight at 4^{o}C. After removing the primary antibody complexes, membranes were incubated with anti-rabbit IgG-HRP labelled antibody [(1:2000); Dako, Ely, UK] for 1 hour at RT. Protein complexes were visualised using ECL plus detection reagent on X-ray films. Membranes were re-probed with total ERK1/2 MAPK antibody [(1:1500); Cell signalling, Beverly, MA, USA] and used as a loading control. The corresponding bands for both phospho-ERK1/2 and total ERK1/2 MAPK were detected as 44/42kDa products. The band intensities were measured using Scion Image™ densitometer (Scion Corporation, Maryland, USA). The data are presented as mean ± SEM of three independent experiments in duplicates ***$p < 0.001$ and **$p < 0.01$ compared to basal.

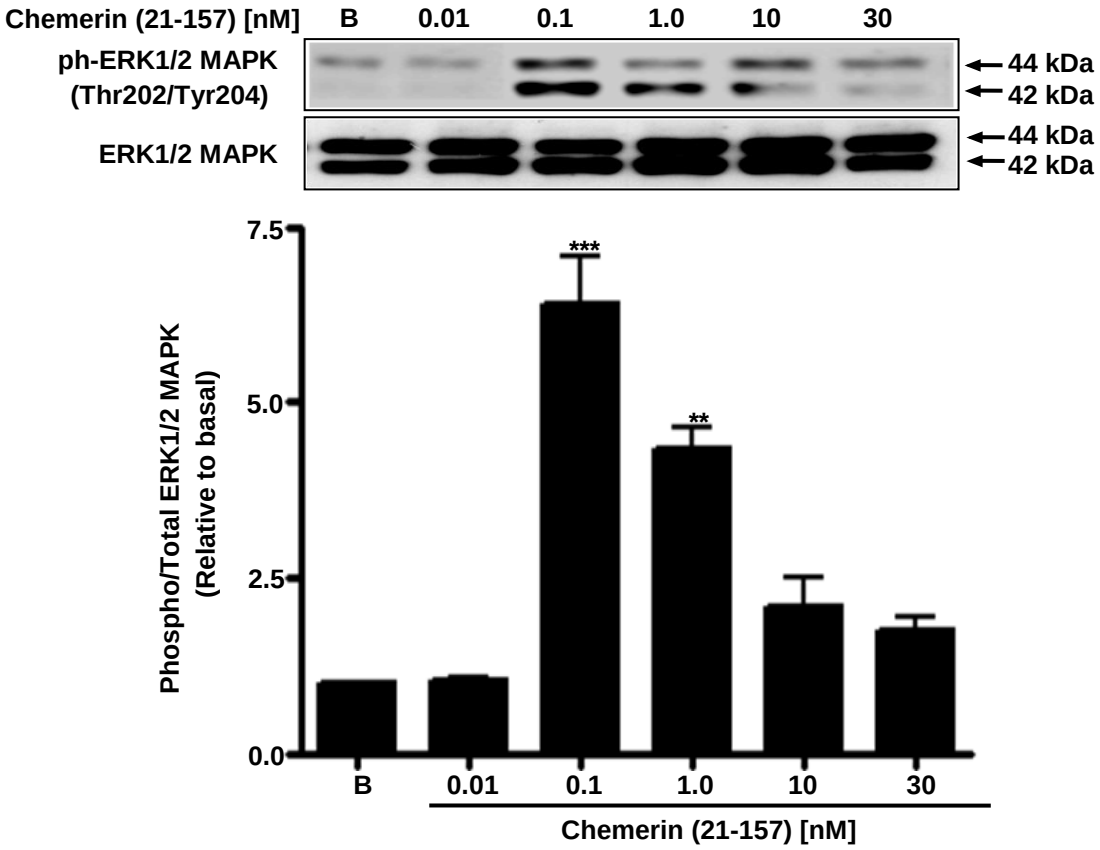

Figure 4.3.1b Chemerin (21-157) lead to ERK1/2 MAPK phosphorylation in a concentration-dependent manner in HMEC-1 cell line

HMEC-1 cells were treated with different chemerin (21-157) concentrations [0-30nM] for 5 minutes. Following cell lysis and sample preparations, the proteins were separated using 12% polyacrylamide gels, and transferred to PVDF membranes at 100V for 1 hour. Membranes were incubated with specific phospho-ERK1/2 (Thr202/Tyr204) antibody [(1:1500); Cell signalling, Beverly, MA, USA] overnight at 4^{o}C. After removing the primary antibody complexes, membranes were incubated with anti-rabbit IgG-HRP labelled antibody [(1:2000); Dako, Ely, UK] for 1 hour at RT. Protein complexes were visualised using ECL plus detection reagent on X-ray films. Membranes were re-probed with total ERK1/2 antibody [(1:1500); Cell signalling, Beverly, MA, USA] and used as a loading control. The corresponding bands for both phospho-ERK1/2 and total ERK1/2 MAPK were detected as 44/42kDa products. The band intensities were measured using Scion Image™ densitometer (Scion Corporation, Maryland, USA). The data are presented as mean ± SEM of three independent experiments in duplicates ***$p < 0.001$ and **$p < 0.01$ compared to basal.

4.3.2 Chemerin (21-157) Lead to ERK5 MAPK Phosphorylation in a Time- and Concentration-dependent Manner in HMEC-1 Cell Line

HMEC-1 cells were cultured in 6-well plates in MCDB cell medium containing 10% FCS, and were serum starved in the same medium containing 1% FCS overnight before performing different treatments. To study time-dependent ERK5 MAPK phosphorylation, HMEC-1 cells were treated with [10nM] chemerin (21-157) at different time-points for a maximum of 30 minutes. For concentration-dependent ERK5 MAPK phosphorylation, HMEC-1 cells were treated with different chemerin (21-157) [0-10nM] concentrations for 15 minute. Cells were lysed in 1x RIPA buffer and protein lysates were separated using SDS-PAGE. Chemerin (21-157) increased ERK5 (Thr218/Tyr220) MAPK phosphorylation both in a time-dependent manner with significant increase at 15 minutes ($p < 0.01$) (Fig. 4.3.2a), and also in a concentration-dependent manner significantly at [0.01-10nM] chemerin (21-157) concentrations compared to basal (Fig. 4.3.2b).

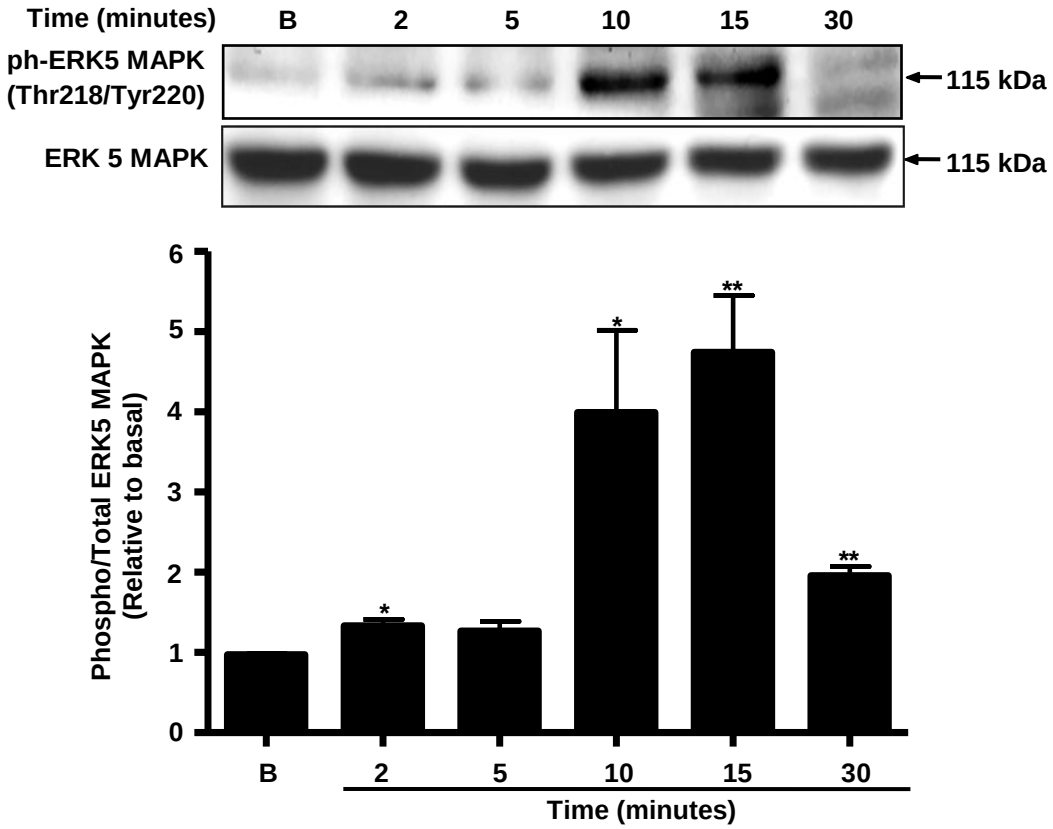

Figure 4.3.2a Chemerin (21-157) lead to ERK5 MAPK in a time-dependent manner in HMEC-1 cell line

HMEC-1 cells were treated with [10nM] chemerin (21-157) for 0-30 minutes. Following cell lysis and sample preparations, the proteins were separated using 8% polyacrylamide gels, and transferred to PVDF membranes at 100V for 1 hour. Membranes were incubated with specific phospho-ERK5 (Thr218/Tyr220) MAPK antibody [(1:1500); Cell signalling, Beverly, MA, USA] overnight at 4^{o}C. After removing the primary antibody complexes, membranes were incubated with anti-rabbit IgG-HRP labelled antibody [(1:2000); Dako, Ely, UK] for 1 hour at RT. Protein complexes were visualised using ECL plus detection reagent on X-ray films. Membranes were re-probed with ERK5 MAPK antibody [(1:1500); Cell signalling, Beverly, MA, USA] and used as a loading control. The corresponding bands for both phospho-ERK5 and total ERK5 MAPK were detected as 115kDa products. The band intensities were measured using Scion Image™ densitometer (Scion Corporation, Maryland, USA). The data are presented as mean ± SEM of three independent experiments in duplicates $^{**}p < 0.01$ and $^{*}p < 0.05$ compared to basal.

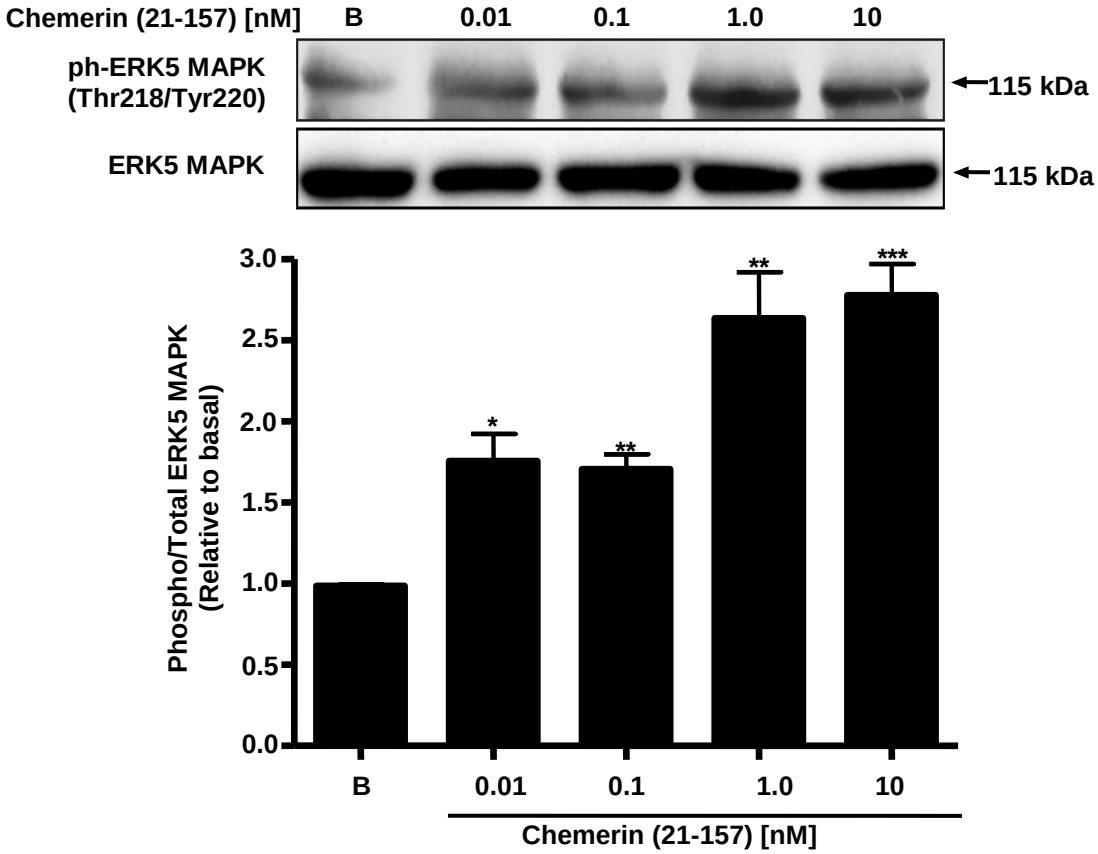

Figure 4.3.2b Chemerin (21-157) lead to ERK5 MAPK phosphorylation in a concentration-dependent manner in HMEC-1 cell line

HMEC-1 cells were treated with different chemerin (21-157) concentrations [0-10nM] for 15 minutes. Following cell lysis and sample preparations, the proteins were separated using 8% polyacrylamide gels, and transferred to PVDF membranes at 100V for 1 hour. Membranes were incubated with specific phospho-ERK5 (Thr218/Tyr220) MAPK antibody [(1:1500); Cell signalling, Beverly, MA, USA] overnight at 4^{o}C. After removing the primary antibody complexes, membranes were incubated with anti-rabbit IgG-HRP labelled antibody [(1:2000); Dako, Ely, UK] for 1 hour at RT. Protein complexes were visualised using ECL plus detection reagent on X-ray films. Membranes were re-probed with ERK5 MAPK antibody [(1:1500); Cell signalling, Beverly, MA, USA] and used as a loading control. The corresponding bands for both phospho-ERK5 and total ERK5 MAPK were detected as 115kDa products. The band intensities were measured using Scion Image™ densitometer (Scion Corporation, Maryland, USA). The data are presented as mean ± SEM of three independent experiments in duplicates ***$p < 0.001$, **$p < 0.01$ and *$p < 0.05$ compared to basal.

4.3.3 Chemerin (21-157) Lead to p38 MAPK Phosphorylation in a Time- and Concentration-dependent Manner in HMEC-1 Cell Line

HMEC-1 cells were cultured in 6-well plates in MCDB cell medium containing 10% FCS, and were serum starved in the same medium containing 1% FCS overnight before performing different treatments. To study time-dependent p38 MAPK phosphorylation, HMEC-1 cells were treated with [0.1nM] chemerin (21-157) at different time-points for a maximum of 30 minutes. For concentration-dependent p38 MAPK phosphorylation, HMEC-1 cells were treated with different chemerin (21-157) [0-30nM] concentrations for 15 minute. Cells were lysed in 1x RIPA buffer and protein lysates were separated using SDS-PAGE. Chemerin (21-157) increased p38 (Thr180/Tyr182) MAPK phosphorylation in a time-dependent manner with a significant increase at 10 and 15 minutes ($p < 0.001$) and decreasing at 30 minutes compared to basal (Fig. 4.3.3a). Chemerin (21-157) significantly increased p38 (Thr180/Tyr182) MAPK phosphorylation at lower concentrations ($p < 0.001$) which then decreased at 10 and 30nM chemerin (21-157) concentrations compared to basal (Fig. 4.3.3b).

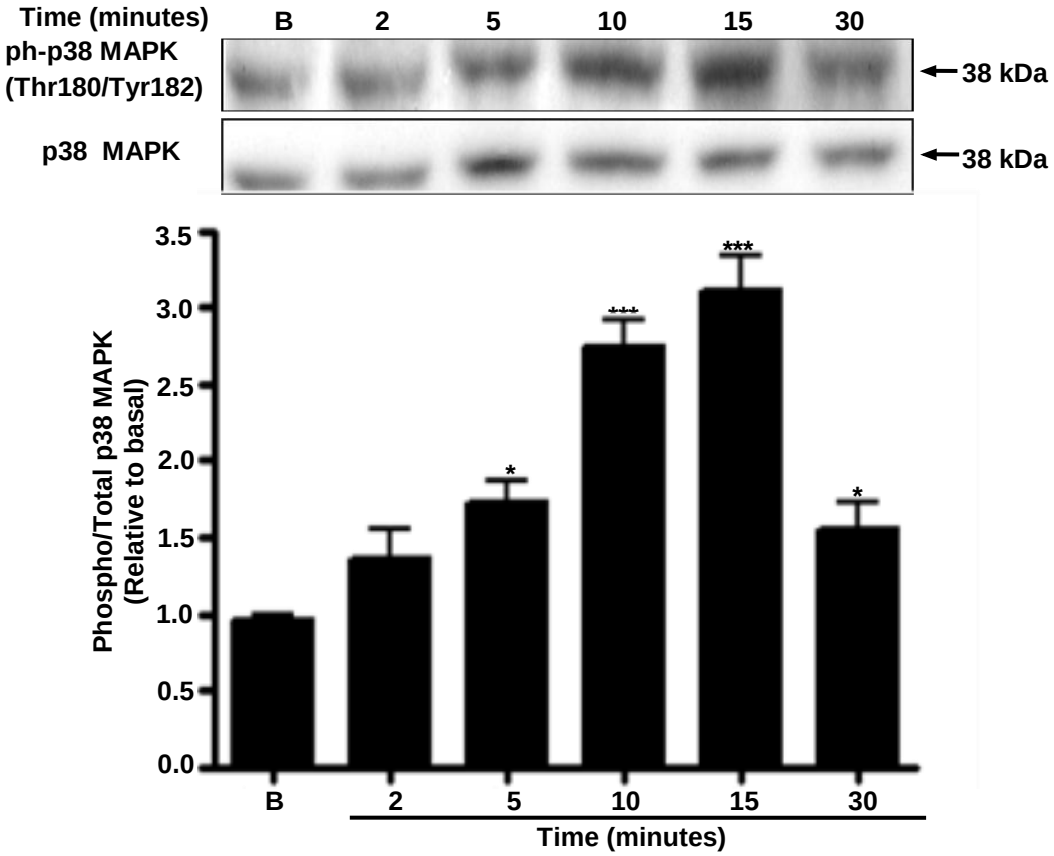

Figure 4.3.3a Chemerin (21-157) lead to p38 MAPK phosphorylation in a time-dependent manner in HMEC-1 cell line

HMEC-1 cells were treated with [0.1nM] chemerin (21-157) for 0-30 minutes. Following cell lysis and sample preparations, the proteins lysates were separated using 12% polyacrylamide gels, and transferred to PVDF membranes at 100V for 1 hour. Membranes were incubated with specific phospho-p38 (Thr180/Tyr182) MAPK antibody [(1:1500); Cell signalling, Beverly, MA, USA] overnight at 4^{o}C. After removing the primary antibody complexes, membranes were incubated with anti-rabbit IgG-HRP labelled antibody [(1:2000); Dako, Ely, UK] for 1 hour at RT. Protein complexes were visualised using ECL plus detection reagent on X-ray films. Membranes were re-probed with total p38 MAPK [(1:1500); Cell signalling, Beverly, MA, USA] and used as a loading control. The corresponding bands for both phospho-p38 (Thr180/Tyr182) and total p38 MAPK were detected as 38kDa products. The band intensities were measured using Scion Image™ densitometer (Scion Corporation, Maryland, USA). The data are presented as mean ± SEM of three independent experiments in duplicates ***$p < 0.001$ and *$p < 0.05$ compared to basal.

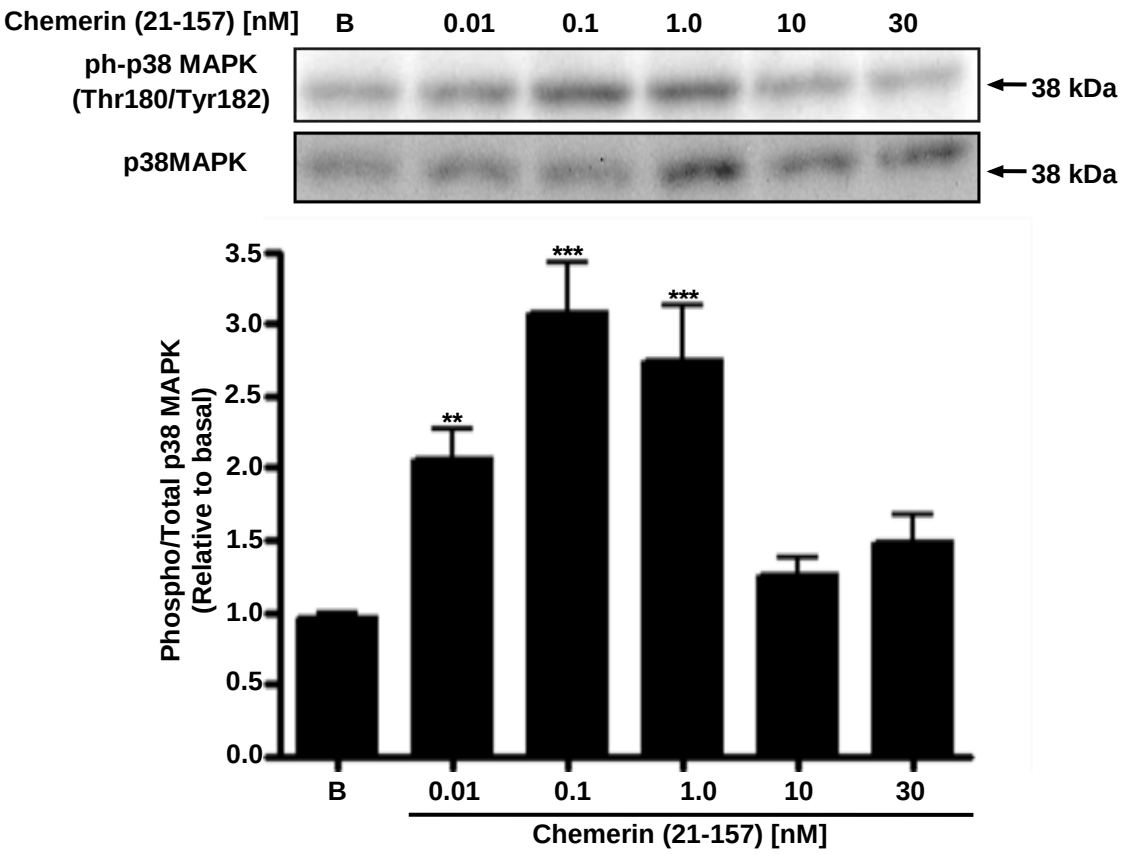

Figure 4.3.3b Chemerin (21-157) lead to p38 MAPK phosphorylation in a concentration-dependent manner in HMEC-1 cell line

HMEC-1 cells were treated with chemerin (21-157) [0-30nM] for 10 minutes. Following cell lysis and sample preparations, the proteins lysates were separated using 12% polyacrylamide gels, and transferred to PVDF membranes at 100V for 1 hour. Membranes were incubated with specific phospho-p38 (Thr180/Tyr182) MAPK antibody [(1:1500); Cell signalling, Beverly, MA, USA] overnight at 4^{o}C. After removing the primary antibody complexes, membranes were incubated with anti-rabbit IgG-HRP labelled antibody [(1:2000); Dako, Ely, UK] for 1 hour at RT. Protein complexes were visualised using ECL plus detection reagent on X-ray films. Membranes were re-probed with total p38 MAPK [(1:1500); Cell signalling, Beverly, MA, USA] and used as a loading control. The corresponding bands for both phospho-p38 (Thr180/Tyr182) and total p38 MAPK were detected as 38kDa products. The band intensities were measured using Scion Image™ densitometer (Scion Corporation, Maryland, USA). The data are presented as mean ± SEM of three independent experiments in duplicates ***$p < 0.001$ and **$p < 0.01$ compared to basal.

4.3.4 Chemerin (21-157) Lead to Akt/PKB Kinase Phosphorylation in a Time- and Concentration-dependent Manner in HMEC-1 Cell Line

HMEC-1 cells were cultured in 6-well plates in MCDB cell medium containing 10% FCS, and were serum starved in the same medium containing 1% FCS overnight before performing different treatments. To study time-dependent Akt phosphorylation, HMEC-1 cells were treated with [10nM] chemerin (21-157) at different time-points for a maximum of 30 minutes. For concentration-dependent Akt phosphorylation, HMEC-1 cells were treated with different chemerin (21-157) concentrations [0-30nM] for 5 minute. Cells were lysed in 1x RIPA buffer and protein lysates were separated using SDS-PAGE. Chemerin (21-157) increased Akt (Ser473) phosphorylation in a time-dependent manner with a significant increase at 5 minutes ($p < 0.001$) compared to basal (Fig. 4.3.4a). Chemerin (21-157) significantly increased Akt (Ser473) phosphorylation at lower concentrations ($p < 0.001$ and $p < 0.01$), decreasing at [30nM] compared to basal (Fig. 4.3.4b).

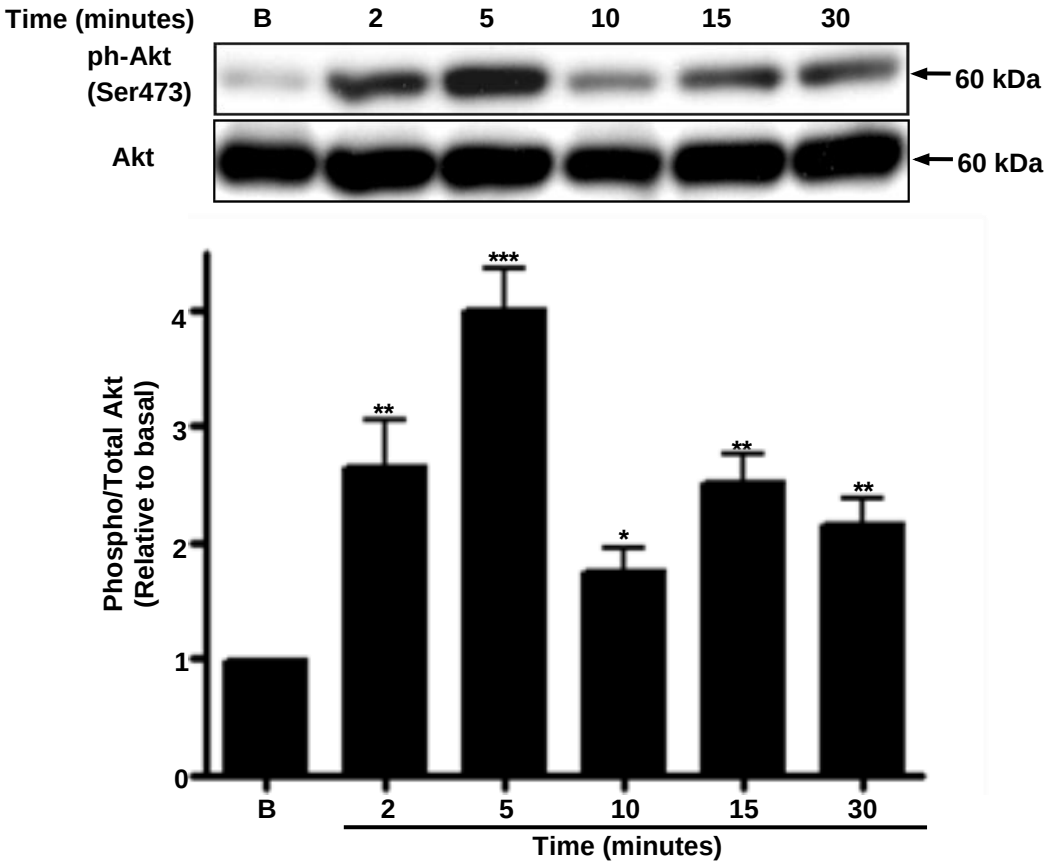

Figure 4.3.4a Chemerin (21-157) lead to Akt/PKB kinase phosphorylation in a time-dependent manner in HMEC-1 cell line

HMEC-1 cells were treated with chemerin [10nM] (21-157) for 0-30 minutes. Following cell lysis and sample preparations, the proteins lysates were separated using 10% polyacrylamide gels, and transferred to PVDF membranes at 100V for 1 hour. Membranes were incubated with specific phospho-Akt (Ser473) antibody [(1:1500); Cell signalling, Beverly, MA, USA] overnight at 4^{o}C. After removing the primary antibody complexes, membranes were incubated with anti-rabbit IgG-HRP labelled antibody [(1:2000); Dako, Ely, UK] for 1 hour at RT. Protein complexes were visualised using ECL plus detection reagent on X-ray films. Membranes were re-probed with total Akt [(1:1500); Cell signalling, Beverly, MA, USA] and used as a loading control. The corresponding bands for both phospho-Akt and total Akt were detected as 60kDa products. The band intensities were measured using Scion Image™ densitometer (Scion Corporation, Maryland, USA). The data are presented as mean ± SEM of three independent experiments in duplicates ***$p < 0.001$, **$p < 0.01$ and *$p < 0.05$ compared to basal.

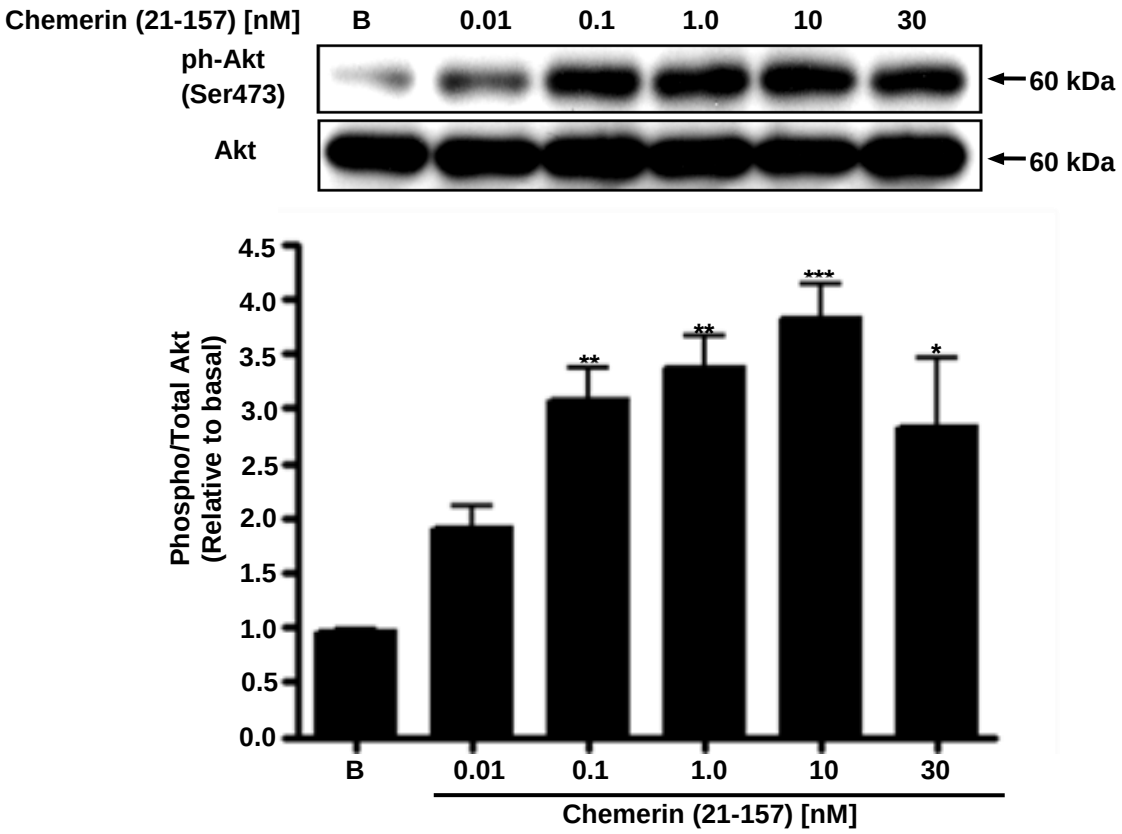

Figure 4.3.4b Chemerin (21-157) lead to Akt/PKB kinase phosphorylation in a concentration-dependent manner in HMEC-1 cell line

HMEC-1 cells were treated with different chemerin (21-157) concentrations [0-30nM] for 10 minutes. Following cell lysis and sample preparations, the proteins were separated using 10% polyacrylamide gels, and transferred to PVDF membranes at 100V for 1 hour. Membranes were incubated with specific phospho-Akt (Ser473) antibody [(1:1500); Cell signalling, Beverly, MA, USA] overnight at 4^{o}C. After removing the primary antibody complexes, membranes were incubated with anti-rabbit IgG-HRP labelled antibody [(1:2000); Dako, Ely, UK] for 1 hour at RT. Protein complexes were visualised using ECL plus detection reagent on X-ray films. Membranes were re-probed with total Akt [(1:1500); Cell signalling, Beverly, MA, USA] and used as a loading control. The corresponding bands for both phospho-Akt and total Akt protein were detected as 60kDa products. The band intensities were measured using Scion Image™ densitometer (Scion Corporation, Maryland, USA). The data are presented as mean ± SEM of three independent experiments in duplicates ***$p < 0.001$, **$p < 0.01$ and *$p < 0.05$ compared to basal.

4.3.5 Chemerin (21-157) Decreased VEGF165 Protein Expressions in HMEC-1 Cell Line

HMEC-1 cells were cultured in 6-well plates in MCDB cell medium containing 10% FCS, and were serum starved in the same medium containing 1% FCS overnight before performing different treatments. HMEC-1 cells were treated with different chemerin (21-157) [0-30nM] concentrations for 12 and 24 hours. Cells were lysed in 1x RIPA buffer and protein lysates were separated using SDS-PAGE. After 12 hours, chemerin (21-157) decreased VEGF165 protein expression levels in HMEC-1 cells in a concentration-dependent manner with the most significant decrease at [30nM] ($p < 0.001$) (Fig. 4.3.5a). Also, at 24 hours, chemerin (21-157) decreased VEGF165 protein expression levels in a concentration-dependent manner compared to basal (Fig. 4.3.5b).

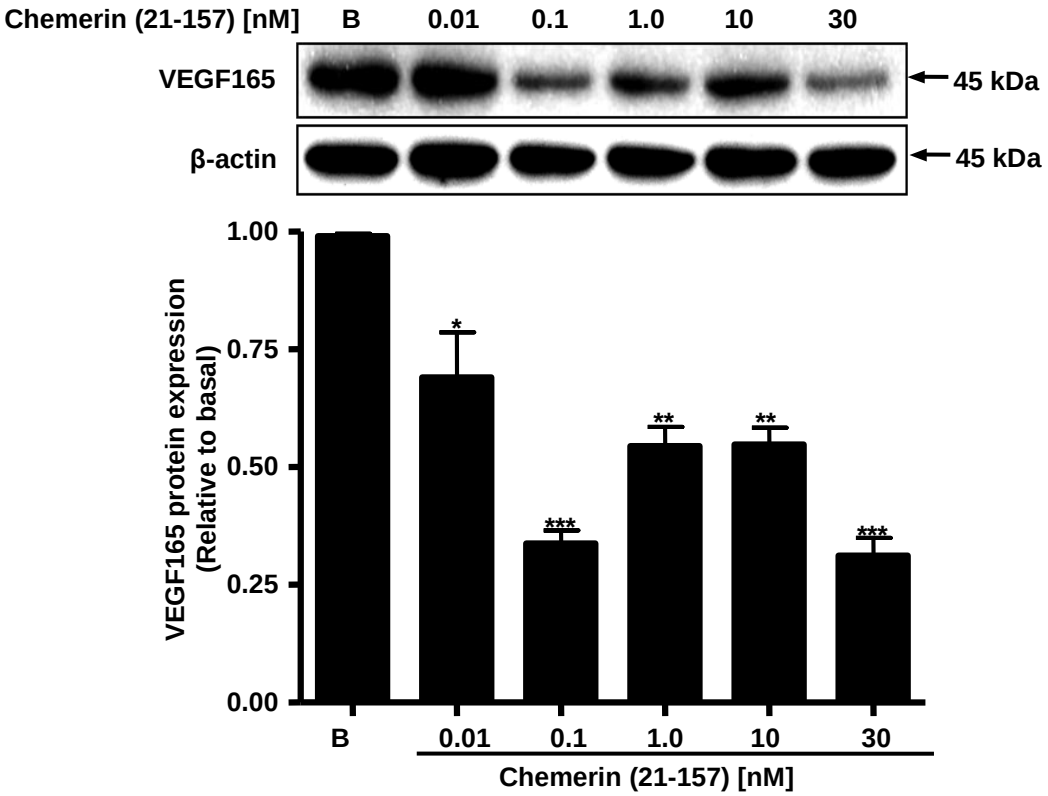

Figure 4.3.5a Chemerin (21-157) decreased VEGF165 protein expression in HMEC-1 cell line after 12 hours

HMEC-1 cells were treated with different chemerin (21-157) concentrations [0-30nM] for 12 hours. Following cell lysis and sample preparations, the proteins were separated using 12% polyacrylamide gels, and transferred to PVDF membranes at 100V for 1 hour. Membranes were incubated with specific mouse anti-VEGF165 antibody [(1:1000); Santa Cruz, USA] overnight at 4^{o}C. After removing the primary antibody complexes, membranes were incubated with anti-mouse IgG-HRP labelled antibody [(1:8000); Sigma-Aldrich, UK] for 1 hour at RT. Protein complexes were visualised using ECL plus detection reagent on X-ray films. Membranes were re-probed with rabbit β-actin antibody [(1:1500); Cell signalling, Beverly, MA, USA] and used as a loading control. The corresponding bands for both VEGF165 and β-actin were detected as 45kDa products. The band intensities were measured using Scion Image™ densitometer (Scion Corporation, Maryland, USA). The data are presented as mean ± SEM of three independent experiments in duplicates ***p < 0.001, **p < 0.01 and *p < 0.05 compared to basal.

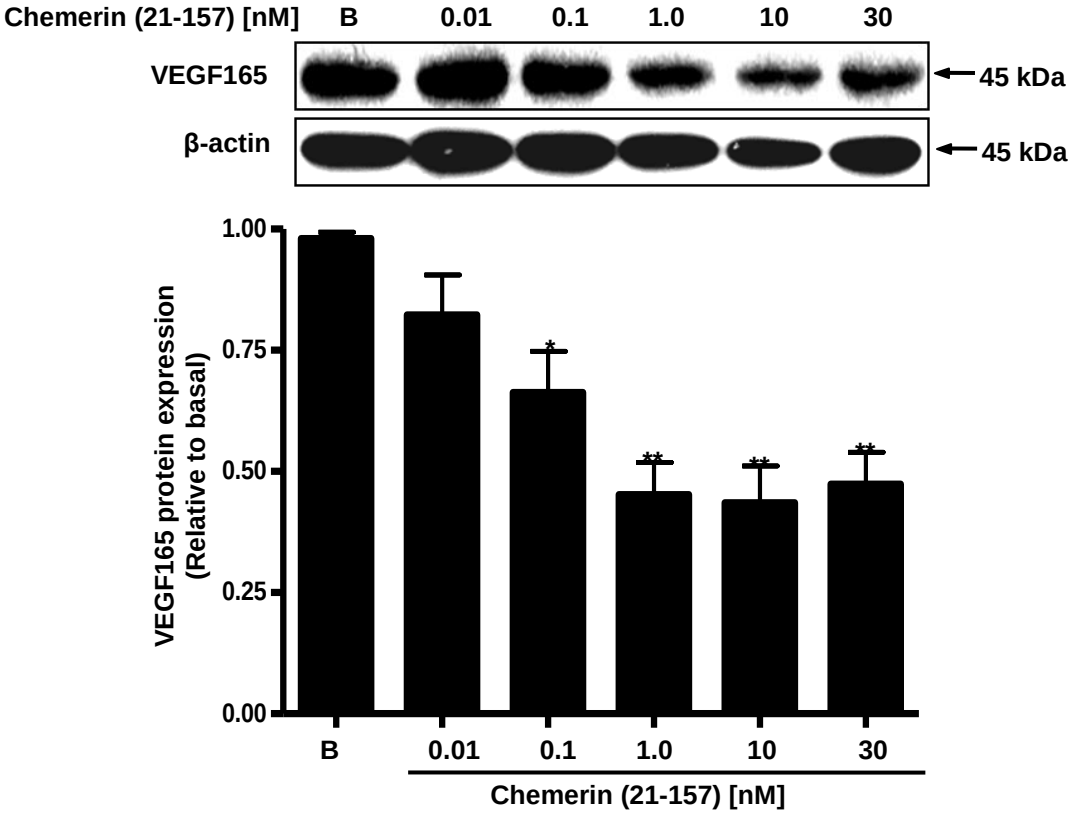

Figure 4.3.5b Chemerin (21-157) decreased VEGF165 protein expression in HMEC-1 cell line after 24 hours

HMEC-1 cells were treated with different chemerin (21-157) concentrations [0-30nM] for 24 hours. Following cell lysis and sample preparations, the proteins were analysed using 12% polyacrylamide gels, and transferred to PVDF membranes at 100V for 1 hour. Membranes were incubated with specific mouse anti-VEGF165 antibody [(1:1000); Santa Cruz, USA] overnight at 4^{o}C. After removing the primary antibody complexes, membranes were incubated with anti-mouse IgG-HRP labelled antibody [(1:8000); Sigma-Aldrich, UK] for 1 hour at RT. Protein complexes were visualised using ECL plus detection reagent on X-ray films. Membranes were re-probed with rabbit β-actin antibody [(1:1500); Cell signalling, Beverly, MA, USA] and used as a loading control. The corresponding bands for both VEGF165 and β-actin were detected as 45kDa products. The band intensities were measured using Scion Image™ densitometer (Scion Corporation, Maryland, USA). The data are presented as mean ± SEM of three independent experiments in duplicates $^{**}p < 0.01$ and $^{*}p < 0.05$ compared to basal.

4.3.6 Chemerin (21-157) Increased VEGF165b Protein Expression in HMEC-1 Cell Line

HMEC-1 cells were cultured in 6-well plates in MCDB cell medium containing 10% FCS, and were serum starved in the same medium containing 1% FCS overnight before performing different treatments. HMEC-1 cells were treated with different chemerin (21-157) [0-30nM] concentrations for 12 and 24 hours. Cells were lysed in 1x RIPA buffer and protein lysates were separated using SDS-PAGE. In both 12 and 24 hours treated HMEC-1 cells, chemerin (21-157) significantly increased VEGF165b protein expression levels in HMEC-1 cells in a concentration-dependent manner with significant increase at [10nM] and [30nM] concentrations ($p < 0.001$) (Fig. 4.3.6a and b respectively).

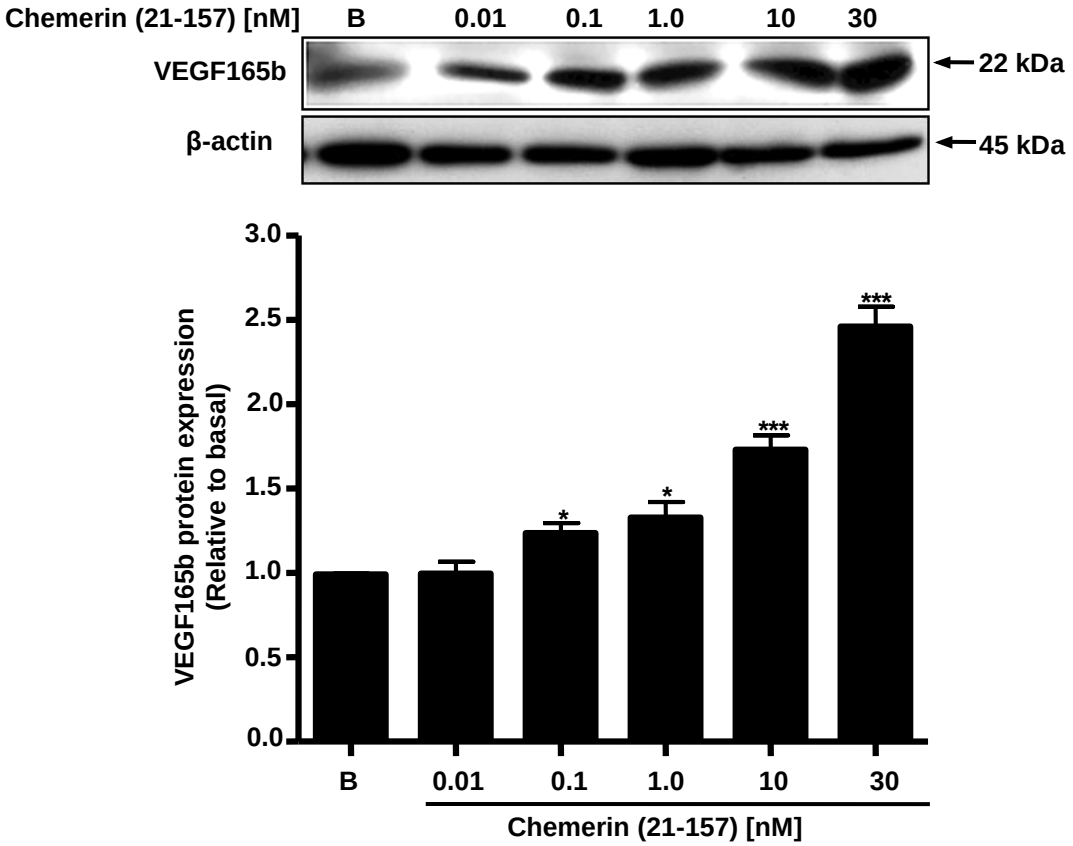

Figure 4.3.6a Chemerin (21-157) increased VEGF165b protein expression in HMEC-1 cell line after 12 hours

HMEC-1 cells were treated with different chemerin (21-157) concentrations [0-30nM] for 12 hours. Following cell lysis and sample preparations, the proteins were separated using 15% polyacrylamide gels, and transferred to PVDF membranes at 100V for 1 hour. Membranes were incubated with specific mouse anti-VEGF165b antibody [(1:1000); R and D Systems, UK] overnight at 4^{o}C. After removing the primary antibody complexes, membranes were incubated with anti-mouse IgG-HRP labelled antibody [(1:8000); Sigma-Aldrich, UK] for 1 hour at RT. Protein complexes were visualised using ECL plus detection reagent on X-ray films. Membranes were re-probed with rabbit β-actin antibody [(1:1500); Cell signalling, Beverly, MA, USA] and used as a loading control. The corresponding bands for VEGF165b and β-actin were detected as 22kDa and 45kDa products. The band intensities were measured using Scion Image™ densitometer (Scion Corporation, Maryland, USA). The data are presented as mean ± SEM of three independent experiments in duplicates ***$p < 0.001$ and *$p < 0.05$ compared to basal.

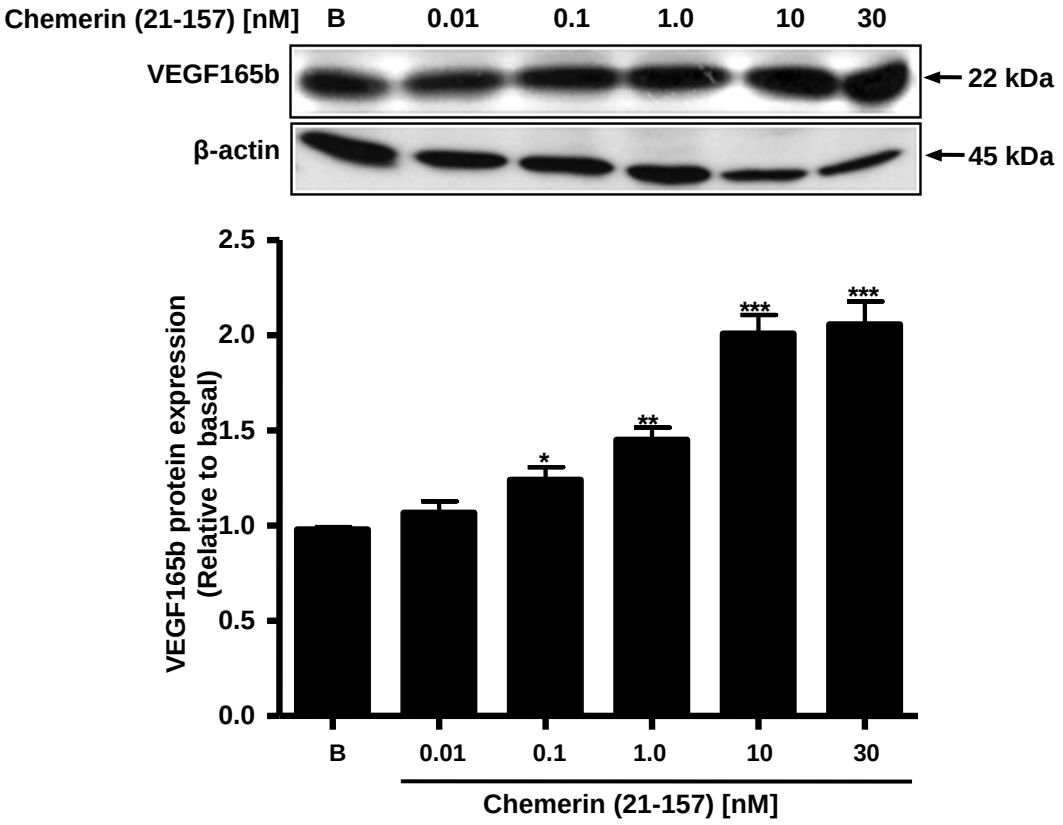

Figure 4.3.6b Chemerin (21-157) increased VEGF165b protein expression in HMEC-1 cell line after 24 hours

HMEC-1 cells were treated with different chemerin (21-157) concentrations [0-30nM] for 24 hours. Following cell lysis and sample preparations, the proteins were separated using 15% polyacrylamide gels, and transferred to PVDF membranes at 100V for 1 hour. Membranes were incubated with specific mouse anti-VEGF165b antibody [(1:1000); R and D Systems, UK] overnight at 4^{o}C. After removing the primary antibody complexes, membranes were incubated with anti-mouse IgG-HRP labelled antibody [(1:8000); Sigma-Aldrich, UK] for 1 hour at RT. Protein complexes were visualised using ECL plus detection reagent on X-ray films. Membranes were re-probed with rabbit β-actin antibody [(1:1500); Cell signalling, Beverly, MA, USA] and used as a loading control. The corresponding bands for VEGF165b and β-actin were detected as 22kDa and 45kDa products. The band intensities were measured using Scion Image™ densitometer (Scion Corporation, Maryland, USA). The data are presented as mean ± SEM of three independent experiments in duplicates ***$p < 0.001$, **$p < 0.01$ and *$p < 0.05$ compared to basal.

4.3.7 Chemerin (21-157) Lead to VEGFR2 Phosphorylation in a Time- and Concentration-dependent Manner in HMEC-1 Cell Line

HMEC-1 cells were cultured in 6-well plates in MCDB cell medium containing 10% FCS, and were serum starved in the same medium containing 1% FCS overnight before performing different treatments. To study time-dependent VEGFR2 phosphorylation, HMEC-1 cells were treated with [10nM] chemerin (21-157) at different time-points for a maximum of 30 minutes. For concentration-dependent VEGFR2 phosphorylation, HMEC-1 cells were treated with different chemerin (21-157) [0-30nM] concentrations for 1 minute. Cells were lysed in 1x RIPA buffer and protein lysates were separated using SDS-PAGE. Chemerin (21-157) increased VEGFR2 receptor phosphorylation both in a time-dependent manner with a significant increase at 0.5 minutes ($p < 0.001$) (Fig. 4.3.7a), and also in a concentration-dependent manner at [1.0nM], [10nM] and [30nM] chemerin (21-157) concentrations ($p < 0.001$ and $p < 0.01$) compared to basal (Fig. 4.3.7b). VEGF [10ng/ml] was used as a positive control.

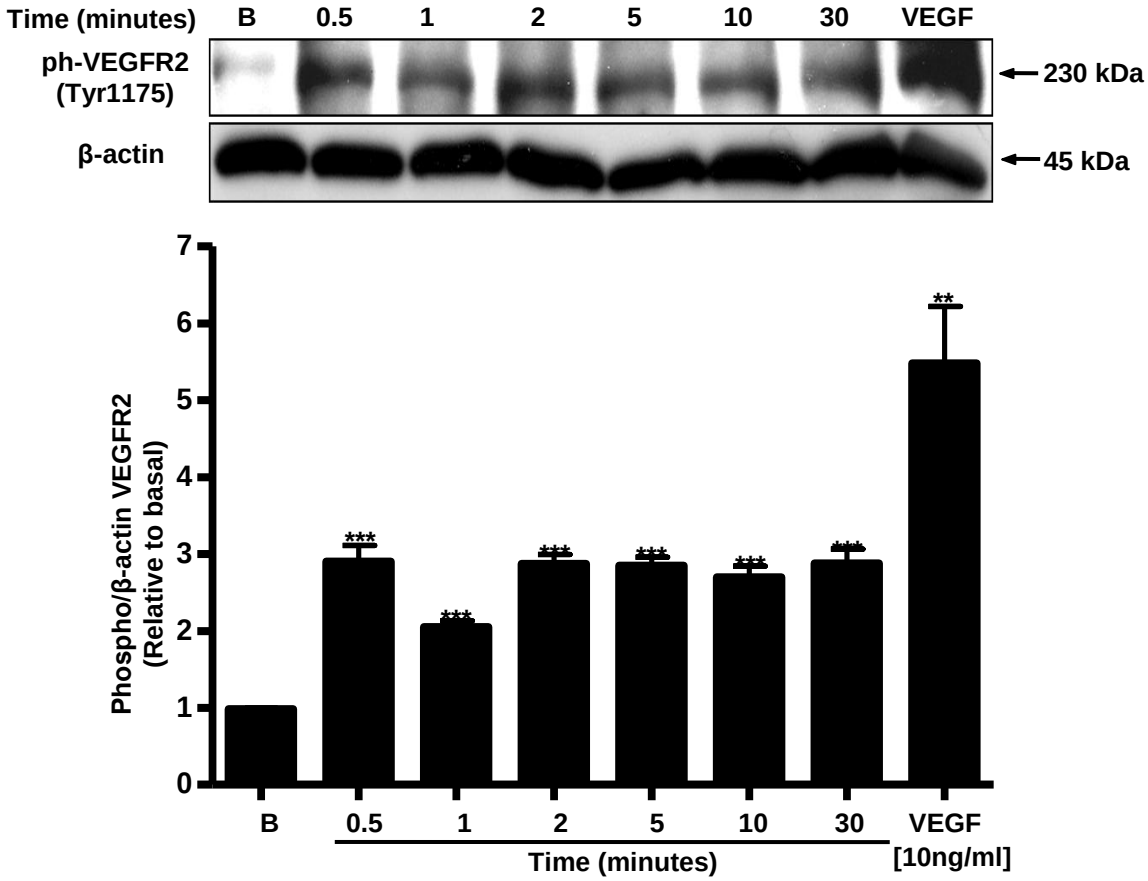

Figure 4.3.7a Chemerin (21-157) lead to VEGFR2 phosphorylation in a time-dependent manner in HMEC-1 cell line

HMEC-1 cells were treated with [10nM] chemerin (21-157) for 0-30 minutes. Following cell lysis and sample preparations, the proteins were separated using 6% polyacrylamide gels, and transferred to PVDF membranes at 100V for 1 hour. Membranes were incubated with specific phospho-VEGFR2 (Tyr1175) antibody [(1:1500); Cell signalling, Beverly, MA, USA] overnight at 4^{o}C. After removing the primary antibody complexes, membranes were incubated with anti-rabbit IgG-HRP labelled antibody [(1:2000); Dako, Ely, UK] for 1 hour at RT. Protein complexes were visualised using ECL plus detection reagent on X-ray films. Membranes were re-probed with rabbit β-actin antibody [(1:1500); Cell signalling, Beverly, MA, USA] and used as a loading control. The corresponding bands for phospho-VEGFR2 (Tyr1175) protein and β-actin were detected as 230kDa and 45kDa products. The band intensities were measured using Scion Image™ densitometer (Scion Corporation, Maryland, USA). The data are presented as mean ± SEM of three independent experiments in duplicates ***$p < 0.001$ and **$p < 0.01$ compared to basal. VEGF [10ng/ml] was used as a positive control.

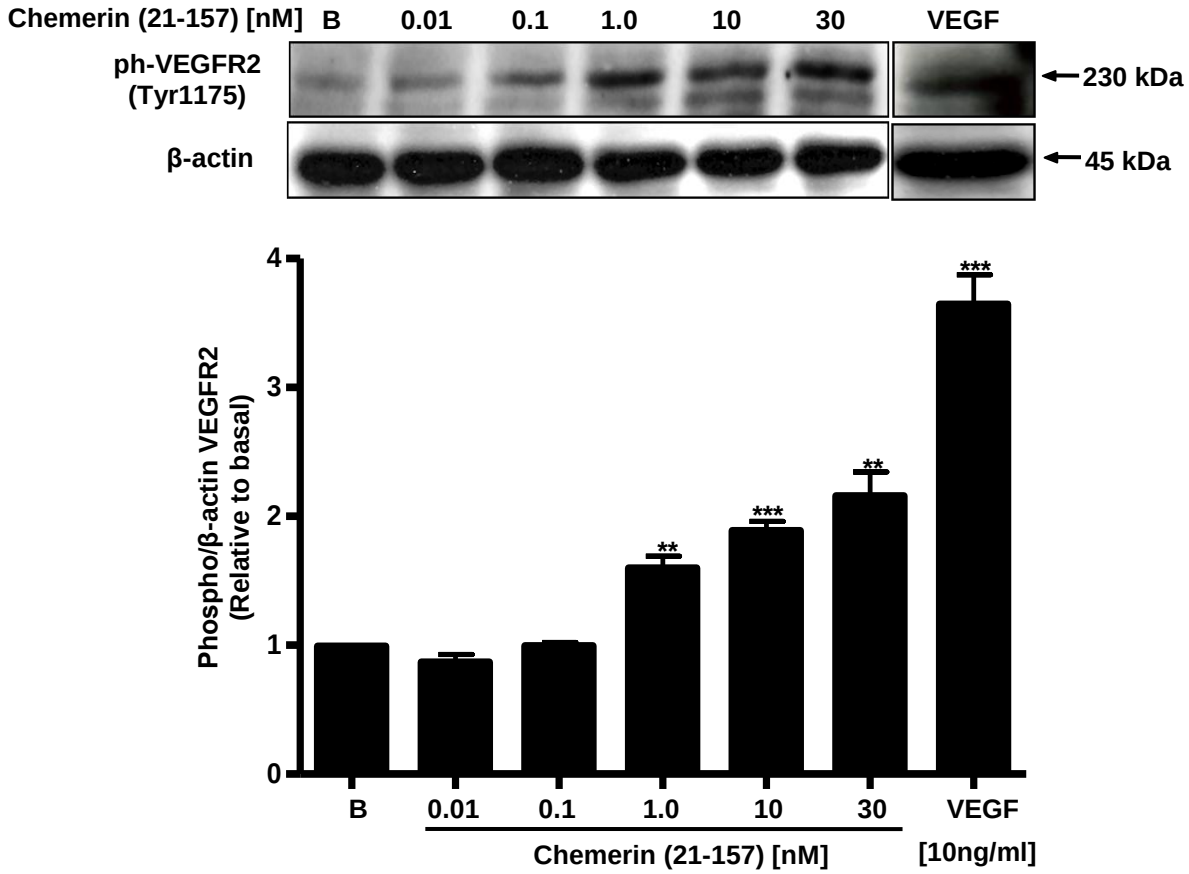

Figure 4.3.7b Chemerin (21-157) lead to VEGFR2 phosphorylation in a concentration-dependent manner in HMEC-1 cell line

HMEC-1 cells were treated with different chemerin (21-157) concentrations [0-30nM] for 1 minute. Following cell lysis and sample preparations, the proteins were separated using 6% polyacrylamide gels, and transferred to PVDF membranes at 100V for 1 hour. Membranes were incubated with specific phospho-VEGFR2 (Tyr1175) antibody [(1:1500); Cell signalling, Beverly, MA, USA] overnight at 4^{o}C. After removing the primary antibody complexes, membranes were incubated with anti-rabbit IgG-HRP labelled antibody [(1:2000); Dako, Ely, UK] for 1 hour at RT. Protein complexes were visualised using ECL plus detection reagent on X-ray films. Membrane was re-probed with rabbit β-actin antibody [(1:1500); Cell signalling, Beverly, MA, USA] and used as a loading control. The corresponding bands for phospho-VEGFR2 (Tyr1175) protein and β-actin were detected as 230kDa and 45kDa products. The band intensities were measured using Scion Image™ densitometer (Scion Corporation, Maryland, USA). The data are presented as mean ± SEM of three independent experiments in duplicates ***$p < 0.001$ and **$p < 0.01$ compared to basal. VEGF [10ng/ml] was used as a positive control.

4.3.8 Chemerin (21-157) Increased MMP-2 and -9 Gelatinolytic Activity in a Concentration-dependent Manner in HMEC-1 Cell Line

HMEC-1 cells were cultured in 6-well plates in MCDB cell medium containing 10% FCS, and were serum starved in the same medium containing 1% FCS overnight before performing various different treatments. HMEC-1 cells were treated with different chemerin (21-157) concentrations [0-30nM] for 24 hours and cell supernatants were collected. Gelatin zymography was used to determine the gelatinolytic activity of secreted MMP-2 and -9 in cell supernatants. Chemerin (21-157) significantly increased the activities of both MMP-2 and -9 in a concentration-dependent manner with a peak response at [10nM] and [30nM] concentrations ($p < 0.001$) (Fig. 4.3.8a and b respectively). VEGF [10ng/ml] was used as a positive control.

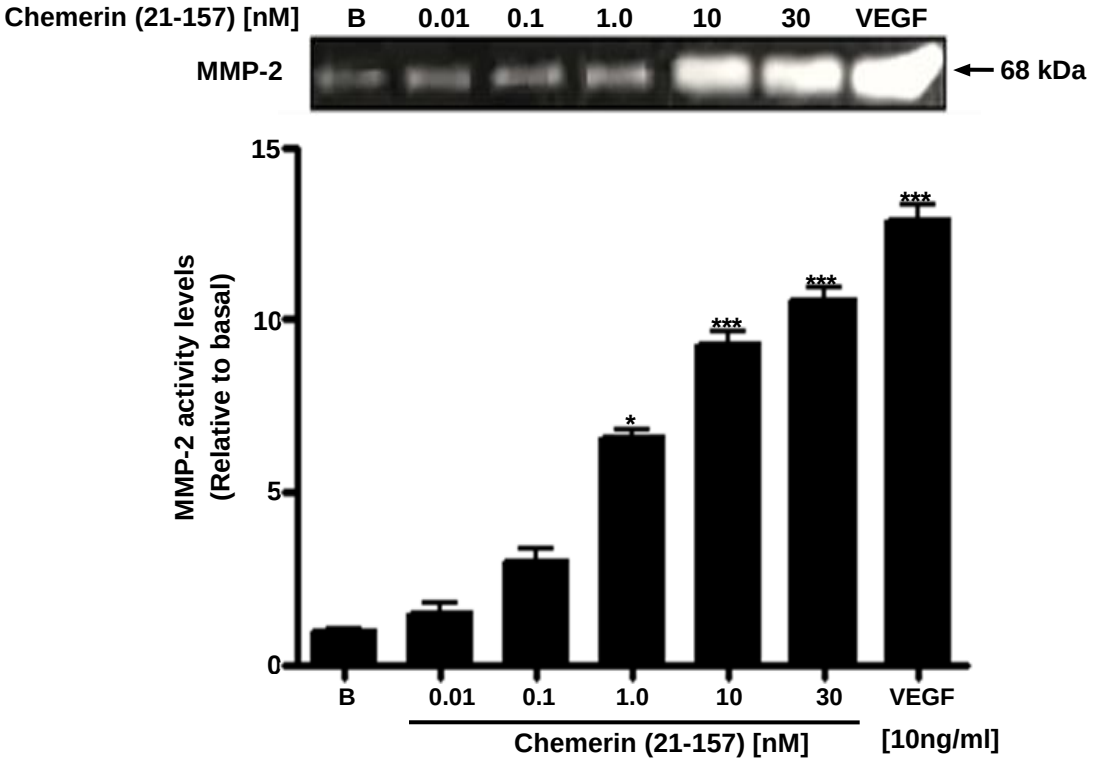

Figure 4.3.8a Chemerin (21-157) increased MMP-2 gelatinolytic activity in a concentration-dependent manner in HMEC-1 cell supernatants

10µl of cell culture supernatant sample was mixed with 10µl zymography sample buffer and resolved on 10% SDS-PAGE containing 1 mg/ml of gelatin (Sigma, St. Louis, USA) under non-reducing conditions. Following electrophoresis at 4^{o}C, gels were washed twice for 30 minutes with denaturation buffer (2.5% Triton X-100) at RT, and incubated overnight in incubation buffer (50mM Tris-HCl pH 7.5, 200mM NaCl, 10mM CaCl2, 1µM ZnCl2) at 37^{o}C. Characterisation of MMPs activity was determined by inhibition with EDTA [10mM]. Following incubation, gels were stained for 1 hour (0.25% Coomassie brilliant blue R-250 in 45% methanol, 10% acetic acid), and de-stained in the same buffer without Coomassie. The white bands against a blue background were observed following de-staining of gels. The corresponding bands for MMP-2 were detected as a 68kDa products. The band intensities were measured using Gel Pro image analysis [Gel Pro image analysis (Gel Pro 4.5, Media Cybernetics, USA)]. The data are represented as mean ± SEM of three independent experiments in duplicates ***$p < 0.001$ and *$p < 0.05$ compared to basal. VEGF [10ng/ml] used as a positive control.

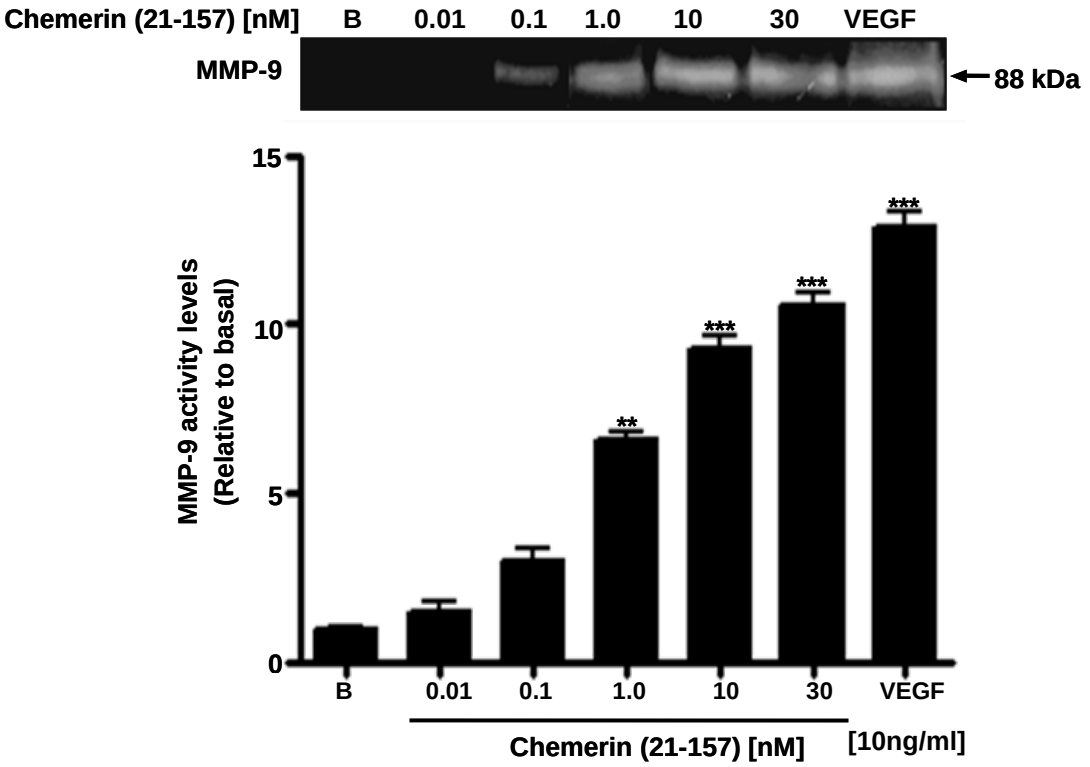

Figure 4.3.8b Chemerin (21-157) increased MMP-9 gelatinolytic activity in a concentration-dependent manner in HMEC-1 cell supernatants

10µl of cell culture supernatant sample was mixed with 10µl zymography sample buffer and resolved on 10% SDS-PAGE containing 1 mg/ml of gelatin (Sigma, St. Louis, USA) under non-reducing conditions. Following electrophoresis at 4^{o}C, gels were washed twice for 30 minutes with denaturation buffer (2.5% Triton X-100) at RT, and incubated overnight in incubation buffer (50mM Tris-HCl pH 7.5, 200mM NaCl, 10mM CaCl2, 1µM ZnCl2) at 37^{0}C. Characterisation of MMPs activity was determined by inhibition with EDTA [10mM]. Following incubation, gels were stained for 1 hour (0.25% Coomassie brilliant blue R-250 in 45% methanol, 10% acetic acid), and de-stained in the same buffer without Coomassie. The white bands against a blue background were observed following de-staining of gels. The corresponding bands for MMP-9 were detected as a 68kDa product. The band intensities were measured using Gel Pro image analysis [Gel Pro image analysis (Gel Pro 4.5, Media Cybernetics, USA)]. The data are represented as mean ± SEM of three independent experiments in duplicates ***$p < 0.001$ and **$p < 0.01$ compared to basal. VEGF [10ng/ml] used as a positive control.

4.3.9 Chemerin (21-157) Increased HMEC-1 Cell Proliferation in a Concentration-dependent Manner

HMEC-1 cell proliferation was determined using CellTiter 96 AQueous One Solution cell proliferation assay (Chapter 2, section 2.4.2, page number 60). HMEC-1 cells were trypsinised and cultured in 96-well plate (provided in the kit) at the cell density of $2.5x10^5$ cells/well for 24 hours in a humidified incubator at 37^oC at 5% CO_2 environment. Cells were serum-starved overnight and treated with different chemerin (21-157) [0-30nM] concentrations for a maximum of 24 hours. After 24 hours of incubation, the cell medium was replaced with 100µl of fresh culture medium, 20µl MTS reagent was added to each well, and incubated for 1 hour. The absorbance was recorded at 490nm using an ELISA plate reader (EL800, Bio-Tek Instruments, Inc., Winooski, VT, USA). Chemerin (21-157) significantly increased HMEC-1 cell proliferation at the concentrations of [0.1nM] and [1.0nM] ($p < 0.01$), and decreasing at higher chemerin (21-157) concentrations compared to basal (Fig. 4.3.9a). VEGF [10ng/ml] was used as a positive control.

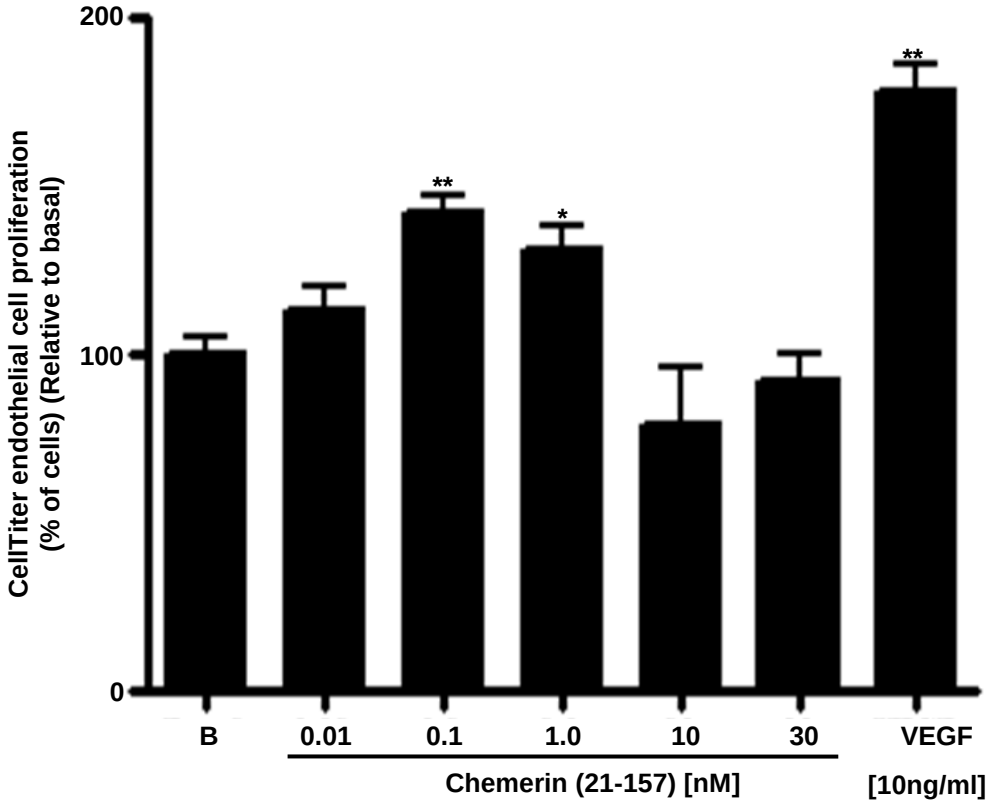

Figure 4.3.9a Chemerin (21-157) induced HMEC-1 cell proliferation in a concentration-dependent manner

HMEC-1 cells were plated at the cell density of $2.5x10^5$ in a 96-well culture for 24 hours in a humidified incubator at 37°C at 5% CO_2 environment. Serum-starved HMEC-1 cells were treated with different chemerin (21-157) concentrations [0-30 nM] for 24 hours. Following chemerin treatments, 20µl MTS reagent was added to 100µl of cell culture medium per well. After 1 hour at 37°C in a humidified, 5% CO_2 atmosphere, the absorbance was recorded at 490nm using an ELISA plate reader (EL800, Bio-Tek Instruments, Inc., Winooski, VT, USA). The percentage increase in absorbance was calculated against untreated cells. The results are presented as percentage of cells in relation to basal (untreated), and represents the mean of triplicates in duplicates $^{**}p < 0.01$ and $^{*}p < 0.05$ compared to basal. VEGF [10ng/ml] was used as a positive control.

4.3.10 Chemerin (21-157) Increased HMEC-1 Cell Migration in a Concentration-dependent Manner

HMEC-1 cell migration was studied using Wound-healing Motility Assay as well as I*n Vitro* Cell Invasion Assay. For Wound-healing Motility Assay (Chapter 2, section 2.4.3, page numbers 64-5), HMEC-1 cells were trypsinised and plated in 6-well plates at the final cell density of $1x10^5$ cells/ml in MCDB cell medium containing 10% FCS and incubated overnight. In 75-80% confluent cells, a single scratch wound was created using a sterile p10 micropipette tip. Cell medium was replaced with MCDB medium containing 1% FCS and incubated overnight. Cells were treated with different chemerin (21-157) [0-30nM] concentrations and incubated for a maximum of 24 hours. Chemerin (21-157) increased the number of migrated ECs in a concentration-dependent manner (Fig. 4.3.10a). VEGF [10ng/ml] was used as a positive control. I*n Vitro* Cell Invasion Assay was performed using BD BioCoat™ Matrigel™ Invasion Chamber. 750µl of 1% FCS containing MCDB medium treated with different chemerin (21-157) [0-30nM] concentrations was added to the BD Falcon™ TC Companion Plate. The rehydrated Culture Inserts were placed in the plates, and 250µl of HMEC-1 cell suspension containing approximately $3x10^4$ cells/ml was added, and incubated for 24 hours in a humidified incubator at 37^oC at 5% CO_2 environment. After incubations, the non-invading cells were scrubbed off using a cotton-tipped swab from the Culture Inserts, and cells invaded through the Matrigel™ Matrix were labelled with 4µg/ml Calcein-AM for 90 minutes. Fluorescence of migrated cells was read at 494/517nm (excitation/emission) using a fluorescence plate reader. Chemerin (21-157) significantly increased the number of migrating endothelial cells in a concentration-dependent manner ($p < 0.01$) (Fig. 4.3.10b). VEGF [10ng/ml] was used as a positive control.

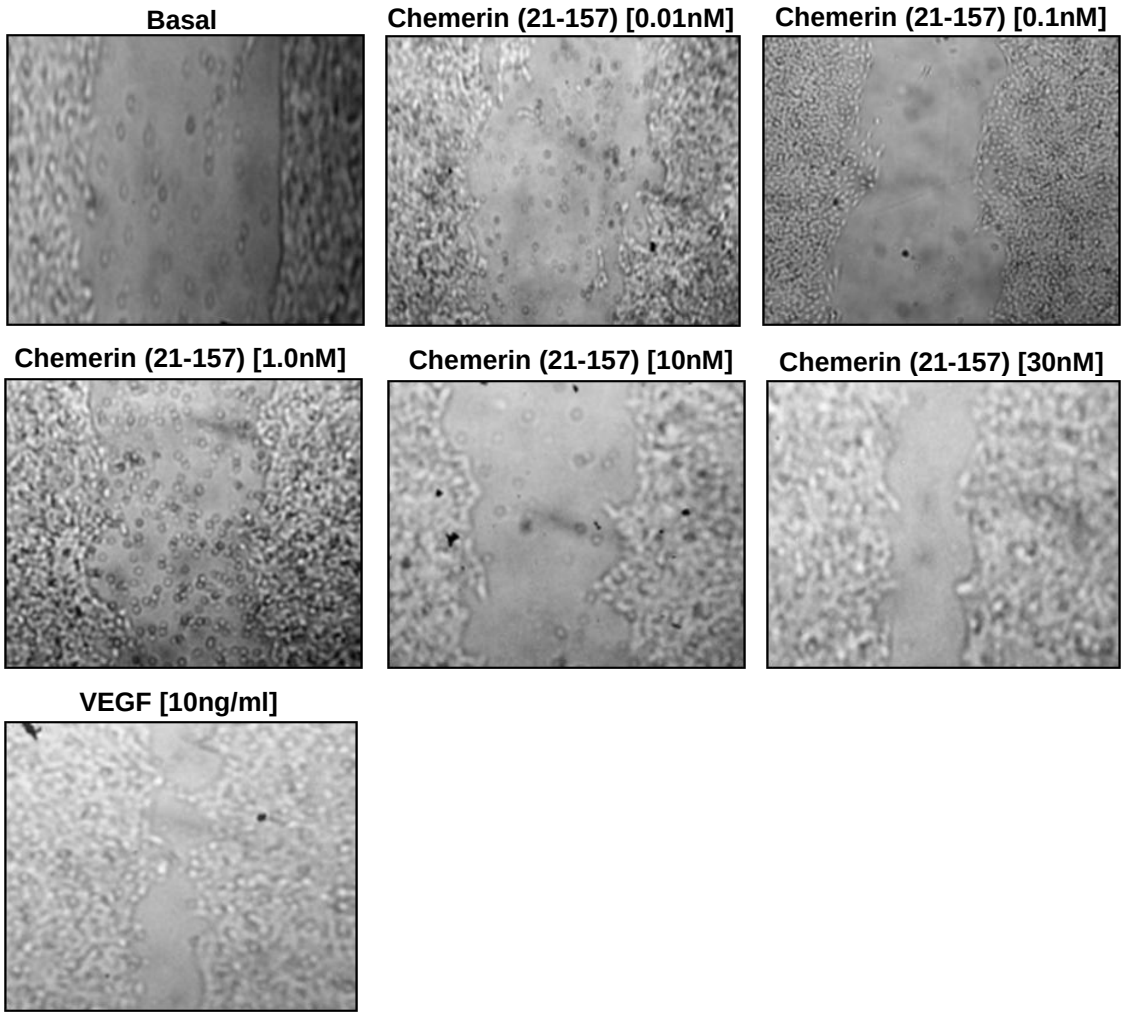

Figure 4.3.10a Chemerin (21-157) induced EC migration in HMEC-1 cell line in a concentration-dependent manner

HMEC-1 cells were trypsinised and plated in 6-well plates at the final cell density of $1x10^5$ cells/ml in MCDB cell medium containing 10% FCS and incubated overnight. In 75-80% confluent cells, a single scratch wound was created using a sterile p10 micropipette tip, and markings were created to serve as reference points in order to eliminate any possible variation caused by the difference in the width of the scratches. Cell medium was replaced with MCDB medium containing 1% FCS and incubated overnight. Cells were treated with different human recombinant chemerin (21-157) concentrations [0-30nM] (R and D systems, Abingdon, UK) and incubated for a maximum of 24 hours. VEGF [10ng/ml] (Sigma Aldrich, Dorset, UK) was used as a positive control. Images were captured using invert phase microscope.

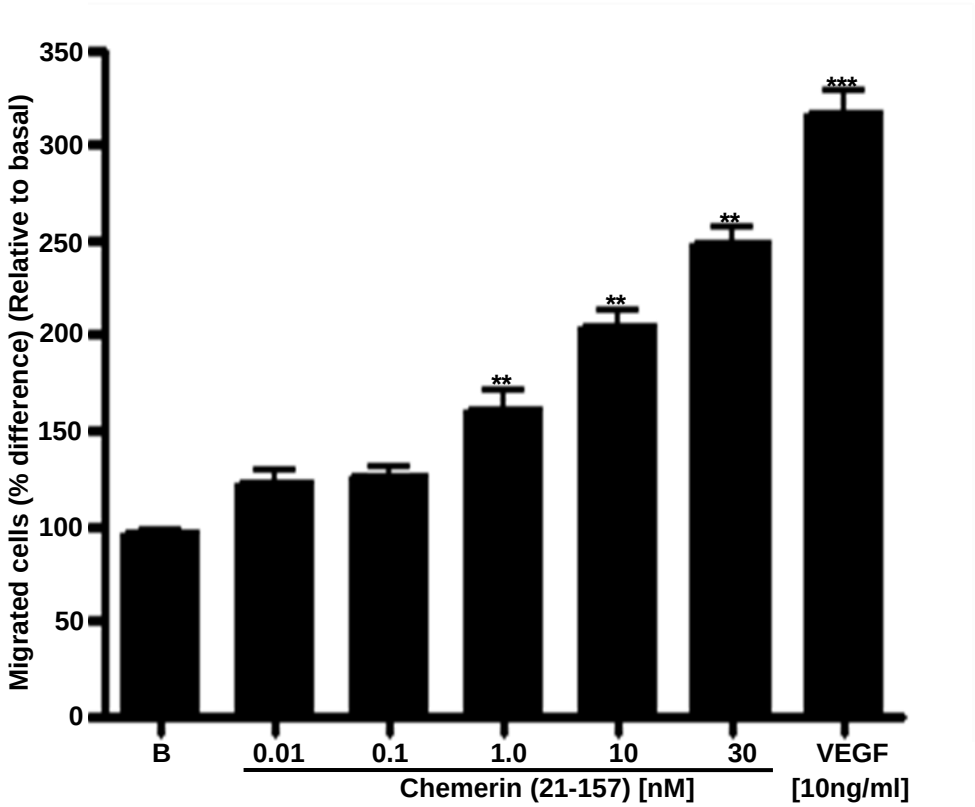

Figure 4.3.10b Chemerin (21-157) induced EC migration in a concentration-dependent manner in HMEC-1 cell line

HMEC-1 cells were trypsinised and final cell suspension of $3x10^4$ cell/ml was prepared. 250µl of resultant cell suspension was added to each Culture Inserts suspended in 750µl of chemerin (21-157) treated starvation medium in the lower chamber and incubated overnight in a humidified incubator at 37^oC at 5% CO_2 environment. After incubations, the non-invading cells were scrubbed off using a cotton-tipped swab from the Culture Inserts, and cells invaded through the Matrigel™ Matrix were labelled with 4µg/ml Calcein-AM (BD Biosciences, UK) for 90 minutes. Fluorescence of migrated cells was read at 494/517nm (excitation/emission) using a fluorescence plate reader. The migrated cells were expressed as the ratio of the fluorescence value compared to the basal. This figure shows graphical representation of migratory distance (expressed as a percentage difference relative to basal). The data are presented as mean ± SEM of three independent experiments in duplicates ***$p < 0.001$ and **$p < 0.01$ compared to basal. VEGF [10ng/ml] was used as a positive control.

4.3.11 Chemerin (21-157) and Capillary Tube Formation in HMEC-1 Cell Line

Endothelial cell capillary tube formation was studied using Growth Factor Reduced Matrigel Matrix (Chapter 2, section 2.4.5, page number 65-6). HMEC-1 cells were trypsinised in MCDB cell medium and cell suspension containing $2x10^4$ cells/well was prepared and added to pre-coated Matrigel plate, and incubated for 2 hours to encourage cell attachment. Post incubation, cell medium was carefully removed from the wells avoiding any damage to the coated gel, and was replaced with cell medium containing 1% FCS and incubated for 4 hours. Cells were treated with different chemerin (21-157) [0-30nM] concentrations for 24 hours, and capillary tube formation images were captured with a digital microscope camera system (Olympus, Tokyo, Japan) under 100x magnification using invert phase microscope (Fig.4.3.11a). The tube lengths in 3-4 randomly selected fields in each of the wells were measured and compared against untreated groups using Image-Pro Plus software. Chemerin (21-157) significantly increased capillary tube length in a concentration-dependent manner, with a maximum tube length formation at higher chemerin (21-157) concentrations ($p < 0.001$) (4.3.11b). VEGF [10ng/ml] was used as a positive control.

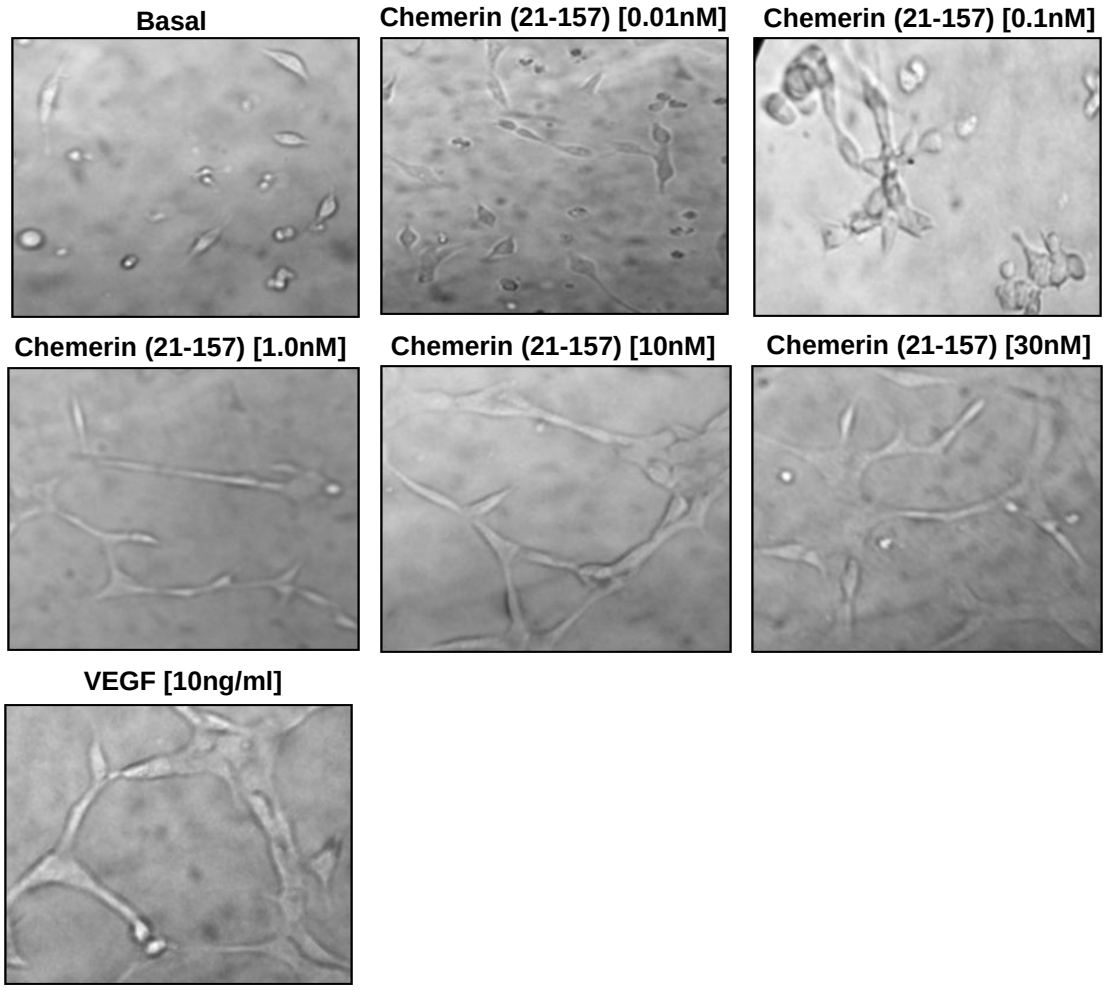

Figure 4.3.11a Chemerin (21-157) induced capillary tube formation in a concentration-dependent manner in HMEC-1 cell line

HMEC-1 cells were trypsinised and seeded onto the Matrigel coated plates at the cell density of $2x10^3$cells/well in the fresh medium and incubated for 2 hours. Cell medium was replaced with MCDB medium containing 1% FCS and incubated for 4 hours. Post incubations, HMEC-1 cells were treated with different chemerin (21-157) concentrations [0-30nM] and VEGF [0.5nM] and incubated for a maximum of 24 hours. Capillary tube formation images were captured using a digital microscope camera system (Olympus, Tokyo, Japan) under 100x magnification. Image-Pro Plus software was used to quantify the tube length formation. The tube lengths in 3-4 randomly selected fields in each of the wells were measured and compared against untreated groups. VEGF [10ng/ml] was used as a positive control.

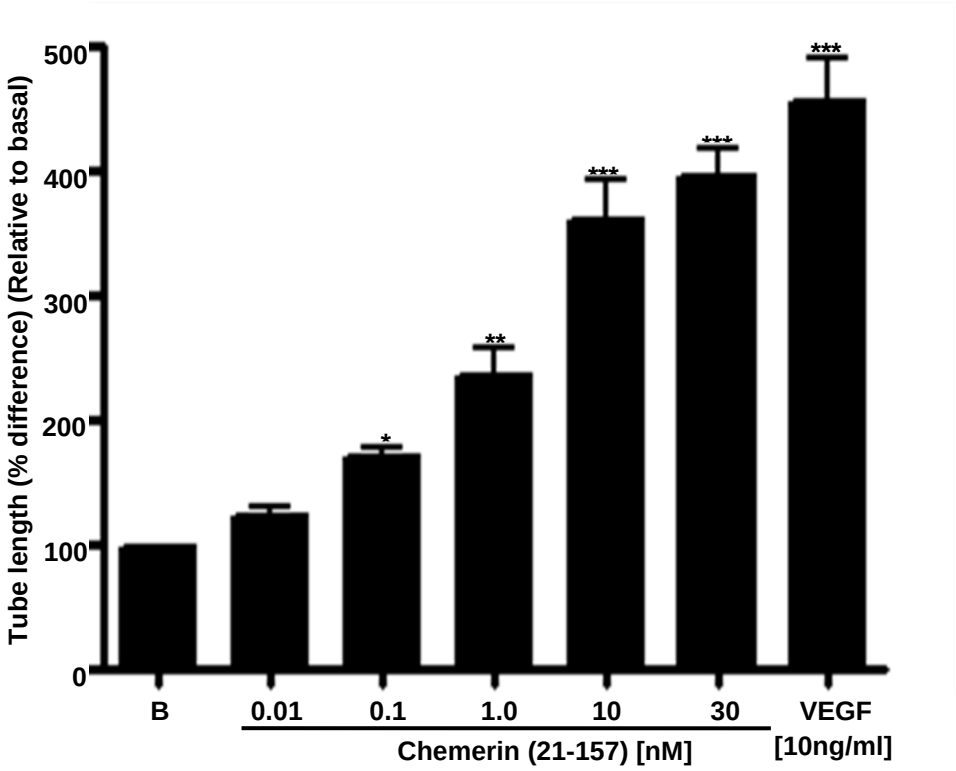

Figure 4.3.11b Graphical presentation of chemerin (21-157)-induced capillary tube formation in HMEC-1 cell line

This figure represents the capillary tube length measurement, expressed as relative to basal; HMEC-1 cells were incubated with different chemerin (21-157) concentrations [0-30nM] for a maximum of 24 hours. Image-Pro Plus software was used to quantify the tube length. The length of tubes in 3-4 randomly selected fields in each of the treatment group was compared with the untreated groups. The data are presented as mean ± SEM of three independent experiments in duplicates ***p < 0.001, **p < 0.01 and *p < 0.05 compared to basal. VEGF [10ng/ml] was used as a positive control.

4.3.12 Chemerin (21-157) Increased HMEC-1 Cell Apoptosis in a Concentration-dependent Manner

Endothelial cell apoptosis assay was studied using Cellular DNA Fragmentation ELISA kit (Chapter 2, section 2.4.6, page numbers 66-7). HMEC-1 cells were trypsinised and plated in 96-well plates at the cell density of $1x10^3$ cells/ml and incubated overnight in a humidified incubator at 37^oC at 5% CO_2 environment. Cells were treated with different chemerin (21-157) concentrations [0-30nM] for 24 hours. Following incubations, cell supernatants were carefully removed and 200µl of 1x incubation solution (solution 5) was added to each well and incubated for 30 minutes at RT. Cells were centrifuged at 250g for 10 minutes and 100µl of the cell supernatants from lysed cells were transferred to pre-coated anti-DNA antibody microplates, ELISA was performed, and the absorbance was recorded at 450 nm using a plate reader. Chemerin (21-157) significantly increased EC death in a concentration-dependent manner ($p < 0.001$) (Fig. 4.3.12a). Camptothecin [2µM] was used as a positive control.

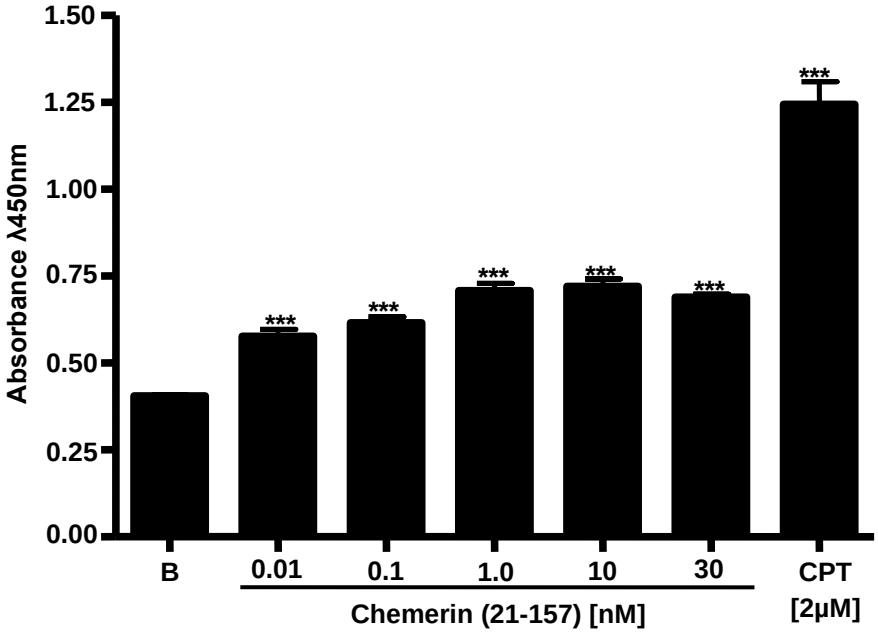

Figure 4.3.12a Chemerin (21-157) and cell apoptosis in HMEC-1 cell line

HMEC-1 cells were trypsinised and plated in 96-well plate at the cell density of $1x10^3$ cells/ml and incubated overnight in a humidified incubator at 37^oC at 5% CO_2 environment. Cells were labelled with anti-BrdU solution (solution 7) at the final concentration of [10μM] and incubated for 24 hours before treating with different chemerin (21-157) concentrations [0-30nM] for another 24 hours. After incubation, cell supernatants were carefully removed and 200μl of 1x incubation solution (solution 5) was added to each well for cell lysis and incubated for 30 minutes at RT. Cells were centrifuged at 250*g* for 10 minutes and 100μl of the cell supernatants were transferred to pre-coated ELISA microplates and absorbance was measured using a spectrophotometer (Beckman Instruments Inc., California, USA). The data are presented as mean ± SEM of three independent experiments in duplicates ***$p <$ 0.001 compared to basal. Camptothecin [2μM] was used as a positive control.

4.4 Summary of Results

Chemerin (21-157) lead to ERK1/2 MAPK and ERK5 MAPKs phosphorylation in a time- and concentration-dependent manner (Fig. 4.3.1a (time response) and b (concentration response), and Fig. 4.3.2a and b respectively). Chemerin (21-157) also resulted in p38 MAPK phosphorylation in a time- and concentration-dependent manner (Fig. 4.3.3a and b respectively) which is an important MAPK implicated in cell apoptosis. SAPK/JNK is another important MAPK known to play crucial role in cell death, and was phosphorylated by chemerin (21-157) in a time- and concentration-dependent manner (Appendix 11, Fig. 11.1a and b respectively, page numbers 277-79).

Chemerin (21-157) also lead to the phosphorylation of Akt/PKB kinase at Ser473 phosphorylation site in a time- and concentration-dependent manner (Fig. 4.3.4a and b respectively). Akt/PKB kinase phosphorylation at Ser473 site is known to increase EC angiogenesis upstream of VEGF protein and regulates the production of endothelium NO (Michell et al., 1999). Akt/PKB kinase regulates protein expression of VEGF, which is the most potent angiogenic molecule known to promote angiogenesis; and Akt/PKB kinase activation is suggested to be sufficient for angiogenesis to take place (Ackah et al., 2005).

Chemerin (21-157) treated HMEC-1 cells showed an increased expression of HIF-1α protein in a concentration-dependent manner (Appendix 3, Fig. 3.1a, page numbers 245-6). HIF-1α is a transcription factor that is known to regulate mRNA expression of a number of genes under normal and hypoxic conditions. Essentially, under hypoxic conditions, increased HIF-1α activity is reported to increase VEGF protein expression; however, quite interestingly, chemerin (21-157) decreased VEGF165 protein expression in a concentration-dependent manner both at 12 and 24

hours in HMEC-1 cell line (Fig. 4.3.5a and b respectively). An anti-angiogenic form of VEGF, VEGF165b, which is formed upon alternative splicing of VEGF gene at exon 8b (Appendix 5, Fig. 5.1a, page number 248); was significantly increased with increasing chemerin (21-157) concentrations in HMEC-1 cell line (Fig. 4.3.6a and b respectively). VEGF165b is an opposite counterpart of VEGF165, and competes with VEGF165 for the binding site (s) on tyrosine kinase receptor, VEGFR2 – the main signalling receptor involved in VEGF-dependent angiogenesis and exerts anti-angiogenic properties (Neufeld et al., 1999, Nowak et al., 2008).

Chemerin (21-157) lead to VEGFR2 phosphorylation at Tyr1175 site both in a time- and concentration-dependent manner (Fig. 4.3.7a and b respectively). VEGFR2 receptor phosphorylation at Tyr1175 is suggested to be the key tyrosine residue involved in VEGF-dependent angiogenesis (Koch et al., 1995, Palframan et al., 2001). Waltenberger and colleagues reported that, in porcine aortic ECs although both VEGFR2 and VEGFR1 receptors undergo phosphorylation, only VEGFR2 transfected cells displayed migratory and proliferative responses (Waltenberger et al., 1994). VEGFR2 receptor activation is also known to recruit adaptor proteins such as PI3K and many other protein tyrosine phosphatases, ultimately resulting in promoting angiogenesis (Kroll and Waltenberger, 1997).

Chemerin (21-157) increased the activities of MMP-2 and -9 in a concentration-dependent manner (4.3.8a and b respectively). A number of cytokines and growth factors are reported to regulate the MMPs balance in the vasculature (Kobayashi et al., 1997), which when disturbed is known to cause diseases of the endothelial-barrier function. Chemerin (21-157) promoted EC proliferation (Fig. 4.3.9a), migration (4.3.10a and b), and capillary tube formation (Fig. 4.3.11a and b) in HMEC-1 cell line in a concentration-dependent manner which further suggests

angiogenic chemerin (21-157) properties. The angiogenic chemerin (21-157) behaviour in the presence of decreased VEGF165, and increased VEGF165b proteins protein expressions, suggests the involvement of angiogenic pathways independent of VEGF, for example Notch/DLL4 (Appendix 4, Fig. 4.1a, page number 247).

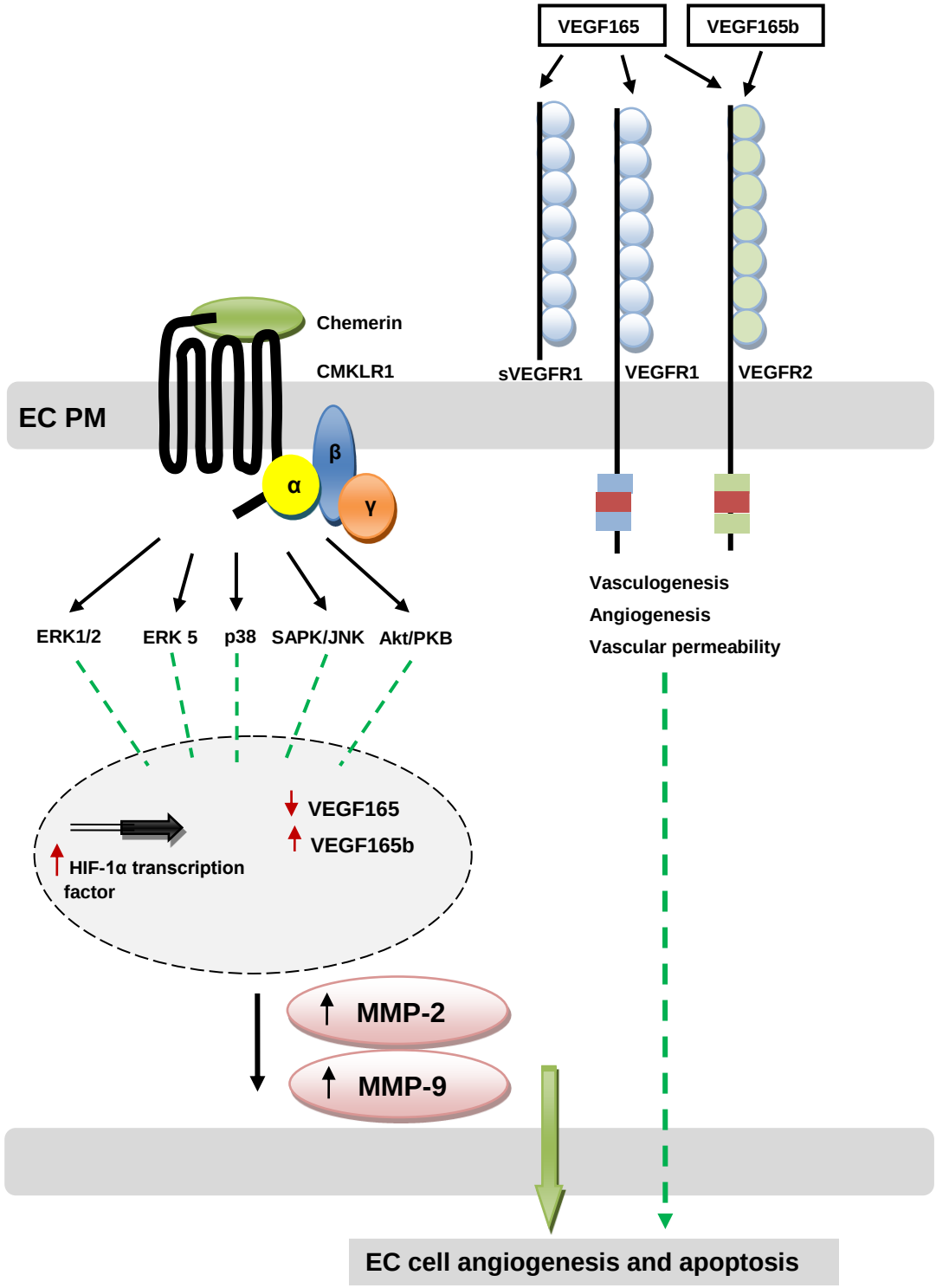

Figure 4.4.1a Schematic representation of the findings in this chapter

This picture shows the schematic representation of involvement and localisation of different MAPKs and Akt/PKB kinases in a cell. The transcription factor, HIF-1α and the expression regulation of VEGF165 and VEGF165b proteins, resulting in altering the activities of MMP-2 and MMP-9 enzymes, and ultimately, affecting the biological responses in a cell; for example EC proliferation, migration and capillary tube formation. This picture also shows the RTKs, VEGFR1 and VEGFR2 on the EC wall and their involvement in endothelial cell angiogenesis.

5.1 Introduction

The specific aims of this part of the project were to study the role (s) of chemerin (21-157) in; (1) endothelial Cell Adhesion Molecules (CAMs) such as E-selectin, Vascular Cell Adhesion Molecule (VCAM)-1 and Intracellular Cell Adhesion Molecule (ICAM)-1 protein expression and secretion in both HMEC-1 cell lysates and supernatants, (2) CAM protein expression in HMEC-1 cells when co-treated with chemerin (21-157) and a known pro-inflammatory mediator, Interleukin (IL)-1β, (3) mediating the activity of Nuclear Factor (NF)-κB pathway, (4) Monocyte Chemoattractant protein (MCP)-1 protein expression, when treated with chemerin (21-157) alone, and in combination with IL-1β, and finally (5) Endothelial (HMEC-1) and monocyte (THP-1) cell adhesion.

Endothelium possess cell-surface glycoproteins, such as E-selectin, VCAM-1, and ICAM-1 which are upregulated in response to different inflammatory stimuli. These inflammatory stimuli encourage leukocyte recruitment and adherence to the endothelium surface at very early stages of vascular inflammation, that ultimately leads to vascular inflammatory disease initiation and progression such as atherosclerosis (Blankenberg et al., 2003). Upon chronic cell activation, selectin molecules and other adhesion molecules including ICAM-1 and VCAM-1 are rapidly cleaved off from the cell surface by a number of different mechanisms and circulate freely in the bloodstream. Soluble isoforms of these molecules are detectable in blood and plasma and are considered as an independent markers of endothelial cell dysfunction and diseases of cardiovascular system (Blankenberg et al., 2003, Ridker et al., 1998, Ingelsson et al., 2008, Soro-Paavonen et al., 2006, Hwang et al., 1997, Tardif et al., 2006).

Activation of Nuclear Factor (NF)-κB pathway in an injured endothelium is known to play a significant role in the early development of inflammatory responses in diseased states such as atherosclerosis (Collins et al., 1995, Savoia and Schiffrin, 2007, Read et al., 1997, Hu et al., 2000, Blankenberg et al., 2003). Several inflammatory cytokines secreted by the adipose tissue cause EC activation and inflammation, causing the diseases of cardiovascular system such (Karkkainen et al., 2000a, Karkkainen et al., 2000b, Fiumara et al., 1989).

5.2 Materials and Methods

The cellular protein expression and phosphorylation was determined by SDS-PAGE (Chapter 2, section 2.3.7, page numbers 57-60) using different percentage polyacrylamide gels for separating different proteins (Table 5.2.1a). NF-κB activity was studied using Luciferase activity assay (Chapter 2, section 2.4.7, page number 68). Endothelial-Monocyte cell adhesion was studied using BD BioCoat Endothelial Cell Adhesion Assay kit (Chapter 2, section 2.4.8, page numbers 69-70).

Table 5.2.1a

The molecular weights of different proteins and gel percentages used for SDS-PAGE analysis

Protein name	Molecular weight (kDa)	Percentage gels used
E-selectin	115	8
ICAM-1	85	10
MCP-1	11	15
VCAM-1	110	8

5.3 Data Presentation and Analyses

5.3.1 Chemerin (21-157) and E-selectin Protein Expression and Secretion in HMEC-1 Cell Line

HMEC-1 cells were cultured in 6-well plates in MCDB cell medium containing 10% FCS, and were serum starved in the same medium containing 1% FCS overnight before performing different treatments. To study cellular protein expression of E-selectin, HMEC-1 cells were treated with different chemerin (21-157) [0-10nM] concentrations for 12 and 24 hours. Cells were lysed in 1x RIPA buffer and protein lysates were separated using SDS-PAGE. To study secreted levels of E-selectin protein in ECs, HMEC-1 cells were treated with different chemerin (21-157) [0-30nM] concentrations for 4, 12 and 24 hours. Cell supernatants were collected and soluble E-selectin (see-selectin) protein levels were determined using Luminex® 100 instrument in all three different treatment groups. In addition, in 24 hours cell supernatants, sE-selectin protein expression was studied using SDS-PAGE. Chemerin (21-157) significantly increased cellular E-selectin protein expression in a concentration-dependent manner in both 12 hours (Fig. 5.3.1a) and 24 hours (Fig. 5.3.1b) HMEC-1 cell lysates ($p < 0.001$, $p < 0.01$ and $p < 0.05$). In 24 hours treated cell supernatants, chemerin (21-157) significantly increased sE-selectin expression in a concentration-dependent manner ($p < 0.01$ and $p < 0.05$) (Fig. 5.3.1c). In contrast, no sE-selectin proteins were detected in HMEC-1 cell supernatants in multiplex ELISA, and also, different chemerin (21-157) treatments failed to show any change in sE-selectin protein secretion in all different treatment groups (Appendix 7.1, Table 7.1a, b and c respectively; page numbers 253-56). TNF-α [10ng/ml] and IL-1β [10ng/ml] were used as positive controls.

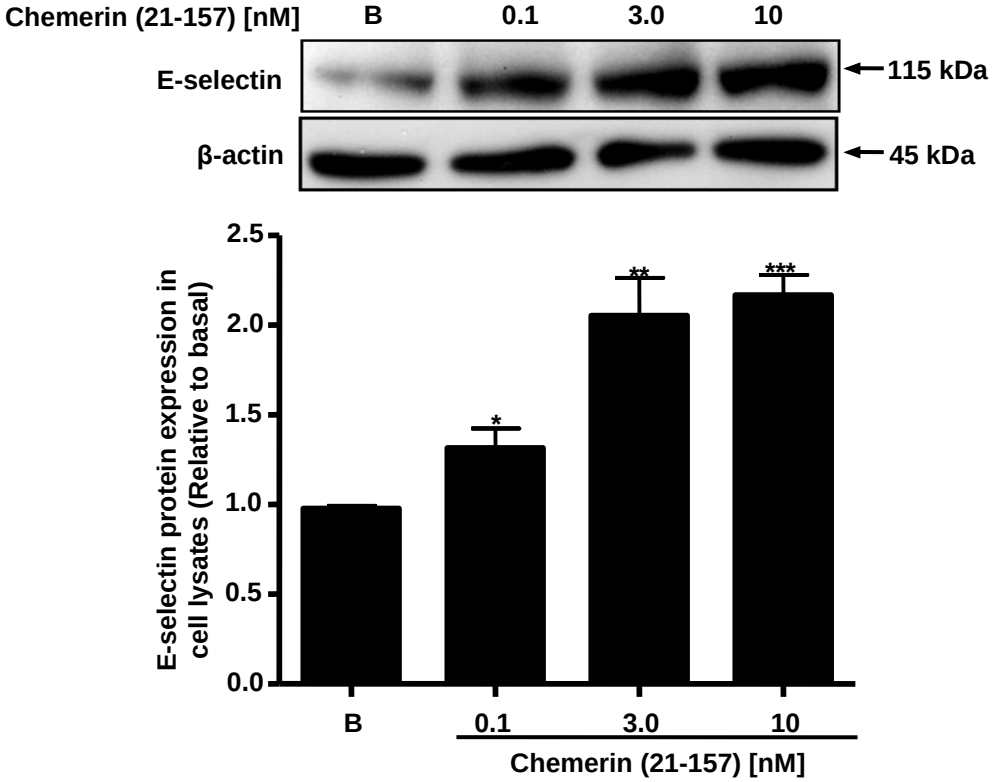

Figure 5.3.1a Chemerin (21-157) increased E-selectin protein expression in a concentration-dependent manner in HMEC-1 cell line after 12 hours

HMEC-1 cells were treated with different chemerin (21-157) concentrations [0-10nM] for 12 hours. Following cell lysis and sample preparations, the protein lysates were separated using 8% polyacrylamide gels, and transferred to PVDF membranes at 100V for 1 hour. Membranes were incubated with specific mouse E-selectin antibody [(1:800); Santa Cruz, USA] overnight at 4^{o}C. After removing the primary antibody complexes, membranes were incubated with anti-mouse IgG-HRP labelled antibody [(1:8000); Sigma-Aldrich, UK] for 1 hour at RT. Protein complexes were visualised using ECL plus detection reagent on X-ray films. Membrane was re-probed with rabbit β-actin antibody [(1:1500); Cell signalling, Beverly, MA, USA] and used as a loading control. The corresponding bands for both E-selectin and β-actin were detected as 115kDa and 45kDa products. The band intensities were measured using Scion Image™ densitometer (Scion Corporation, Maryland, USA). The data are presented as mean ± SEM of three independent experiments in duplicates ***$p < 0.001$, **$p < 0.01$ and *$p < 0.05$ compared to basal.

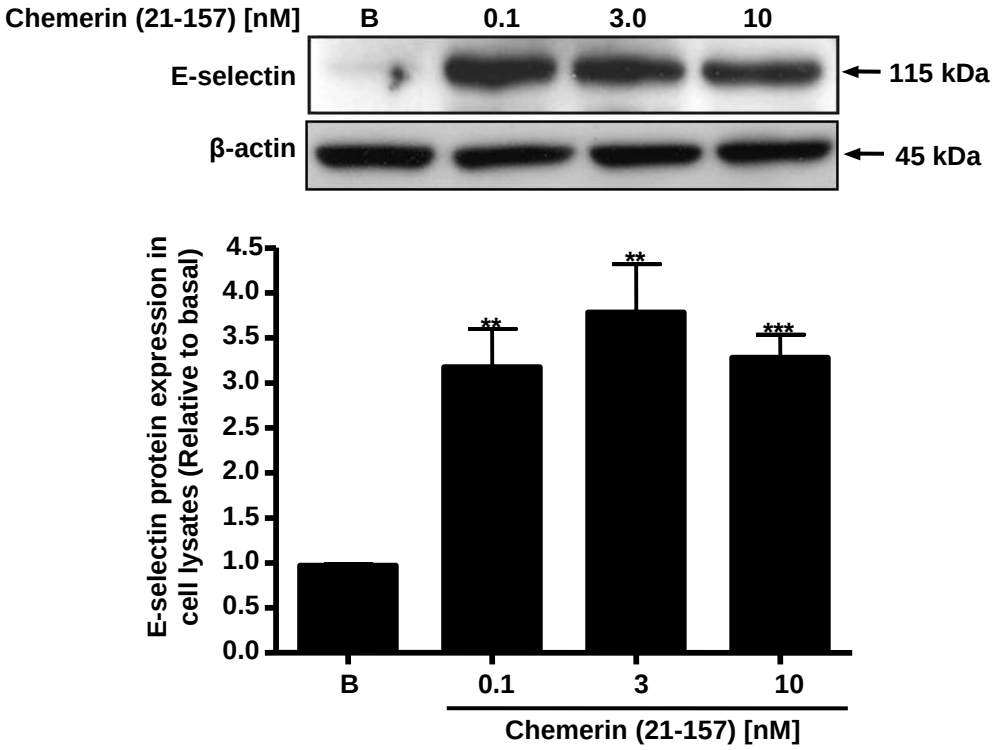

Figure 5.3.1b Chemerin (21-157) increased E-selectin protein expression in a concentration-dependent manner in HMEC-1 cell line after 24 hours

HMEC-1 cells were treated with different chemerin (21-157) concentrations [0-10nM] for 24 hours. Following cell lysis and sample preparations, the protein lysates were separated using 8% polyacrylamide gels, and transferred to PVDF membranes at 100V for 1 hour. Membranes were incubated with specific mouse E-selectin antibody [(1:800); Santa Cruz, USA] overnight at 4^{o}C. After removing the primary antibody complexes, membranes were incubated with anti-mouse IgG-HRP labelled antibody [(1:8000); Sigma-Aldrich, UK] for 1 hour at RT. Protein complexes were visualised using ECL plus detection reagent on X-ray films. Membrane was re-probed with rabbit β-actin antibody [(1:1500); Cell signalling, Beverly, MA, USA] and used as a loading control. The corresponding bands for both E-selectin and β-actin were detected as 115kDa and 45kDa products. The band intensities were measured using Scion Image™ densitometer (Scion Corporation, Maryland, USA). The data are presented as mean ± SEM of three independent experiments in duplicates ***$p < 0.001$, **$p < 0.01$ and *$p < 0.05$ compared to basal.

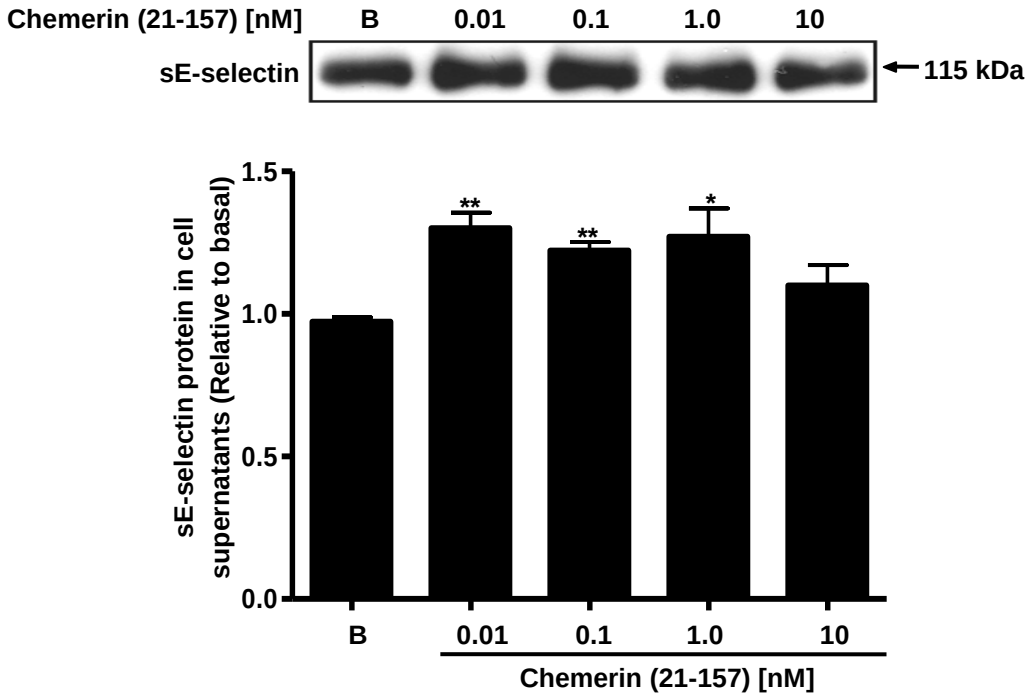

Figure 5.3.1c Chemerin (21-157) increased sE-selectin protein secretion in HMEC-1 cell supernatants in a concentration-dependent manner after 24 hours

HMEC-1 cells were treated with different chemerin (21-157) concentrations [0-10nM] for 24 hours and cell supernatants were collected. Samples were prepared by mixing equal volumes of cell supernatants with 1x Laemmili buffer solution. Following sample preparations, the proteins were separated using 8% polyacrylamide gels, and transferred to PVDF membranes at 100V for 1 hour. Membranes were incubated with specific mouse E-selectin antibody [(1:800); Santa Cruz, USA] overnight at 4^{o}C. After removing the primary antibody complexes, membranes were incubated with anti-mouse IgG-HRP labelled antibody [(1:8000); Sigma-Aldrich, UK] for 1 hour at RT. Protein complexes were visualised using ECL plus detection reagent on X-ray films. The corresponding band for sE-selectin was detected as a 115kDa product. The band intensities were measured using Scion Image™ densitometer (Scion Corporation, Maryland, USA). The data are presented as mean ± SEM of three independent experiments in duplicates $^{**}p < 0.01$ and $^{*}p < 0.05$ compared to basal.

5.3.2 Chemerin (21-157) and VCAM-1 Protein Expression and Secretion in HMEC-1 Cell Line

HMEC-1 cells were cultured in 6-well plates in MCDB cell medium containing 10% FCS, and were serum starved in the same medium containing 1% FCS overnight before performing various different treatments. To study cellular protein expression of VCAM-1, HMEC-1 cells were treated with different chemerin (21-157) [0-10nM] concentrations for 12 and 24 hours. Cells were lysed in 1x RIPA buffer and protein lysates were separated using SDS-PAGE. To study secreted levels of VCAM-1 protein in EC supernatants, HMEC-1 cells were treated with different chemerin (21-157) [0-30nM] concentrations for 4, 12 and 24 hours. Cell supernatants were collected and soluble VCAM-1 (sVCAM-1) levels were determined using Luminex® 100 instrument in all three different treatment groups. In addition, in 24 hours cell supernatants, sVCAM-1 protein expression was studied using SDS-PAGE. Chemerin (21-157) significantly upregulated cellular VCAM-1 protein expression in a concentration-dependent manner in both 12 hours (Fig. 5.3.2a) and 24 hours (Fig. 5.3.2b) cell lysates ($p < 0.01$, $p < 0.01$ and $p < 0.05$). In 24 hours treated cell supernatants, chemerin (21-157) significantly increased sVCAM-1 protein expression in a concentration-dependent manner ($p < 0.01$, $p < 0.01$ and $p < 0.05$) (Fig. 5.3.2c). In contrast, sVCAM-1 proteins were not detected in HMEC-1 cell supernatants in all chemerin (21-157) treated cell supernatants in all treatment groups by multiplex ELISA (Appendix 7.2, Table 7.2a, b and c; page numbers 257-60). TNF-α [10ng/ml] and IL-1β [10ng/ml] were used as positive controls.

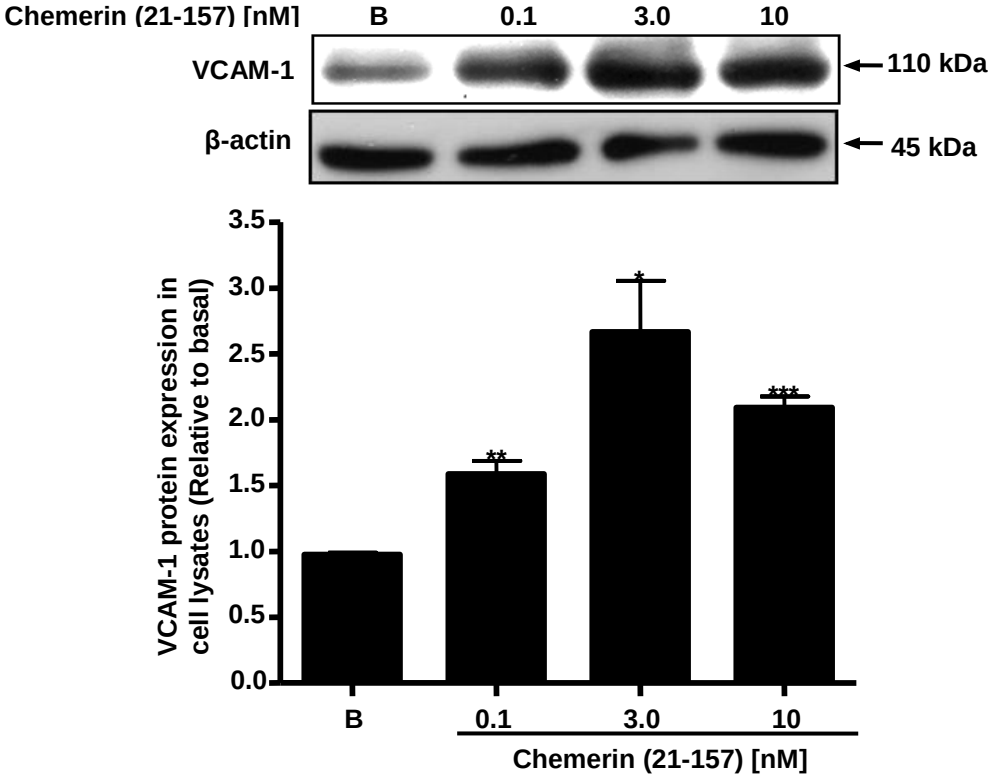

Figure 5.3.2a Chemerin (21-157) increased VCAM-1 protein expression in a concentration-dependent manner in HMEC-1 cell line after 12 hours

HMEC-1 cells were treated with chemerin (21-157) [0-10nM] for 12 hours. Following cell lysis and sample preparations, the protein lysates were separated using 8% polyacrylamide gels, and transferred to PVDF membranes at 100V for 1 hour. Membranes were incubated with specific mouse anti-VCAM-1 antibody [(1:800); Santa Cruz, USA] overnight at 4^{o}C. After removing the primary antibody complexes, membranes were incubated with anti-mouse IgG-HRP labelled antibody [(1:8000); Sigma-Aldrich, UK] for 1 hour at RT. Protein complexes were visualised using ECL plus detection reagent on X-ray films. Membrane was re-probed with rabbit β-actin antibody [(1:1500); Cell signalling, Beverly, MA, USA] and used as a loading control. The corresponding bands for VCAM-1 and β-actin were detected as 110kDa and 45kDa products. The band intensities were measured using Scion Image™ densitometer (Scion Corporation, Maryland, USA). The data are presented as mean ± SEM of three independent experiments in duplicates ***$p < 0.001$, **$p < 0.01$ and *$p < 0.05$ compared to basal.

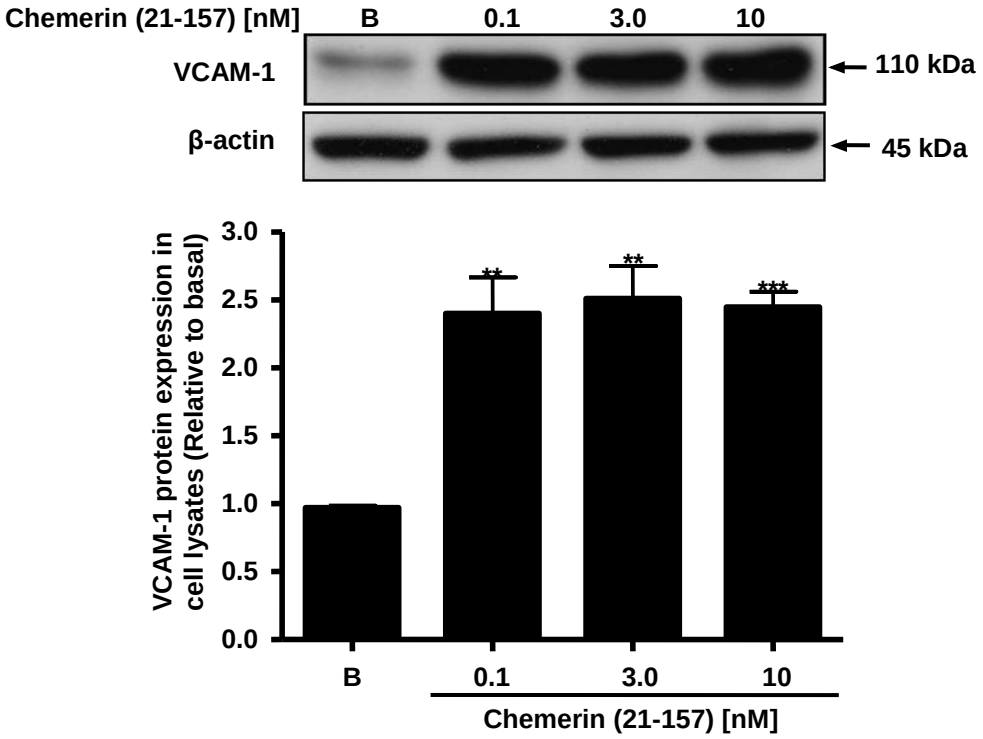

Figure 5.3.2b Chemerin (21-157) increased VCAM-1 protein expression in a concentration-dependent manner in HMEC-1 cell line after 24 hours

HMEC-1 cells were treated with chemerin (21-157) [0-10nM] for 24 hours. Following cell lysis and sample preparations, the protein lysates were separated using 8% polyacrylamide gels, and transferred to PVDF membranes at 100V for 1 hour. Membranes were incubated with specific mouse anti-VCAM-1 antibody [(1:800); Santa Cruz, USA] overnight at 4^{o}C. After removing the primary antibody complexes, membranes were incubated with anti-mouse IgG-HRP labelled antibody [(1:8000); Sigma-Aldrich, UK] for 1 hour at RT. Protein complexes were visualised using ECL plus detection reagent on X-ray films. Membrane was re-probed with rabbit β-actin antibody [(1:1500); Cell signalling, Beverly, MA, USA] and used as a loading control. The corresponding bands for VCAM-1 and β-actin were detected as 110kDa and 45kDa products. The band intensities were measured using Scion Image™ densitometer (Scion Corporation, Maryland, USA). The data are presented as mean ± SEM of three independent experiments in duplicates ***$p < 0.001$ and **$p < 0.01$ compared to basal.

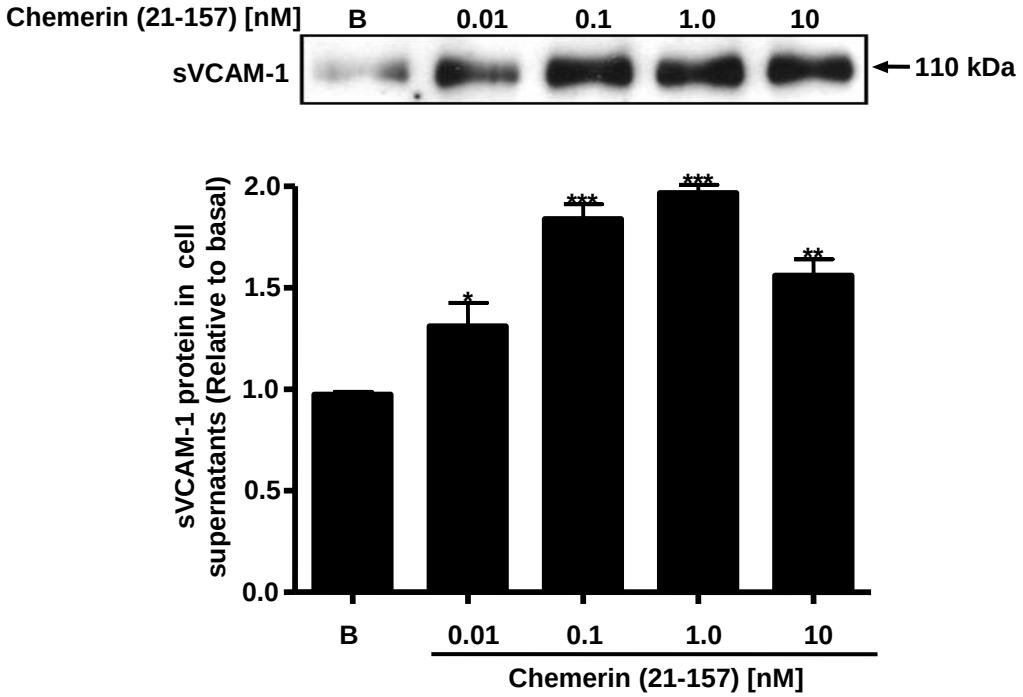

Figure 5.3.2c Chemerin (21-157) increased VCAM-1 protein secretion in HMEC-1 supernatants a concentration-dependent manner after 24 hours

HMEC-1 cells were treated with chemerin (21-157) [0-10nM] for 24 hours and cell supernatants were collected. Samples were prepared by mixing equal volumes of cell supernatants and 1xLaemmili buffer solution. Following sample preparations, the proteins were separated using 8% polyacrylamide gels, and transferred to PVDF membranes at 100V for 1 hour. Membranes were incubated with specific mouse anti-VCAM-1 antibody [(1:800); Santa Cruz, USA] overnight at 4^{o}C. After removing the primary antibody complexes, membranes were incubated with anti-mouse IgG-HRP labelled antibody [(1:8000); Sigma-Aldrich, UK] for 1 hour at RT. Protein complexes were visualised using ECL plus detection reagent on X-ray films. The corresponding band for sVCAM-1 was detected as a 110kDa product. The band intensities were measured using Scion Image™ densitometer (Scion Corporation, Maryland, USA). The data are presented as mean ± SEM of three independent experiments in duplicates ***$p < 0.001$, **$p < 0.01$ and **$p < 0.05$ compared to basal.

5.3.3 Chemerin (21-157) and ICAM-1 Protein Expression and Secretion in HMEC-1 Cell Line

HMEC-1 cells were cultured in 6-well plates in specific cell medium containing 10% FCS, and were serum starved in the same medium containing 1% FCS overnight before performing various different treatments. To study cellular protein expression of ICAM-1, HMEC-1 cells were treated with different chemerin (21-157) concentrations [0-10nM] for 12 and 24 hours. Cells were lysed in 1x RIPA buffer and protein lysates were separated using SDS-PAGE. To study secreted levels of ICAM-1 in endothelial cells, HMEC-1 cells were treated with different chemerin (21-157) concentrations [0-30nM] for 4, 12 and 24 hours. Cell supernatants were collected and soluble ICAM-1 (sICAM-1) levels were determined using Luminex® 100 instrument in all three different treatment groups. In addition, in 24 hours cell supernatants, sVCAM-1 protein expression was studied using SDS-PAGE. Chemerin (21-157) significantly increased cellular ICAM-1 protein expression in a concentration-dependent manner in both 12 hours (Fig. 5.3.3a) and 24 hours (Fig. 5.3.3b) cell lysates ($p < 0.001$, $p < 0.01$ and $p < 0.05$). In 24 hours treated cell supernatants, chemerin (21-157) significantly increased sICAM-1 protein expression in a concentration-dependent manner ($p < 0.01$, $p < 0.01$ and $p < 0.01$) (Fig. 5.3.3c). Multiplex ELISA failed to detect any sICAM-1 protein levels, and different chemerin (21-157) treatments failed to show any change in sICAM-1 protein levels in HMEC-1 cell supernatants in all three different treatment groups (Appendix 7.3, Table 7.3a, b and c; page numbers 261-64). TNF-α [10ng/ml] and IL-1β [10ng/ml] were used as positive controls.

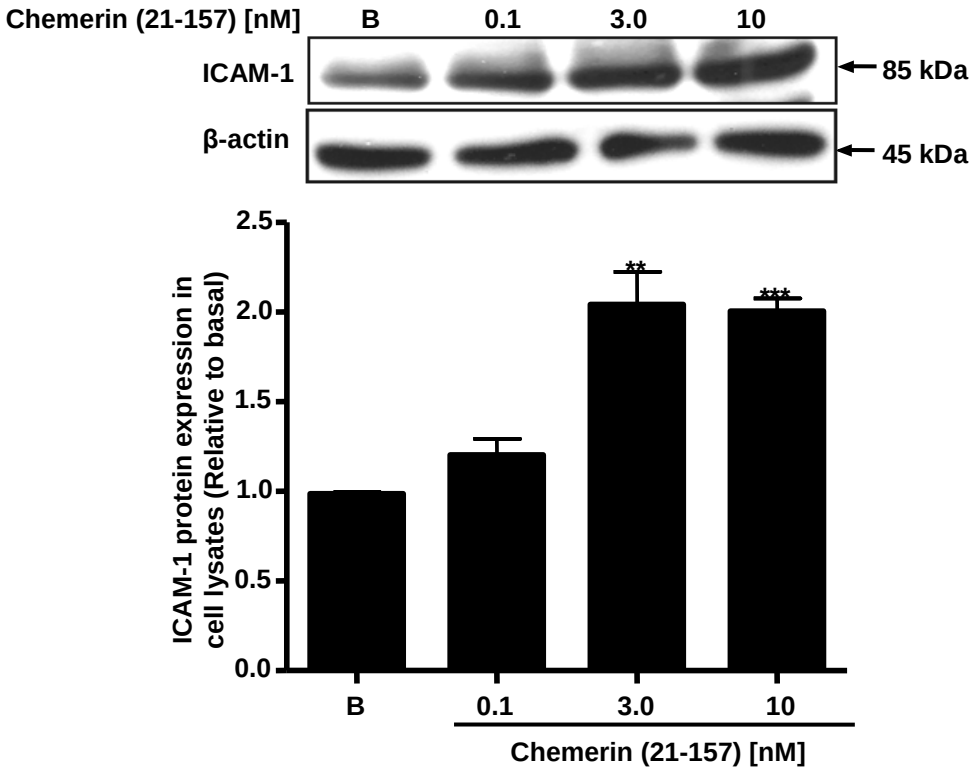

Figure 5.3.3a Chemerin (21-157) increased ICAM-1 protein expression in a concentration-dependent manner in HMEC-1 cell line after 12 hours

HMEC-1 cells were treated with chemerin (21-157) [0-10nM] for 12 hours. Following cell lysis and sample preparations, protein lysates were separated using 10% polyacrylamide gels and transferred to PVDF membranes at 100V for 1 hour. Membranes were incubated with specific mouse anti-ICAM-1 antibody [(1:800); Santa Cruz, USA] overnight at 4^{o}C. After removing the primary antibody complexes, membranes were incubated with anti-mouse IgG-HRP labelled antibody [(1:8000); Sigma-Aldrich, UK] for 1 hour at RT. Protein complexes were visualised using ECL plus detection reagent on X-ray films. Membrane was re-probed with rabbit β-actin antibody [(1:1500); Cell signalling, Beverly, MA, USA] and used as a loading control. The corresponding bands for ICAM-1 and β-actin were detected as 85kDa and 45kDa products. The band intensities were measured using Scion Image™ densitometer (Scion Corporation, Maryland, USA). The data are presented as mean ± SEM of three independent experiments in duplicates ***$p < 0.001$ and **$p < 0.01$ compared to basal.

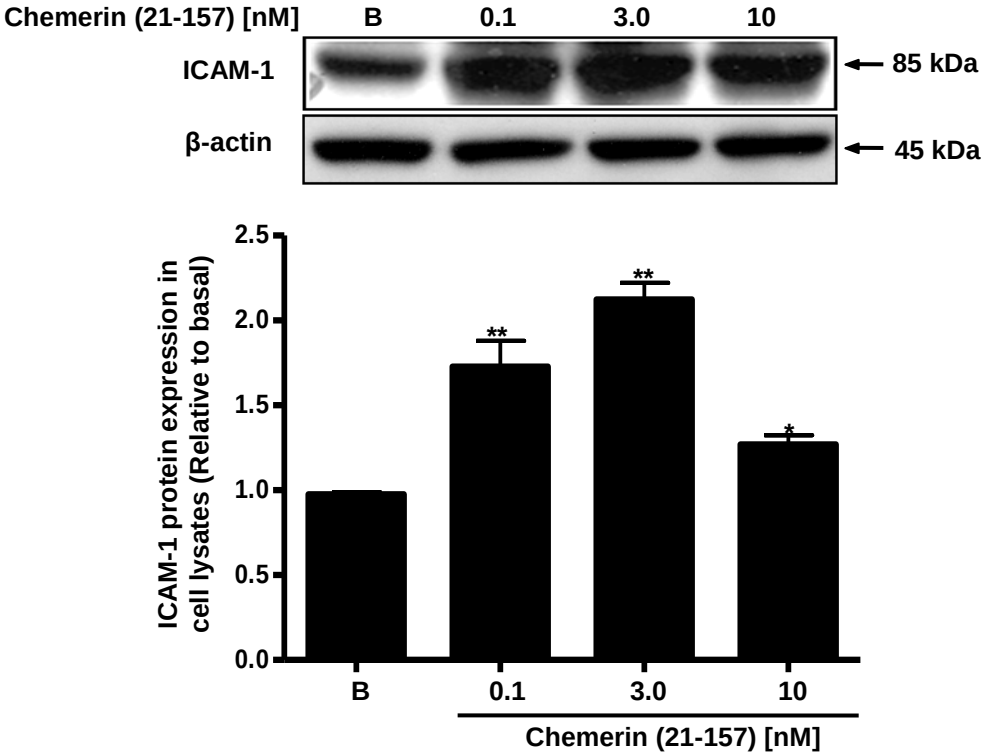

Figure 5.3.3b Chemerin (21-157) increased ICAM-1 protein expression in a concentration-dependent manner in HMEC-1 cell line after 24 hours

HMEC-1 cells were treated with chemerin (21-157) [0-10nM] for 12 hours. Following cell lysis and sample preparations, the protein lysates were separated using 10% polyacrylamide gels, and transferred to PVDF membranes at 100V for 1 hour. Membranes were incubated with specific mouse anti-ICAM-1 antibody [(1:800); Santa Cruz, USA] overnight at 4^{o}C. After removing the primary antibody complexes, membranes were incubated with anti-mouse IgG-HRP labelled antibody [(1:8000); Sigma-Aldrich, UK] for 1 hour at RT. Protein complexes were visualised using ECL plus detection reagent on X-ray films. Membrane was re-probed with rabbit β-actin antibody [(1:1500); Cell signalling, Beverly, MA, USA] and used as a loading control. The corresponding bands for ICAM-1 and β-actin were detected as 85kDa and 45kDa products. The band intensities were measured using Scion Image™ densitometer (Scion Corporation, Maryland, USA). The data are presented as mean ± SEM of three independent experiments in duplicates $^{**}p < 0.01$ and $^{*}p < 0.05$ compared to basal.

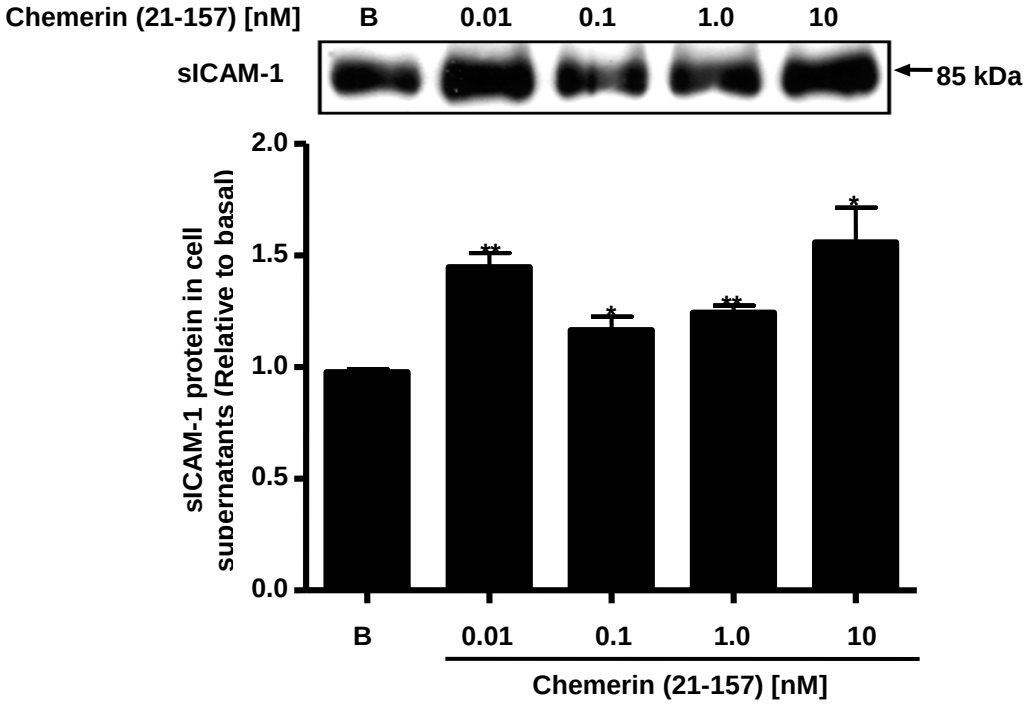

Figure 5.3.3c Chemerin (21-157) increased ICAM-1 protein secretion in HMEC-1 cell supernatants in a concentration-dependent manner after 24 hours

HMEC-1 cells were treated with chemerin (21-157) [0-10nM] for 24 hours and cell supernatants were collected. Samples were prepared by mixing equal volumes of cell supernatants and 1x Laemmili buffer solution. Following sample preparations, the proteins were separated using 10% polyacrylamide gels and transferred to PVDF membranes at 100V for 1 hour. Membranes were incubated with specific mouse anti-ICAM-1 antibody [(1:800); Santa Cruz, USA] overnight at 4^{o}C. After removing the primary antibody complexes, membranes were incubated with anti-mouse IgG-HRP labelled antibody [(1:8000); Sigma-Aldrich, UK] for 1 hour at RT. Protein complexes were visualised using ECL plus detection reagent on X-ray films. The corresponding band for sICAM-1 was detected as a 85kDa product. The band intensities were measured using Scion Image™ densitometer (Scion Corporation, Maryland, USA). The data are presented as mean ± SEM of three independent experiments in duplicates $^{**}p < 0.01$ and $^{*}p < 0.01$ compared to basal.

5.3.4 Combined Chemerin (21-157) and Interleukin-1β Treatments Resulted in Altered E-selectin, VCAM-1 and ICAM-1 Protein Expression in HMEC-1 Cell Line

HMEC-1 cells were cultured in 6-well plates in MCDB cell medium containing 10% FCS, and cells were serum starved in the same medium containing 1% FCS overnight before performing different treatments. HMEC-1 cells were incubated with IL-1β [10ng/ml] at different time-points for a maximum of 18 hours. At 6 hours incubation, IL-1β [10ng/ml] showed maximum VCAM-1 and ICAM-1 protein expressions (Appendix 6, Fig. 6.1a and b respectively, page numbers 249-51). To study the combined effects of chemerin (21-157) and IL-1β on E-selectin, VCAM-1 and ICAM-1 protein expressions, HMEC-1 cells were pre-incubated with IL-1β [10ng/ml] for 6 hours, and then treated with [3.0nM] chemerin (21-157) for further 12 hours. Cells were lysed in 1x RIPA buffer and protein lysates were separated using SDS-PAGE. Combined IL-1β and chemerin (21-157) treatments in HMEC-1 cells resulted in altered protein expression levels of E-selectin ($p < 0.01$ and $p < 0.05$) (Fig. 5.3.4a), VCAM-1 ($p < 0.001$ and $p < 0.01$) (Fig. 5.3.4b) and ICAM-1 ($p < 0.001$ and $p < 0.01$) compared to chemerin (21-157) and IL-1β alone (relative to basal) (Fig. 5.3.4c). For all three different adhesion molecules, same β-actin loading control was used and was run separately using 10% gels.

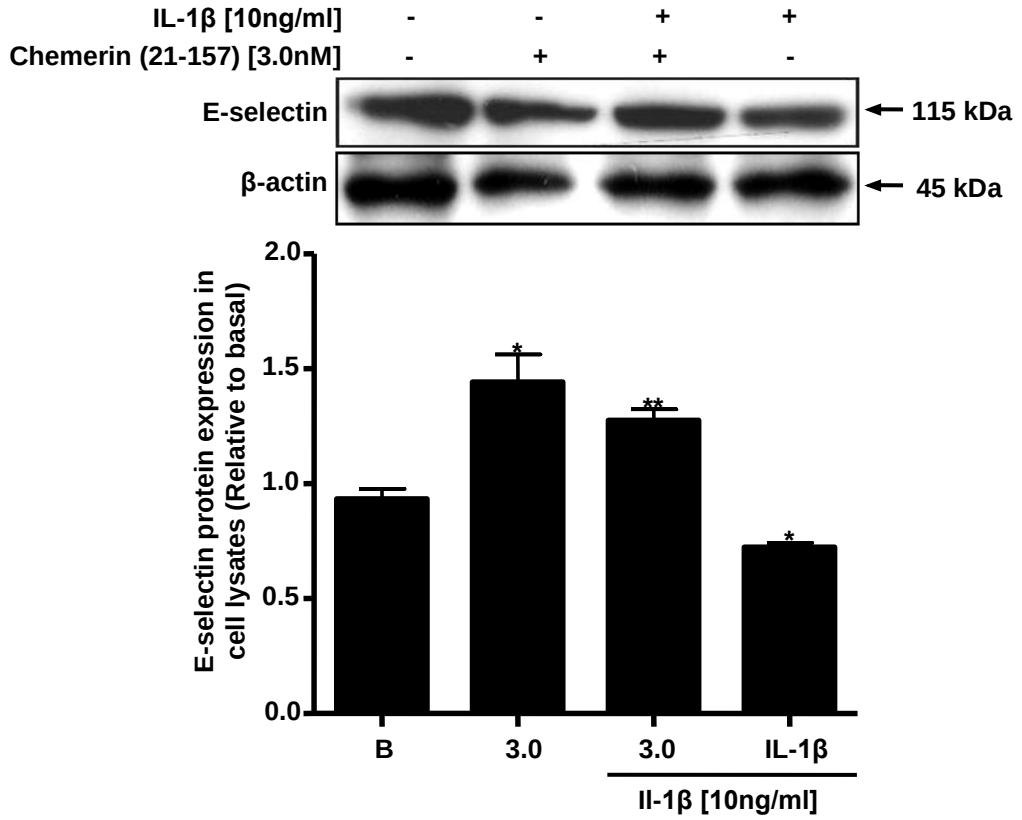

Figure 5.3.4a Combined chemerin (21-157) and interleukin-1β treatments resulted in altered E-selectin protein expression in HMEC-1 cell line after 12 hours

HMEC-1 cells were pre-treated with IL-1β [10ng/ml] for 6 hours followed by chemerin (21-157) [3.0nM] stimulation for 12 hours. Following cell lysis and sample preparations, the protein lysates were separated using 8% polyacrylamide gels, and transferred to PVDF membranes at 100V for 1 hour. Membranes were incubated with specific mouse E-selectin antibody [(1:800); Santa Cruz, USA] overnight at 4^{o}C. After removing the primary antibody complexes, membranes were incubated with anti-mouse IgG-HRP labelled antibody [(1:8000); Sigma-Aldrich, UK] for 1 hour at RT. Protein complexes were visualised using ECL plus detection reagent on X-ray films. Membrane was re-probed with rabbit β-actin antibody [(1:1500); Cell signalling, Beverly, MA, USA] and used as a loading control. The corresponding bands for both E-selectin and β-actin were detected as 115kDa and 45kDa products. The band intensities were measured using Scion Image™ densitometer (Scion Corporation, Maryland, USA). The data are presented as mean ± SEM of three independent experiments in duplicates $^{**}p < 0.01$ and $^{*}p < 0.05$ compared to basal.

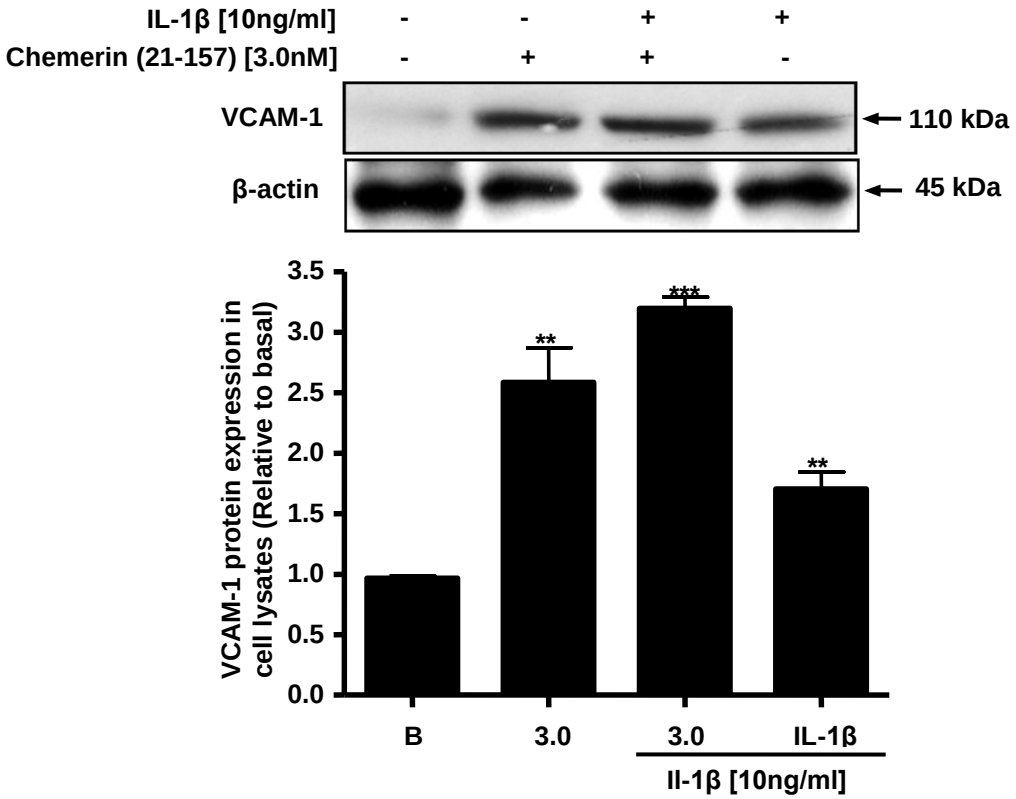

Figure 5.3.4b Combined chemerin (21-157) and interleukin-1β treatments resulted in altered VCAM-1 protein expression in HMEC-1 cell line after 12 hours

HMEC-1 cells were pre-treated with IL-1β [10ng/ml] for 6 hours followed by chemerin [3.0nM] stimulation for 12 hours. Following cell lysis and sample preparations, the protein lysates were separated using 8% polyacrylamide gels, and transferred to PVDF membranes at 100V for 1 hour. Membranes were incubated with specific mouse anti-VCAM-1 antibody [(1:800); Santa Cruz, USA] overnight at 4^{o}C. After removing the primary antibody complexes, membranes were incubated with anti-mouse IgG-HRP labelled antibody [(1:8000); Sigma-Aldrich, UK] for 1 hour at RT. Protein complexes were visualised using ECL plus detection reagent on X-ray films. Membrane was re-probed with rabbit β-actin antibody [(1:1500); Cell signalling, Beverly, MA, USA] and used as a loading control. The corresponding bands for VCAM-1 and β-actin were detected as 110kDa and 45kDa products. The band intensities were measured using Scion Image™ densitometer (Scion Corporation, Maryland, USA). The data are presented as mean ± SEM of three independent experiments in duplicates ***$p < 0.001$ and **$p < 0.01$ compared to basal.

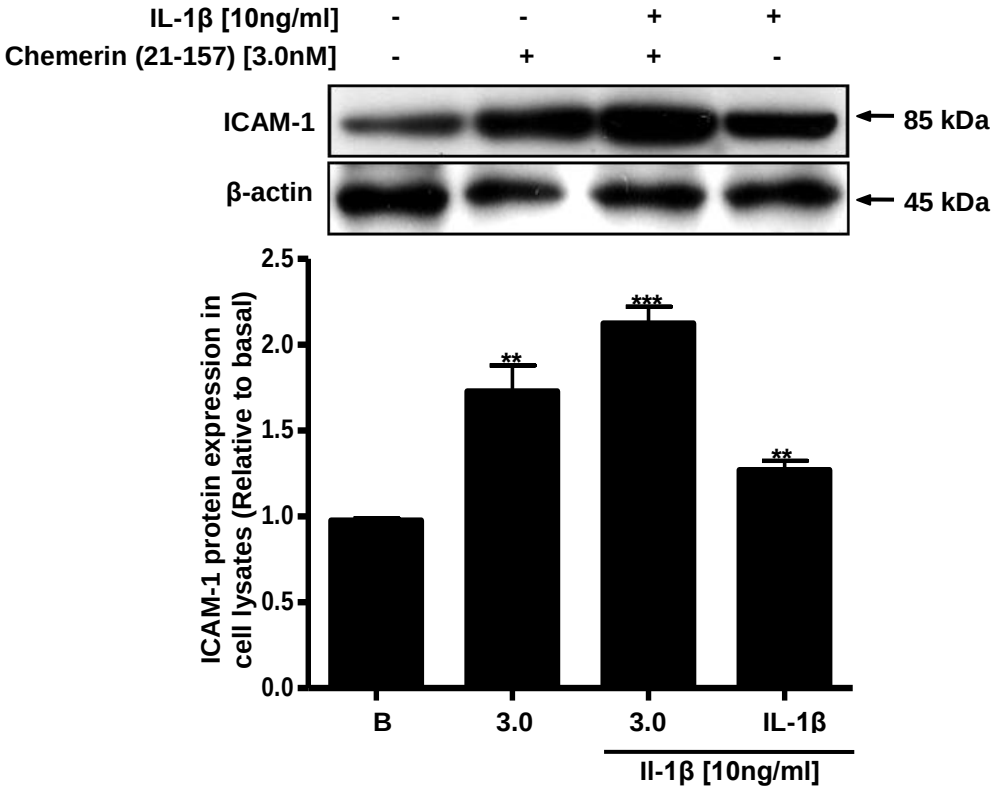

Figure 5.3.4c Combined chemerin (21-157) and interleukin-1β treatments resulted in altered ICAM-1 protein expression in HMEC-1 cell line after 12 hours

HMEC-1 cells were pre-treated with IL-1β [10ng/ml] for 6 hours followed by chemerin [3.0nM] stimulation for 12 hours. Following cell lysis and sample preparations, the protein lysates were separated using 10% polyacrylamide gels, and transferred to PVDF membranes at 100V for 1 hour. Membranes were incubated with specific mouse anti-ICAM-1 antibody [(1:800); Santa Cruz, USA] overnight at 4^{o}C. After removing the primary antibody complexes, membranes were incubated with anti-mouse IgG-HRP labelled antibody [(1:8000); Sigma-Aldrich, UK] for 1 hour at RT. Protein complexes were visualised using ECL plus detection reagent on X-ray films. Membrane was re-probed with rabbit β-actin antibody [(1:1500); Cell signalling, Beverly, MA, USA] and used as a loading control. The corresponding bands for ICAM-1 and β-actin were detected as 85kDa and 45kDa products. The band intensities were measured using Scion Image™ densitometer (Scion Corporation, Maryland, USA). The data are presented as mean ± SEM of three independent experiments in duplicates ***$p < 0.001$ and **$p < 0.01$ compared to basal.

5.3.5 Chemerin (21-157) and MCP-1 Protein Expression in HMEC-1 Cell Line

HMEC-1 cells were cultured in 6-well plates in MCDB cell medium containing 10% FCS, and were serum starved in the same medium containing 1% FCS overnight before performing different treatments. To study cellular protein expression of MCP-1, HMEC-1 cells were treated with different chemerin (21-157) concentrations [0-10nM] for 12 and 24 hours. Cells were lysed in 1x RIPA buffer and protein lysates were separated using SDS-PAGE. Chemerin (21-157) significantly increased MCP-1 protein expression in a concentration-dependent manner at 12 hours and 24 hours ($p < 0.001$, $p < 0.01$ and $p < 0.05$) (Fig. 5.3.5a and b respectively).

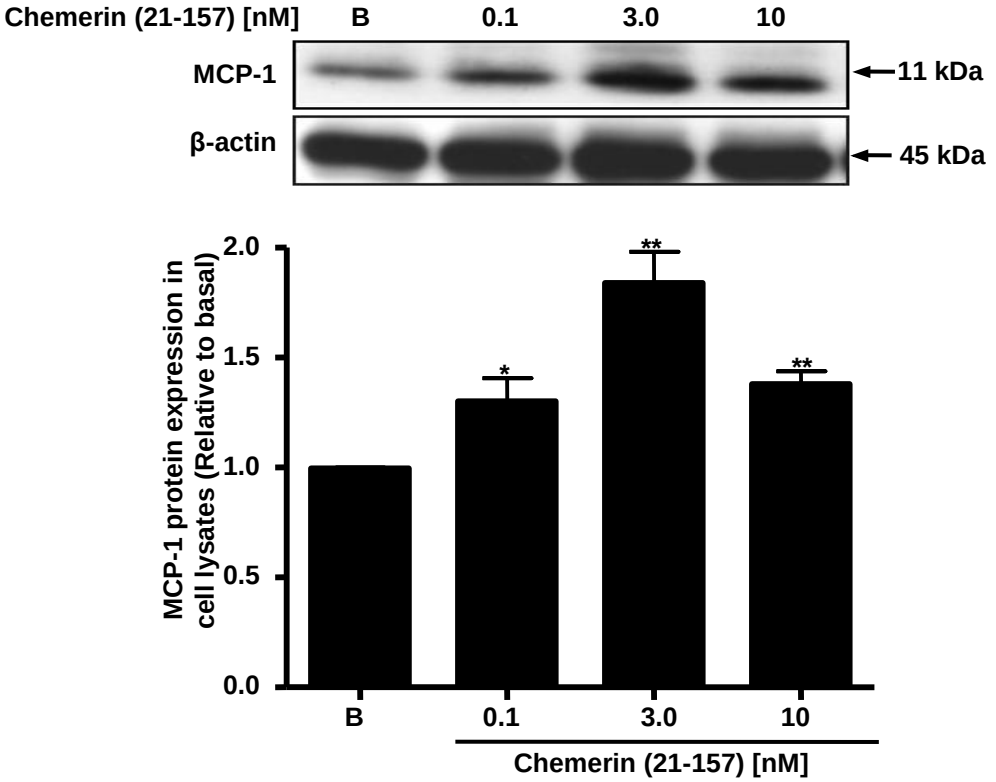

Figure 5.3.5a Chemerin (21-157) increased MCP-1 protein expression in a concentration-dependent manner in HMEC-1 cell line after 12 hours

HMEC-1 cells were treated with chemerin (21-157) [0-10nM] for 12 hours. Following cell lysis and sample preparations, the protein lysates were separated using 15% polyacrylamide gels, and transferred to PVDF membranes at 100V for 1 hour. Membranes were incubated with specific mouse anti-MCP-1 antibody [(1:800); Santa Cruz, USA] overnight at 4^{o}C. After removing the primary antibody complexes, membranes were incubated with anti-mouse IgG-HRP labelled antibody [(1:8000); Sigma-Aldrich, UK] for 1 hour at RT. Protein complexes were visualised using ECL plus detection reagent on X-ray films. Membranes were re-probed with rabbit β-actin antibody [(1:1500); Cell signalling, Beverly, MA, USA] and used as a loading control. The corresponding bands for MCP-1 and β-actin were detected as 11kDa and 45kDa products. The band intensities were measured using Scion Image™ densitometer (Scion Corporation, Maryland, USA). The data are presented as mean ± SEM of three independent experiments in duplicates $^{**}p < 0.01$ and $^{*}p < 0.05$ compared to basal.

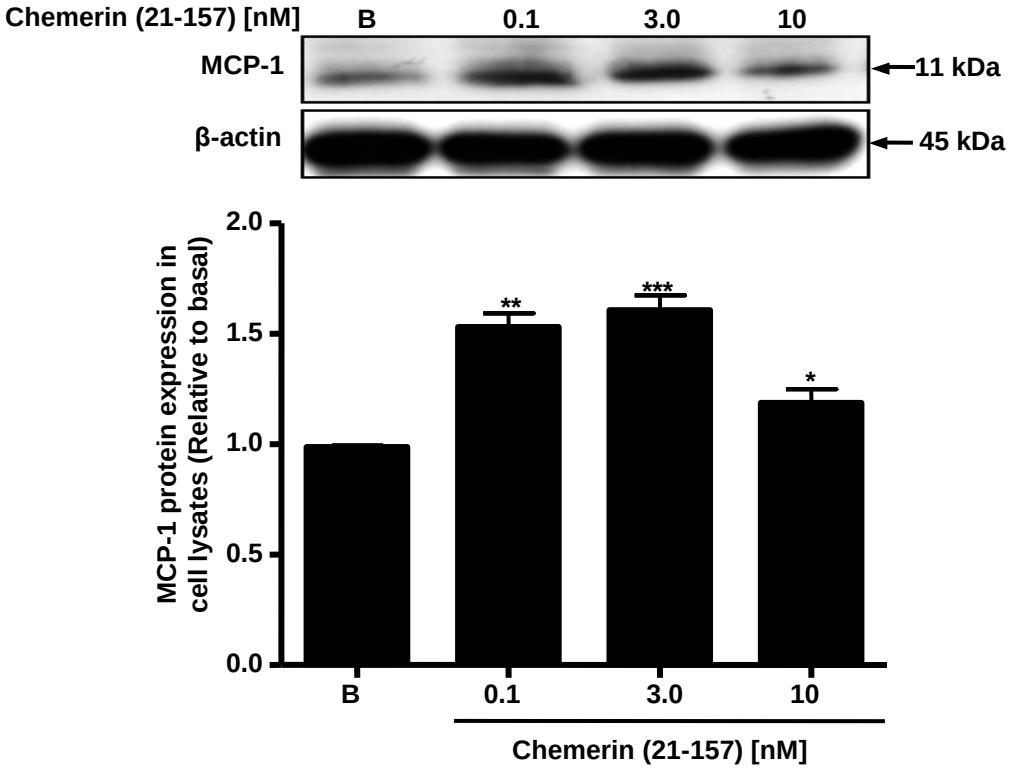

Figure 5.3.5b Chemerin (21-157) increased MCP-1 protein expression in a concentration-dependent manner in HMEC-1 cell line after 24 hours

HMEC-1 cells were treated with chemerin (21-157) [0-10nM] for 24 hours. Following cell lysis and sample preparations, the protein lysates were separated using 15% polyacrylamide gels, and transferred to PVDF membranes at 100V for 1 hour. Membranes were incubated with specific mouse anti-MCP-1 antibody [(1:800); Santa Cruz, USA] overnight at 4^{o}C. After removing the primary antibody complexes, membranes were incubated with anti-mouse IgG-HRP labelled antibody [(1:8000); Sigma-Aldrich, UK] for 1 hour at RT. Protein complexes were visualised using ECL plus detection reagent on X-ray films. Membranes were re-probed with rabbit β-actin antibody [(1:1500); Cell signalling, Beverly, MA, USA] and used as a loading control. The corresponding bands for MCP-1 and β-actin were detected as 11kDa and 45kDa products. The band intensities were measured using Scion Image™ densitometer (Scion Corporation, Maryland, USA). The data are presented as mean ± SEM of three independent experiments in duplicates ***$p < 0.001$, **$p < 0.01$ and **$p < 0.05$ compared to basal.

5.3.6 Combined Chemerin (21-157) and Interleukin-1β Treatments Resulted in Altered MCP-1 Protein Expression in HMEC-1 Cell Line

HMEC-1 cells were cultured in 6-well plates in MCDB cell medium containing 10% FCS, and were serum starved in the same medium containing 1% FCS overnight before performing various different treatments. To study the combined effects of chemerin (21-157) and IL-1β on MCP-1 protein expression, HMEC-1 cells were pre-incubated with IL-1β [10ng/ml] for 6 hours and then with [3.0nM] chemerin (21-157) for 12 hours. Combined IL-1β and chemerin (21-157) treatments resulted in significant increase in MCP-1 protein expression in HMEC-1 cells compared to chemerin (21-157) and IL-1β alone ($p < 0.001$ and $p < 0.01$) (Fig. 5.3.6a).

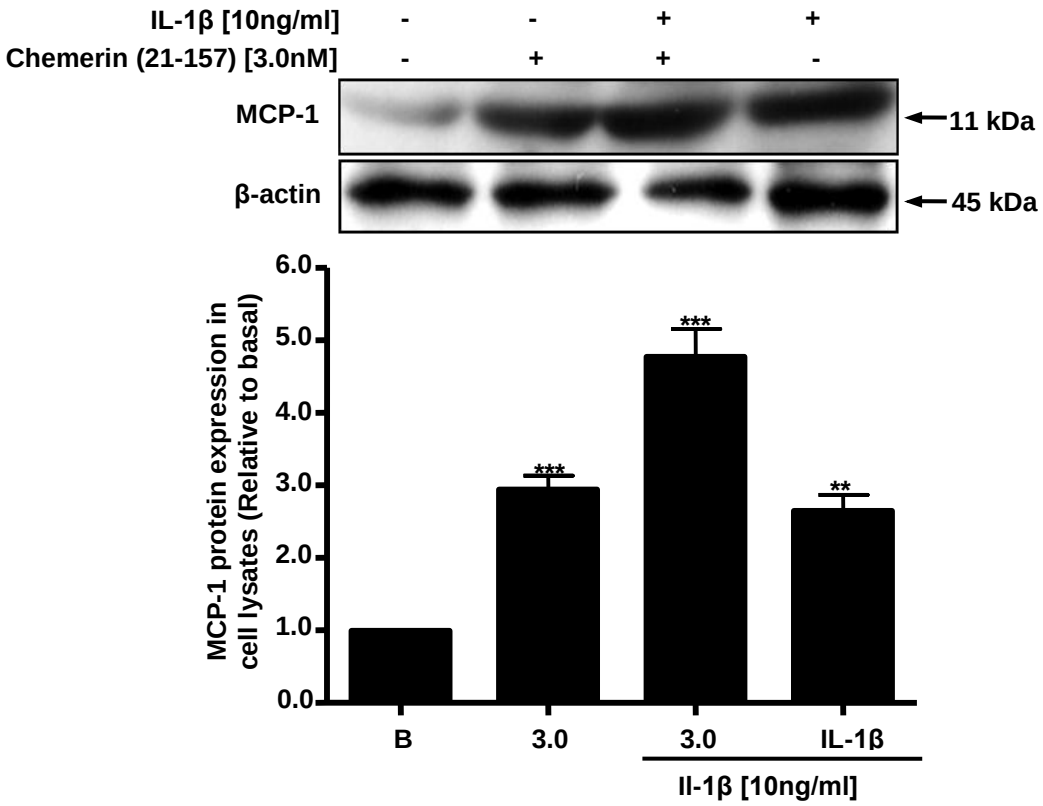

Figure 5.3.6a Combined chemerin (21-157) and interleukin-1β treatments resulted in altered MCP-1 protein expression in HMEC-1 cell line after 12 hours

HMEC-1 cells were pre-treated with IL-1β [10ng/ml] for 6 hours followed by chemerin [3.0nM] stimulation for 12 hours. Following cell lysis and sample preparations, the protein lysates were separated using 15% polyacrylamide gels, and transferred to PVDF membranes at 100V for 1 hour. Membranes were incubated with specific mouse anti-MCP-1 antibody [(1:800); Santa Cruz, USA] overnight at 4^{o}C. After removing the primary antibody complexes, membranes were incubated with anti-mouse IgG-HRP labelled antibody [(1:8000); Sigma-Aldrich, UK] for 1 hour at RT. Protein complexes were visualised using ECL plus detection reagent on X-ray films. Membranes were re-probed with rabbit β-actin antibody [(1:1500); Cell signalling, Beverly, MA, USA] and used as a loading control. The corresponding bands for MCP-1 and β-actin were detected as 11kDa and 45kDa products. The band intensities were measured using Scion Image™ densitometer (Scion Corporation, Maryland, USA). The data are presented as mean ± SEM of three independent experiments in duplicates ***$p < 0.01$ and **$p < 0.01$ compared to basal.

5.3.7 Chemerin (21-157) Increased NF-κB Activity in a Concentration-dependent Manner in HMEC-1 Cell Line

NF-κB activity was measured using NF-κB Luciferase Activity Assay. pcDNA3.1-NF-κB-Luc [0.35µg/µl] plasmid was transfected into the HMEC-1 cells using Lipofectamine and Opti-MEM® medium (Chapter 2, section 2.4.7, page number 68). Following 12 hours incubation, the cell medium was replaced with MCDB medium containing 10% FCS and further incubated for 12 hours. Cells were treated with different chemerin (21-157) [0-10nM] concentrations, and IL-1β [10ng/ml] for a maximum of 24 hours. Following cell treatments, cell lysates were collected and luminescence was measured using a dual luciferase reporter assay system (Luminometer, Promega, UK). Chemerin (21-157) significantly increased NF-κB activity in a concentration-dependent manner, showing an additive increase when co-stimulated with IL-1β and chemerin (21-157) together ($p < 0.001$ and $p < 0.01$) (Fig. 5.3.7a).

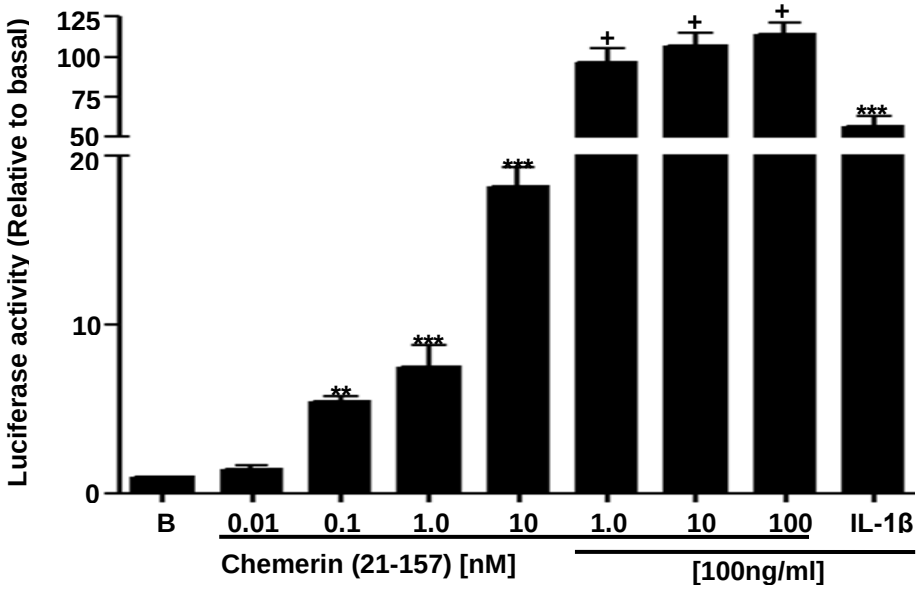

Figure 5.3.7a Chemerin (21-157) and NF-κB activity in HMEC-1 cell line

The pcDNA3.1-NF-κB-Luc was transfected into HMEC-1 using Lipofectamine reagent (Invitrogen, Paisley, UK) and were cultured in 75 cm^2 flask for 24 hours. Cells were trypsinised and cultured in a 6-well plates at the cell density of $3x10^5$ cells/well in cell medium containing 10% FCS for 24 hours. Cells were treated with different chemerin (21-157) concentrations [0-10nM] for 24 hours. Following cell treatments, cell lysates were collected and luminescence was measured using a dual luciferase reporter assay system (Luminometer, Promega, UK). The data are presented as mean ± SEM of three independent experiments in duplicates ***p < 0.001 and **p < 0.01 compared to basal.

5.3.8 Chemerin (21-157)-induced VCAM-1 Protein Expression in the Presence of NF-κB Inhibitor in HMEC-1 Cell Line

HMEC-1 cells were cultured in 6-well plates in MCDB cell medium containing 10% FCS, and were serum starved in the same medium containing 1% FCS overnight before performing various different treatments. HMEC-1 cells were pre-incubated with BAY11-7085, a specific NF-κB inhibitor [10μM] for 1 hour and were treated with [3.0nM] chemerin (21-157) for 12 hours. Cells were lysed in 1x RIPA buffer and protein lysates were separated using SDS-PAGE. Chemerin (21-157) [3.0nM] treatment in BAY11-7085 pre-treated HMEC-1 cells resulted in decreased VCAM-1 protein expression compared to chemerin (21-157) and BAY11-7085 alone ($p < 0.01$ and $p < 0.01$) (relative to basal) (Fig. 5.3.8a).

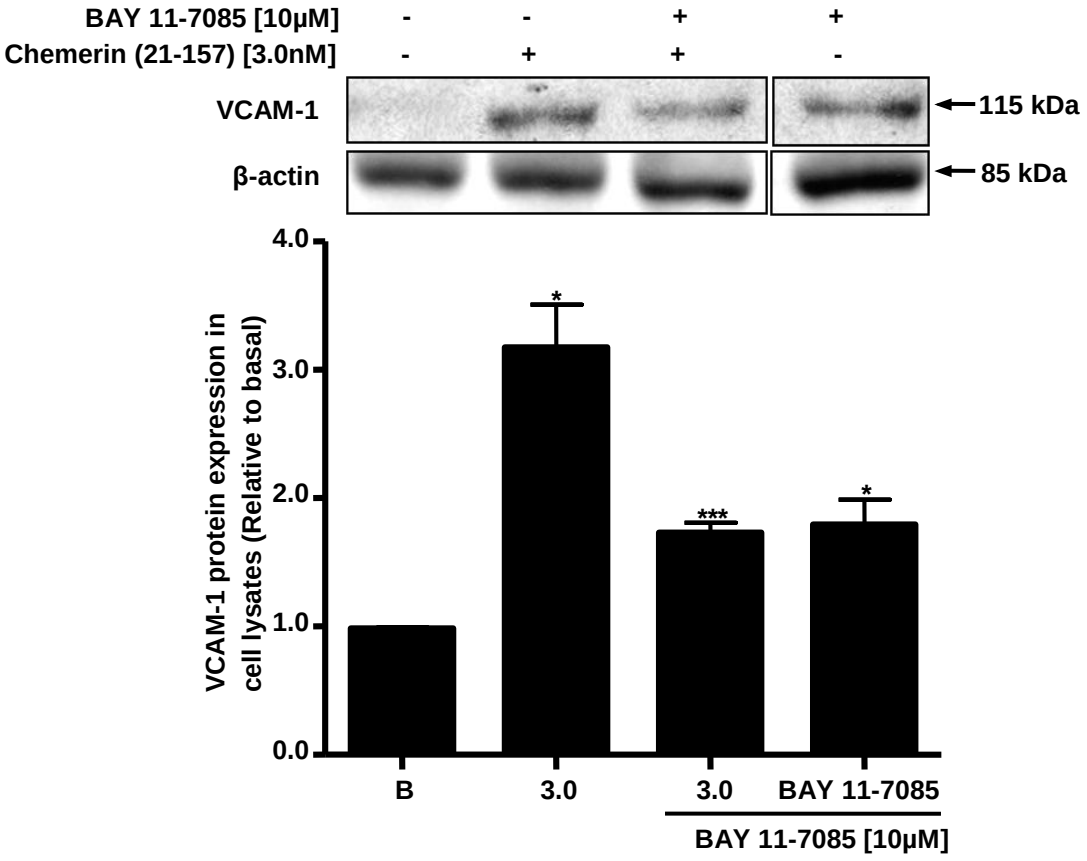

Figure 5.3.8a Chemerin (21-157) decreased VCAM-1 protein expression in HMEC-1 cell line in the presence of BAY11-7085 after 12 hours

HMEC-1 cells were pre-incubated with BAY 11-7085 [10 μM] for 1 hour and were treated with chemerin [3.0nM] for 12 hours. Following cell lysis and sample preparations, the protein lysates were separated using 8% polyacrylamide gels, and transferred to PVDF membranes at 100V for 1 hour. Membranes were incubated with specific mouse anti-VCAM-1 antibody [(1:800); Santa Cruz, USA] overnight at 4^{o}C. After removing the primary antibody complexes, membranes were incubated with anti-mouse IgG-HRP labelled antibody [(1:8000); Sigma-Aldrich, UK] for 1 hour at RT. Protein complexes were visualised using ECL plus detection reagent on X-ray films. Membranes were re-probed with rabbit β-actin antibody [(1:1500); Cell signalling, Beverly, MA, USA] and used as a loading control. The corresponding bands for VCAM-1 and β-actin were detected as 110kDa and 45kDa products. The band intensities were measured using Scion Image™ densitometer (Scion Corporation, Maryland, USA). The data are presented as mean ± SEM of three independent experiments in duplicates $^{**}p < 0.01$ and $^{*}p < 0.05$ compared to basal.

5.3.9 Chemerin (21-157) Induced Endothelial-Monocyte Cell Adhesion in a Concentration-dependent Manner in HMEC-1 Cell Line

Endothelial-Monocyte cell adhesion assay was performed using BD BioCoat Endothelial Cell Adhesion Assay kit (BD Biosciences, San Jose, CA, USA). HMEC-1 cells were trypsinised and a cell suspension containing $2x10^6$ cells/ml in a MCDB cell medium was prepared. 100µl of HMEC-1 cell suspension was added to each 96-well tissue culture plate (included in the kit) and incubated for 3 hours to allow attachment of cells to the plate surface. Post incubation, cell medium was aspirated out and 100µl of Cycloheximide solution was added to the control wells, and 100µl of fresh 10% FCS MCDB cell medium. Endothelial cells were activated by adding 10µl of TNF-α [20ng/ml] to respective wells. Cells were pre-treated with different inhibitors; BAY11-7085 [10µM] for 1 hour, U0126 [10µM] for 1 hour, SB203580 [10µM] for 30minutes, and LY294002 [10µM] for 1 hour; and were treated with different chemerin (21-157) [0-10nM] concentrations for 6 hours. 75µl of medium was aspirated out from the plate wells and washed gently with 200µl of Assay Buffer twice. After the last wash, 50µl of Assay Buffer solution was added to each well and 100µl of Calcein AM labelled THP-1 monocytes (~50,000 to 200,000 cells) were added and incubated for 30 minutes at 37^oC. Approximately, 120µl solution was aspirated out from the plate wells, and two 200µl cell washes were performed using Assay Buffer solution. An additional wash was performed to remove any remaining unbound cells in order to eliminate non-specific binding. 100µl of Assay Buffer was added to each well and the plate reading was performed using a fluorescent plate reader with an excitation/emission filter of 485/530nm. Chemerin (21-157) significantly increased monocyte-endothelial cell adhesion in a concentration-dependent manner ($p < 0.05$ and $p < 0.01$), and was significantly afflicted in cells

pre-treated with U0126 ($p < 0.05$), SB203580 ($p < 0.01$) and LY294002 ($p < 0.01$) (Fig. 5.3.9a) inhibitors.

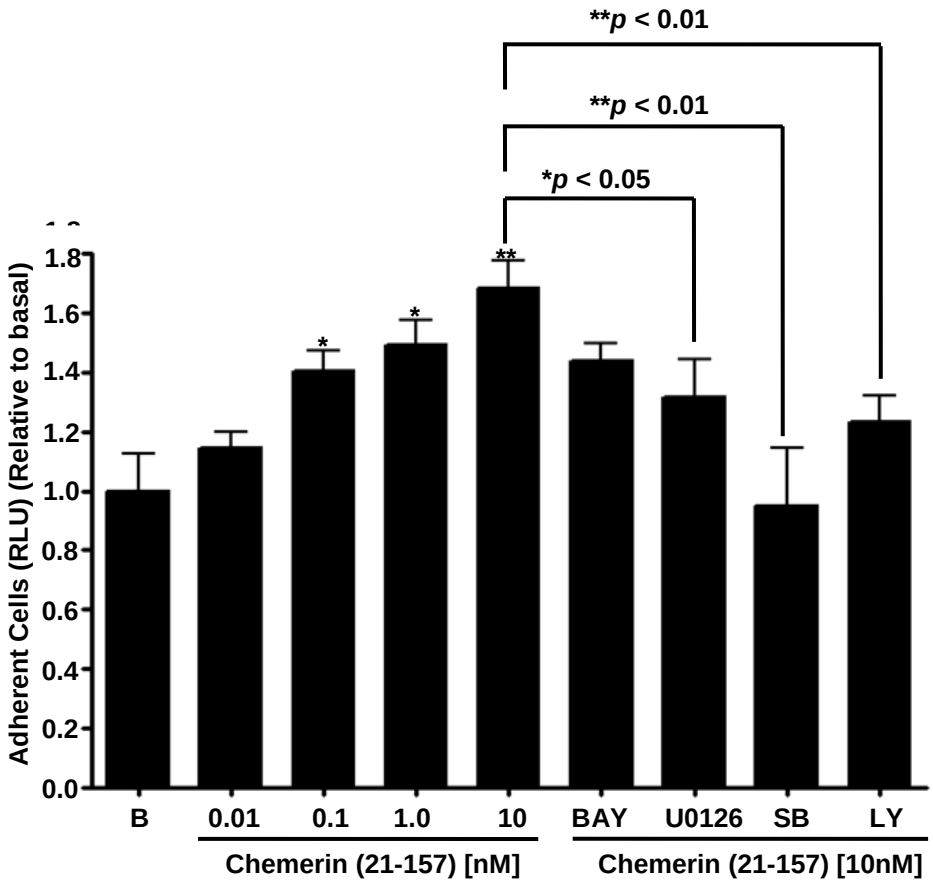

Figure 5.3.9a Chemerin (21-157) increased Endothelial-Monocyte cell adhesion in a concentration-dependent manner

HMEC-1 cells were trypsinised and a cell suspension containing $2x10^6$ cells/ml in a MCDB cell medium was prepared. 100µl of HMEC-1 cell suspension was added to each 96-well tissue culture plate (included in the kit) and incubated for 3 hours to allow attachment of cells to the plate surface. Post incubation, cell medium was aspirated out and 100µl of Cycloheximide solution was added to the control wells, and 100µl of fresh 10% FCS MCDB cell medium. Endothelial cells were activated by adding 10 µl of TNF-α [20ng/ml] to respective wells. Cells were pre-treated with different inhibitors; BAY11-7085 [10µM] for 1 hour, U0126 [10µM] for 1 hour, SB203580 [10µM] for 30minutes and LY294002 [10µM] for 1 hour, and were treated with different chemerin (21-157) concentrations [0-10nM] for 6 hours. 75µl of medium was aspirated out from the plate wells and washed gently with 200µl of Assay Buffer twice. After the last wash, 50µl of Assay Buffer solution was added to each well and 100µl of Calcein AM labelled THP-1 monocytes (~50,000 to 200,000 cells) were added and incubated for 30 minutes at 37^oC. Approximately, 120µl solution was aspirated out from the plate wells and two 200µl cell washes were performed using Assay Buffer solution. An additional wash was performed to remove any remaining unbound cells in order to eliminate non-specific binding. 100µl of Assay Buffer was added to each well and the plate reading was performed using a fluorescent plate reader with an excitation/emission filter of 485/530nm. The data are presented as mean ± SEM of three independent experiments in duplicates $**p < 0.01$ and $*p < 0.05$ compared to basal.

5.4 Summary of Results

Chemerin (21-157) significantly upregulated the cellular protein expression levels of E-selectin (Fig. 5.3.1a and b), VCAM-1 (Fig. 5.3.2a and b) and ICAM-1 (Fig. 5.3.3a and b) adhesion molecules in a concentration-dependent manner at 12 and 24 hours (respectively). In addition, chemerin (21-157) also increased secreted levels of E-selectin (sE-selectin), VCAM-1 (sVCAM-1) and ICAM-1 (sICAM-1) adhesion molecules in a concentration-dependent manner (Fig. 5.3.1c, 5.3.2c and 5.3.3c respectively). The protein expression levels of E-selectin, VCAM-1 and ICAM-1 were altered in HMEC-1 cell line, when combined chemerin (21-157) and known inflammatory mediator IL-1β treatments were performed, compared to chemerin (21-157) and IL-1β alone (5.3.4a, b and c respectively).

Chemerin (21-157) significantly upregulated the protein expression of MCP-1 in a concentration-dependent manner after 12 and 24 hours of incubation (Fig. 5.3.5a and 5.3.5b respectively). Also, combined HMEC-1 cells treatments with chemerin (21-157) and IL-1β resulted in additive increase in MCP-1 protein expression, compared to chemerin (21-157) and IL-1β alone (Fig. 5.3.6a).

Chemerin (21-157) increased NF-κB pathway activity, a well studied inflammatory pathway in a concentration-dependent manner, showing an additive increase when co-stimulated with chemerin (21-157) and IL-1β together in HMEC-1 cell line (Fig. 5.3.7a). HMEC-1 cell treatments with BAY11-7085, a specific NF-κB inhibitor, prior to stimulating with chemerin (21-157) resulted in VCAM-1 protein expression down-regulation compared to chemerin (21-157) and BAY11-7085 alone (Fig. 5.3.8b). NF-κB modulates a number of genes regulating inflammatory and acute phase responses (Vereecke and Carmeliet, 2000), as well as play an important role in body's immune responses and other process such as thymus development,

apoptosis, embryonic development, growth regulation, malignant transformation and viral mRNA expression (Baes et al., 2000, Bautch et al., 2000). The NF-κB activity is stimulated by a number of stimuli including various bacterial and viral stimuli, and other cellular and environmental stressors such as irradiation, osmotic shock, osmotic stress, hyperglycaemia and haemorrhage also stimulate NF-κB activity (Dvorak et al., 1995b).

Chemerin (21-157) dose-dependently encouraged monocyte cell adhesion to ECs in a concentration-dependent manner, and was inhibited when pre-incubated with a specific NF-κB inhibitor; BAY11-7085, a MAPK inhibitor; U0126, a p38 MAPK inhibitor, SB203580; and an Akt/PI3K inhibitor, LY294002 (Fig. 5.3.9a).

CAM expression is kept under check by the endothelium NO, a molecule produced by endothelial Nitric Oxide Synthase (eNOS), which is an enzyme constitutively expressed on the walls of ECs and regulates NO production. The final aim of this project explored the role of chemerin (21-157) in the activity of eNOS enzyme (chapter 6); the key signalling pathways involved, and finally, in the production of NO in HMEC-1 cell line.

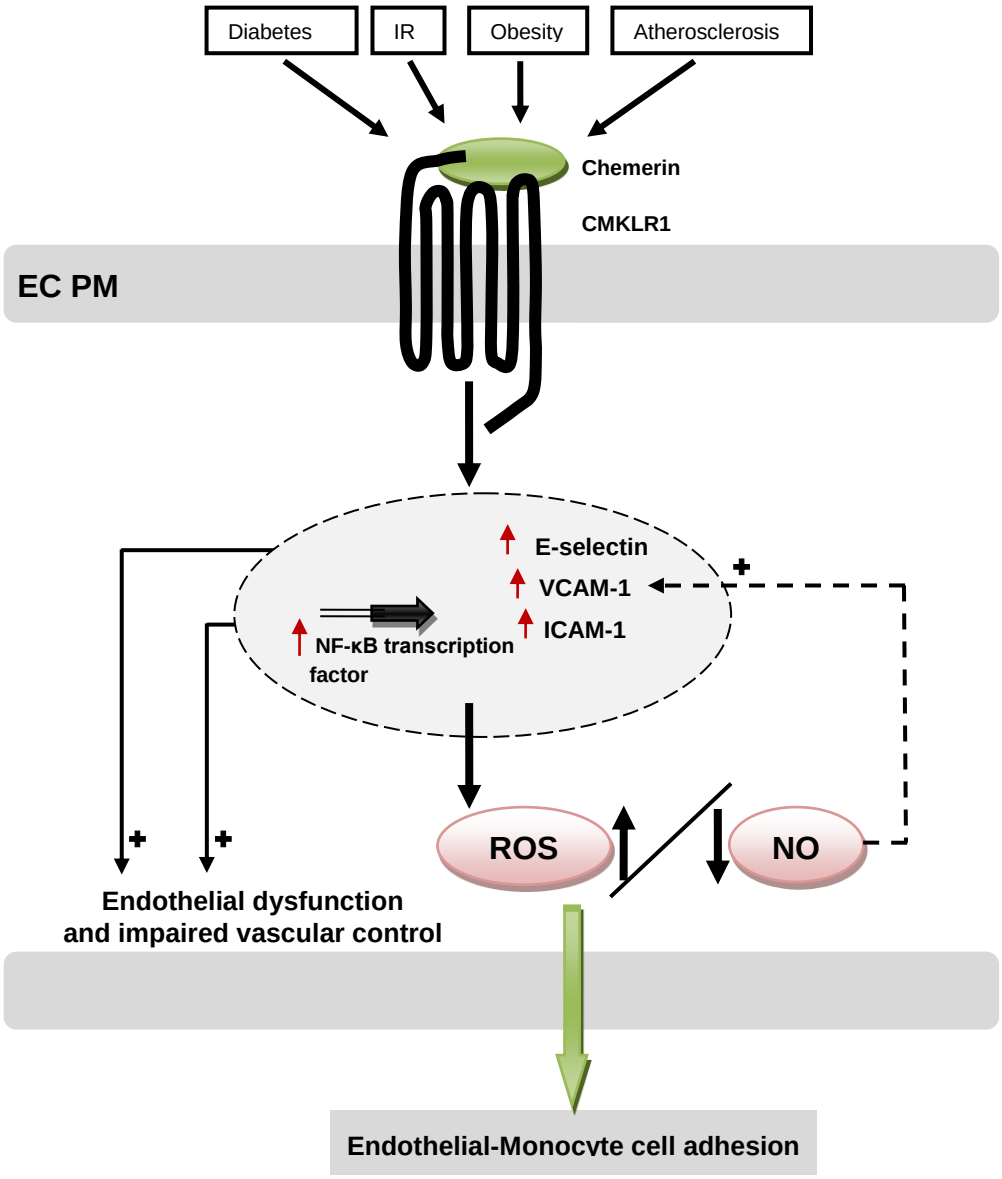

Figure 5.4.1a Schematic representation of the findings in this chapter

This picture shows the schematic representation of the role of chemerin (21-157) in E-selectin, ICAM-1 and VCAM-1 endothelial cell adhesion molecules protein expression inside a cell. This picture also shows the involvement of NF-κB pathway in regulating the expression of these adhesion molecules, which finally results in endothelial-monocyte cell adhesion resulting in vascular inflammation. The role and implication of increased Reactive Oxygen Species (ROS) and decreased Nitric Oxide (NO) levels in the expression of endothelial cell adhesion molecules, consequently resulting in vascular pathology.

6.1 Introduction

The specific aims of this part of the project were to explore the role (s) of chemerin (21-157) in; (1) the activity of endothelial Nitric Oxide Synthase (eNOS) by studying eNOS phosphorylation at Ser1177, and dephosphorylation at Thr495 sites both in a time- and concentration-dependent manner, (2) the involvement of Akt/PI3 kinase, Protein Kinase A (PKA) and Protein Kinase C (PKC) signalling pathways in the regulation of eNOS activity, (3) the levels of nitrites and nitrates; the end products of Nitric Oxide (NO) catabolism, and finally (4) the inducible Nitric Oxide Synthase (iNOS) protein expression in HMEC-1 cell line.

NO is secreted by the vascular endothelium and acts as a potent vasodilator, promotes angiogenesis, and reduces the expression of adhesion molecules on the EC surface. NO production is regulated by endothelial specific enzyme, endothelial Nitric Oxide Synthase (eNOS) which is constitutively expressed on EC surfaces. eNOS activity is regulated by phosphorylation and dephosphorylation on a number of different sites, however, eNOS phosphorylation at Ser1177 and dephosphorylation at Thr495 sites contribute as the two most significant sites of eNOS regulatory activity. In this project, eNOS phosphorylation at Ser1177, and dephosphorylation at Thr495 sites were studied in relation to the activity of eNOS enzyme. A number of different upstream pathways may be involved in regulating the activity of eNOS (Fig. 6.4.1a, page number 199). However, in relation to chemerin (21-157), involvement of three pathways including Akt/PI3K, PKA and PKC pathways was studied in inducing eNOS phosphorylation at Ser1177 site only. Nitrites and nitrates are end products of NO metabolism, which are detectable in cell supernatants and lysates. Inducible Nitric Oxide Synthase (iNOS) is induced during injury or inflammation and secretes 100- to 1000-fold more NO compared to eNOS (Morris and Billiar, 1994, Nathan and Xie, 1994).

6.2 Materials and Methods

The protein expression levels and phosphorylation were determined by SDS-PAGE (Chapter 2, section 2.3.7, page numbers 57-60) using different percentage polyacrylamide gels for separating different proteins (Table 6.2.1a). Amount of nitrites and nitrates was determined using Griess reagent test (Chapter 2, section 2.4.10, page numbers 71-2).

Table 6.2.1a

The molecular weights of different proteins and gel percentages used for SDS-PAGE analysis

Protein name	Molecular weight (kDa)	Percentage gels used
eNOS	120	8
iNOS	130	8

6.3 Data Presentation and Analyses

6.3.1 Chemerin and endothelial Nitric Oxide Synthase (eNOS) Activity in HMEC-1 Cell Line

HMEC-1 cells were cultured in 6-well plates in MCDB cell medium containing 10% FCS, and were serum starved in the same medium containing 1% FCS overnight before performing different treatments. To study time-dependent eNOS phosphorylation, HMEC-1 cells were treated with [3.0nM] chemerin (21-157) at different time-points for a maximum of 30 minutes. For concentration-dependent eNOS phosphorylation, HMEC-1 cells were treated with different chemerin (21-157) [0-30nM] concentrations for 3 minutes. Cells were lysed in 1x RIPA buffer and protein lysates were separated using SDS-PAGE. Chemerin (21-157) increased eNOS activity by phosphorylating at Ser1177 [eNOS (Ser1177)] in a time-dependent manner with a significant increase at 3 minutes ($p < 0.01$) (Fig. 6.3.1a), and by dephosphorylation at Thr495 [eNOS(Thr495)] ($p < 0.001$ and $p < 0.01$) (Fig. 6.3.1b). Chemerin (21-157) increased eNOS activity in a concentration-dependent manner by phosphorylating at Ser1177 [eNOS (Ser1177)] with a significant increase at [10nM] ($p < 0.001$) (Fig. 6.3.1c), and by dephosphorylation at Thr495 [eNOS(Thr495)] ($p < 0.001$ and $p < 0.01$) (Fig. 6.3.1d).

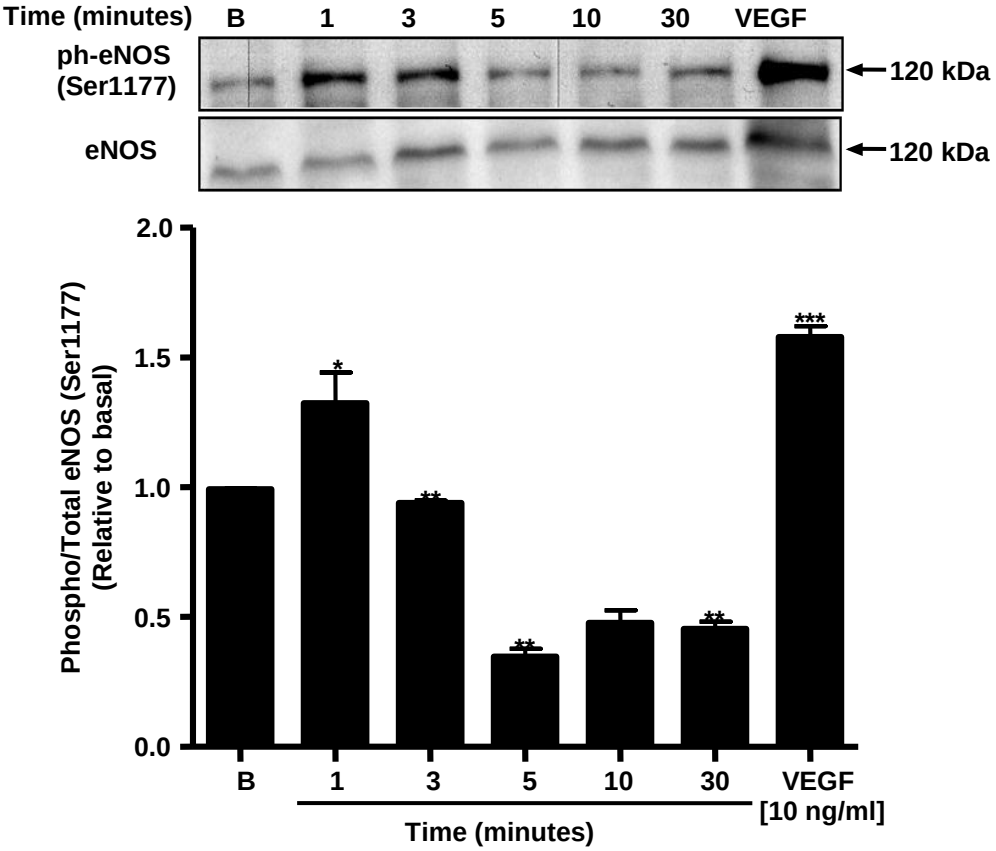

Figure 6.3.1a Chemerin (21-157) lead to eNOS (Ser1177) phosphorylation in a time-dependent manner in HMEC-1 cell line

HMEC-1 cells were treated with [3.0nM] chemerin (21-157) for 0-30 minutes. Following cell lysis and sample preparations, the protein lysates were separated using 8% polyacrylamide gels, and transferred to PVDF membranes at 100V for 1 hour. Membranes were incubated with specific eNOS (Ser1177) antibody [(1:1500); Cell signalling, Beverly, MA, USA] overnight at 4^{o}C. After removing the primary antibody complexes, membranes were incubated with anti-rabbit IgG-HRP labelled antibody [(1:2000); Dako, Ely, UK] for 1 hour at RT. Protein complexes were visualised using ECL plus detection reagent on X-ray films. Membrane was re-probed with total eNOS [(1:1500); Cell signalling, Beverly, MA, USA] and used as a loading control. The corresponding bands for both phospho-eNOS (Ser1177) and total eNOS were observed as 120kDa products. The band intensities were measured using Scion Image™ densitometer (Scion Corporation, Maryland, USA). The data are presented as mean ± SEM of three independent experiments in duplicates ***$p <$ 0.001, **$p < 0.01$ and *$p < 0.05$ compared to basal. VEGF was [10ng/ml] used as a positive control.

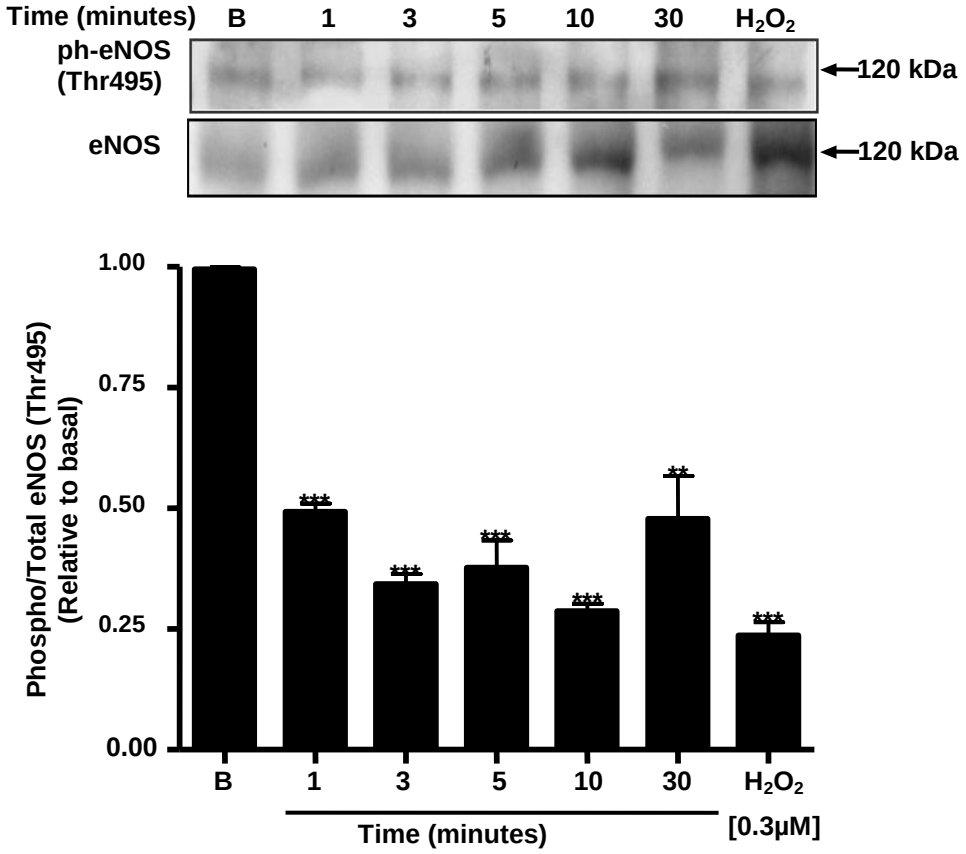

Figure 6.3.1b Chemerin (21-157) lead to eNOS (Thr495) dephosphorylation in a time-dependent manner in HMEC-1 cell line

HMEC-1 cells were treated with [3.0nM] chemerin (21-157) for 0-30 minutes. Following cell lysis and sample preparations, the protein lysates were separated using 8% polyacrylamide gels, and transferred to PVDF membranes at 100V for 1 hour. Membranes were incubated with specific eNOS (Thr495) antibody [(1:1500); Cell signalling, Beverly, MA, USA] overnight at 4^{o}C. After removing the primary antibody complexes, membranes were incubated with anti-rabbit IgG-HRP labelled antibody [(1:2000); Dako, Ely, UK] for 1 hour at RT. Protein complexes were visualised using ECL plus detection reagent on X-ray films. Membrane was re-probed with total eNOS [(1:1500); Cell signalling, Beverly, MA, USA] and used as a loading control. The corresponding bands for both phospho-eNOS (Thr495) and total eNOS were observed as 120kDa products. The band intensities were measured using Scion Image™ densitometer (Scion Corporation, Maryland, USA). The data are presented as mean ± SEM of three independent experiments in duplicates ***$p <$ 0.01 and **$p < 0.01$ compared to basal. H_2O_2 was [0.3μM] used as a positive control.

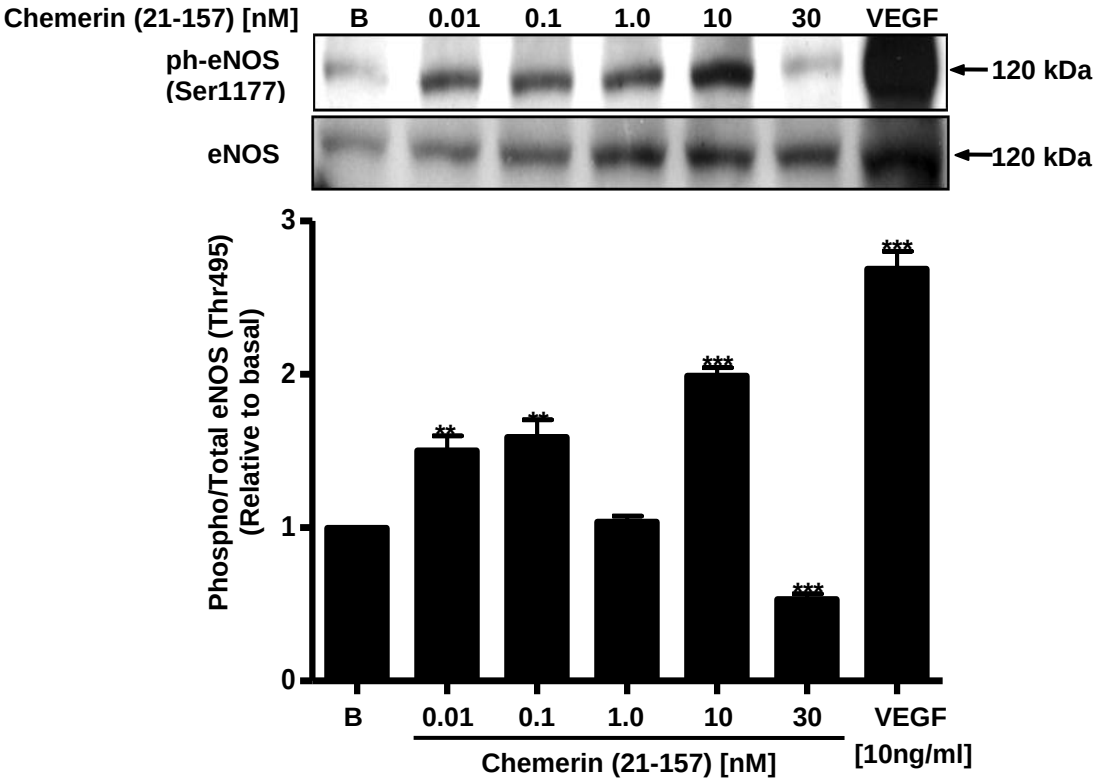

Figure 6.3.1c Chemerin (21-157) lead to eNOS (Ser1177) phosphorylation in a concentration-dependent manner in HMEC-1 cell line

HMEC-1 cells were treated with different chemerin (21-157) [0-30nM] concentrations for 3 minutes. Following cell lysis and sample preparations, the protein lysates were separated using 8% polyacrylamide gels, and transferred to PVDF membranes at 100V for 1 hour. Membranes were incubated with specific eNOS (Ser1177) antibody [(1:1500); Cell signalling, Beverly, MA, USA] overnight at 4^{o}C. After removing the primary antibody complexes, membranes were incubated with anti-rabbit IgG-HRP labelled antibody [(1:2000); Dako, Ely, UK] for 1 hour at RT. Protein complexes were visualised using ECL plus detection reagent on X-ray films. Membrane was re-probed with total eNOS [(1:1500); Cell signalling, Beverly, MA, USA] and used as a loading control. The corresponding bands for both phospho-eNOS (Ser1177) and total eNOS were observed as 120kDa products. The band intensities were measured using Scion Image™ densitometer (Scion Corporation, Maryland, USA). The data are presented as mean ± SEM of three independent experiments in duplicates ***$p < 0.01$ and **$p < 0.01$ compared to basal. VEGF [10ng/ml] was used as a positive control.

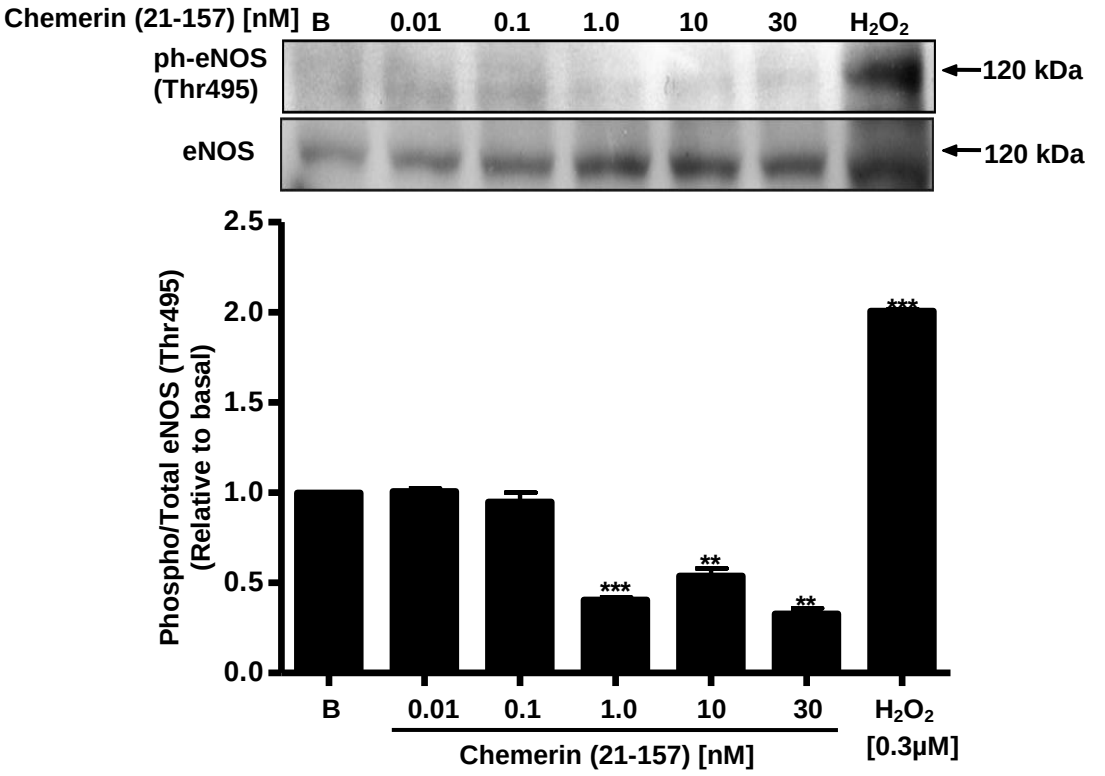

Figure 6.3.1d Chemerin (21-157) lead to eNOS (Thr495) dephosphorylation in a concentration-dependent manner in HMEC-1 cell line

HMEC-1 cells were treated with different chemerin (21-157) [0-30nM] concentrations for 3 minutes. Following cell lysis and sample preparations, the protein lysates were separated using 8% polyacrylamide gels, and transferred to PVDF membranes at 100V for 1 hour. Membranes were incubated with specific eNOS (Thr495) antibody [(1:1500); Cell signalling, Beverly, MA, USA] overnight at 4^{o}C. After removing the primary antibody complexes, membranes were incubated with anti-rabbit IgG-HRP labelled antibody [(1:2000); Dako, Ely, UK] for 1 hour at RT. Protein complexes were visualised using ECL plus detection reagent on X-ray films. Membrane was re-probed with total eNOS [(1:1500); Cell signalling, Beverly, MA, USA] and used as a loading control. The corresponding bands for both phospho-eNOS (Thr495) and total eNOS were observed as 120kDa products. The band intensities were measured using Scion Image™ densitometer (Scion Corporation, Maryland, USA). The data are presented as mean ± SEM of three independent experiments in duplicates ***$p < 0.001$ and **$p < 0.01$ compared to basal. H_2O_2 was [0.3µM] used as a positive control.

6.3.2 Chemerin (21-157) Induced eNOS (Ser1177) Phosphorylation via Akt/PI3K, PKA and PKC Pathways in HMEC-1 Cell Line

HMEC-1 cells were cultured in 6-well plates in MCDB cell medium containing 10% FCS, and were serum starved in the same medium containing 1% FCS overnight before performing various different treatments. HMEC-1 cells were pre-treated with LY294002 [30µmol/L] for 1 hour, H-89 [10µmol/L] and BIS II [10µmol/L] for 40 minutes, and were treated with [3.0nM] chemerin (21-157) for 3 minutes. Cells were lysed in 1x RIPA buffer and protein lysates were separated using SDS-PAGE. Chemerin (21-157) increased eNOS activity by phosphorylating at Ser1177 [eNOS (Ser1177)] which was inhibited significantly by Akt/PI3K inhibitor, LY294002 [30µmol/L] (Fig. 6.3.2a); PKA inhibitor, H-89 [10µmol/L] (Fig. 6.3.2b); and PKC inhibitor, BIS II [10µmol/L] (Fig. 6.3.2c) treatments ($p < 0.001$, $p < 0.01$ and $p < 0.05$) compared to basal.

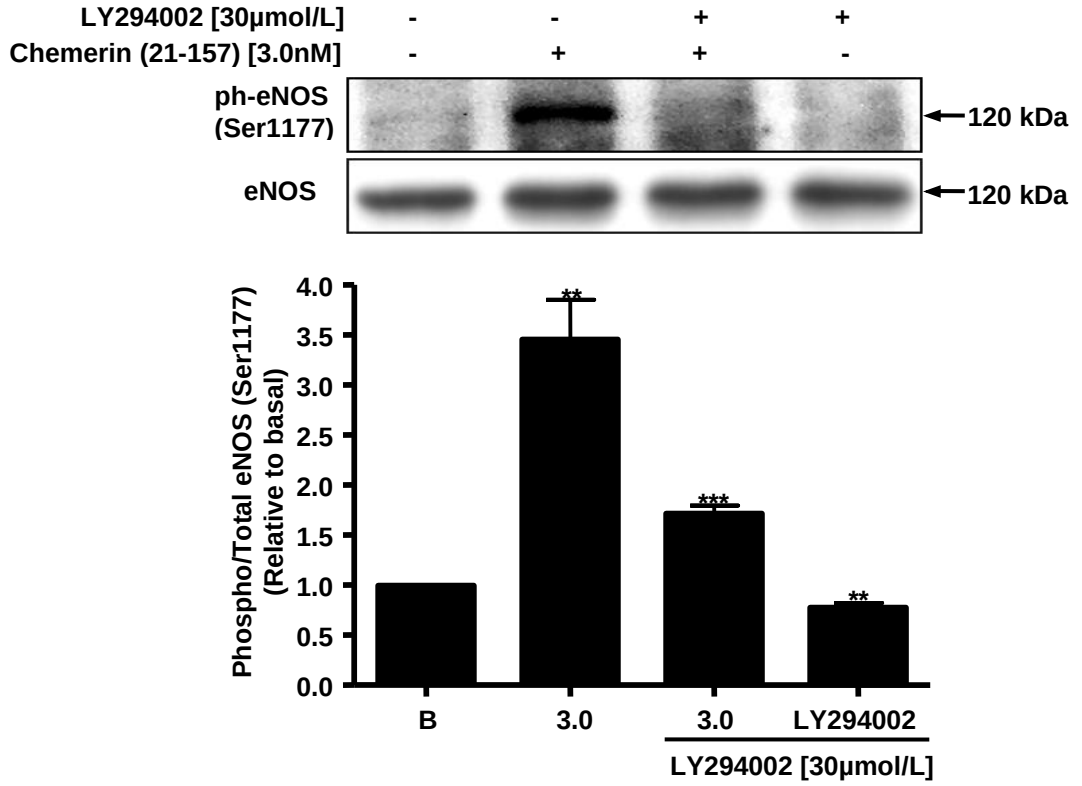

Figure 6.3.2a Chemerin (21-157) induced eNOS (Ser1177) phosphorylation via Akt/PKB kinase pathway in HMEC-1 cell line

HMEC-1 cells were pre-incubated with LY294002 [30µmol/L] for 1 hour and were treated with [3.0nM] chemerin (21-157) for 3 minutes. Following cell lysis and sample preparations, the protein lysates were separated using 8% polyacrylamide gels, and transferred to PVDF membranes at 100V for 1 hour. Membranes were incubated with specific eNOS (Ser1177) antibody [(1:1500); Cell signalling, Beverly, MA, USA] overnight at 4^{o}C. After removing the primary antibody complexes, membranes were incubated with anti-rabbit IgG-HRP labelled antibody [(1:2000); Dako, Ely, UK] for 1 hour at RT. Protein complexes were visualised using ECL plus detection reagent on X-ray films. Membrane was re-probed with total eNOS [(1:1500); Cell signalling, Beverly, MA, USA] and used as a loading control. The corresponding bands for both phospho-eNOS (Ser1177) and total eNOS were observed as 120kDa products. The band intensities were measured using Scion Image™ densitometer (Scion Corporation, Maryland, USA). The data are presented as mean ± SEM of three independent experiments in duplicates ***$p < 0.001$ and **$p < 0.01$ compared to basal.

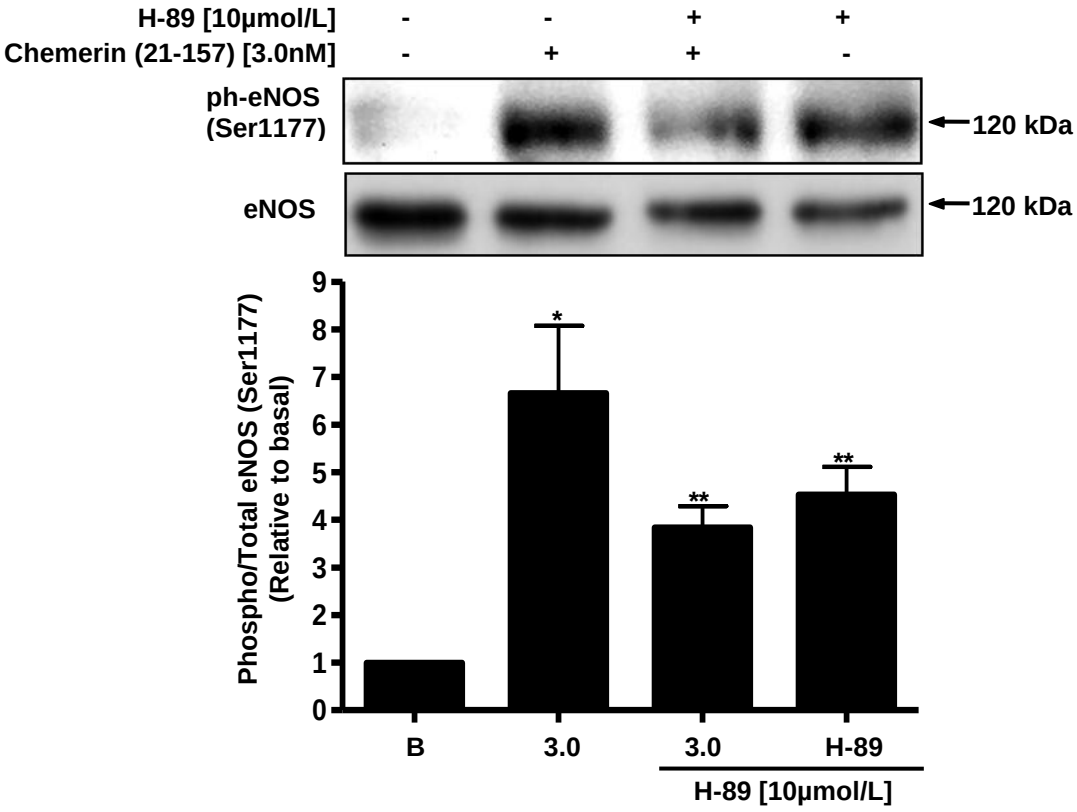

Figure 6.3.2b Chemerin (21-157) induced eNOS (Ser1177) phosphorylation via PKA pathway in HMEC-1 cell line

HMEC-1 cells were incubated with H-89 [10µmol/L] for 40 minutes and were treated with [3.0nM] chemerin (21-157) for 3 minutes. Following cell lysis and sample preparations, the protein lysates were separated using 8% polyacrylamide gels, and transferred to PVDF membrane at 100V for 1 hour. Membranes were incubated with specific eNOS (Ser1177) antibody [(1:1500); Cell signalling, Beverly, MA, USA] overnight at 4^{o}C. After removing the primary antibody complexes, membranes were incubated with anti-rabbit IgG-HRP labelled antibody [(1:2000); Dako, Ely, UK] for 1 hour at RT. Protein complexes were visualised using ECL plus detection reagent on X-ray films. Membrane was re-probed with total eNOS [(1:1500); Cell signalling, Beverly, MA, USA] and used as a loading control. The corresponding bands for both phospho-eNOS (Ser1177) and total eNOS were observed as 120kDa products. The band intensities were measured using Scion Image™ densitometer (Scion Corporation, Maryland, USA). The data are presented as mean ± SEM of three independent experiments in duplicates $^{**}p < 0.01$ and $^{*}p < 0.05$ compared to basal.

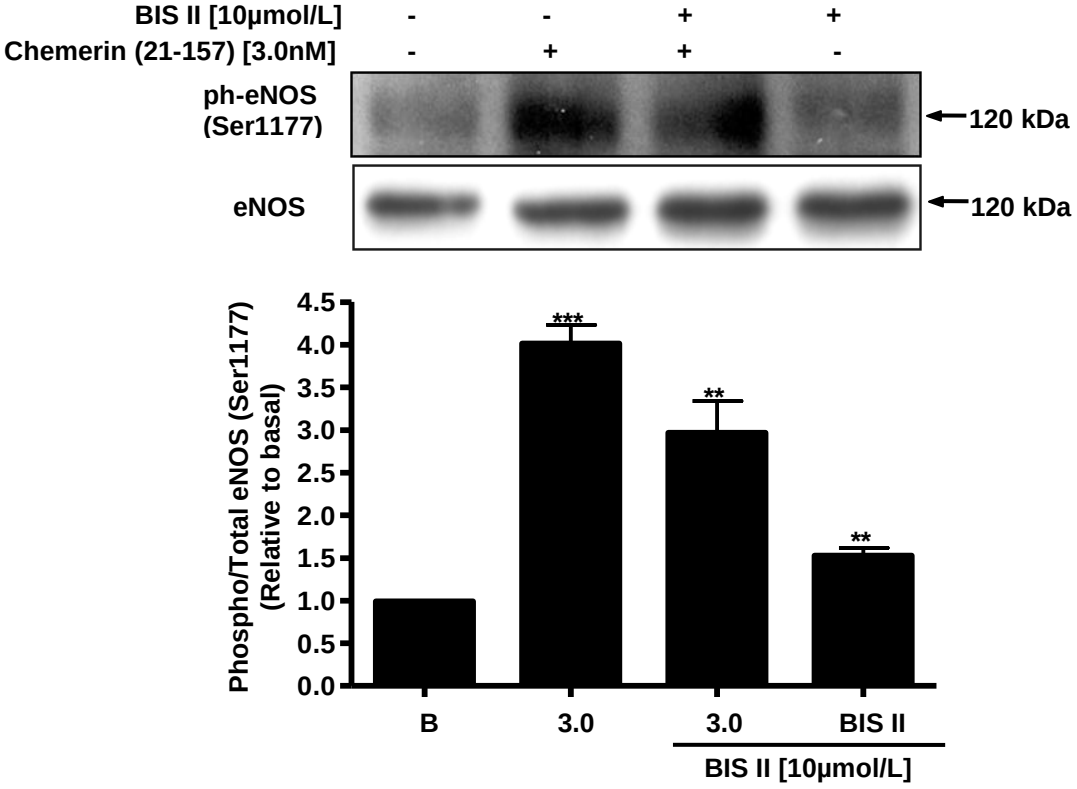

Figure 6.3.2c Chemerin (21-157) induced eNOS (Ser1177) phosphorylation via PKC pathway in HMEC-1 cell line

HMEC-1 cells were incubated with BIS II [10µmol/L] for 40 minutes and were treated with [3.0nM] chemerin (21-157) for 3 minutes. Following cell lysis and sample preparations, the protein lysates were separated using 8% polyacrylamide gels, and transferred to PVDF membranes at 100V for 1 hour. Membranes were incubated with specific eNOS (Ser1177) antibody [(1:1500); Cell signalling, Beverly, MA, USA] overnight at 4^{o}C. After removing the primary antibody complexes, membranes were incubated with anti-rabbit IgG-HRP labelled antibody [(1:2000); Dako, Ely, UK] for 1 hour at RT. Protein complexes were visualised using ECL plus detection reagent on X-ray films. Membrane was re-probed with total eNOS [(1:1500); Cell signalling, Beverly, MA, USA] and used as a loading control. The corresponding bands for both phospho-eNOS (Ser1177) and total eNOS were observed as 120kDa products. The band intensities were measured using Scion Image™ densitometer (Scion Corporation, Maryland, USA). The data are presented as mean ± SEM of three independent experiments in duplicates ***$p < 0.001$ and **$p < 0.01$ compared to basal.

6.3.3 Chemerin (21-157) Increased inducible Nitric Oxide Synthase (iNOS) Protein Expression in HMEC-1 Cell Line

HMEC-1 cells were cultured in 6-well plates in MCDB cell medium containing 10% FCS, and were serum starved in the same medium containing 1% FCS overnight before performing different treatments. For studying time-point response, HMEC-1 cells were treated with [10nM] chemerin (21-157) at different time-points for a maximum of 12 hours. For concentration-dependent response, HMEC-1 cells were treated with different chemerin (21-157) [0-30nM] concentrations for 6 hours. Cells were lysed in 1x RIPA buffer and protein lysates were separated using SDS-PAGE. Chemerin (21-157) increased iNOS protein expression in HMEC-1 cell line in a time-dependent manner showing a peak response at 6 hours (Fig. 6.3.3a). Chemerin (21-157) increased iNOS protein expression in a concentration-dependent manner showing maximum response at [10nM] chemerin (21-157) (Fig. 6.3.3b).

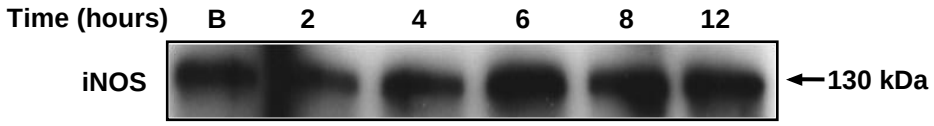

Figure 6.3.3a Chemerin (21-157) increased iNOS protein expression in a time-dependent manner in HMEC-1 cell line

HMEC-1 cells were treated with [10nM] chemerin (21-157) for a maximum of 12 hours. Following cell lysis and sample preparation, the protein lysates were separated using 8% polyacrylamide gels, and transferred to PVDF membranes at 100V for 1 hour. Membranes were incubated with specific iNOS antibody [(1:1500); Abcam Cambridge, UK] overnight at 4^{o}C. After removing the primary antibody complexes, membranes were incubated with anti-mouse IgG-HRP labelled antibody [(1:8000); Sigma-Aldrich, UK] for 1 hour at RT. Protein complexes were visualised using ECL plus detection reagent on X-ray films. The corresponding bands for iNOS were detected as 130kDa products.

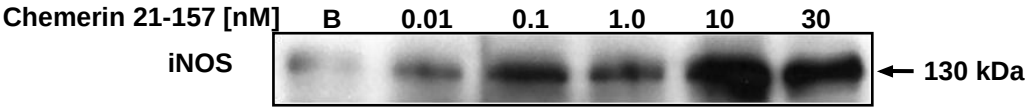

Figure 6.3.3b Chemerin (21-157) increased iNOS protein expression in a concentration-dependent manner in HMEC-1 cell line

HMEC-1 cells were treated with different chemerin (21-157) [0-30nM] concentrations for 6 hours. Following cell lysis and sample preparation, the protein lysates were separated using 8% polyacrylamide gels, and transferred to PVDF membranes at 100V for 1 hour. Membranes were incubated with specific iNOS antibody [(1:1500); Abcam Cambridge, UK] overnight at 4^{o}C. After removing the primary antibody complexes, membranes were incubated with anti-mouse IgG-HRP labelled antibody [(1:8000); Sigma-Aldrich, UK] for 1 hour at RT. Protein complexes were visualised using ECL plus detection reagent on X-ray films. The corresponding bands for iNOS were detected as 130kDa products.

6.3.4 Chemerin and Nitrites and Nitrates in HMEC-1 Cell Lysates and Supernatants

HMEC-1 cells were cultured in 6-well plates in MCDB cell medium containing 10% FCS, and were serum starved in the same medium containing 1% FCS overnight before performing different treatments. Cell medium was aspirated out, washed with PBS, and was replaced with 1ml fresh PBS. HMEC-1 cells were treated with different chemerin (21-157) [0-30nM] concentrations for 15 minutes and cell supernatants were collected. Cells were washed with ice cold PBS twice, and 500µl of dH_2O was added to the wells, lysed, and cell lysates were collected in eppendorf tubes. Amounts of combined nitrite and nitrate (NOx), as well as nitrite ($NO2^-$) only were determined using Griess reagent method. Griess reagent failed to detect any NOx levels in chemerin (21-157) treated HMEC-1 cell supernatants (data not shown), and remained unchanged in EC lysates with increasing chemerin (21-157) concentrations (Fig. 6.3.4a). Different chemerin (21-157) [0-30nM] concentrations significantly down-regulated $NO2^-$ levels in a concentration-dependent manner ($p < 0.001$) (Fig. 6.3.4b) in EC supernatants, and were not detected in EC lysates (data not shown).

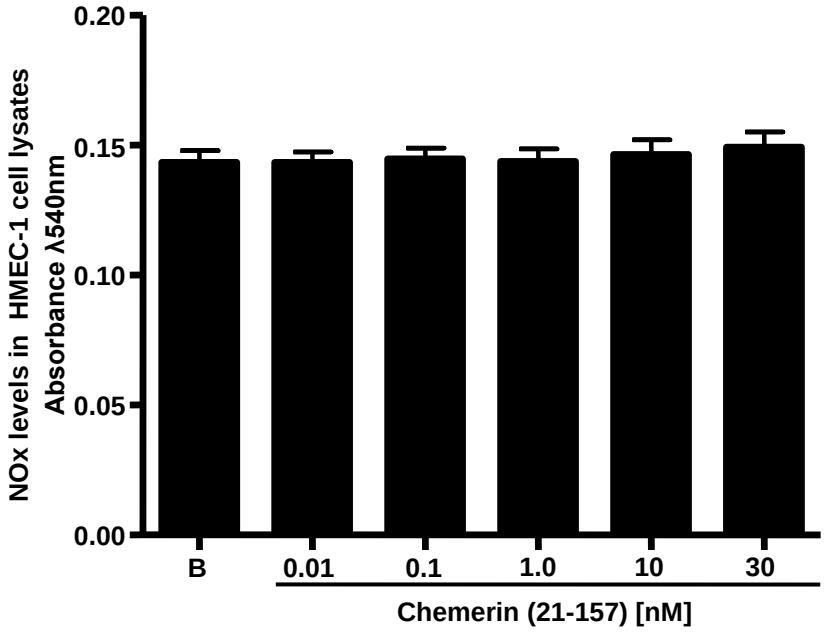

Figure 6.3.4a Chemerin (21-157) and NOx levels in HMEC-1 cell lysates

HMEC-1 cells were treated with different chemerin (21-157) concentrations [0-30nM] for 15 minutes. Cell lysates were collected in 500µl of dH_2O and NOx levels were determined using Griess reagent test. 100µl of each standard or sample was added into a 96-well plate, followed by 100µl of Vanadium chloride solution. Griess reagent mix (50µl of NEDD + 50µl SULF) was prepared and 100µl of the mixture was added to each well and incubated for 45 minutes. The absorbance was recorded at 550nm. The data are presented as mean ± SEM of three independent experiments in duplicates.

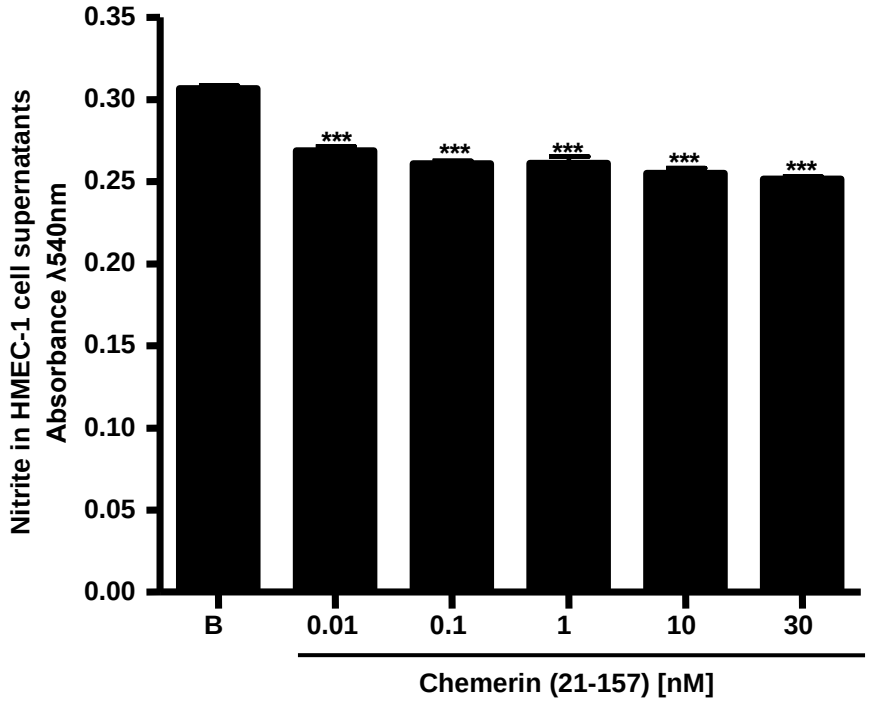

Figure 6.3.4b Chemerin (21-157) and $NO2^-$ levels in HMEC-1 cell supernatants

HMEC-1 cells were treated with different chemerin (21-157) concentrations [0-30nM] for 15 minutes. Cell supernatants were collected and nitrite levels were determined using Griess reagent test. 300µl of each standard or sample solution (both cell lysates and supernatants) was added to the pre-labelled 1.5ml eppendorf tubes. Griess reagent mix (150µl of NEDD+150µl SULF) was prepared and resultant 300µl of mix was added to each standard or sample, mixed gently and 300µl was transferred to 96-well plate and incubated for 10 minutes. The absorbance was recorded at 550nm. The data are presented as mean ± SEM of three independent experiments in duplicates ***$p < 0.001$ compared to basal.

6.4 Summary of Results

Chemerin (21-157) increased eNOS enzyme activity in a time-dependent manner by causing eNOS phosphorylation at Ser1177 [eNOS (Ser1177)] (Fig. 6.3.1a), and dephosphorylation at Thr495 site [eNOS (Thr495)] (Fig. 6.3.1b). Chemerin (21-157) increased eNOS activity in a concentration-dependent manner by causing eNOS phosphorylation at Ser1177 [eNOS (Ser1177)] (Fig. 6.3.1c), and dephosphorylation at Thr495 [eNOS (Thr495)] (Fig. 6.3.1d). [eNOS (Ser1177)] and [eNOS (Thr495)] sites are the main regulatory sites that are reported to regulate the activity of eNOS enzyme in the endothelium.

Upstream signalling kinases such as Akt/PI3K, PKA and PKC pathways were found to be involved in chemerin (21-157)-mediated activity of eNOS enzyme. In HMEC-1 cells, chemerin (21-157)-induced eNOS activity at Ser1177 [eNOS (Ser1177)] site was inhibited significantly when pre-incubated with an Akt/PI3K inhibitor, LY294002 (Fig. 6.3.2a); a PKA inhibitor, H-89 (Fig. 6.3.2b) and a PKC inhibitor, BIS II (Fig. 6.3.2c).

Chemerin (21-157) increased iNOS protein expression in a time- and concentration-dependent manner in HMEC-1 cell line (Fig. 6.3.4a and b respectively).

Chemerin (21-157) increased caveolin-1 protein expression in a time- and concentration-dependent manner (Appendix 8, Fig. 8.1a and 8.1b respectively, page numbers 265-7).

Chemerin (21-157) increased HSP90 protein expression in a time- and concentration-dependent manner in HMEC-1 cell line (Appendix 9, Fig. 9.1a and 9.1b respectively, page numbers 268-70).

Interestingly, Griess reagent test failed to detect any change in NOx levels in chemerin (21-157)-treated HMEC-1 cell supernatants (data not shown), and amount of NOx in cell lysates remain unchanged with increasing chemerin (21-157) concentrations (Fig. 6.3.3a). Different chemerin (21-157) [0-30nM] concentrations significantly down-regulated $NO2^-$ levels in a concentration-dependent manner in HMEC-1 cell supernatants (Fig. 6.3.3b); however, $NO2^-$ levels remained undetected in cell supernatants (data not shown).

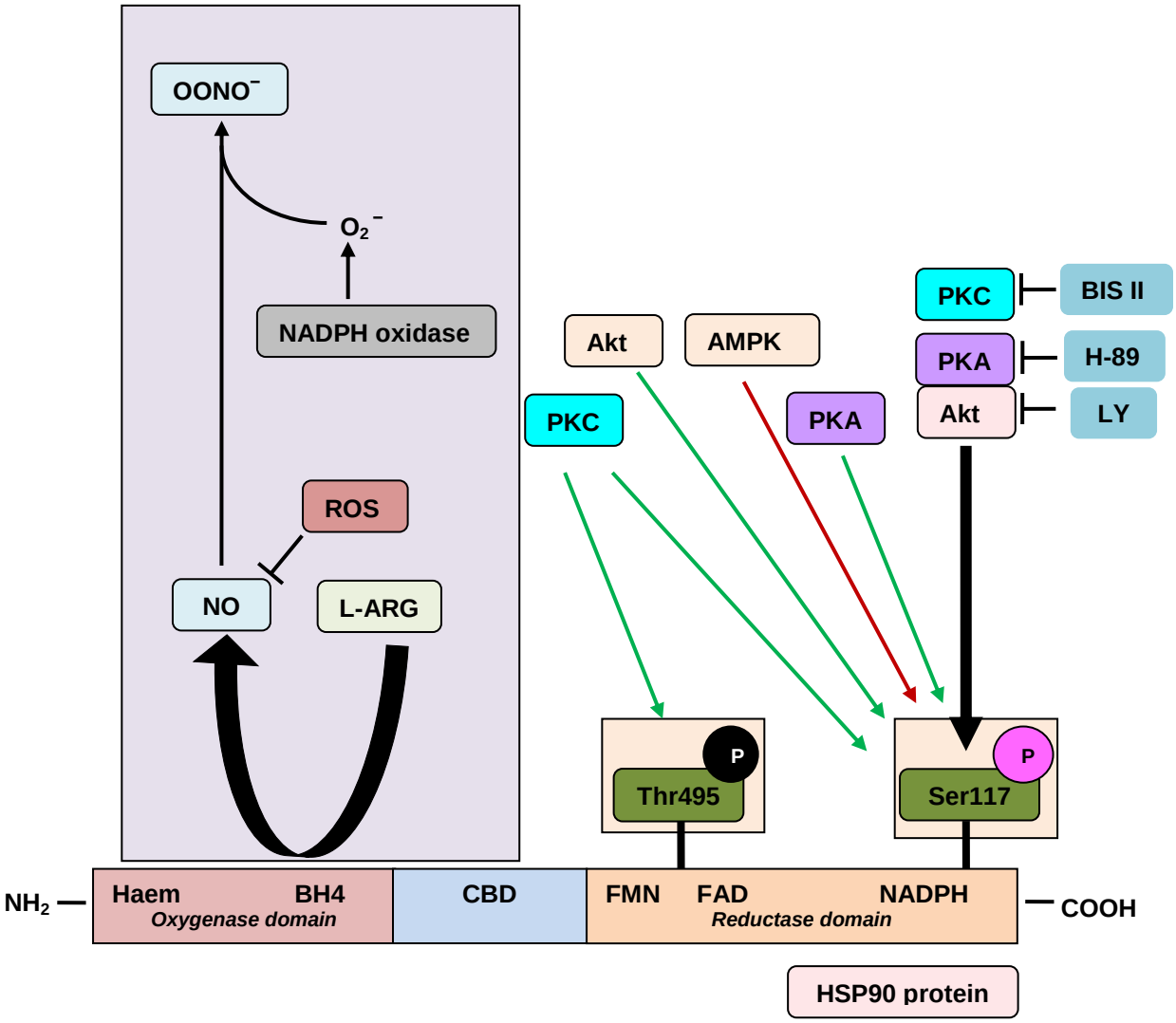

Figure 6.4.1a Schematic representation of the findings in this chapter

The figure shows the eNOS monomer and the two main phosphorylation sites – eNOS (Thr495) and eNOS (Ser1177), and the involvement of different kinases in eNOS (Ser1177) phosphorylation. This figure also shows the NO production, L-arginine acting as a precursor molecule, ROS involvement, and formation of peroxynitrite ($OONO^-$).

7.1 Identification of chemerin and its receptors in human microvascular and macrovascular ECs: CMKLR1 receptor regulation by inflammatory cytokines

Both human chemerin and its natural GPCR receptor, CMKLR1 were identified and confirmed at gene and protein levels in both microvascular (HMEC-1) and macrovascular (EA.hy926) endothelial cell lines, as well as in primary HUVEC cells. In addition to CMKLR1, two human orphan chemerin GPCRs, CCRL2 and GPR1 receptors were also identified in ECs at both gene and protein levels. Chemerin mainly functions via CMKLR1 receptor, CCRL2 is known to act as a non-functional decoy receptor (Cash et al., 2008), whereas, the functional effects of chemerin upon GPR1 receptor binding still remain unknown (Barnea et al., 2008). Chemerin is a newly identified cytokine and is expressed in a number of body tissues, however, adipose tissue acts as a major source of chemerin expression and secretion in the human body (Roh et al., 2007, Bozaoglu et al., 2007, Goralski et al., 2007). Chemerin functions via its natural GPCR, CMKLR1 and is known to mediate adipogenesis, adipocyte metabolism (Roh et al., 2007, Goralski et al., 2007) and recruitment of cells of immune system to the sites of inflammation (Wittamer et al., 2005, Wittamer et al., 2003). Chemerin expression is reported to be upregulated in inflammatory diseases such as psoriatic skin lesions (Albanesi et al., 2009) and rheumatoid arthritis (Kaneko et al., 2011). Circulating chemerin levels positively correlate with various facets of metabolic syndrome such as high circulating glucose levels, triglycerides, high blood pressure and low levels of HDL and high LDL levels (Bozaoglu et al., 2007, Bozaoglu et al., 2009). Abnormal circulating metabolites in the bloodstream are implicated in the development and progression of diseases associated with chronic inflammation, EC injury, T2D and related cardiovascular complications (Kukk et al., 1996b, Grundy et al., 2004). In HMEC-1 cells, known

inflammatory cytokines such as TNF-α, IL-6 and IL-1β treatments resulted in increased protein expression of CMKLR1 which suggests that under inflammatory conditions, CMKLR1 receptor availability is increased (Kaur et al., 2010), hence encouraging the participation of chemerin/CMKLR1 axis in causing inflammatory responses in a cell, and mediating the occurrence of inflammation-related pathologies in the body. CMKLR1, is primarily expressed on cells of the immune system, and under inflammatory conditions, the receptor expression is reported to be increased. A number of other molecules such as Lipopolysaccharide (LPS), an endotoxin, is also reported to increase CMKLR1 receptor expression in lower concentrations, however, is down-regulated when treated with higher LPS concentrations (Luangsay et al., 2009). In macrophages, Transforming Growth Factor-β (TGF-β), an anti-inflammatory protein, decreased CMKLR1 receptor protein expression (Zabel et al., 2006a). CMKLR1 receptor protein expression is also reported to change upon maturation of immature plasmacytoid dendritic cells (pDCs) into mature pDCs suggesting that chemerin may play an important role in pDCs trafficking (Vermi et al., 2005).

7.2 Chemerin (21-157) lead to ERK1/2, ERK5, p38 and SAPK/JNK MAPKs and Akt/PKB Kinases phosphorylation: role in EC proliferation, migration and capillary tube formation in HMEC-1 cell line

It is well documented that a number of MAPKs mediate critical cellular processes such as cell proliferation, apoptosis and differentiation depending on the type of stimuli involved and certain cell types. The Ras-Raf-MEK-ERK and MEK2/3-MEK5-ERK5 MAPKs signalling cascades are activated by a number of external stimuli (Fig. 1.5.1a, page number 35). These MAPK are known to play important roles in cell proliferation and differentiation (Nishimoto and Nishida, 2006), the key processes implicated in biological responses such as vasculogenesis and angiogenesis. ERK1/2 MAPK is known to play an important role from cell morphogenesis to whole organism development (Nishimoto and Nishida, 2006). Mice lacking ERK2 and MEK1 showed defects in embryo development, whereas, mice lacking ERK1 and MEK2 showed normal development (Hatano et al., 2003). Activation of ERK2 MAPK is of particular importance as mice deficient in ERK2 showed abnormal mesoderm differentiation, suggesting that ERK2 plays a crucial role in mesoderm formation (Yao et al., 2003). ERK5 MAPK is essential in the processes of cell proliferation, migration and angiogenesis as mice embryos deficient in ERK5 MAPK are reported to die due to lack of angiogenesis and failure to develop fully functional cardiovascular system. Also, mice lacking $ERK5^{-/-}$ showed decreased VEGF/VEGF165 expression, altered expression and secretion of other mitogenic factors, hence, leading to defective angiogenic responses (Sohn et al., 2002). A number of adipose-tissue derived hormones such as leptin, TNF-α and IL-1β are known to cause ERK1/2 MAPK phosphorylation and promote angiogenesis (Bouloumie et al., 1998), however, the roles of these MAPK in cell death remain to be fully understood (Mebratu and Tesfaigzi, 2009). p38 and SAPK/JNK MAPKs are

important MAPK known to play crucial roles in a number of biological processes including inflammation, cell cycle and death, development, and cell differentiation. Akt/PKB kinase phosphorylation at Ser473 site is known to increase EC angiogenesis upstream of VEGF protein and regulates the production of NO by the vascular endothelium (Michell et al., 1999). Akt/PKB kinase regulate protein expression of VEGF, which is the most potent angiogenic molecule known to promote angiogenesis, and activation of Akt/PKB kinase is suggested to be sufficient for angiogenesis to take place (Ackah et al., 2005). EC angiogenesis is a tightly regulated process in normo-physiological and pathological conditions and involves EC proliferation, migration and elongation of the EC tips to form capillary-like structures, such as embryo development and wound healing (Klagsbrun and D'Amore, 1991), and is balanced by a number of pro- and anti-angiogenic molecules (Folkman, 2006). Dysregulated angiogenesis in diseased states such as ischaemia, chronic inflammation, diabetes, and atherosclerosis is initiated by a number of risk factors affecting the normal EC functioning. Abnormal fat-cell secreted adipokines or chemokines circulating in the blood stream cause cell injury or inflammation of the endothelium vessel wall. Increased circulating chemerin levels in obese patients with metabolic disease risk factors suggest a role of chemerin in mediating EC injury, initiation, progression and pathogenesis of diseases such as dysregulated angiogenesis in tumour formation; atherosclerosis and causing diseases including heart attack and myocardial infarction by disrupting the functions of a number of different enzymes and proteins leading to defective functional outcome. VEGF also plays an important role in mediating pathological angiogenesis, such as that associated with tumour growth (Ferrara and Davis-Smyth, 1997). VEGF is supported heavily as a mitogen known to induce angiogenic responses in different animal

models (Zhang et al., 2011), and is a survival factor for ECs both *in vivo* and *in vitro* (Ohuchi et al., 1997b, Semenza et al., 2001). Many studies focussed on the actions of VEGF in ECs, and is demonstrated to be a potent stimulator of EC proliferation (Yamane et al., 1994, Ferrara and Henzel, 1989, Plouet et al., 1989, Connolly et al., 1989) and migration (Rousseau et al., 1997). Also, Watanabe and colleagues suggested that VEGF promotes endothelial survival by encouraging scaffold formation and cell attachment in microvascular ECs (Watanabe and Dvorak, 1997). Chemerin (21-157) upregulated the protein expression of HIF-1α, a transcription factor that regulates the mRNA expression of a number of genes including VEGF under normal and hypoxic conditions. Under hypoxic conditions, HIF-1α is known to increase VEGF protein expression, however, chemerin (21-157) down-regulated VEGF165 protein expression in a concentration-dependent manner. VEGF165b, which is formed upon alternative splicing of VEGF gene at exon 8 is an anti-angiogenic form of VEGF. VEGF165b is the opposite counterpart of VEGF165, and is the most abundant anti-angiogenic form of VEGFxxxb family (xxx representing the number of amino acids) (Appendix 5, Fig. 5.1a, page number 248), and competes for the binding site on tyrosine kinase receptor, VEGFR2, which is the main signalling receptor involved in VEGF-dependent angiogenesis and known to exert anti-angiogenic properties (Neufeld et al., 1999, Nowak et al., 2008). VEGF165b is reported to inhibit VEGF165-induced EC proliferation, migration and vasodilation (Bates et al., 2002). VEGF165b is implicated in the inhibition of VEGF165-induced EC proliferation, migration and vasodilation (Bates et al., 2002). VEGF165b is also reported to inhibit physiological angiogenesis and tumour growth (Woolard et al., 2004). In comparison to VEGF165, VEGF165b is down-regulated in cancers including renal-cell carcinoma (Bates et al., 2002), prostate (Woolard et al., 2004),

colon carcinoma (Varey et al., 2008) and malignant melanoma (Pritchard-Jones et al., 2007). VEGF165b contains the receptor-binding domain in its structure and acts as a competitive inhibitor of VEGF165 for VEGF receptor binding, however, failing to induce the full tyrosine phosphorylation of the receptor (Woolard et al., 2004). Increased VEGF165b protein expression in HMEC-1 cell line after Chemerin (21-157) treatments suggests that chemerin (21-157) may activate pathways independent of VEGF to promote EC angiogenesis, for example Notch/DLL4 (Appendix 4, page number 247). The balance between the pro- and anti-angiogenic VEGFR2 is the main signalling receptor for VEGF-dependent angiogenesis and was phosphorylated by chemerin (21-157) at Tyr1175 site both in a time- and concentration-dependent manner. VEGFR2 receptor phosphorylation at Tyr1175 is reported to be the key tyrosine residue involved in VEGF-dependent angiogenesis (Koch et al., 1995, Palframan et al., 2001). Waltenberger and colleagues reported that in porcine aortic ECs, although both VEGFR2 and VEGFR1 receptors undergo phosphorylation, only VEGFR2 transfected cells displayed migratory and proliferative responses (Waltenberger et al., 1994). VEGFR2 receptor activation further resulted in the recruitment of adaptor proteins such as PI3K and many other protein tyrosine phosphatases (Kroll and Waltenberger, 1997). VEGF is the most important and specific isoform of VEGF (Ferrara and Henzel, 1989) and is also known to initiate and accelerate other inflammatory diseases such as atherogenesis (Miura et al., 1997, Tabuchi et al., 1997) via activating VEGFR2 receptor (Terman et al., 1992). Chemerin (21-157) increased the activity of MMP-2 and -9 in a concentration-dependent manner in ECs. MMP-2 and MMP-9 are important metalloproteinases that are known to degrade the extracellular matrix and facilitate cell proliferation, migration and resulting capillary tube formation. A number of cytokines and growth

factors are reported to regulate the MMPs balance in the vasculature (Kobayashi et al., 1997) which when disturbed caused disease of endothelial-barrier function. Chemerin (21-157) also induced EC proliferation and capillary tube formation in a concentration-dependent manner. Cell proliferation and capillary tube formation are critically controlled processes in the normal and pathological angiogenesis.

In this project, HMEC-1 cell treatments with different chemerin (21-157) concentrations resulted in delayed ERK5 activity as compared with ERK1/2 MAPK, and could be due to the involvement of GPCR signalling pathways acting independent of GPCR receptors without the involvement of intracellular G-proteins, for example G Protein-Coupled Receptor Kinases (GRKs) and β-arrestins. Concentration-dependent biphasic response in the activities of p38 MAPK, ERK1/2 MAPK and Akt/PKB kinases; and also in HMEC-1 cell proliferation, in the presence of linear concentration-response observed in cell apoptosis assay, when treated with different chemerin (21-157) concentrations could be owing to the involvement of neighbouring receptors, either GPCR or non-GPCR receptors, for example Receptor Tyrosine Kinases (RTKs) or Epidermal Growth Factor Receptors (EGFRs). In order to eliminate the assumption if higher chemerin (21-157) concentrations prove to be toxic to the endothelial cells, performing a cell count before treatments with desired chemical could help to determine the limitation of endothelial cell apoptosis used in this project.

In conclusion, the role of chemerin (21-157) in sFlt-1 (soluble form of VEGFR1) secretion and production, VEGFR1 phosphorylation, and most importantly, the question of how the VEGF receptor signalling network is integrated and co-ordinated with other receptor tyrosine kinases in the ECs, such as angiopoietins and Tie receptors (Gale and Yancopoulos, 1999) must be addressed. Also, the involvement of different MAPKs and other signalling kinases in chemerin (21-157)-mediated angiogenesis and cell death remains to be elucidated. Bozaoglu and colleagues reported the involvement of ERK1/2 MAPK in angiogenesis (Bozaoglu et al., 2010), however, the role of other important MAPK such as p38, SAPK/JNK, ERK5 MAPK and Akt/PKB kinases needs to be understood. Role of chemerin (21-157) in mediating angiogenesis via pathways which are independent of VEGF such as Notch/DLL4 remains to be explored. Involvement of different MAPK in mediating the activities of MMPs enzymes, and also elucidate the role of Tissue Inhibitors of Metalloproteinases (TIMPs) in angiogenesis. In order to fully appreciate the role of chemerin (21-157) in mediating important biological responses such as angiogenesis, the finding must be carried out in *in vivo* models.

7.3 Chemerin (21-157) increased cell adhesion molecules protein expression and Nuclear Factor (NF)-κB activity: role in endothelial-monocyte cell adhesion in HMEC-1 cell line

Chemerin (21-157) significantly upregulated the cellular protein expression levels of cell adhesion molecules including E-selectin, VCAM-1, and ICAM-1 in a concentration-dependent manner at 12 and 24 hours. In addition, chemerin (21-157) also increased soluble protein expression of E-selectin (sE-selectin), VCAM-1 (sVCAM-1) and ICAM-1 (sICAM-1) adhesion molecules in a concentration-dependent manner. Combined treatments of HMEC-1 cells with chemerin (21-157) alone and in combination with IL-1β resulted in altered protein expression levels of E-selectin, VCAM-1 and ICAM-1. Adhesion molecules expression is known to increase in inflammatory states, for example ICAM-1 protein expression is induced by inflammatory cytokines and is highly expressed on the activated endothelium which is particularly important in mediating the firm adhesion of neutrophils on ECs as well as trans-endothelial migration. Under transcriptional regulation, VCAM-1 protein expression is considered as one of the earliest markers of lesions in animal model of atherogenesis (Cybulsky and Gimbrone, 1991). VCAM-1 is a key adhesion molecule expressed on the ECs that mediates monocyte recruitment to early lesions in an experimental model of atherogenesis (Cybulsky et al., 2001). Chemerin (21-157) increased NF-κB pathway activity, a well studied inflammatory pathway in a concentration-dependent manner, showing an additive increase when co-stimulated with chemerin (21-157) and IL-1β together in HMEC-1 cell line. HMEC-1 pre-treatments with BAY11-7085, a specific NF-κB inhibitor, prior to stimulating with chemerin (21-157) resulted in the down-regulation of VCAM-1 protein expression compared to chemerin (21-157) only treatments. Interestingly, BAY11-7085 only treatments in HMEC-1 cells resulted in increased VCAM-1 protein expression,

however, no current explanation is supported in the literature at present. Chemerin (21-157) significantly upregulated the protein expression of the chemoattractant protein, MCP-1 in a concentration-dependent manner after 12 and 24 hours of incubation; also showing an additive increase when co-stimulated with chemerin (21-157) and IL-1β, in comparison to chemerin (21-157) and IL-1β alone. MCP-1 is a chemoattractant protein and is implicated in the recruitment of monocytes to the inflamed endothelium (Gerszten et al., 1999, Luscinskas et al., 2000). Low molecular weight cytokines such as MCP-1 are capable of crossing the epithelial cell barriers such as EC, and establish a chemokine gradient across the cell wall, and attract monocytes to the extravascular spaces. Chemerin (21-157) encouraged monocyte cell adhesion to ECs in a concentration-dependent manner, and was inhibited when pre-incubated with specific inhibitors for NF-κB, p38 MAPK, ERK1/2 MAPK and Akt/PI3K pathways; suggesting the involvement of NF-κB transcription factor, and other mentioned key MAPKs, and kinases such as Akt/PKB in monocyte-endothelial cell adhesion respectively. MCP-1 is a chemoattractant protein and is primarily implicated in the recruitment of monocytes to the inflamed endothelium (Gerszten et al., 1999, Luscinskas et al., 2000). Leukocyte adhesion to EC involves initial leukocyte cell adhesion to the EC, rolling and tethering on the EC surface, followed by firm adhesion and trans-endothelial migration. In particular, recruitment and transmigration of monocyte cells to the extravascular spaces and formation of foam cells after the ingestion of lipids results in the production of inflammatory cytokines, recruiting smooth muscle cells to the inflammatory site and promoting cell proliferation; which again results in the formation of more unstable and complex plaques leading to complications associated with CVDs.

In conclusion, involvement of important kinases such as ERK1/2, p38 and ERK5 MAPKs in inducing NF-κB pathway activation remains to be elucidated. As different chemerin fragments are reported to show different functional effects, for example murine chemerin 15 (140-154) is reported to show anti-inflammatory properties (Cash et al., 2008). Therefore, not only the role of other chemerin fragments in inducing EC inflammation and pathology must be explored, but also the involvement of one or more chemerin receptors in mediating those effects must be understood (Fig. 1.3.1a, page number 26). In addition, finding must be carried out in *in vivo* animal models in order to fully understand the pro- or anti-inflammatory chemerin (21-157) behaviour.

7.4 Chemerin (21-157) increased endothelial Nitric Oxide Synthase (eNOS) activity via Akt/PI3 Kinase, PKA and PKC Pathways in ECs: role in nitrite and nitrate production in HMEC-1 cell line

Chemerin (21-157) increased eNOS activity by phosphorylating eNOS at Ser1177 [eNOS (Ser1177)] and dephosphorylating at Thr 495 [eNOS (Thr495)] in a time- and concentration-dependent manner; which are reported to be the main sites that regulate the activity of eNOS enzyme. In addition to Ser1177 and Thr495, eNOS is reported to be phosphorylated on a number of different sites that are known to increase the activity of eNOS; including Ser116 and Ser617, where the consequences of Ser116 phosphorylation remain unclear. More recently, eNOS phosphorylation or dephosphorylation at Thr495 site has been suggested as an intrinsic switch mechanism that determines whether eNOS enzyme results in the generation of NO or O_2^- (Lin et al., 2003). eNOS, which is an enzyme constitutively expressed on the cells of the endothelium, is the main enzyme that regulates the production of vascular NO, which maintains vascular homeostasis. ED marks early stages of vascular disease and is suggested as a direct result of NO deficiency (Cooke, 2004). NO inhibits key processes in atherogenesis such as down-regulating the expression of cell adhesion molecules (De Caterina et al., 1995, Khan et al., 1996, Biffl et al., 1996), monocyte adhesion, platelet aggregation, and vascular smooth muscle proliferation (Garg and Hassid, 1989). A variety of stimuli such as shear stress (Marsden et al., 1993), chronic exercise (Kojda et al., 2001), VEGF (Bouloumie et al., 1999), TGF-β (B et al., 2002); and a number of other cytokines are reported to alter eNOS expression and activity (Chen et al., 2003, Lu et al., 1996). Chemerin (21-157) increased the activity of eNOS at Ser1177 [eNOS (Ser1177)] via Akt/PI3, PKA, and PKC pathways. Chemerin (21-157)-induced eNOS (Ser1177) phosphorylation is reduced in ECs when pre-incubated with Akt/PI3 kinase, PKA

and PKC inhibitors, which suggests the involvement of these pathways in chemerin (21-157)-induced eNOS activity. Moreover, both PKA and PKC inhibitor pre-incubations in HMEC-1 cells, in the absence of chemerin (21-157), lead to eNOS phosphorylation at Ser1177, however, no current explanation is supported in the literature at present. Akt/PKB kinase phosphorylation at Ser473 site is crucial as it then phosphorylates eNOS at Ser1177 site resulting in the release of NO (Dimmeler et al., 1999, Fulton et al., 1999, Luo et al., 2000). In addition, AMPKα kinase phosphorylation at Thr172 (Appendix 12, Fig. 12.1a and b respectively, page numbers 280-82) is also known to increase the activity of eNOS by directly phosphorylating at Ser1177 [eNOS(Ser1177)]. VEGF, in addition to its mitogenic and chemotactic activities, is also known to release NO in primary HUVEC cells (van der Zee et al., 1997, Ahmed et al., 1997). Chemerin (21-157) increased the protein expression of caveolin-1 in a time- and concentration-dependent manner (Appendix 8, Fig. 8.1a and b respectively, page numbers 265-67). eNOS interaction with caveolin proteins including caveolin-1 and -3 is known to inhibit the activity of eNOS thus interfering with the production of NO (Bucci et al., 2000). Also, chemerin (21-157) increased HSP90 protein expression in a time- and concentration-dependent manner (Appendix 9, Fig. 9.1a and b respectively, page numbers 268-70). eNOS interaction with HSP90 is suggested to result in increased eNOS activity (Garcia-Cardena et al., 1998). Chemerin (21-157) increased iNOS protein expression in a time- and concentration-dependent manner; which is known to produce 100- to 1000- times more NO compared to that of eNOS (Nathan and Xie, 1994). In atherosclerosis, iNOS expression is increased, whereas, eNOS expression is low (Fukuchi and Giaid, 1999). iNOS protein expression is also increased in response to ischaemia (Azadzoi et al., 2004) and due to involvement of ROS (Aliev et al., 1998).

However, chemerin (21-157) failed to induce any changes in NOx levels in HMEC-1 cells, and caused decrease in $NO2^-$ levels. No or reduced availability of NO metabolites, in the presence of increased eNOS activity and iNOS expression, suggests the involvement of ROS. Although chemerin (21-157) increased eNOS activity, and also increased iNOS protein expression in a time- and concentration-dependent manner in HMEC-1 cell line, unfortunately, the assessment of NO metabolites in this project remained inconclusive.

Hence, in conclusion, in order to fully understand the role of chemerin (21-157) in EC functioning and NO production in the endothelium, better NO assessment method must be considered. Involvement of ROS in endothelium NO production and depletion needs to be elucidated; as ROS are known to act as signalling molecules in the vascular endothelium and activate a number of downstream signalling molecules such as MAPKs and different ion channels; which in turn are implicated in a number of different biological processes such as EC proliferation, migration, extracellular matrix degradation and expression of various different pro-inflammatory cytokines. In addition to ROS-mediated NO reduced bioavailability, oxidative stress is also known to inhibit eNOS activity via a number of different mechanisms such as depletion or toxicity of eNOS substrates, eNOS uncoupling and involvement of different endogenous inhibition of eNOS. One of these important mechanisms that is increasingly becoming popular is the involvement of endogenous inhibitors of eNOS. Asymmetrical N^G, N^G-dimethyl-L-arginine (ADMA), first characterised by Vallance P and colleagues (1991), is reported to act as a competitive inhibitor of eNOS, and its accumulation is reported to cause increased blood pressure and reduced blood flow (Vallance et al., 1992a). N^G-monomethyl-L-arginine (MMA) is reported to be another endogenous inhibitor of eNOS (Vallance et al., 1992b). Similar to ADMA

and MMA, Symmetric Dimethylarginine (SDMA) competes with eNOS substrate, L-arginine; however, is inactive and does not inhibit eNOS activity (Teerlink et al., 2009). Therefore, role of chemerin (21-157) in all above mentioned processed must be accounted for, and again *in vivo* animal models must be developed to fully understand the role of chemerin in different aspects of EC biology.

As previously mentioned, a number of active and inactive chemerin fragments are formed upon proteolytic cleavage of precursor protein, pre-prochemerin (Fig. 1.2.3a.1, page number 16). Chemerin (149-157) is the shortest chemerin fragment known to retain most of the activity of full length chemerin (21-157) *in vitro,* and binds to CMKLR1 in micromolar concentrations (Wittamer et al., 2004, Wong et al., 2011). The future work will be focussed on studying the role of chemerin (149-157) in EC biology. So far, similar to chemerin (21-157), chemerin (149-157) induced the phosphorylation of important MAPKs including ERK1/2, p38, SAPK/JNK MAPKs, and Akt/PKB and AMPKα kinases in a time- and concentration-dependent manner in HMEC-1 cell line. In addition, chemerin (149-157) also induced EC capillary tube formation in a concentration-dependent manner in HMEC-1 cell line.

8.1 Chemerin (149-157) Lead to ERK1/2 MAPK Phosphorylation in a Time- and Concentration-dependent Manner in HMEC-1 Cell Line

HMEC-1 cells were cultured in 6-well plates in MCDB cell medium containing 10% FCS, and were serum starved in the same medium containing 1% FCS overnight before performing different treatments. To study time-dependent ERK1/2 MAPK phosphorylation, HMEC-1 cells were treated with [3.0µM] chemerin (149-157) at different time-points for a maximum of 30 minutes. For concentration-dependent ERK1/2 MAPK phosphorylation, HMEC-1 cells were treated with different chemerin (149-157) [0-1000nM] concentrations for 15 minutes, however, failed to show ERK1/2 MAPK phosphorylation in nanomolar concentrations (Appendix 13, Fig. 13.1a, page numbers 283). HMEC-1 cells were then treated with different, micromolar chemerin (149-157) [0-30µM] concentrations for 15 minute. Cells were lysed in 1x RIPA buffer and protein lysates were separated using SDS-PAGE. Chemerin (149-157) phosphorylated ERK1/2 MAPK in a time- and concentration-dependent manner (Fig. 8.1a and b respectively).

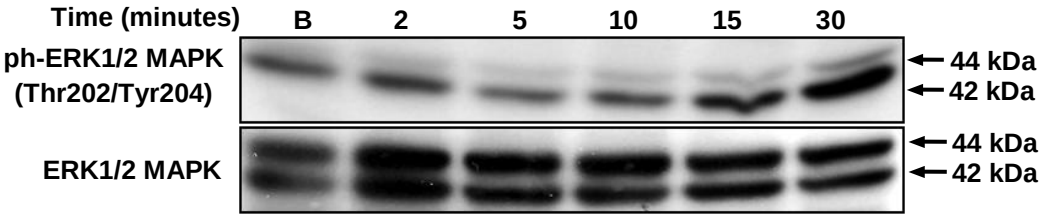

Figure 8.1a Chemerin (149-157) lead to ERK1/2 MAPK phosphorylation in a time-dependent manner in HMEC-1 cell line

HMEC-1 cells were treated with [3.0µM] chemerin (149-157) for 0-30 minutes. Following cell lysis and sample preparations, the proteins were separated using 12% polyacrylamide gels, and transferred to PVDF membranes at 100V for 1 hour. Membranes were incubated with specific phospho-ERK1/2 (Thr202/Tyr204) MAPK antibody [(1:1500); Cell signalling, Beverly, MA, USA] overnight at 4^{o}C. After removing the primary antibody complexes, membranes were incubated with anti-rabbit IgG-HRP labelled antibody [(1:2000); Dako, Ely, UK] for 1 hour at RT. Protein complexes were visualised using ECL plus detection reagent on X-ray films. Membranes were re-probed with total ERK1/2 MAPK antibody [(1:1500); Cell signalling, Beverly, MA, USA] and used as a loading control. The corresponding bands for both phospho-ERK1/2 and total ERK1/2 MAPK were detected as 44/42kDa products.

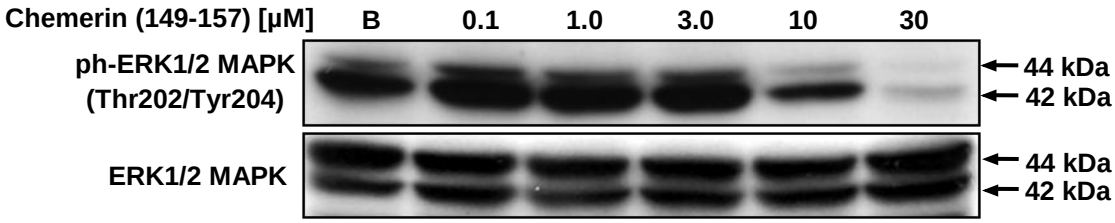

Figure 8.1b Chemerin (149-157) lead to ERK1/2 MAPK phosphorylation in a concentration-dependent manner in HMEC-1 cell line

HMEC-1 cells were treated with different chemerin (149-157) concentrations [0-30µM] for 15 minutes. Following cell lysis and sample preparations, the proteins were separated using 12% polyacrylamide gels, and transferred to PVDF membranes at 100V for 1 hour. Membranes were incubated with specific phospho-ERK1/2 (Thr202/Tyr204) MAPK antibody [(1:1500); Cell signalling, Beverly, MA, USA] overnight at 4^{o}C. After removing the primary antibody complexes, membranes were incubated with anti-rabbit IgG-HRP labelled antibody [(1:2000); Dako, Ely, UK] for 1 hour at RT. Protein complexes were visualised using ECL plus detection reagent on X-ray films. Membranes were re-probed with total ERK1/2 MAPK antibody [(1:1500); Cell signalling, Beverly, MA, USA] and used as a loading control. The corresponding bands for both phospho-ERK1/2 and total ERK1/2 MAPK were detected as 44/42kDa products.

8.2 Chemerin (149-157) Lead to p38 MAPK Phosphorylation in a Time- and Concentration-dependent Manner in HMEC-1 Cell Line

HMEC-1 cells were cultured in 6-well plates in MCDB cell medium containing 10% FCS, and were serum starved in the same medium containing 1% FCS overnight before performing different treatments. To study time-dependent p38 MAPK phosphorylation, HMEC-1 cells were treated with [3.0µM] chemerin (149-157) at different time-points for a maximum of 30 minutes. For concentration-dependent p38 MAPK phosphorylation, HMEC-1 cells were treated with different chemerin (149-157) [0-30µM] concentrations for 15 minute. Cells were lysed in 1x RIPA buffer and protein lysates were separated using SDS-PAGE. Chemerin (149-157) phosphorylated p38 MAPK in a time- and concentration-dependent manner (Fig. 8.2a and b respectively).

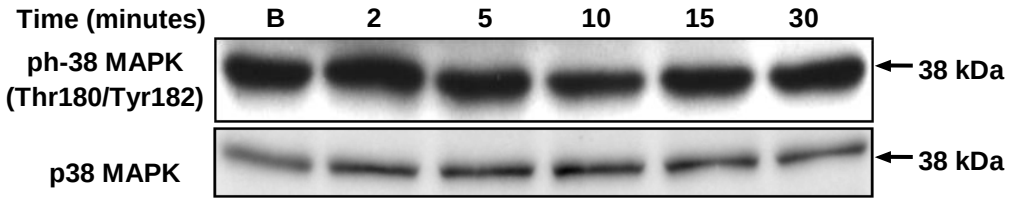

Figure 8.2a Chemerin (149-157) lead to p38 MAPK phosphorylation in a time-dependent manner in HMEC-1 cell line

HMEC-1 cells were treated with [3.0µM] chemerin (149-157) for 0-30 minutes. Following cell lysis and sample preparations, the protein lysates were separated using 12% polyacrylamide gels, and transferred to PVDF membranes at 100V for 1 hour. Membranes were incubated with specific phospho-p38 (Thr180/Tyr182) MAPK antibody [(1:1500); Cell signalling, Beverly, MA, USA] overnight at 4^{o}C. After removing the primary antibody complexes, membranes were incubated with anti-rabbit IgG-HRP labelled antibody [(1:2000); Dako, Ely, UK] for 1 hour at RT. Protein complexes were visualised using ECL plus detection reagent on X-ray films. Membranes were re-probed with total p38 MAPK antibody [(1:1500); Cell signalling, Beverly, MA, USA] and used as a loading control. The corresponding bands for both phospho-p38 and total p38 were detected as 38kDa products.

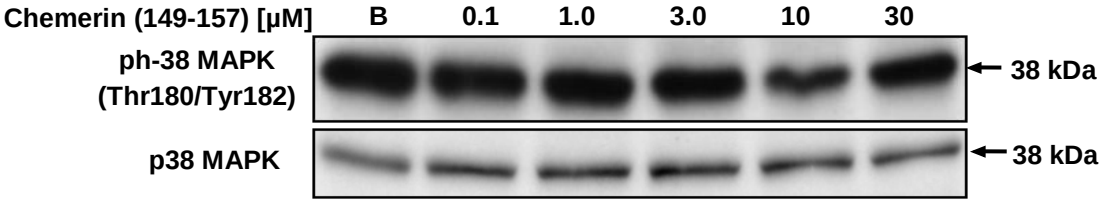

Figure 8.2b Chemerin (149-157) lead to p38 MAPK phosphorylation in a concentration-dependent manner in HMEC-1 cell line

HMEC-1 cells were treated with different chemerin (149-157) concentrations [0-30μM] for 15 minutes. Following cell lysis and sample preparations, the protein lysates were separated using 12% polyacrylamide gels, and transferred to PVDF membranes at 100V for 1 hour. Membranes were incubated with specific phospho-p38 (Thr180/Tyr182) MAPK antibody [(1:1500); Cell signalling, Beverly, MA, USA] overnight at 4^{o}C. After removing the primary antibody complexes, membranes were incubated with anti-rabbit IgG-HRP labelled antibody [(1:2000); Dako, Ely, UK] for 1 hour at RT. Protein complexes were visualised using ECL plus detection reagent on X-ray films. Membranes were re-probed with total p38 MAPK antibody [(1:1500); Cell signalling, Beverly, MA, USA] and used as a loading control. The corresponding bands for both phospho-p38and total p38 were detected as 38kDa products.

8.3 Chemerin (149-157) lead to SAPK/JNK MAPK Phosphorylation in a Time- and Concentration-dependent Manner in HMEC-1 Cell Line

HMEC-1 cells were cultured in 6-well plates in MCDB cell medium containing 10% FCS, and were serum starved in the same medium containing 1% FCS overnight before performing different treatments. To study time-dependent SAPK/JNK MAPK phosphorylation, HMEC-1 cells were treated with [1.0µM] chemerin (149-157) at different time-points for a maximum of 30 minutes. For concentration-dependent SAPK/JNK MAPK phosphorylation, HMEC-1 cells were treated with different chemerin (149-157) [0-30µM] concentrations for 30 minute. Cells were lysed in 1x RIPA buffer and protein lysates were separated using SDS-PAGE. Chemerin (149-157) phosphorylated SAPK/JNK MAPK in a time- and concentration-dependent manner (Fig. 8.3a and b respectively).

.

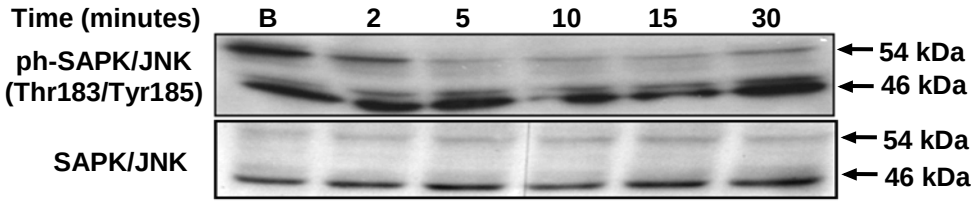

Figure 8.3a Chemerin (149-157) lead to SAPK/JNK MAPK phosphorylation in a time-dependent manner in HMEC-1 cell line

HMEC-1 cells were treated with [1.0µM] chemerin (149-157) for 0-30 minutes. Following cell lysis and sample preparations, the protein lysates were separated using 10% polyacrylamide gels, and transferred to PVDF membranes at 100V for 1 hour. Membranes were incubated with phospho-SAPK/JNK (Thr183/Tyr185) MAPK antibody [(1:1500); Cell signalling, Beverly, MA, USA] overnight at 4^{o}C. After removing the primary antibody complexes, membranes were incubated with anti-rabbit IgG-HRP labelled antibody [(1:2000); Dako, Ely, UK] for 1 hour at RT. Protein complexes were visualised using ECL plus detection reagent on X-ray films. Membranes were re-probed with total SAPK/JNK MAPK antibody [(1:1500); Cell signalling, Beverly, MA, USA] and used as a loading control. The corresponding bands for both phospho-SAPK/JNK and total SAPK/JNK were detected as 54/46kDa products.

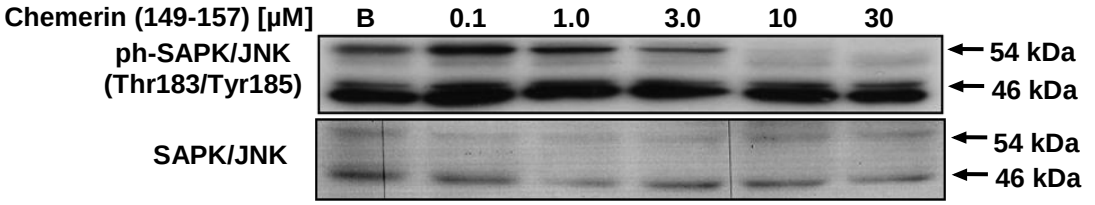

Figure 8.3b Chemerin (149-157) lead to SAPK/JNK MAPK phosphorylation in a concentration-dependent manner in HMEC-1 cell line

HMEC-1 cells were treated with different chemerin (149-157) concentrations [0-30μM] for 30 minutes. Following cell lysis and sample preparations, the protein lysates were separated using 10% polyacrylamide gels, and transferred to PVDF membranes at 100V for 1 hour. Membranes were incubated with phospho-SAPK/JNK (Thr183/Tyr185) MAPK antibody [(1:1500); Cell signalling, Beverly, MA, USA] overnight at 4^{o}C. After removing the primary antibody complexes, membranes were incubated with anti-rabbit IgG-HRP labelled antibody [(1:2000); Dako, Ely, UK] for 1 hour at RT. Protein complexes were visualised using ECL plus detection reagent on X-ray films. Membranes were re-probed with total SAPK/JNK MAPK antibody [(1:1500); Cell signalling, Beverly, MA, USA] and used as a loading control. The corresponding bands for both phospho-SAPK/JNK and total SAPK/JNK were detected as 54/46kDa products.

8.4 Chemerin (149-157) Lead to Akt/PKB Kinase Phosphorylation in a Time- and Concentration-dependent Manner in HMEC-1 Cell Line

HMEC-1 cells were cultured in 6-well plates in MCDB cell medium containing 10% FCS, and were serum starved in the same medium containing 1% FCS overnight before performing various different treatments. To study time-dependent Akt/PKB kinase phosphorylation, HMEC-1 cells were treated with [3.0µM] chemerin (149-157) at different time-points for a maximum of 30 minutes. For concentration-dependent Akt/PKB kinases phosphorylation, HMEC-1 cells were treated with different chemerin (149-157) [0-30µM] concentrations for 15 minute. Cells were lysed in 1x RIPA buffer and protein lysates were separated using SDS-PAGE. Chemerin (149-157) phosphorylated Akt/PKB Kinase in a time- and concentration-dependent manner (Fig. 8.4a and b respectively).

.

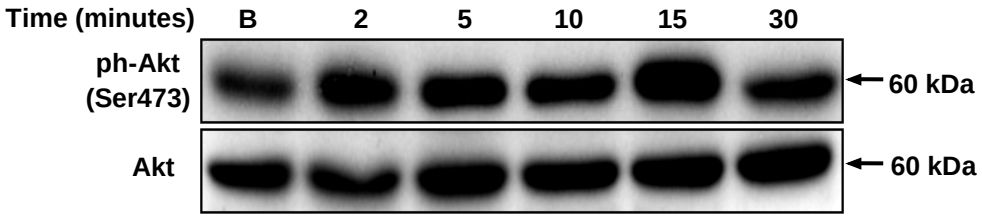

Figure 8.4a Chemerin (149-157) lead to Akt/PKB Kinase phosphorylation in a time-dependent manner in HMEC-1 cell line

HMEC-1 cells were treated with [3.0μM] chemerin (149-157) for 0-30 minutes. Following cell lysis and sample preparations, the protein lysates were separated using 10% polyacrylamide gels, and transferred to PVDF membranes at 100V for 1 hour. Membranes were incubated with phospho-Akt (Ser473) antibody [(1:1500); Cell signalling, Beverly, MA, USA] overnight at 4^{o}C. After removing the primary antibody complexes, membranes were incubated with anti-rabbit IgG-HRP labelled antibody [(1:2000); Dako, Ely, UK] for 1 hour at RT. Protein complexes were visualised using ECL plus detection reagent on X-ray films. Membranes were re-probed with total Akt antibody [(1:1500); Cell signalling, Beverly, MA, USA] and used as a loading control. The corresponding bands for both phospho-Akt and total Akt were detected as 60kDa products.

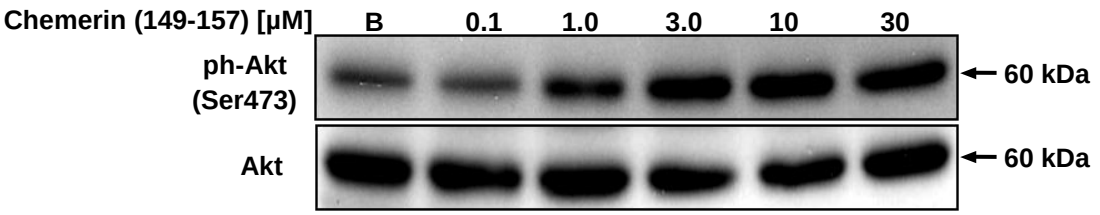

Figure 8.4b Chemerin (149-157) lead to Akt/PKB Kinase phosphorylation in a concentration-dependent manner in HMEC-1 cell line

HMEC-1 cells were treated with different chemerin (149-157) concentrations [0-30μM] for 15 minutes. Following cell lysis and sample preparations, the protein lysates were separated using 10% polyacrylamide gels, and transferred to PVDF membranes at 100V for 1 hour. Membranes were incubated with phospho-Akt (Ser473) antibody [(1:1500); Cell signalling, Beverly, MA, USA] overnight at 4^{o}C. After removing the primary antibody complexes, membranes were incubated with anti-rabbit IgG-HRP labelled antibody [(1:2000); Dako, Ely, UK] for 1 hour at RT. Protein complexes were visualised using ECL plus detection reagent on X-ray films. Membranes were re-probed with total Akt antibody [(1:1500); Cell signalling, Beverly, MA, USA] and used as a loading control. The corresponding bands for both phospho-Akt and total Akt were detected as 60kDa products.

8.5 Chemerin (149-157) Lead to AMPKα Kinase Phosphorylation in a Time- and Concentration-dependent Manner in HMEC-1 Cell Line

HMEC-1 cells were cultured in 6-well plates in MCDB cell medium containing 10% FCS, and were serum starved in the same medium containing 1% FCS overnight before performing different treatments. To study time-dependent AMPKα kinases phosphorylation, HMEC-1 cells were treated with [10μM] chemerin (149-157) at different time-points for a maximum of 30 minutes. For concentration-dependent AMPKα kinase phosphorylation, HMEC-1 cells were treated with different chemerin (149-157) [0-30μM] concentrations for 10 minute. Cells were lysed in 1x RIPA buffer and protein lysates were separated using SDS-PAGE. Chemerin (149-157) phosphorylated AMPKα kinase in a time- and concentration-dependent manner (Fig. 8.5a and b respectively).

.

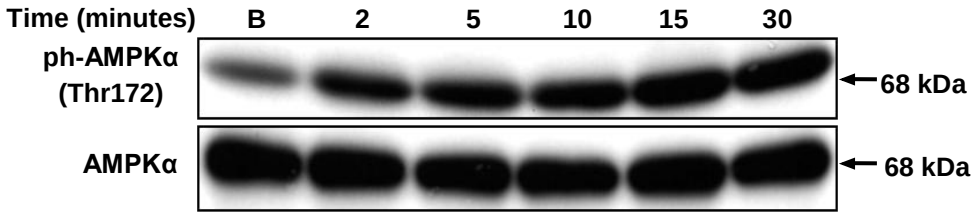

Figure 8.5a Chemerin (149-157) lead to AMPKα kinase phosphorylation in a time-dependent manner in HMEC-1 cell line

HMEC-1 cells were treated with [10μM] chemerin (149-157) for 0-30 minutes. Following cell lysis and sample preparations, the protein lysates were separated using 10% polyacrylamide gels, and transferred to PVDF membranes at 100V for 1 hour. Membranes were incubated with phospho-AMPKα (Thr172) antibody [(1:1500); Cell signalling, Beverly, MA, USA] overnight at 4^{o}C. After removing the primary antibody complexes, membranes were incubated with anti-rabbit IgG-HRP labelled antibody [(1:2000); Dako, Ely, UK] for 1 hour at RT. Protein complexes were visualised using ECL plus detection reagent on X-ray films. Membranes were re-probed with total AMPKα antibody [(1:1500); Cell signalling, Beverly, MA, USA] and used as a loading control. The corresponding bands for both phospho-AMPKα and total AMPKα were detected as 68kDa products.

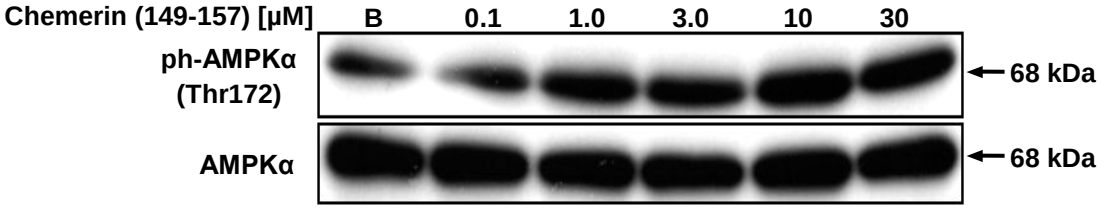

Figure 8.5b Chemerin (149-157) lead to AMPKα kinase phosphorylation in a concentration-dependent manner in HMEC-1 cell line

HMEC-1 cells were treated with different chemerin (149-157) concentrations [0-30μM] for 10 minutes. Following cell lysis and sample preparations, the protein lysates were separated using 10% polyacrylamide gels, and transferred to PVDF membranes at 100V for 1 hour. Membranes were incubated with phospho-AMPKα (Thr172) antibody [(1:1500); Cell signalling, Beverly, MA, USA] overnight at 4^{o}C. After removing the primary antibody complexes, membranes were incubated with anti-rabbit IgG-HRP labelled antibody [(1:2000); Dako, Ely, UK] for 1 hour at RT. Protein complexes were visualised using ECL plus detection reagent on X-ray films. Membranes were re-probed with total AMPKα antibody [(1:1500); Cell signalling, Beverly, MA, USA] and used as a loading control. The corresponding bands for both phospho-AMPKα and total AMPKα were detected as 68kDa products.

8.6 Chemerin (149-157) Induced Capillary Tube Formation in HMEC-1 Cell Line

Chemerin (149-157) induced capillary tube formation in a concentration-dependent manner in HMEC-1 cell line. VEGF [10ng/ml] was used as a positive control (Fig. 8.6a).

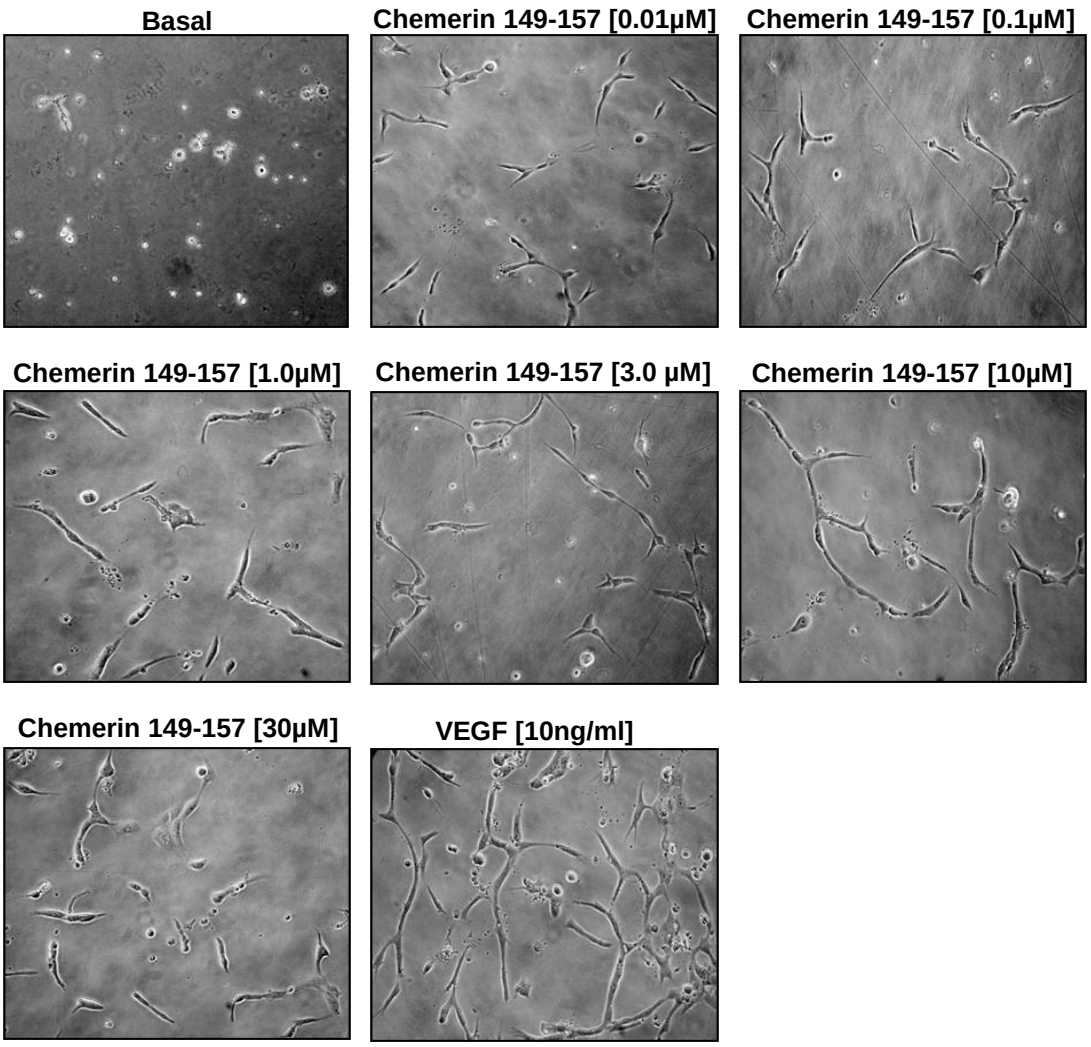

Figure 8.6a Chemerin (149-157) induced capillary tube formation in a concentration-dependent manner in HMEC-1 cell line

HMEC-1 cells were trypsinised and seeded onto the Matrigel coated plates at the cell density of $2x10^3$cells/well in the fresh medium and incubated for 2 hours. Cell medium was replaced with MCDB medium containing 1% FCS and incubated for 4 hours. Post incubations, HMEC-1 cells were treated with different chemerin (149-157) concentrations [0-30µM] and VEGF [10ng/ml] and incubated for a maximum of 24 hours. Capillary tube formation images were captured using a digital microscope camera system (Olympus, Tokyo, Japan) under 100x magnification. VEGF [10ng/ml] was used as a positive control.

1. Materials Used

1.1 List of buffers and cell media solution

List of Buffers and Cell Media Solution
Blocking solution – 5% Bovine Serum Albumin
DMEM medium – Invitrogen, Paisley, UK
HMEC-1 cell line - CDC, Atlanta, Georgia, USA
MCDB medium - Sigma-Aldrich, Dorset, UK
Medium 199 (M199) cell medium – Invitrogen, Paisley, UK L-glutamine
Membrane Stripping Buffer
Opti-MEM® medium - Invitrogen, Paisley, UK)
SDS-PAGE Transfer Buffer – 10% Tris/Glycine solution, 20% methanol and water
SDS-PAGE Running Buffer (10x) 30.3g Tris base, 144g glycine, 10g SDS – total volume 1000ml with distilled water
PBS containing 0.01% Triton X-100 (PBS-T)
Phosphate Buffer Solution (PBS)
Tris Borate-EDTA (TBE)
Tris Buffered Saline (TBS) wash buffer
Tris Buffered Saline-0.1% Tween-20 (TBS-T) wash buffer
Trypan Blue solution - Invitrogen, Paisley, UK
Trypsin EDTA

All the buffer solutions were prepared by Media Preparation Laboratory, Department of Life Sciences, The University of Warwick, UK; unless otherwise stated.

1.2 DNA and protein markers

Markers	Supplier name
GeneRuler™ 1kb DNA ladder	Fermentas, UK
GeneRuler™ 50bp DNA ladder	Fermentas, UK
PageRuler™ Prestained Protein	Fermentas, UK
Spectra™ Multicolour Broad Range Protein Ladder	Fermentas, UK

1.3 List of chemicals and reagents

Chemicals/Reagents	Supplier name
Ammonium Persulphate (APS)	Sigma Aldrich, Dorset, UK
Chemerin (21-157)	R and D systems, Abingdon, UK
Chemerin 149-157	AnaSpec, Cambridge, UK
β-Mercaptoethanol	Sigma Aldrich, Dorset, UK
Dimethylsulphoxide (DMSO)	Sigma Aldrich, Dorset, UK
Endothelial Cell Growth Supplement (ECGS)	BD Biosciences, Bedford, MA, UK
Epidermal Growth Factor (EGF)	Invitrogen, Paisley, UK
Ethidium Bromide	Sigma Aldrich, Dorset, UK
Fetal Calf Serum (FCS)	Sigma Aldrich, Dorset, UK
Glacial Acetic Acid	Sigma Aldrich, Dorset, UK
Glutamine	Sigma Aldrich, Dorset, UK
Heparin	Aventis Pharma, Milan, Italy
H_2O_2	Sigma Aldrich, Dorset, UK
Interleukine-1 beta (IL-1β)	Abcam, Cambridge, UK
Interleukine-6	NBS Biologicals, Cambridgeshire, UK
Lipofectamine	Invitrogen, Paisley, UK
$MgCl_2$	Biogene, Kimbolton, UK
(M-MuLV) reverse transcriptase	Fermentas, York, UK
N-(1-Naphthyl) ethylenediamine dihydrochloride	Sigma Aldrich, Dorset, UK
NF-κB binding sites (pcDNA3.1-NF-κB-Luc)	Stratagene, La Jolla, CA

N, N, N', N'- tetramethyl-ethylenediamine	Sigma Aldrich, Dorset, UK
Penicillin	Sigma Aldrich, Dorset, UK
Protogel [30% Acrylamide: Bisacrylamide (37.5:1)	GENEFLOW, Limited, UK
Poly-L-lysine	Sigma Aldrich, Dorset, UK
Sodium nitrite	Sigma Aldrich, Dorset, UK
Sodium nitrate	Sigma Aldrich, Dorset, UK
Streptomycin	Sigma Aldrich, Dorset, UK
Sulfanilamide	Sigma Aldrich, Dorset, UK
Tumour Necrosis factor (TNF)-alpha	Calbiochem, UK
Trypsin/EDTA	Sigma Aldrich, Dorset, UK
Vanadium chloride	Sigma Aldrich, Dorset, UK
VECTASHIELD mounting medium with DAPI	Vector Laboratories, Inc Orton Southgate, Peterborough, UK
VEGF	Sigma Aldrich, Dorset, UK
1M HCL solution	Sigma Aldrich, Dorset, UK
4´,6-Diamidino-2-phenylindole dihydrochloride	Sigma-Aldrich, Dorset, UK
70% Ethanol	Sigma Aldrich, Dorset, UK

1.4 Inhibitors

Inhibitors	Supplier name
BAY11-7085	Calbiochem, UK
LY294002	Calbiochem, san Diego, CA, USA
Pertussis toxin	Sigma-Aldrich, UK
PKA inhibitor - H-89	Calbiochem, san Diego, CA, USA
PKC inhibitor - BIS II	Sigma-Aldrich, UK
SB203580	Calbiochem, san Diego, CA, USA
U0126	Calbiochem, san Diego, CA, USA

1.5 Lab apparatus and glass and plastic ware

Lab apparatus and glass and plastic ware
Gilson pipettes
Glassware – cylinders, beakers, conical flasks, storage bottles and funnels
Filters
Gloves
Liquid Broth (LB) plates
Petri dishes
Pipette tips
Syringes
0.5, 1 and 1.5ml eppendorf tubes
6, 12, 24 and 96 well plates
5, 10 and 20ml eppendorf tubes
Tissue culture flasks
Universal containers

Liquid Broth (LB) plates were prepared by Media Preparation Laboratory, Department of Life Sciences, The University of Warwick, UK.

1.6 Lab equipment

Lab apparatus
Automated analyser – Abbott Architect, Abbott Laboratories, Abbott Park, IL, USA
Digital microscope camera – Olympus, Tokyo, Japan
DMRE Laser-scanning confocal microscope – Leica, Milton Keynes, UK
DNA sequencer – Molecular Biology Lab, Department of Life Sciences, University of Warwick, UK
ELISA plate reader – EL800, Bio-Tek Instruments, Inc., Winooski, VT, USA
Freezing container – Nalgene® Mr Frosty, Sigma-Aldrich, UK
Fuji medical X-ray film – Fuji Photo Film Company, Tokyo, Japan
Luminex® 100 instrument
Leica model DMRE laser-scanning confocal microscope – Milton Keynes, UK
Mr Frosty cryofreezing container – Fischer Scientific, Loughborough, UK
NanoDrop spectrophotometer – Labtech International, Ringmer, UK
Plate reader – Multiskan Ascent 96/384 Plate Reader
Pro-plus software – Media Cybernetics, Bethesda, MD
Roche Light Cycler™ System – Roche Molecular Biochemicals, Mannheim, Germany
Scion Image™ – Scion Corporation, Maryland, USA
Spectrophotomer – Beckman Instruments Inc., California, USA

1.7 Specialised assay kits

Assay kits	Supplier name
BioCoat Angiogenesis System	BD Biosciences, UK
Cell DNA Fragmentation Assay	Roche Diagnostics, UK
CellTitre 96 Aqueous one solution Cell Proliferation assay kit	Promega, UK
GenElute Plasmid Miniprep Kit	Qiagen, Crawley, UK
Growth Factor Reduced Matrigel	BD Biosciences, San Jose, CA, USA
QIAquick Gel Extraction kit	Qiagen, Crawley, UK
QIAGEN Plasmid Maxi Kit	Qiagen, Crawley, UK
sE-selectin, sICAM-1, sVCAM-1 and sPAI-1 multiplex assay kit	Millipore, UK

1.8 Antibodies

Antibodies	Supplier name
Akt antibody	Cell Signalling, Beverly, MA, USA
Anti-MMP-2 antibody	Abcam, Cambridge, UK
Anti-MMP-9 antibody	Abcam, Cambridge, UK
Anti-rabbit horseradish peroxide-conjugated antibody	Dako, Ely, UK
Alexa 680 conjugated anti-mouse IgG	Cell Signalling, Beverly, MA, USA
AMPKα antibody	Cell Signalling, Beverly, MA, USA
β-actin antibody Rabbit	Cell signalling, Beverly, MA, USA
Caveolin-1 antibody	Cell Signalling, Beverly, MA, USA
Chemerin antibody	R and D Systems, UK
Chemerin receptor, CMKLR1 antibody	Santa Cruz, California, USA
E-selectin antibody	Santa Cruz, California, USA
ERK 44/42 MAPK (Erk1/2)	Cell Signalling, Beverly, MA, USA
GPR-1 antibody	Santa Cruz, California, USA
ICAM-1 antibody	Santa Cruz, California, USA
MCP-1 monoclonal antibody	Cell Signalling, Beverly, MA, USA
PAI-1 antibody	Abcam, Cambridge, UK
Phospho-Akt (Ser473) (193H12) Rabbit mAb	Cell Signalling, Beverly, MA, USA
Phospho-AMPKα (Thr172) (40H9) Rabbit mAb	Cell Signalling, Beverly, MA, USA
Phospho ERK-44/42 MAPK (Erk1/2) (Thr202/Tyr204) Rabbit mAb	Cell Signalling, Beverly, MA, USA

p38 MAPK Antibody	Cell Signalling, Beverly, MA, USA
VCAM-1 antibody	Santa Cruz, California, USA
VEGF (Ab)-1 antibody	Lab Vision, Suffolk, UK
VEGF165b antibody	R and D Systems, UK
VEGFR2 antibody	Cell Signalling, Beverly, MA, USA

All chemical reagents and materials were stored at temperatures of 4-6^{o}C, - 20^{o}C and - 80^{o}C according to manufacturer's instructions.

2. CMKLR1 Receptor Staining Using Immunostaining

HMEC-1 cells were immunostained for CMKLR1 receptor; cells were plated on sterilised coverslips, and slides were prepared using Immunostaining method (Chapter 2, section 2.3.8, page numbers 59-61). CMKLR1 receptor was present in HMEC-1 cells (Fig. 2.1a). TNF-α [10ng/ml] was used as a positive control.

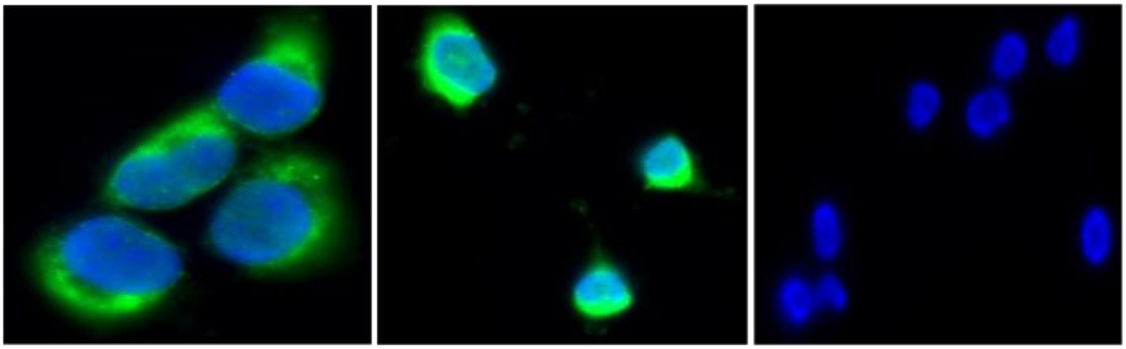

CMKLR1 TNF-α [10ng/ml] (-ve DAPI stain)

Figure 2.1a CMKLR1 receptor localisation and distribution in HMEC-1 cell line

HMEC-1 cells were incubated with anti-CMKLR1 antibody [(1:400); Santa Cruz, USA] constituted in PBS-T overnight at 4^{o}C. After removing the antibody, cells were washed with PBS and incubated with anti-mouse Alexa 680-conjugated IgG antibody [(1:400); Sigma, UK] and incubated in the dark for 2 hours. Cells were mounted in VECTASHIELD mounting medium with DAPI (Vector Laboratories, Inc Orton Southgate, Peterborough, UK) on microscope slides. Cells were observed under an oil immersion objective lens using a Leica model DMRE laser-scanning confocal microscope (Milton Keynes, UK). TNF-α [10ng/ml] served as a positive control and DAPI stain was used as a negative control.

3. Chemerin (21-157) Upregulated Hypoxia-inducible Factor (HIF)-1α Protein Expression in HMEC-1 Cell Line

HMEC-1 cells were cultured in 6-well plates in MCDB cell medium containing 10% FCS, and were serum starved in the same medium containing 1% FCS overnight before performing different treatments. HMEC-1 cells were treated with different chemerin (21-157) [0-10nM] concentrations for 6 hours. Cells were lysed in 1x RIPA buffer and protein lysates were separated using SDS-PAGE. Chemerin (21-157) significantly increased HIF-1α cellular protein expressions at [0.01-1nM] concentrations ($p < 0.001$) and decreasing significantly at [10nM] ($p < 0.01$) (Fig. 3.1a).

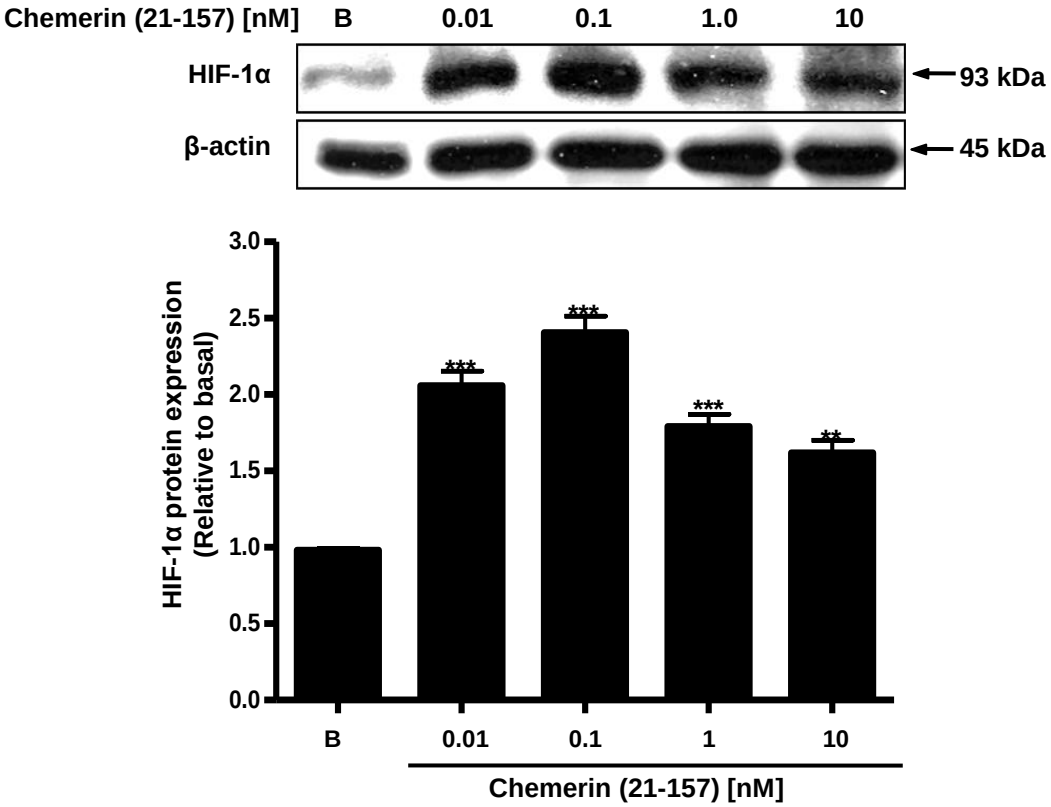

Figure 3.1a Chemerin (21-157) upregulated HIF-1α protein expression in HMEC-1 cell line

HMEC-1 cells were treated with different chemerin (21-157) concentrations [0-10nM] for 6 hours. Following cell lysis and sample preparations, the protein lysates were separated using 10% polyacrylamide gels, and transferred to PVDF membranes at 100V for 1 hour. Membranes were incubated with specific mouse HIF-1α antibody [(1:1000); Santa Cruz, USA] overnight at 4^{o}C. After removing the primary antibody complexes, membranes were incubated with anti-mouse IgG-HRP labelled antibody [(1:8000); Sigma-Aldrich, UK] for 1 hour at RT. Protein complexes were visualised using ECL plus detection reagent on X-ray films. Membrane were re-probed with rabbit β-actin antibody [(1:1500); Cell signalling, Beverly, MA, USA] and used as a loading control. The corresponding bands for HIF-1α and β-actin were detected as 93kDa and 45kDa products. The band intensities were measured using Scion Image™ densitometer (Scion Corporation, Maryland, USA). The data are presented as mean ± SEM of three independent experiments in duplicates ***p < 0.001 and **p < 0.01 compared to basal.

4. Angiogenic Pathways Independent of VEGF – Notch/DLL4

Cellular signalling pathways independent of VEGF/VEGFR1/VEGFR2 system are also known to mediate angiogenesis. Inter-endothelial signalling via Delta-like 4 (DLL4) and Notch has recently emerged as important regulators of endothelial heterogeneity, and controls arterial cell specification as well as tip versus stalk cell selection. Tip cell formation during angiogenesis is mediated by VEGF-dependent angiogenesis and Notch/DLL4-mediated through stalk cell phenotype. VEGFR2 system is also required by Notch. Notch receptors are required during vascular development and morphogenesis (Harrington et al., 2008).

5. Anti-angiogenic VEGF Isoforms and Angiogenesis

In 2002, VEGF165b was the first anti-angiogenic isoform identified (Bates et al., 2002) formed by differential splice-acceptor-site selection in the 3` UTR within exon 8 of the VEGF gene (Fig. 5.1a). The alternate splicing of VEGF gene results in the formation of anti-antigenic isoforms of VEGF which are grouped together in VEGFxxxb family; where xxx represents the number of amino acids. The VEGFxxxb isoforms correspond to that of their existing angiogenic counterparts of VEGF and are denoted as VEGF121b, VEGF145b, VEGF165b and VEGF189b (Perrin et al., 2005). The VEGF165b is an opposite counterpart of VEGF165 and inhibits VEGF165-induced endothelial cell proliferation, migration and vasodilation (Bates et al., 2002). In addition, VEGF165b also inhibits *in vivo* experimental and physiological angiogenesis and tumour growth and is reported to be down-regulated in cancers.

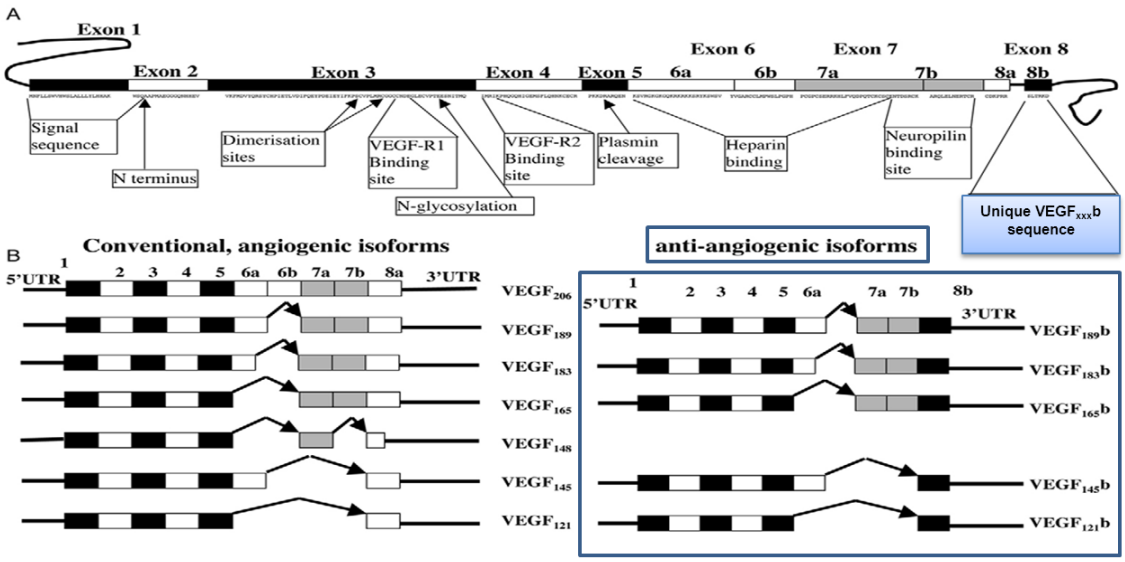

Figure 5.1a The alternative splicing of VEGF gene

Figure shows the alternative splicing of VEGF gene at exon 8. Exon 8b translates anti-angiogenic VEGF isoforms which are grouped together in VEGFxxxb, xxx representing the number of amino acids. VEGF121b, VEGF145b, VEGF165b, VEGF183b and VEGF189b are different anti-angiogenic VEGF isoforms formed by alternative splicing. Adapted from (Nowak et al., 2008).

6. Interleukin (IL)-1β Increased VCAM-1 and ICAM-1 Protein Expression in HMEC-1 Cell Line

HMEC-1 cells were cultured in 6-well plates in MCDB cell medium containing 10% FCS, and were serum starved in the same medium containing 1% FCS overnight before performing various different treatments. For studying optimum incubation time for IL-1β-induced VCAM-1 and ICAM-1 protein expressions in HMEC-1 cell line, cells were treated with [10ng/ml] IL-1β at different time-point for a maximum of 18 hours. Cells were lysed in 1x RIPA buffer and protein lysates were separated using SDS-PAGE. IL-1β increased both VCAM-1 (Fig. 6.1a) and ICAM-1 (Fig. 6.1b) protein expression in HMEC-1 cells, showing maximum protein expression at 6 hours, which then decreased with prolonged incubation times.

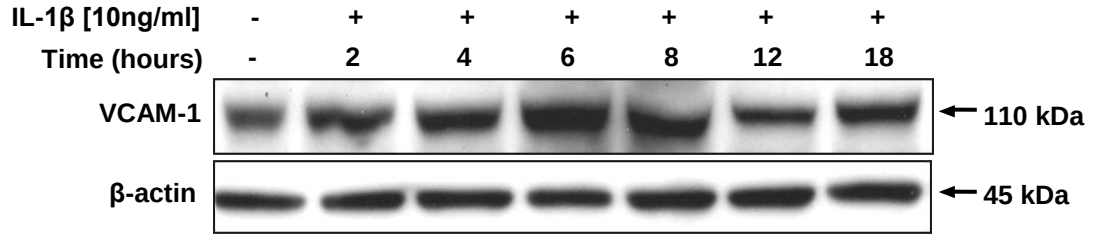

Figure 6.1a IL-1β increased VCAM-1 protein expression in HMEC-1 cell line

HMEC-1 cells were treated with IL-1β [10ng/ml] at different time-points for a maximum of 18 hours. Following cell lysis and sample preparations, the protein lysates were separated using 8% polyacrylamide gels, and transferred to PVDF membranes at 100V for 1 hour. Membranes were incubated with specific mouse anti-VCAM-1 antibody [(1:800); Santa Cruz, USA] overnight at 4^{o}C. After removing the primary antibody complexes, membranes were incubated with anti-mouse IgG-HRP labelled antibody [(1:8000); Sigma-Aldrich, UK] for 1 hour at RT. Protein complexes were visualised using ECL plus detection reagent on X-ray films. Membrane was re-probed with rabbit β-actin antibody [(1:1500); Cell signalling, Beverly, MA, USA] and used as a loading control. The corresponding bands for VCAM-1 and β-actin were detected as 110kDa and 45kDa products.

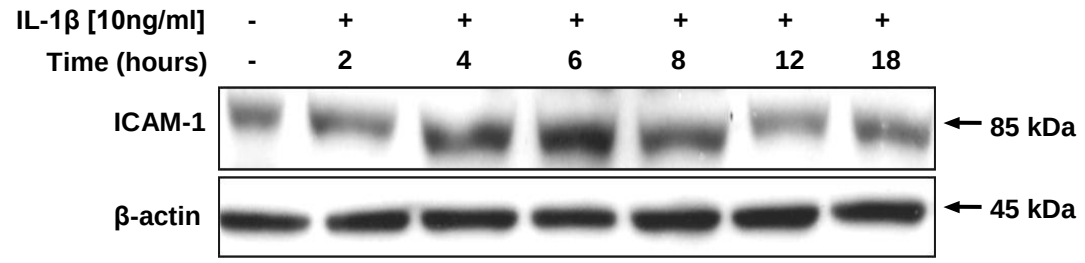

Figure 6.1b IL-1β increased ICAM-1 protein expression in HMEC-1 cell line

HMEC-1 cells were treated with IL-1β [10ng/ml] at different time-points for a maximum of 18 hours. Following cell lysis and sample preparations, the protein lysates were separated using 8% polyacrylamide gels, and transferred to PVDF membranes at 100V for 1 hour. Membranes were incubated with specific mouse anti-ICAM-1 antibody [(1:800); Santa Cruz, USA] overnight at 4^{o}C. After removing the primary antibody complexes, membranes were incubated with anti-mouse IgG-HRP labelled antibody [(1:8000); Sigma-Aldrich, UK] for 1 hour at RT. Protein complexes were visualised using ECL plus detection reagent on X-ray films. Membrane was re-probed with rabbit β-actin antibody [(1:1500); Cell signalling, Beverly, MA, USA] and used as a loading control. The corresponding bands for ICAM-1 and β-actin were detected as 85kDa and 45kDa products.

7. Cell Adhesion Molecules Secretion in HMEC-1 Cell Supernatants

HMEC-1 cells were treated with different chemerin (21-157) [0-30nM] concentrations for 4, 12 and 24 hours and cell supernatants were collected. Luminex® 100 system (Chapter 2, section 2.4.9, page numbers 70-1) was used to quantify the secreted levels of E-selectin (sE-selectin), VCAM-1 (sVCAM-1) and ICAM-1 (sICAM-1) proteins in HMEC-1 cell culture supernatants. TNF-α [10ng/ml] and IL-1β [10ng/ml] were used as positive controls.

7.1 sE-selectin protein secretion in HMEC-1 cell supernatants

HMEC-1 cells were treated with different chemerin (21-157) [0-30nM] concentrations for 4, 12 and 24 hours. Post incubations, HMEC-1 cell supernatants were collected and protein secretion levels were measured using Luminex® 100 system. Different chemerin (21-157) treatments failed to show any change in sE-selectin protein secretion in HMEC-1 cell supernatants at all three different time-points (Table 7.1a, b and c respectively).

Table 7.1a

Chemerin (21-157) and sE-selectin protein secretion in HMEC-1 cell supernatants after 4 hours

Treatments	4 hours (n=1) pg/mL	4 hours (n=2) pg/mL
Basal	0.1	nd
[0.01nM] chemerin (21-157)	0.05	0.05
[0.1nM] chemerin (21-157)	0.08	nd
[1nM] chemerin (21-157)	0.05	0.08
[10nM] chemerin (21-157)	nd	0.08
[30nM] chemerin (21-157)	nd	0.08
TNF-α [10ng/ml]	0.05	0.05
TNF-α [10ng/ml]	0.03	0.03
IL-1β [10ng/ml]	0	0

Table 7.1b

Chemerin (21-157) and sE-selectin protein secretion in HMEC-1 cell supernatants after 12 hours

Treatments	12 hours (n=1) pg/mL	12 hours (n=2) pg/mL
Basal	nd	nd
[0.01nM] chemerin (21-157)	nd	0.07
[0.1nM] chemerin (21-157)	0.08	0.04
[1nM] chemerin (21-157)	nd	nd
[10nM] chemerin (21-157)	nd	0.07
[30nM] chemerin (21-157)	0.07	0.05
TNF-α [10ng/ml]	0.05	0.05
TNF-α [10ng/ml]	0.03	0.03
IL-1β [10ng/ml]	0	0

Table 7.1c

Chemerin (21-157) and sE-selectin protein secretion in HMEC-1 cell supernatants after 24 hours

Treatments	24 hours (n=1) pg/mL	24hours (n=2) pg/mL
Basal	nd	nd
[0.01nM] chemerin (21-157)	0.02	nd
[0.1nM] chemerin (21-157)	nd	nd
[1nM] chemerin (21-157)	nd	nd
[10nM] chemerin (21-157)	nd	nd
[30nM] chemerin (21-157)	nd	nd
TNF-α [10ng/ml]	0.05	0.05
TNF-α [10ng/ml]	0.03	0.03
IL-1β [10ng/ml]	0	0

7.2 sVCAM-1 protein secretion in HMEC-1 cell supernatants

HMEC-1 cells were treated with different chemerin (21-157) [0-30nM] concentrations for 4, 12 and 24 hours. Post incubations, HMEC-1 cell supernatants were collected and protein secretion levels were measured using Luminex® 100 system. sVCAM-1 protein levels were not detected in HMEC-1 cell supernatants in any treatment group (Table 7.2a, b and c respectively).

Table 7.2a

Chemerin (21-157) and sVCAM-1 protein secretion in HMEC-1 cell supernatants after 4 hours

Treatments	4 hours (n=1) pg/mL	4hours (n=2) pg/mL
Basal	nd	nd
[0.01nM] chemerin (21-157)	nd	nd
[0.1nM] chemerin (21-157)	nd	nd
[1nM] chemerin (21-157)	nd	nd
[10nM] chemerin (21-157)	nd	nd
[30nM] chemerin (21-157)	nd	nd
TNF-α [10ng/ml]	9.62	9.00
TNF-α [10ng/ml]	57.88	54.63
IL-1β [10ng/ml]	129.68	125.76

Table 7.2b

Chemerin (21-157) and sVCAM-1 protein secretion in HMEC-1 cell supernatants after 12 hours

Treatments	12 hours (n=1) pg/mL	12hours (n=2) pg/mL
Basal	nd	nd
[0.01nM] chemerin (21-157)	nd	nd
[0.1nM] chemerin (21-157)	nd	nd
[1nM] chemerin (21-157)	nd	nd
[10nM] chemerin (21-157)	nd	nd
[30nM] chemerin (21-157)	nd	nd
TNF-α [10ng/ml]	10	9.58
TNF-α [10ng/ml]	50	47.25
IL-1β [10ng/ml]	250	245.46

Table 7.2c

Chemerin (21-157) and sVCAM-1 protein secretion in HMEC-1 cell supernatants after 24 hours

Treatments	24 hours (n=1) pg/mL	24 hours (n=2) pg/mL
Basal	nd	nd
[0.01nM] chemerin (21-157)	nd	nd
[0.1nM] chemerin (21-157)	nd	nd
[1nM] chemerin (21-157)	nd	nd
[10nM] chemerin (21-157)	nd	nd
[30nM] chemerin (21-157)	nd	nd
TNF-α [10ng/ml]	96	94.56
TNF-α [10ng/ml]	116	105.26
IL-1β [10ng/ml]	52	49.56

7.3 sICAM-1 protein secretion in HMEC-1 cell supernatants

HMEC-1 cells were treated with different chemerin (21-157) [0-30nM] concentrations for 4, 12 and 24 hours. Post incubations, HMEC-1 cell supernatants were collected and protein secretion levels were determined using Luminex® 100 system. Different chemerin (21-157) treatments failed to show any changes in sICAM-1 protein secretion in HMEC-1 cell supernatants at all three different time-points (Table 7.3a, b and c respectively).

Table 7.3a

Chemerin (21-157) and sICAM-1 protein secretion in HMEC-1 cell supernatants after 4 hours

Treatments	4 hours (n=1) pg/mL	4 hours (n=2) pg/mL
Basal	0.33	0.3
[0.01nM] chemerin (21-157)	0.26	0.26
[0.1nM] chemerin (21-157)	0.29	0.25
[1nM] chemerin (21-157)	0.24	0.25
[10nM] chemerin (21-157)	0.26	0.29
[30nM] chemerin (21-157)	0.22	0.3
TNF-α [10ng/ml]	4.54	4.54
TNF-α [10ng/ml]	3.25	3.25
IL-1β [10ng/ml]	8.04	8.04

Table 7.3b

Chemerin (21-157) and sICAM-1 protein secretion in HMEC-1 cell supernatants after 12 hours

Treatments	12 hours (n=1) pg/mL	12 hours (n=2) pg/mL
Basal	0.6	0.54
[0.01nM] chemerin (21-157)	0.52	0.57
[0.1nM] chemerin (21-157)	0.56	0.59
[1nM] chemerin (21-157)	0.55	0.53
[10nM] chemerin (21-157)	0.76	0.59
[30nM] chemerin (21-157)	0.81	0.73
TNF-α [10ng/ml]	4.54	4.54
TNF-α [10ng/ml]	3.25	3.25
IL-1β [10ng/ml]	8.04	8.04

Table 7.3c

Chemerin (21-157) and sICAM-1 protein secretion in HMEC-1 cell supernatants after 24 hours

Treatments	24 hours (n=1) pg/mL	24 hours (n=2) pg/mL
Basal	1.01	1.42
[0.01nM] chemerin (21-157)	1.06	1.29
[0.1nM] chemerin (21-157)	1.11	1.29
[1nM] chemerin (21-157)	1.01	1.45
[10nM] chemerin (21-157)	1.1	1.65
[30nM] chemerin (21-157)	1.31	1.72
TNF-α [10ng/ml]	4.54	4.54
TNF-α [10ng/ml]	3.25	3.25
IL-1β [10ng/ml]	8.04	8.04

8. Chemerin (21-157) Increased Caveolin-1 Protein Expression in a Time- and Concentration-dependent Manner in HMEC-1 Cell Line

HMEC-1 cells were cultured in 6-well plates in MCDB cell medium containing 10% FCS, and were serum starved in the same medium containing 1% FCS overnight before performing different treatments. To study time-dependent caveolin-1 protein expression, HMEC-1 cells were treated with [30nM] chemerin (21-157) at different time-points for a maximum of 24 hours. For concentration-dependent caveolin-1 protein expression, HMEC-1 cells were treated with different chemerin (21-157) [0-30nM] concentrations for 12 hours. Cells were lysed in 1x RIPA buffer and protein lysates were separated using SDS-PAGE. Chemerin (21-157) increased caveolin-1 protein expression in a time-dependent manner with a maximum response at 12 hours (Fig. 8.1a). Chemerin (21-157) increased caveolin-1 protein expression in a concentration-dependent manner showing maximum response at [30nM] chemerin (21-157) (Fig. 8.1b).

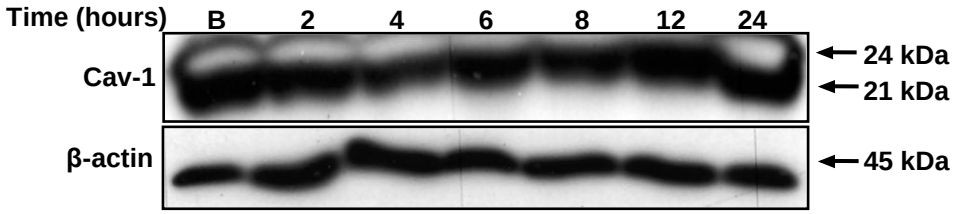

Figure 8.1a Chemerin (21-157) increased caveolin-1 protein expression in a time-dependent manner in HMEC-1 cell line

HMEC-1 cells were treated with [30nM] chemerin (21-157) for a maximum of 24 hours. Following cell lysis and sample preparations, the protein lysates were separated using 15% polyacrylamide gels, and transferred to PVDF membranes at 100V for 1 hour. Membranes were incubated with specific caveolin-1 antibody [(1:2000); Cell signalling, Beverly, MA, USA] overnight at 4^{o}C. After removing the primary antibody complexes, membranes were incubated with anti- rabbit IgG-HRP labelled antibody [(1:2000); Dako, Ely, UK] for 1 hour at RT. Protein complexes were visualised using ECL plus detection reagent on X-ray films. Membranes were re-probed with rabbit β-actin antibody [(1:1500); Cell signalling, Beverly, MA, USA] and used as a loading control. The corresponding bands for both caveolin-1 and β-actin were detected as 24/21kDa and 45kDa products.

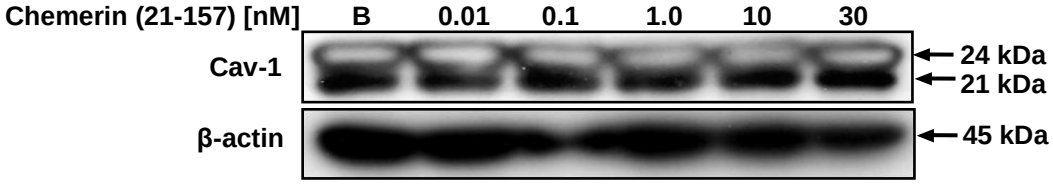

Figure 8.1b Chemerin (21-157) increased caveolin-1 protein expression in a concentration-dependent manner in HMEC-1 cell line

HMEC-1 cells were treated with different chemerin (21-157) concentrations [0-30nM] for 24 hours. Following cell lysis and sample preparations, protein lysates were separated using 15% polyacrylamide gels and transferred to PVDF membranes at 100V for 1 hour. Membranes were incubated with specific caveolin-1 antibody [(1:2000); Cell signalling, Beverly, MA, USA] overnight at 4^{o}C. After removing the primary antibody complexes, membranes were incubated with anti- rabbit IgG-HRP labelled antibody [(1:2000); Dako, Ely, UK] for 1 hour at RT. Protein complexes were visualised using ECL plus detection reagent on X-ray films. Membranes were re-probed with rabbit β-actin antibody [(1:1500); Cell signalling, Beverly, MA, USA] and used as a loading control. The corresponding bands for both caveolin-1 and β-actin were detected as 24/21kDa and 45kDa products.

9. Chemerin Increased Heat-Shock Protein (HSP90) Protein Expression in a Time- and Concentration-dependent Manner in HMEC-1 Cell Line

HMEC-1 cells were cultured in 6-well plates in MCDB cell medium containing 10% FCS, and were serum starved in the same medium containing 1% FCS overnight before performing different treatments. For studying time-point response, HMEC-1 cells were treated with [10nM] chemerin (21-157) at different time-points for a maximum of 24 hours. For concentration-dependent response, HMEC-1 cells were treated with different chemerin (21-157) [0-30nM] concentrations for 6 hours. Cells were lysed in 1x RIPA buffer and protein lysates were separated using SDS-PAGE. Chemerin (21-157) increased HSP90 protein expression in HMEC-1 cell line in a time-dependent manner showing a peak response at 6 hours (Fig. 9.1a). Chemerin (21-157) increased HSP90 protein expression in a concentration-dependent manner showing maximum response at [10nM] chemerin (21-157) (Fig. 9.1b).

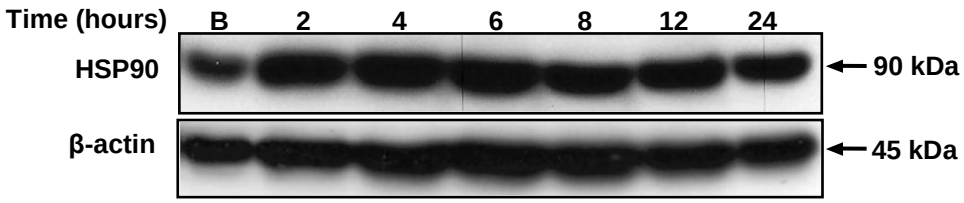

Figure 9.1a Chemerin (21-157) increased HSP90 protein expression in a time-dependent manner in HMEC-1 cell line

HMEC-1 cells were treated with [10nM] chemerin (21-157) for a maximum of 24 hours. Following cell lysis and sample preparations, the protein lysates were separated using 10% polyacrylamide gels, and transferred to PVDF membranes at 100V for 1 hour. Membranes were incubated with specific HSP90 antibody [(1:1500); Abcam Cambridge, UK] overnight at 4^{o}C. After removing the primary antibody complexes, membranes were incubated with rabbit IgG-HRP labelled antibody [(1:2000); Dako, Ely, UK] for 1 hour at RT. Protein complexes were visualised using ECL plus detection reagent on X-ray films. Membranes were re-probed with rabbit β-actin antibody [(1:1500); Cell signalling, Beverly, MA, USA] and used as a loading control. The corresponding bands for HSP90 and β-actin were detected as 90kDa and 45kDa products.

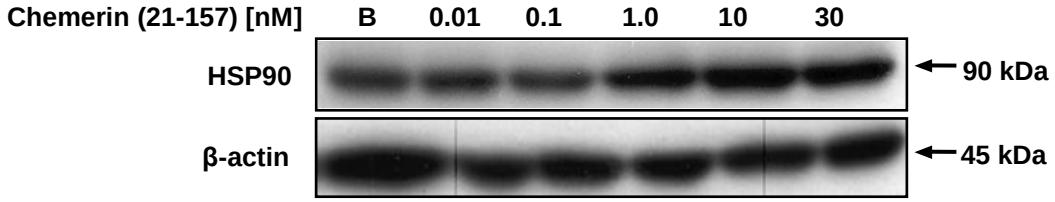

Figure 9.1b Chemerin (21-157) increased HSP90 protein expression in a concentration-dependent manner in HMEC-1 cell line

HMEC-1 cells were treated with different chemerin (21-157) concentrations [0-30nM] for 6 hours. Following cell lysis and sample preparations, the protein lysates were separated using 10% polyacrylamide gels, and transferred to PVDF membranes at 100V for 1 hour. Membranes were incubated with specific HSP90 antibody [(1:1500); Abcam Cambridge, UK] overnight at 4^{o}C. After removing the primary antibody complexes, membranes were incubated with rabbit IgG-HRP labelled antibody [(1:2000); Dako, Ely, UK] for 1 hour at RT. Protein complexes were visualised using ECL plus detection reagent on X-ray films. Membranes were re-probed with rabbit β-actin antibody [(1:1500); Cell signalling, Beverly, MA, USA] and used as a loading control. The corresponding bands for HSP90 and β-actin were detected as 90kDa and 45kDa products.

10. Chemerin (21-157) Increased Plasminogen Activator Inhibitor (PAI)-1 Protein Expression and Secretion in HMEC-1 Cell Line

HMEC-1 cells were cultured in 6-well plates in MCDB cell medium containing 10% FCS, and were serum starved in the same medium containing 1% FCS overnight before performing various different treatments. To study cellular protein expression of PAI-1, HMEC-1 cells were treated with different chemerin (21-157) [0-10nM] concentrations for 6 hours. Cells were lysed in 1x RIPA buffer and protein lysates were separated using SDS-PAGE. To study secreted levels of PAI-1, HMEC-1 cells were treated with different chemerin (21-157) [0-30nM] concentrations for 4, 12 and 24 hours. Cell supernatants were collected and soluble PAI-1 levels were determined using Luminex® 100 system in all three different treatment groups. In addition, in 24 hours cell supernatants, PAI-1 protein expression was also studied using SDS-PAGE. Chemerin (21-157) increased PAI-1 protein expression in a concentration-dependent manner in HMEC-1 cell lysates (Fig. 10.1a). Secreted PAI-1 protein levels were detected by SDS-PAGE in 24 hours cell supernatants (Fig. 10.1b). In contrast, different chemerin (21-157) treatments did not show any changes in PAI-1 levels in HMEC-1 cell supernatants (Table 10.1a, b and c respectively). TNF-α [10ng/ml] and IL-1β [10ng/ml] were used as positive controls.

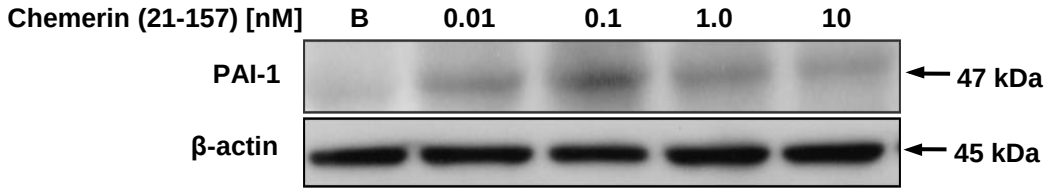

Figure 10.1a Chemerin (21-157) increased PAI-1 protein expression in HMEC-1 cell line

HMEC-1 cells were treated with different chemerin (21-157) concentrations [0-10nM] for 6 hours. Following cell lysis and sample preparations, the protein lysates were separated using 12% polyacrylamide gels, and transferred to PVDF membranes at 100V for 1 hour. Membranes were incubated with specific mouse PAI-1 antibody [(1:1000); Abcam Cambridge, UK] overnight at 4^{o}C. After removing the primary antibody complexes, membranes were incubated with anti-mouse IgG-HRP labelled antibody [(1:8000); Sigma-Aldrich, UK] for 1 hour at RT. Protein complexes were visualised using ECL plus detection reagent on X-ray films. Membranes were re-probed with rabbit β-actin antibody [(1:1500); Cell signalling, Beverly, MA, USA] and used as a loading control. The corresponding bands for PAI-1 and β-actin were detected as 47kDa and 45 kDa products.

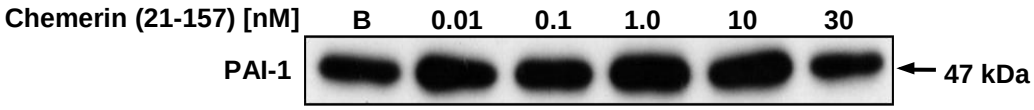

Figure 10.1b Chemerin (21-157) and PAI-1 protein secretion in HMEC-1 cell supernatants

HMEC-1 cells were treated with different chemerin (21-157) concentrations [0-10nM] for 24 hours and cell supernatants were collected. Samples were prepared by mixing equal volumes of cell supernatants and 1x Laemmili buffer solution. Following sample preparations, the proteins were separated using 12% polyacrylamide gels, and transferred to PVDF membranes at 100V for 1 hour. Membranes were incubated with specific mouse PAI-1 antibody [(1:1000); Abcam Cambridge, UK] overnight at 4^{o}C. After removing the primary antibody complexes, membranes were incubated with anti-mouse IgG-HRP labelled antibody [(1:8000); Sigma-Aldrich, UK] for 1 hour at RT. Protein complexes were visualised using ECL plus detection reagent on X-ray films. The corresponding bands for PAI-1 were detected as 47kDa products.

Table 10.1a

Chemerin (21-157) and PAI-1 protein secretion in HMEC-1 cell supernatants after 4 hours

Treatments	4 hours (n=1) pg/mL	4 hours (n=2) pg/mL
Basal	4.75298	5.20259
[0.01nM] chemerin (21-157)	4.89021	7.48906
[0.1nM] chemerin (21-157)	5.16941	3.1263
[1nM] chemerin (21-157)	4.92472	4.70012
[10nM] chemerin (21-157)	4.86558	4.51402
[30nM] chemerin (21-157)	5.0147	5.07345
TNF-α [10ng/ml]	9.02581	9.02581
TNF-α [10ng/ml]	10.34339	10.34339
IL-1β [10ng/ml]	11.18808	11.18808

Table 10.1b

Chemerin (21-157) and sPAI-1 protein secretion in HMEC-1 cell supernatants after 12 hours

Treatments	12 hours (n=1) pg/mL	12 hours (n=2) pg/mL
Basal	8.57681	8.345
[0.01nM] chemerin (21-157)	7.33019	5.145
[0.1nM] chemerin (21-157)	7.4077	6.845
[1nM] chemerin (21-157)	6.35122	7.212
[10nM] chemerin (21-157)	8.46765	7.751
[30nM] chemerin (21-157)	5.76457	6.167
TNF-α [10ng/ml]	9.02581	9.026
TNF-α [10ng/ml]	10.3434	10.34
IL-1β [10ng/ml]	11.1881	11.19

Table 10.1c

Chemerin (21-157) and sPAI-1 protein secretion in HMEC-1 cell supernatants after 24 hours

Treatments	24 hours (n=1) pg/mL	24 hours (n=2) pg/mL
Basal	8.61724	9.12865
[0.01nM] chemerin (21-157)	8.58847	9.97703
[0.1nM] chemerin (21-157)	10.06147	9.48074
[1nM] chemerin (21-157)	8.4005	8.85272
[10nM] chemerin (21-157)	9.38937	0.85836
[30nM] chemerin (21-157)	9.554	8.55766
TNF-α [10ng/ml]	9.02581	9.02581
TNF-α [10ng/ml]	10.34339	10.34339
IL-1β [10ng/ml]	11.18808	11.18808

11. Chemerin (21-157) and SAPK/JNK MAPK Phosphorylation in a Time- and Concentration-dependent Manner in HMEC-1 Cell Line

HMEC-1 cells were cultured in 6-well plates in MCDB cell medium containing 10% FCS, and were serum starved in the same medium containing 1% FCS overnight before performing different treatments. To study time-dependent SAPK/JNK MAPK phosphorylation, HMEC-1 cells were treated with [1.0nM] chemerin (21-157) at different time-points for a maximum of 30 minutes. For concentration-dependent SAPK/JNK MAPK phosphorylation, HMEC-1 cells were treated with different chemerin (21-157) [0-10nM] concentrations for 30 minute. Cells were lysed in 1x RIPA buffer and protein lysates were separated using SDS-PAGE. Chemerin (21-157) phosphorylated SAPK/JNK MAPK in a time- and concentration-dependent manner (Fig. 11.1a and b respectively).

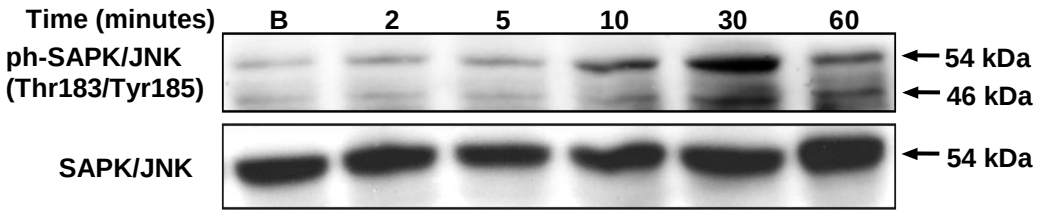

Figure 11.1a Chemerin (21-157) lead to SAPK/JNK MAPK phosphorylation in a time-dependent manner in HMEC-1 cell line

HMEC-1 cells were treated with [1.0nM] chemerin (21-157) for 0-60 minutes. Following cell lysis and sample preparations, the protein lysates were separated using 10% polyacrylamide gels, and transferred to PVDF membranes at 100V for 1 hour. Membranes were incubated with phospho-SAPK/JNK (Thr183/Tyr185) MAPK antibody [(1:1500); Cell signalling, Beverly, MA, USA] overnight at 4^{o}C. After removing the primary antibody complexes, membranes were incubated with anti-rabbit IgG-HRP labelled antibody [(1:2000); Dako, Ely, UK] for 1 hour at RT. Protein complexes were visualised using ECL plus detection reagent on X-ray films. Membrane was re-probed with total SAPK/JNK MAPK antibody [(1:1500); Cell signalling, Beverly, MA, USA] and used as a loading control. The corresponding bands for both phospho-SAPK/JNK and total SAPK/JNK MAPK were detected as 54/46kDa products.

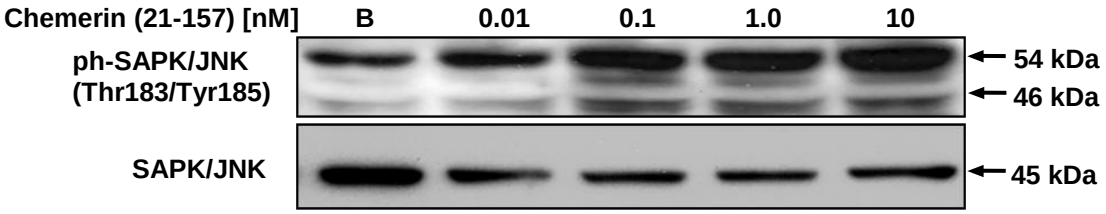

Figure 11.1b Chemerin (21-157) lead to SAPK/JNK MAPK phosphorylation in a concentration-dependent manner in HMEC-1 cell line

HMEC-1 cells were treated with different chemerin (21-157) concentrations for 30 minutes. Following cell lysis and sample preparations, the protein lysates were separated using 10% polyacrylamide gels, and transferred to PVDF membranes at 100V for 1 hour. Membranes were incubated with phospho-SAPK/JNK (Thr183/Tyr185) MAPK antibody [(1:1500); Cell signalling, Beverly, MA, USA] overnight at 4^{o}C. After removing the primary antibody complexes, membranes were incubated with anti-rabbit IgG-HRP labelled antibody [(1:2000); Dako, Ely, UK] for 1 hour at RT. Protein complexes were visualised using ECL plus detection reagent on X-ray films. Membranes were re-probed with total SAPK/JNK MAPK antibody [(1:1500); Cell signalling, Beverly, MA, USA] and used as a loading control. The corresponding bands for both phospho-SAPK/JNK and total SAPK/JNK MAPK were detected as 54/46kDa products.

12. Chemerin (21-157) and AMPKα Phosphorylation in a Time- and Concentration-dependent Manner in HMEC-1 Cell Line

HMEC-1 cells were cultured in 6-well plates in MCDB cell medium containing 10% FCS, and were serum starved in the same medium containing 1% FCS overnight before performing different treatments. To study time-dependent AMPKα kinases phosphorylation, HMEC-1 cells were treated with [1.0M] chemerin (21-157) at different time-points for a maximum of 60 minutes. For concentration-dependent AMPKα kinases phosphorylation, HMEC-1 cells were treated with different chemerin (21-157) [0-10M] concentrations for 10 minute. Cells were lysed in 1x RIPA buffer and protein lysates were separated using SDS-PAGE. Chemerin (21-157) phosphorylated AMPKα in a time- and concentration-dependent manner (Fig. 12.1a and b respectively).

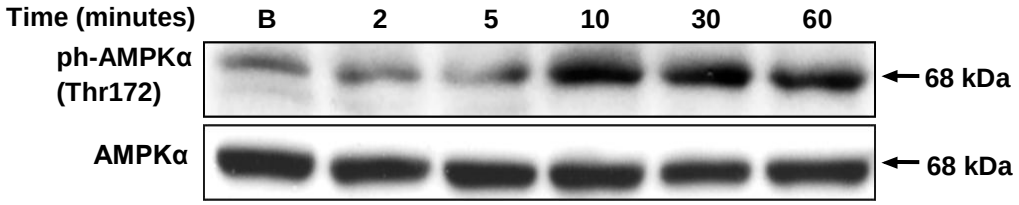

Figure 12.1a Chemerin (21-157) lead to AMPKα kinase phosphorylation in a time-dependent manner in HMEC-1 cell line

HMEC-1 cells were treated with [1.0nM] chemerin (21-157) for 0-60 minutes. Following cell lysis and sample preparations, the protein lysates were separated using 10% polyacrylamide gels, and transferred to PVDF membranes at 100V for 1 hour. Membranes were incubated with phospho-AMPKα (Thr172) antibody [(1:1500); Cell signalling, Beverly, MA, USA] overnight at 4^{o}C. After removing the primary antibody complexes, membranes were incubated with anti-rabbit IgG-HRP labelled antibody [(1:2000); Dako, Ely, UK] for 1 hour at RT. Protein complexes were visualised using ECL plus detection reagent on X-ray films. Membranes were re-probed with total AMPKα antibody [(1:1500); Cell signalling, Beverly, MA, USA] and used as a loading control. The corresponding bands for both phospho-AMPKα and total AMPKα were detected as 68kDs products.

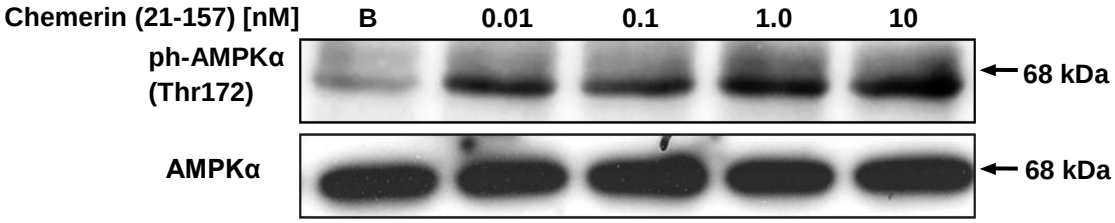

Figure 12.1b Chemerin (21-157) lead to AMPKα kinase phosphorylation in a concentration-dependent manner in HMEC-1 cell line

HMEC-1 cells were treated with different chemerin (21-157) concentrations [0-10nM] for 30 minutes. Following cell lysis and sample preparations, the protein lysates were separated using 10% polyacrylamide gels, and transferred to PVDF membranes at 100V for 1 hour. Membranes were incubated with phospho-AMPKα (Thr172) antibody [(1:1500); Cell signalling, Beverly, MA, USA] overnight at 4^{o}C. After removing the primary antibody complexes, membranes were incubated with anti-rabbit IgG-HRP labelled antibody [(1:2000); Dako, Ely, UK] for 1 hour at RT. Membranes were re-probed with total AMPKα antibody [(1:1500); Cell signalling, Beverly, MA, USA] and used as a loading control. Protein complexes were visualised using ECL plus detection reagent on X-ray films and corresponding bands for both phospho-AMPKα and total AMPKα were detected as 68kDa products.

13. Shortest Chemerin Peptide, Chemerin (149-157), and ERK1/2 Phosphorylation in HMEC-1 Cell Line in Nanomolar Concentrations

In 2004, Wittamer and colleagues found that chemerin (149-157) is the shortest chemerin fragment known to bind CMKLR1, and retains most of the activity of full length chemerin (21-157). Chemerin (149-157) is reported to bind CMKLR1 in micromolar concentrations, compared to nanomolar concentration of full length chemerin (21-157) (Wittamer et al., 2004, Wong et al., 2011) . In order to see the effects of chemerin (149-157) in nanomolar concentrations, HMEC-1 cells were treated with different nanomolar chemerin (149-157) concentrations [0-1000nM] and ERK1/2 MAPK phosphorylation was studied. Chemerin (149-157), at low nanomolar concentrations, failed to show any changes in ERK1/2 MAPK phosphorylation (Fig. 13.1a).

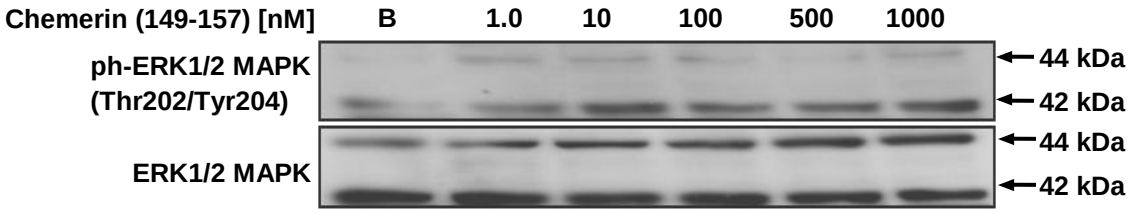

Figure 13.1a Chemerin (149-157) and ERK1/2 MAPK phosphorylation in HMEC-1 cell line

HMEC-1 cells were treated with different chemerin (149-157) concentrations [0-1000nM] for 5 minutes. Following cell lysis and sample preparations, the protein lysates were separated using 12% polyacrylamide gels, and transferred to PVDF membranes at 100V for 1 hour. Membranes were incubated with specific phospho-ERK1/2 (Thr202/Tyr204) MAPK antibody [(1:1500); Cell signalling, Beverly, MA, USA] overnight at 4^{o}C. After removing the primary antibody complexes, membranes were incubated with anti-rabbit IgG-HRP labelled antibody [(1:2000); Dako, Ely, UK] for 1 hour at RT. Protein complexes were visualised using ECL plus detection reagent on X-ray films. Membranes were re-probed with total ERK1/2 MAPK antibody [(1:1500); Cell signalling, Beverly, MA, USA] and used as a loading control. The corresponding bands for both phospho-ERK1/2 and total ERK1/2 MAPK were detected as 44/42kDa products.

14. Chemerin (21-157) and ERK1/2 MAPK Phosphorylation in Stable CMKLR1 Transfected HEK293T Cells

HEK293T cells were stable transfected with pcDNA3.1-CMKLR1 plasmid and stable cell line expressing CMKLR1 was prepared (HEK293T.CMKLR1). HEK293T.CMKLR1 cells were cultured in 6-well plates in DMEM cell medium containing 10% FCS, and were serum starved in the same medium containing 1% FCS overnight before performing different treatments. HEK293T.CMKLR1 cells were treated with different chemerin (21-157) [0-30nM] concentrations for 5 minutes. Cells were lysed in 1x RIPA buffer and protein lysates were separated using SDS-PAGE. Chemerin (21-157) phosphorylated ERK1/2 MAPK in a concentration-dependent manner in HEK293T.CMKLR1 (Fig. 14.1a).

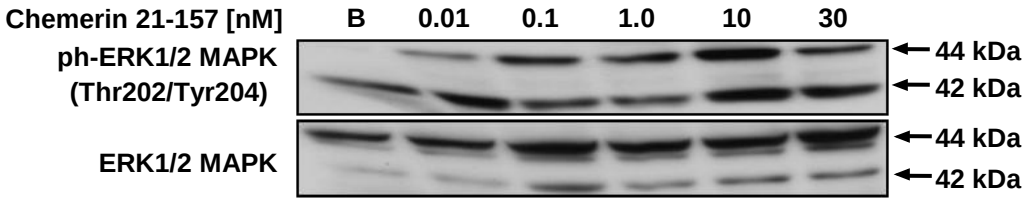

Figure 14.1a Chemerin (21-157) and ERK1/2 MAPK phosphorylation in CMKLR1 stable transfected HEK293T.CMKLR1 cells

HEK293T.CMKLR1 cells were treated with different chemerin (21-157) concentrations [0-10nM] for 5 minutes. Following cell lysis and sample preparations, the protein lysates were separated using 12% polyacrylamide gels, and transferred to PVDF membranes at 100V for 1 hour. Membranes were incubated with specific phospho-ERK1/2 (Thr202/Tyr204) MAPK antibody [(1:1500); Cell signalling, Beverly, MA, USA] overnight at 4^{o}C. After removing the primary antibody complexes, membranes were incubated with anti-rabbit IgG-HRP labelled antibody [(1:2000); Dako, Ely, UK] for 1 hour at RT. Protein complexes were visualised using ECL plus detection reagent on X-ray films. Membranes were re-probed with total ERK1/2 MAPK antibody [(1:1500); Cell signalling, Beverly, MA, USA] and used as a loading control. The corresponding bands for both phospho-ERK1/2 and total ERK1/2 MAPK were detected as 44/42kDa products.

15. List of Experiments and Methods Contributed by Others Researchers

Following is the list of experiments and methods contributed by other researchers

Chapter number	Method/experiments	Person's name	Role I played	Page numbers
2	Primary Human Umbilical Vein endothelial Cells (HUVECs)	Dr R Adya	None	41-3
2	Making competent *E.coli* cells for transformation	Dr J Chen	Observed and assisted	51
2	Transient transfection of NF-κB-Luc plasmid in HMEC-1 cell line	Dr R Adya	None	55-6
2	Stable CMKLR1 transfections in HEK293T Cell Line	Dr J Chen	None	56
2 and 4	Gelatin Zymography	Dr R Adya	Observed only	61
2 and 4	Wound-healing Cell Motility Assay	Dr R Adya	None	63-4
2 and 4	*In vitro* Cell Invasion Assay	Dr R Adya	None	64-5
2 and 4	Endothelial cell capillary tube formation assay for generating data presented on page number 136 (Fig. 4.3.11a)	Dr R Adya	Observed and assisted	65-6
2 and future work	Capillary tube formation experiment using chemerin (149-157) (Fig. 8.6a, page number 232).	myself	n/a	65-6
2 and 5	NF-κB Luciferase Activity Assay	Dr R Adya	None	68
2 and 5	Endothelial-Monocyte Cell Adhesion Assay	Dr R Adya	None	69-70

Bibliography

ABE, J., KUSUHARA, M., ULEVITCH, R. J., BERK, B. C. & LEE, J. D. 1996. Big mitogen-activated protein kinase 1 (BMK1) is a redox-sensitive kinase. *J Biol Chem,* 271**,** 16586-90.

ACKAH, E., YU, J., ZOELLNER, S., IWAKIRI, Y., SKURK, C., SHIBATA, R., OUCHI, N., EASTON, R. M., GALASSO, G., BIRNBAUM, M. J., WALSH, K. & SESSA, W. C. 2005. Akt1/protein kinase Balpha is critical for ischemic and VEGF-mediated angiogenesis. *J Clin Invest,* 115**,** 2119-27.

ADES, E. W., CANDAL, F. J., SWERLICK, R. A., GEORGE, V. G., SUMMERS, S., BOSSE, D. C. & LAWLEY, T. J. 1992. HMEC-1: establishment of an immortalized human microvascular endothelial cell line. *J Invest Dermatol,* 99**,** 683-90.

AHMED, A., DUNK, C., KNISS, D. & WILKES, M. 1997. Role of VEGF receptor-1 (Flt-1) in mediating calcium-dependent nitric oxide release and limiting DNA synthesis in human trophoblast cells. *Lab Invest,* 76**,** 779-91.

AKSELA, H., JAUHIAINEN, J., KUKK, E., NOMMISTE, E., AKSELA, S. & TULKKI, J. 1996a. Electron correlation in the decay of resonantly excited 3d3/2,5/2-15p states of krypton. *Phys Rev A,* 53**,** 290-296.

AKSELA, H., JAUHIAINEN, J., NOMMISTE, E., SAIRANEN, O., KARVONEN, J., KUKK, E. & AKSELA, S. 1996b. Angular distribution of Auger electrons in the decay of resonantly excited 4d3/2,5/2-1 6p states in Xe. *Phys Rev A,* 54**,** 2874-2881.

ALBANESI, C., SCARPONI, C., PALLOTTA, S., DANIELE, R., BOSISIO, D., MADONNA, S., FORTUGNO, P., GONZALVO-FEO, S., FRANSSEN, J. D., PARMENTIER, M., DE PITA, O., GIROLOMONI, G. & SOZZANI, S. 2009. Chemerin expression marks early psoriatic skin lesions and correlates with plasmacytoid dendritic cell recruitment. *J Exp Med,* 206**,** 249-58.

ALIEV, G., BODIN, P. & BURNSTOCK, G. 1998. Free radical generators cause changes in endothelial and inducible nitric oxide synthases and endothelin-1 immunoreactivity in endothelial cells from hyperlipidemic rabbits. *Mol Genet Metab,* 63**,** 191-7.

ALLEN, M., SVENSSON, L., ROACH, M., HAMBOR, J., MCNEISH, J. & GABEL, C. A. 2000. Deficiency of the stress kinase p38alpha results in embryonic lethality: characterization of the kinase dependence of stress responses of enzyme-deficient embryonic stem cells. *J Exp Med,* 191**,** 859-70.

ARITA, M., OHIRA, T., SUN, Y. P., ELANGOVAN, S., CHIANG, N. & SERHAN, C. N. 2007. Resolvin E1 selectively interacts with leukotriene B4 receptor BLT1 and ChemR23 to regulate inflammation. *J Immunol,* 178**,** 3912-7.

AUBIER, M., GUENEGOU, A., BENESSIANO, J., LEYNAERT, B., BOCZKOWSKI, J. & NEUKIRCH, F. 2006. [Association of lung function decline with the microsatellite polymorphism in the heme oxygenase-1 gene promoter, in a general population sample. Results from the Longitudinal European Community Respiratory Health Survey (ECRHS-France)]. *Bull Acad Natl Med,* 190**,** 877-90; discussion 890-1.

AYAJIKI, K., KINDERMANN, M., HECKER, M., FLEMING, I. & BUSSE, R. 1996. Intracellular pH and tyrosine phosphorylation but not calcium determine shear stress-induced nitric oxide production in native endothelial cells. *Circ Res,* 78**,** 750-8.

AZADZOI, K. M., MASTER, T. A. & SIROKY, M. B. 2004. Effect of chronic ischemia on constitutive and inducible nitric oxide synthase expression in erectile tissue. *J Androl,* 25**,** 382-8.

B, M. P., J, M. D. & M, P. G. 2002. Mimotopes and proteome analyses using human genomic and cDNA epitope phage display. *Comp Funct Genomics,* 3**,** 254-63.

BAEKKEVOLD, E. S., YAMANAKA, T., PALFRAMAN, R. T., CARLSEN, H. S., REINHOLT, F. P., VON ANDRIAN, U. H., BRANDTZAEG, P. & HARALDSEN, G. 2001. The CCR7 ligand elc (CCL19) is transcytosed in high endothelial venules and mediates T cell recruitment. *J Exp Med,* 193**,** 1105-12.

BAES, M., HUYGHE, S., CARMELIET, P., DECLERCQ, P. E., COLLEN, D., MANNAERTS, G. P. & VAN VELDHOVEN, P. P. 2000. Inactivation of the peroxisomal multifunctional protein-2 in mice impedes the degradation of not only 2-methyl-branched fatty acids and bile acid intermediates but also of very long chain fatty acids. *J Biol Chem,* 275**,** 16329-36.

BALDI, A., ROSSIELLO, R., DI MARINO, M., FERRARA, N., GROEGER, A. M., ESPOSITO, V., SANTINI, D., KAISER, H. E. & BALDI, F. 2000. Colonic type adenocarcinoma of male urethra. *In Vivo,* 14**,** 487-92.

BARNEA, G., STRAPPS, W., HERRADA, G., BERMAN, Y., ONG, J., KLOSS, B., AXEL, R. & LEE, K. J. 2008. The genetic design of signaling cascades to record receptor activation. *Proc Natl Acad Sci U S A,* 105**,** 64-9.

BATES, D. O., CUI, T. G., DOUGHTY, J. M., WINKLER, M., SUGIONO, M., SHIELDS, J. D., PEAT, D., GILLATT, D. & HARPER, S. J. 2002. VEGF165b, an inhibitory splice variant of vascular endothelial growth factor, is down-regulated in renal cell carcinoma. *Cancer Res,* 62**,** 4123-31.

BAUER, P. M., FULTON, D., BOO, Y. C., SORESCU, G. P., KEMP, B. E., JO, H. & SESSA, W. C. 2003. Compensatory phosphorylation and protein-protein interactions revealed by loss of function and gain of function mutants of multiple serine phosphorylation sites in endothelial nitric-oxide synthase. *J Biol Chem,* 278**,** 14841-9.

BAUTCH, V. L., REDICK, S. D., SCALIA, A., HARMATY, M., CARMELIET, P. & RAPOPORT, R. 2000. Characterization of the vasculogenic block in the absence of vascular endothelial growth factor-A. *Blood,* 95**,** 1979-87.

BECKER, M., RABE, K., LEBHERZ, C., ZUGWURST, J., GOKE, B., PARHOFER, K. G., LEHRKE, M. & BROEDL, U. C. 2010. Expression of human chemerin induces insulin resistance in the skeletal muscle but does not affect weight, lipid levels and atherosclerosis in LDL receptor knockout mice on high fat diet. *Diabetes*.

BELANGER, L. F., ROY, S., TREMBLAY, M., BROTT, B., STEFF, A. M., MOURAD, W., HUGO, P., ERIKSON, R. & CHARRON, J. 2003. Mek2 is dispensable for mouse growth and development. *Mol Cell Biol,* 23**,** 4778-87.

BHAT, N. R. & ZHANG, P. 1999. Hydrogen peroxide activation of multiple mitogen-activated protein kinases in an oligodendrocyte cell line: role of extracellular signal-regulated kinase in hydrogen peroxide-induced cell death. *J Neurochem,* 72**,** 112-9.

BIFFL, W. L., MOORE, E. E., MOORE, F. A. & BARNETT, C. 1996. Nitric oxide reduces endothelial expression of intercellular adhesion molecule (ICAM)-1. *J Surg Res,* 63**,** 328-32.

BLANKENBERG, S., BARBAUX, S. & TIRET, L. 2003. Adhesion molecules and atherosclerosis. *Atherosclerosis,* 170**,** 191-203.

BOO, Y. C., SORESCU, G. P., BAUER, P. M., FULTON, D., KEMP, B. E., HARRISON, D. G., SESSA, W. C. & JO, H. 2003. Endothelial NO synthase phosphorylated at SER635 produces NO without requiring intracellular calcium increase. *Free Radic Biol Med,* 35**,** 729-41.

BOULOUMIE, A., DREXLER, H. C., LAFONTAN, M. & BUSSE, R. 1998. Leptin, the product of Ob gene, promotes angiogenesis. *Circ Res,* 83**,** 1059-66.

BOULOUMIE, A., SCHINI-KERTH, V. B. & BUSSE, R. 1999. Vascular endothelial growth factor up-regulates nitric oxide synthase expression in endothelial cells. *Cardiovasc Res,* 41**,** 773-80.

BOZAOGLU, K., BOLTON, K., MCMILLAN, J., ZIMMET, P., JOWETT, J., COLLIER, G., WALDER, K. & SEGAL, D. 2007. Chemerin is a novel adipokine associated with obesity and metabolic syndrome. *Endocrinology,* 148**,** 4687-94.

BOZAOGLU, K., CURRAN, J. E., STOCKER, C. J., ZAIBI, M. S., SEGAL, D., KONSTANTOPOULOS, N., MORRISON, S., CARLESS, M., DYER, T. D., COLE, S. A., GORING, H. H., MOSES, E. K., WALDER, K., CAWTHORNE, M. A., BLANGERO, J. & JOWETT, J. B. 2010. Chemerin, a novel adipokine in the regulation of angiogenesis. *J Clin Endocrinol Metab,* 95**,** 2476-85.

BOZAOGLU, K., SEGAL, D., SHIELDS, K. A., CUMMINGS, N., CURRAN, J. E., COMUZZIE, A. G., MAHANEY, M. C., RAINWATER, D. L., VANDEBERG, J. L., MACCLUER, J. W., COLLIER, G., BLANGERO, J., WALDER, K. & JOWETT, J. 2009. Chemerin is associated with metabolic syndrome phenotypes in a Mexican American Population. *J Clin Endocrinol Metab*.

BRADHAM, C. & MCCLAY, D. R. 2006. p38 MAPK in development and cancer. *Cell Cycle,* 5**,** 824-8.

BREDT, D. S. & SNYDER, S. H. 1990. Isolation of nitric oxide synthetase, a calmodulin-requiring enzyme. *Proc Natl Acad Sci U S A,* 87**,** 682-5.

BROCK, T. A., DVORAK, H. F. & SENGER, D. R. 1991. Tumor-secreted vascular permeability factor increases cytosolic Ca2+ and von Willebrand factor release in human endothelial cells. *Am J Pathol,* 138**,** 213-21.

BUCCI, M., GRATTON, J. P., RUDIC, R. D., ACEVEDO, L., ROVIEZZO, F., CIRINO, G. & SESSA, W. C. 2000. In vivo delivery of the caveolin-1 scaffolding domain inhibits nitric oxide synthesis and reduces inflammation. *Nat Med,* 6**,** 1362-7.

BUSSE, R. & FLEMING, I. 2006. Vascular endothelium and blood flow. *Handb Exp Pharmacol***,** 43-78.

CARMELIET, P. 2000. Mechanisms of angiogenesis and arteriogenesis. *Nat Med,* 6**,** 389-95.

CARTER, N. M., ALI, S. & KIRBY, J. A. 2003. Endothelial inflammation: the role of differential expression of N-deacetylase/N-sulphotransferase enzymes in alteration of the immunological properties of heparan sulphate. *J Cell Sci,* 116**,** 3591-600.

CASH, J. L., HART, R., RUSS, A., DIXON, J. P., COLLEDGE, W. H., DORAN, J., HENDRICK, A. G., CARLTON, M. B. & GREAVES, D. R. 2008. Synthetic chemerin-derived peptides suppress inflammation through ChemR23. *J Exp Med,* 205**,** 767-75.

CHEN, H., MONTAGNANI, M., FUNAHASHI, T., SHIMOMURA, I. & QUON, M. J. 2003. Adiponectin stimulates production of nitric oxide in vascular endothelial cells. *J Biol Chem,* 278**,** 45021-6.

CHEN, J., BRAET, F., BRODSKY, S., WEINSTEIN, T., ROMANOV, V., NOIRI, E. & GOLIGORSKY, M. S. 2002. VEGF-induced mobilization of caveolae and increase in permeability of endothelial cells. *Am J Physiol Cell Physiol,* 282**,** C1053-63.

CHOI, J., ENIS, D. R., KOH, K. P., SHIAO, S. L. & POBER, J. S. 2004. T lymphocyte-endothelial cell interactions. *Annu Rev Immunol,* 22**,** 683-709.

COLLINS, T., READ, M. A., NEISH, A. S., WHITLEY, M. Z., THANOS, D. & MANIATIS, T. 1995. Transcriptional regulation of endothelial cell adhesion molecules: NF-kappa B and cytokine-inducible enhancers. *FASEB J,* 9**,** 899-909.

CONNOLLY, D. T., HEUVELMAN, D. M., NELSON, R., OLANDER, J. V., EPPLEY, B. L., DELFINO, J. J., SIEGEL, N. R., LEIMGRUBER, R. M. & FEDER, J. 1989. Tumor vascular permeability factor stimulates endothelial cell growth and angiogenesis. *J Clin Invest,* 84**,** 1470-8.

COOKE, J. P. 2004. Asymmetrical dimethylarginine: the Uber marker? *Circulation,* 109**,** 1813-8.

CORTES-GONZALEZ, C., BARRERA-CHIMAL, J., IBARRA-SANCHEZ, M., GILBERT, M., GAMBA, G., ZENTELLA, A., FLORES, M. E. & BOBADILLA, N. A. 2010. Opposite effect of Hsp90alpha and Hsp90beta on eNOS ability to produce nitric oxide or superoxide anion in human embryonic kidney cells. *Cell Physiol Biochem,* 26**,** 657-68.

CRAINE, N. G., RANDOLPH, S. E. & NUTTALL, P. A. 1995. Seasonal variation in the role of grey squirrels as hosts of Ixodes ricinus, the tick vector of the Lyme disease spirochaete, in a British woodland. *Folia Parasitol (Praha),* 42**,** 73-80.

CSERMELY, P., SCHNAIDER, T., SOTI, C., PROHASZKA, Z. & NARDAI, G. 1998. The 90-kDa molecular chaperone family: structure, function, and clinical applications. A comprehensive review. *Pharmacol Ther,* 79**,** 129-68.

CYBULSKY, M. I. & GIMBRONE, M. A., JR. 1991. Endothelial expression of a mononuclear leukocyte adhesion molecule during atherogenesis. *Science,* 251**,** 788-91.

CYBULSKY, M. I., IIYAMA, K., LI, H., ZHU, S., CHEN, M., IIYAMA, M., DAVIS, V., GUTIERREZ-RAMOS, J. C., CONNELLY, P. W. & MILSTONE, D. S. 2001. A major role for VCAM-1, but not ICAM-1, in early atherosclerosis. *J Clin Invest,* 107**,** 1255-62.

DAS, A. K., UHLER, M. D. & HAJRA, A. K. 2000. Molecular cloning and expression of mammalian peroxisomal trans-2-enoyl-coenzyme A reductase cDNAs. *J Biol Chem,* 275**,** 24333-40.

DAVENPECK, K. L., GAUTHIER, T. W. & LEFER, A. M. 1994. Inhibition of endothelial-derived nitric oxide promotes P-selectin expression and actions in the rat microcirculation. *Gastroenterology,* 107**,** 1050-8.

DE CATERINA, R., LIBBY, P., PENG, H. B., THANNICKAL, V. J., RAJAVASHISTH, T. B., GIMBRONE, M. A., JR., SHIN, W. S. & LIAO, J. K. 1995. Nitric oxide decreases cytokine-induced endothelial activation. Nitric oxide selectively reduces endothelial expression of adhesion molecules and proinflammatory cytokines. *J Clin Invest,* 96**,** 60-8.

DE WINTHER, M. P., KANTERS, E., KRAAL, G. & HOFKER, M. H. 2005. Nuclear factor kappaB signaling in atherogenesis. *Arterioscler Thromb Vasc Biol,* 25**,** 904-14.

DIMMELER, S., FLEMING, I., FISSLTHALER, B., HERMANN, C., BUSSE, R. & ZEIHER, A. M. 1999. Activation of nitric oxide synthase in endothelial cells by Akt-dependent phosphorylation. *Nature,* 399**,** 601-5.

DONG, C., DAVIS, R. J. & FLAVELL, R. A. 2002. MAP kinases in the immune response. *Annu Rev Immunol,* 20**,** 55-72.

DOUGHER-VERMAZEN, M., HULMES, J. D., BOHLEN, P. & TERMAN, B. I. 1994. Biological activity and phosphorylation sites of the bacterially expressed cytosolic domain of the KDR VEGF-receptor. *Biochem Biophys Res Commun,* 205**,** 728-38.

DU, X. Y., ZABEL, B. A., MYLES, T., ALLEN, S. J., HANDEL, T. M., LEE, P. P., BUTCHER, E. C. & LEUNG, L. L. 2009. Regulation of chemerin bioactivity by plasma carboxypeptidase N, carboxypeptidase B (activated thrombin-activable fibrinolysis inhibitor), and platelets. *J Biol Chem,* 284**,** 751-8.

DVORAK, H. F., BROWN, L. F., DETMAR, M. & DVORAK, A. M. 1995a. Vascular permeability factor/vascular endothelial growth factor, microvascular hyperpermeability, and angiogenesis. *Am J Pathol,* 146**,** 1029-39.

DVORAK, J., DUBCOVSKY, J., LUO, M. C., DEVOS, K. M. & GALE, M. D. 1995b. Differentiation between wheat chromosomes 4B and 4D. *Genome,* 38**,** 1139-47.

DYE, J., LAWRENCE, L., LINGE, C., LEACH, L., FIRTH, J. & CLARK, P. 2004. Distinct patterns of microvascular endothelial cell morphology are determined by extracellular matrix composition. *Endothelium,* 11**,** 151-67.

EDGELL, C. J., MCDONALD, C. C. & GRAHAM, J. B. 1983. Permanent cell line expressing human factor VIII-related antigen established by hybridization. *Proc Natl Acad Sci U S A,* 80**,** 3734-7.

ENKVIST, M. O., HAMALAINEN, H., JANSSON, C. C., KUKKONEN, J. P., HAUTALA, R., COURTNEY, M. J. & AKERMAN, K. E. 1996. Coupling of astroglial alpha 2-adrenoreceptors to second messenger pathways. *J Neurochem,* 66**,** 2394-401.

ERNST, M. C. & SINAL, C. J. 2010. Chemerin: at the crossroads of inflammation and obesity. *Trends Endocrinol Metab,* 21**,** 660-7.

ERIKSSON, S., RAIVIO, E., KUKKONEN, J. P., ERIKSSON, K. & LINDQVIST, C. 1996. Green fluorescent protein as a tool for screening recombinant baculoviruses. *J Virol Methods,* 59**,** 127-33.

FENG, Y., VENEMA, V. J., VENEMA, R. C., TSAI, N., BEHZADIAN, M. A. & CALDWELL, R. B. 1999. VEGF-induced permeability increase is mediated by caveolae. *Invest Ophthalmol Vis Sci,* 40**,** 157-67.

FERRARA, N. 2000. VEGF: an update on biological and therapeutic aspects. *Curr Opin Biotechnol,* 11**,** 617-24.

FERRARA, N. & DAVIS-SMYTH, T. 1997. The biology of vascular endothelial growth factor. *Endocr Rev,* 18**,** 4-25.

FERRARA, N. & HENZEL, W. J. 1989. Pituitary follicular cells secrete a novel heparin-binding growth factor specific for vascular endothelial cells. *Biochem Biophys Res Commun,* 161**,** 851-8.

FIUMARA, E., GAMBACORTA, M., D'ANGELO, V., FERRARA, M. & CORONA, C. 1989. Chronic encapsulated intracerebral haematoma: pathogenetic and diagnostic considerations. *J Neurol Neurosurg Psychiatry,* 52**,** 1296-9.

FLEMING, I., FISSLTHALER, B., DIMMELER, S., KEMP, B. E. & BUSSE, R. 2001. Phosphorylation of Thr(495) regulates Ca(2+)/calmodulin-dependent endothelial nitric oxide synthase activity. *Circ Res,* 88**,** E68-75.

FOGAR, P., BASSO, D., FADI, E., GRECO, E., PANTANO, G., PADOAN, A., BOZZATO, D., FACCO, M., SANZARI, M. C., TEOLATO, S., ZAMBON, C. F., NAVAGLIA, F., SEMENZATO, G., PEDRAZZOLI, S. & PLEBANI, M. 2011. Pancreatic cancer alters human CD4+ T lymphocyte function: a piece in the immune evasion puzzle. *Pancreas,* 40**,** 1131-7.

FOLKMAN, J. 1992. Is there a field of wound pharmacology? *Ann Surg,* 215**,** 1-2.

FOLKMAN, J. 2006. Angiogenesis. *Annu Rev Med,* 57**,** 1-18.

FOLKMAN, J. & D'AMORE, P. A. 1996. Blood vessel formation: what is its molecular basis? *Cell,* 87**,** 1153-5.

FOLKMAN, J. & INGBER, D. 1992. Inhibition of angiogenesis. *Semin Cancer Biol,* 3**,** 89-96.

FOLKMAN, J. & SHING, Y. 1992a. Angiogenesis. *J Biol Chem,* 267**,** 10931-4.

FOLKMAN, J. & SHING, Y. 1992b. Control of angiogenesis by heparin and other sulfated polysaccharides. *Adv Exp Med Biol,* 313**,** 355-64.

FREDRIKSSON, R., LAGERSTROM, M. C., LUNDIN, L. G. & SCHIOTH, H. B. 2003. The G-protein-coupled receptors in the human genome form five main families. Phylogenetic analysis, paralogon groups, and fingerprints. *Mol Pharmacol,* 63**,** 1256-72.

FRESHNEY, N. W., RAWLINSON, L., GUESDON, F., JONES, E., COWLEY, S., HSUAN, J. & SAKLATVALA, J. 1994. Interleukin-1 activates a novel protein kinase cascade that results in the phosphorylation of Hsp27. *Cell,* 78**,** 1039-49.

FUKUCHI, M. & GIAID, A. 1999. Endothelial expression of endothelial nitric oxide synthase and endothelin-1 in human coronary artery disease. Specific reference to underlying lesion. *Lab Invest,* 79**,** 659-70.

FULTON, D., GRATTON, J. P., MCCABE, T. J., FONTANA, J., FUJIO, Y., WALSH, K., FRANKE, T. F., PAPAPETROPOULOS, A. & SESSA, W. C. 1999. Regulation of endothelium-derived nitric oxide production by the protein kinase Akt. *Nature,* 399**,** 597-601.

FURCHGOTT, R. F. & ZAWADZKI, J. V. 1980. The obligatory role of endothelial cells in the relaxation of arterial smooth muscle by acetylcholine. *Nature,* 288**,** 373-6.

GALE, N. W. & YANCOPOULOS, G. D. 1999. Growth factors acting via endothelial cell-specific receptor tyrosine kinases: VEGFs, angiopoietins, and ephrins in vascular development. *Genes Dev,* 13**,** 1055-66.

GANTZ, I., KONDA, Y., YANG, Y. K., MILLER, D. E., DIERICK, H. A. & YAMADA, T. 1996. Molecular cloning of a novel receptor (CMKLR1) with homology to the chemotactic factor receptors. *Cytogenet Cell Genet,* 74**,** 286-90.

GARCIA-CARDENA, G., FAN, R., SHAH, V., SORRENTINO, R., CIRINO, G., PAPAPETROPOULOS, A. & SESSA, W. C. 1998. Dynamic activation of endothelial nitric oxide synthase by Hsp90. *Nature,* 392**,** 821-4.

GARCIA-CARDENA, G., OH, P., LIU, J., SCHNITZER, J. E. & SESSA, W. C. 1996. Targeting of nitric oxide synthase to endothelial cell caveolae via palmitoylation: implications for nitric oxide signaling. *Proc Natl Acad Sci U S A,* 93**,** 6448-53.

GARG, U. C. & HASSID, A. 1989. Nitric oxide-generating vasodilators and 8-bromo-cyclic guanosine monophosphate inhibit mitogenesis and proliferation of cultured rat vascular smooth muscle cells. *J Clin Invest,* 83**,** 1774-7.

GARTHWAITE, J., GARTHWAITE, G., PALMER, R. M. & MONCADA, S. 1989. NMDA receptor activation induces nitric oxide synthesis from arginine in rat brain slices. *Eur J Pharmacol,* 172**,** 413-6.

GERSZTEN, R. E., GARCIA-ZEPEDA, E. A., LIM, Y. C., YOSHIDA, M., DING, H. A., GIMBRONE, M. A., JR., LUSTER, A. D., LUSCINSKAS, F. W. & ROSENZWEIG, A. 1999. MCP-1 and IL-8 trigger firm adhesion of monocytes to vascular endothelium under flow conditions. *Nature,* 398**,** 718-23.

GIROUX, S., TREMBLAY, M., BERNARD, D., CARDIN-GIRARD, J. F., AUBRY, S., LAROUCHE, L., ROUSSEAU, S., HUOT, J., LANDRY, J., JEANNOTTE, L. & CHARRON, J. 1999. Embryonic death of Mek1-deficient mice reveals a role for this kinase in angiogenesis in the labyrinthine region of the placenta. *Curr Biol,* 9**,** 369-72.

GO, Y. M., PARK, H., MALAND, M. C., DARLEY-USMAR, V. M., STOYANOV, B., WETZKER, R. & JO, H. 1998. Phosphatidylinositol 3-kinase gamma mediates shear stress-dependent activation of JNK in endothelial cells. *Am J Physiol,* 275**,** H1898-904.

GOLDSMITH, Z. G. & DHANASEKARAN, D. N. 2007. G protein regulation of MAPK networks. *Oncogene,* 26**,** 3122-42.

GORALSKI, K. B., MCCARTHY, T. C., HANNIMAN, E. A., ZABEL, B. A., BUTCHER, E. C., PARLEE, S. D., MURUGANANDAN, S. & SINAL, C. J. 2007. Chemerin, a novel adipokine that regulates adipogenesis and adipocyte metabolism. *J Biol Chem,* 282**,** 28175-88.

GROSS, C. M., LELIEVRE, D., WOODWARD, C. K. & BARANY, G. 2005. Preparation of protected peptidyl thioester intermediates for native chemical ligation by Nalpha-9-fluorenylmethoxycarbonyl (Fmoc) chemistry: considerations of side-chain and backbone anchoring strategies, and compatible protection for N-terminal cysteine. *J Pept Res,* 65**,** 395-410.

GRUNDY, S. M., BREWER, H. B., JR., CLEEMAN, J. I., SMITH, S. C., JR. & LENFANT, C. 2004. Definition of metabolic syndrome: report of the National Heart, Lung, and Blood Institute/American Heart Association conference on scientific issues related to definition. *Arterioscler Thromb Vasc Biol,* 24**,** e13-8.

GUILLABERT, A., WITTAMER, V., BONDUE, B., GODOT, V., IMBAULT, V., PARMENTIER, M. & COMMUNI, D. 2008. Role of neutrophil proteinase 3 and mast cell chymase in chemerin proteolytic regulation. *J Leukoc Biol,* 84**,** 1530-8.

HAGEMANN, T., ROBINSON, S. C., SCHULZ, M., TRUMPER, L., BALKWILL, F. R. & BINDER, C. 2004. Enhanced invasiveness of breast cancer cell lines upon co-cultivation with macrophages is due to TNF-alpha dependent up-regulation of matrix metalloproteases. *Carcinogenesis,* 25**,** 1543-9.

HAINZL, O., LAPINA, M. C., BUCHNER, J. & RICHTER, K. 2009. The charged linker region is an important regulator of Hsp90 function. *J Biol Chem,* 284**,** 22559-67.

HAJRA, L., EVANS, A. I., CHEN, M., HYDUK, S. J., COLLINS, T. & CYBULSKY, M. I. 2000. The NF-kappa B signal transduction pathway in aortic endothelial cells is primed for activation in regions predisposed to atherosclerotic lesion formation. *Proc Natl Acad Sci U S A,* 97**,** 9052-7.

HARRINGTON, L. S., SAINSON, R. C., WILLIAMS, C. K., TAYLOR, J. M., SHI, W., LI, J. L. & HARRIS, A. L. 2008. Regulation of multiple angiogenic pathways by Dll4 and Notch in human umbilical vein endothelial cells. *Microvasc Res,* 75**,** 144-54.

HART, R. & GREAVES, D. R. 2010. Chemerin contributes to inflammation by promoting macrophage adhesion to VCAM-1 and fibronectin through clustering of VLA-4 and VLA-5. *J Immunol,* 185**,** 3728-39.

HATANO, N., MORI, Y., OH-HORA, M., KOSUGI, A., FUJIKAWA, T., NAKAI, N., NIWA, H., MIYAZAKI, J., HAMAOKA, T. & OGATA, M. 2003. Essential role for ERK2 mitogen-activated protein kinase in placental development. *Genes Cells,* 8**,** 847-56.

HATTORI, H., OKUDA, K., MURASE, T., SHIGETSURA, Y., NARISE, K., SEMENZA, G. L. & NAGASAWA, H. 2011. Isolation, identification, and biological evaluation of HIF-1-modulating compounds from Brazilian green propolis. *Bioorg Med Chem,* 19**,** 5392-401.

HAYASHI, M., KIM, S. W., IMANAKA-YOSHIDA, K., YOSHIDA, T., ABEL, E. D., ELICEIRI, B., YANG, Y., ULEVITCH, R. J. & LEE, J. D. 2004. Targeted deletion of BMK1/ERK5 in adult mice perturbs vascular integrity and leads to endothelial failure. *J Clin Invest,* 113**,** 1138-48.

HAYASHI, M. & LEE, J. D. 2004. Role of the BMK1/ERK5 signaling pathway: lessons from knockout mice. *J Mol Med (Berl),* 82**,** 800-8.

HENKART, P. A. 1996. ICE family proteases: mediators of all apoptotic cell death? *Immunity,* 4**,** 195-201.

HERLIDOU, S., GREBE, R., GRADOS, F., LEUYER, N., FARDELLONE, P. & MEYER, M. E. 2004. Influence of age and osteoporosis on calcaneus trabecular bone structure: a preliminary in vivo MRI study by quantitative texture analysis. *Magn Reson Imaging,* 22**,** 237-43.

HIRASAWA, N., MUE, S. & OHUCHI, K. 1997a. Negative regulation of MAP kinase by diacylglycerol-dependent mechanisms via G protein-coupled receptors in rat basophilic RBL-2H3 (ml) cells. *Cell Signal,* 9**,** 319-22.

HIRASAWA, N., SHIRAISHI, M., TOKUHARA, N., HIRANO, Y., MIZUTANI, A., MUE, S. & OHUCHI, K. 1997b. Pharmacological analysis of the inflammatory exudate-induced histamine production in bone marrow cells. *Immunopharmacology,* 36**,** 87-94.

HOOD, J. D., MEININGER, C. J., ZICHE, M. & GRANGER, H. J. 1998. VEGF upregulates ecNOS message, protein, and NO production in human endothelial cells. *Am J Physiol,* 274**,** H1054-8.

HOUVENAEGHEL, G., LELIEVRE, L., GONZAGUE-CASABIANCA, L., BUTTARELLI, M., MOUTARDIER, V., GONCALVES, A. & RESBEUT, M. 2006. Long-term survival after concomitant chemoradiotherapy prior to surgery in advanced cervical carcinoma. *Gynecol Oncol,* 100**,** 338-43.

HU, Y., KIELY, J. M., SZENTE, B. E., ROSENZWEIG, A. & GIMBRONE, M. A., JR. 2000. E-selectin-dependent signaling via the mitogen-activated protein kinase pathway in vascular endothelial cells. *J Immunol,* 165**,** 2142-8.

HWANG, S. J., BALLANTYNE, C. M., SHARRETT, A. R., SMITH, L. C., DAVIS, C. E., GOTTO, A. M., JR. & BOERWINKLE, E. 1997. Circulating adhesion molecules VCAM-1, ICAM-1, and E-selectin in carotid atherosclerosis and incident coronary heart disease cases: the Atherosclerosis Risk In Communities (ARIC) study. *Circulation,* 96**,** 4219-25.

INGELSSON, E., HULTHE, J. & LIND, L. 2008. Inflammatory markers in relation to insulin resistance and the metabolic syndrome. *Eur J Clin Invest,* 38**,** 502-9.

JACOBY, E., BOUHELAL, R., GERSPACHER, M. & SEUWEN, K. 2006. The 7 TM G-protein-coupled receptor target family. *ChemMedChem,* 1**,** 761-82.

JAFFE, E. A., HOYER, L. W. & NACHMAN, R. L. 1973a. Synthesis of antihemophilic factor antigen by cultured human endothelial cells. *J Clin Invest,* 52**,** 2757-64.

JAFFE, E. A., NACHMAN, R. L., BECKER, C. G. & MINICK, C. R. 1973b. Culture of human endothelial cells derived from umbilical veins. Identification by morphologic and immunologic criteria. *J Clin Invest,* 52**,** 2745-56.

JANSSENS, S. P., SHIMOUCHI, A., QUERTERMOUS, T., BLOCH, D. B. & BLOCH, K. D. 1992. Cloning and expression of a cDNA encoding human endothelium-derived relaxing factor/nitric oxide synthase. *J Biol Chem,* 267**,** 14519-22.

JENKINS, D. C., CHARLES, I. G., THOMSEN, L. L., MOSS, D. W., HOLMES, L. S., BAYLIS, S. A., RHODES, P., WESTMORE, K., EMSON, P. C. & MONCADA, S. 1995. Roles of nitric oxide in tumor growth. *Proc Natl Acad Sci U S A,* 92**,** 4392-6.

JIANG, Y., CHEN, C., LI, Z., GUO, W., GEGNER, J. A., LIN, S. & HAN, J. 1996. Characterization of the structure and function of a new mitogen-activated protein kinase (p38beta). *J Biol Chem,* 271**,** 17920-6.

JIANG, Y., GRAM, H., ZHAO, M., NEW, L., GU, J., FENG, L., DI PADOVA, F., ULEVITCH, R. J. & HAN, J. 1997. Characterization of the structure and function of the fourth member of p38 group mitogen-activated protein kinases, p38delta. *J Biol Chem,* 272**,** 30122-8.

JOHN, H., HIERER, J., HAAS, O. & FORSSMANN, W. G. 2007. Quantification of angiotensin-converting-enzyme-mediated degradation of human chemerin 145-154 in plasma by matrix-assisted laser desorption/ionization-time-of-flight mass spectrometry. *Anal Biochem,* 362**,** 117-25.

JOUKOV, V., PAJUSOLA, K., KAIPAINEN, A., CHILOV, D., LAHTINEN, I., KUKK, E., SAKSELA, O., KALKKINEN, N. & ALITALO, K. 1996. A novel vascular endothelial growth factor, VEGF-C, is a ligand for the Flt4 (VEGFR-3) and KDR (VEGFR-2) receptor tyrosine kinases. *EMBO J,* 15**,** 1751.

KANEKO, K., MIYABE, Y., TAKAYASU, A., FUKUDA, S., MIYABE, C., EBISAWA, M., YOKOYAMA, W., WATANABE, K., IMAI, T., MURAMOTO, K., TERASHIMA, Y., SUGIHARA, T., MATSUSHIMA, K., MIYASAKA, N. & NANKI, T. 2011. Chemerin activates fibroblast-like synoviocytes in patients with rheumatoid arthritis. *Arthritis Res Ther,* 13**,** R158.

KARKKAINEN, M. J., FERRELL, R. E., LAWRENCE, E. C., KIMAK, M. A., LEVINSON, K. L., MCTIGUE, M. A., ALITALO, K. & FINEGOLD, D. N. 2000a. Missense mutations interfere with VEGFR-3 signalling in primary lymphoedema. *Nat Genet,* 25**,** 153-9.

KARKKAINEN, U. M., IKAHEIMO, R., KATILA, M. L., SIVONEN, A. & SIITONEN, A. 2000b. Low virulence of Escherichia coli strains causing urinary tract infection in renal disease patients. *Eur J Clin Microbiol Infect Dis,* 19**,** 254-9.

KATO, Y., TAPPING, R. I., HUANG, S., WATSON, M. H., ULEVITCH, R. J. & LEE, J. D. 1998. Bmk1/Erk5 is required for cell proliferation induced by epidermal growth factor. *Nature,* 395**,** 713-6.

KAUR, J., ADYA, R., TAN, B. K., CHEN, J. & RANDEVA, H. S. 2010. Identification of chemerin receptor (ChemR23) in human endothelial cells: chemerin-induced endothelial angiogenesis. *Biochem Biophys Res Commun,* 391**,** 1762-8.

KESWANI, S. C., BOSCH-MARCE, M., REED, N., FISCHER, A., SEMENZA, G. L. & HOKE, A. 2011. Nitric oxide prevents axonal degeneration by inducing HIF-1-dependent expression of erythropoietin. *Proc Natl Acad Sci U S A,* 108**,** 4986-90.

KHAN, B. V., HARRISON, D. G., OLBRYCH, M. T., ALEXANDER, R. W. & MEDFORD, R. M. 1996. Nitric oxide regulates vascular cell adhesion molecule 1 gene expression and redox-sensitive transcriptional events in human vascular endothelial cells. *Proc Natl Acad Sci U S A,* 93**,** 9114-9.

KLAGSBRUN, M. & D'AMORE, P. A. 1991. Regulators of angiogenesis. *Annu Rev Physiol,* 53**,** 217-39.

KLEINMAN, H. K., MCGARVEY, M. L., HASSELL, J. R., STAR, V. L., CANNON, F. B., LAURIE, G. W. & MARTIN, G. R. 1986. Basement membrane complexes with biological activity. *Biochemistry,* 25**,** 312-8.

KOBAYASHI, S., OHUCHI, T. & MAKI, T. 1997. [A case of probable Creutzfeldt-Jakob disease with a point mutation of prion protein gene codon 180 and atypical MRI findings]. *Rinsho Shinkeigaku,* 37**,** 671-4.

KOCH, A. E., HALLORAN, M. M., HASKELL, C. J., SHAH, M. R. & POLVERINI, P. J. 1995. Angiogenesis mediated by soluble forms of E-selectin and vascular cell adhesion molecule-1. *Nature,* 376**,** 517-9.

KOJDA, G., CHENG, Y. C., BURCHFIELD, J. & HARRISON, D. G. 2001. Dysfunctional regulation of endothelial nitric oxide synthase (eNOS) expression in response to exercise in mice lacking one eNOS gene. *Circulation,* 103**,** 2839-44.

KOLLIGS, F. T., KOLLIGS, B., HAJRA, K. M., HU, G., TANI, M., CHO, K. R. & FEARON, E. R. 2000. gamma-catenin is regulated by the APC tumor suppressor and its oncogenic activity is distinct from that of beta-catenin. *Genes Dev,* 14**,** 1319-31.

KRISHNA, M. & NARANG, H. 2008. The complexity of mitogen-activated protein kinases (MAPKs) made simple. *Cell Mol Life Sci,* 65**,** 3525-44.

KROLL, J. & WALTENBERGER, J. 1997. The vascular endothelial growth factor receptor KDR activates multiple signal transduction pathways in porcine aortic endothelial cells. *J Biol Chem,* 272**,** 32521-7.

KROLL, J. & WALTENBERGER, J. 1998. VEGF-A induces expression of eNOS and iNOS in endothelial cells via VEGF receptor-2 (KDR). *Biochem Biophys Res Commun,* 252**,** 743-6.

KUBES, P. 1995. Nitric oxide affects microvascular permeability in the intact and inflamed vasculature. *Microcirculation,* 2**,** 235-44.

KUKK, E., AKSELA, S. & AKSELA, H. 1996a. Features of the Auger resonant Raman effect in experimental spectra. *Phys Rev A,* 53**,** 3271-3277.

KUKK, E., LYMBOUSSAKI, A., TAIRA, S., KAIPAINEN, A., JELTSCH, M., JOUKOV, V. & ALITALO, K. 1996b. VEGF-C receptor binding and pattern of expression with VEGFR-3 suggests a role in lymphatic vascular development. *Development,* 122**,** 3829-37.

KUKKONEN, H. T., FOSTER, D. H., WOOD, J. R., WAGEMANS, J. & VAN GOOL, L. 1996a. Qualitative cues in the discrimination of affine-transformed minimal patterns. *Perception,* 25**,** 195-206.

KUKKONEN, J. P., HAUTALA, R. & AKERMAN, K. E. 1996b. Muscarinic depolarization of SH-SY5Y human neuroblastoma cells as determined using oxonol V. *Neurosci Lett,* 212**,** 57-60.

KUKKONEN, S., HEIKKILA, L., VERKKALA, K., MATTILA, S. & TOIVONEN, H. 1996c. Abnormal in vivo response to sodium nitroprusside after porcine single lung transplantation. *Transplantation,* 61**,** 1435-9.

KUKKONEN, S., HEIKKILA, L., VERKKALA, K., MATTILA, S. & TOIVONEN, H. 1996d. Thromboxane receptor blockade does not attenuate pulmonary pressor response in porcine single lung transplantation. *J Heart Lung Transplant,* 15**,** 409-14.

LAUGHNER, E., TAGHAVI, P., CHILES, K., MAHON, P. C. & SEMENZA, G. L. 2001. HER2 (neu) signaling increases the rate of hypoxia-inducible factor 1alpha (HIF-1alpha) synthesis: novel mechanism for HIF-1-mediated vascular endothelial growth factor expression. *Mol Cell Biol,* 21**,** 3995-4004.

LEIBOVICH, S. J., POLVERINI, P. J., FONG, T. W., HARLOW, L. A. & KOCH, A. E. 1994. Production of angiogenic activity by human monocytes requires an L-arginine/nitric oxide-synthase-dependent effector mechanism. *Proc Natl Acad Sci U S A,* 91**,** 4190-4.

LEWIS, T. S., SHAPIRO, P. S. & AHN, N. G. 1998. Signal transduction through MAP kinase cascades. *Adv Cancer Res,* 74**,** 49-139.

LEY, K. & REUTERSHAN, J. 2006. Leucocyte-endothelial interactions in health and disease. *Handb Exp Pharmacol***,** 97-133.

LI, Z., JIANG, Y., ULEVITCH, R. J. & HAN, J. 1996. The primary structure of p38 gamma: a new member of p38 group of MAP kinases. *Biochem Biophys Res Commun,* 228**,** 334-40.

LIN, M. I., FULTON, D., BABBITT, R., FLEMING, I., BUSSE, R., PRITCHARD, K. A., JR. & SESSA, W. C. 2003. Phosphorylation of threonine 497 in endothelial nitric-oxide synthase coordinates the coupling of L-arginine metabolism to efficient nitric oxide production. *J Biol Chem,* 278**,** 44719-26.

LISANTI, M. P., SCHERER, P. E., VIDUGIRIENE, J., TANG, Z., HERMANOWSKI-VOSATKA, A., TU, Y. H., COOK, R. F. & SARGIACOMO, M. 1994. Characterization of caveolin-rich membrane domains isolated from an endothelial-rich source: implications for human disease. *J Cell Biol,* 126**,** 111-26.

LIU, J., WANG, X. B., PARK, D. S. & LISANTI, M. P. 2002. Caveolin-1 expression enhances endothelial capillary tubule formation. *J Biol Chem,* 277**,** 10661-8.

LOVELOCK, J. E. & BISHOP, M. W. 1959. Prevention of freezing damage to living cells by dimethyl sulphoxide. *Nature,* 183**,** 1394-5.

LU, J. L., SCHMIEGE, L. M., 3RD, KUO, L. & LIAO, J. C. 1996. Downregulation of endothelial constitutive nitric oxide synthase expression by lipopolysaccharide. *Biochem Biophys Res Commun,* 225**,** 1-5.

LUANGSAY, S., WITTAMER, V., BONDUE, B., DE HENAU, O., ROUGER, L., BRAIT, M., FRANSSEN, J. D., DE NADAI, P., HUAUX, F. & PARMENTIER, M. 2009. Mouse ChemR23 is expressed in dendritic cell subsets and macrophages, and mediates an anti-inflammatory activity of chemerin in a lung disease model. *J Immunol,* 183**,** 6489-99.

LUO, W. & SEMENZA, G. L. 2011. Pyruvate kinase M2 regulates glucose metabolism by functioning as a coactivator for hypoxia-inducible factor 1 in cancer cells. *Oncotarget,* 2**,** 551-6.

LUO, Z., FUJIO, Y., KUREISHI, Y., RUDIC, R. D., DAUMERIE, G., FULTON, D., SESSA, W. C. & WALSH, K. 2000. Acute modulation of endothelial Akt/PKB activity alters nitric oxide-dependent vasomotor activity in vivo. *J Clin Invest,* 106**,** 493-9.

LUSCINSKAS, F. W., GERSZTEN, R. E., GARCIA-ZEPEDA, E. A., LIM, Y. C., YOSHIDA, M., DING, H. A., GIMBRONE, M. A., JR., LUSTER, A. D. & ROSENZWEIG, A. 2000. C-C and C-X-C chemokines trigger firm adhesion of monocytes to vascular endothelium under flow conditions. *Ann N Y Acad Sci,* 902**,** 288-93.

MAJUMDER, V., SAHA, B., HAJRA, S. K., BISWAS, S. K. & SAHA, K. 2000. Efficacy of single-dose ROM therapy plus low-dose convit vaccine as an adjuvant for treatment of paucibacillary leprosy patients with a single skin lesion. *Int J Lepr Other Mycobact Dis,* 68**,** 283-90.

MARSDEN, P. A., HENG, H. H., SCHERER, S. W., STEWART, R. J., HALL, A. V., SHI, X. M., TSUI, L. C. & SCHAPPERT, K. T. 1993. Structure and chromosomal localization of the human constitutive endothelial nitric oxide synthase gene. *J Biol Chem,* 268**,** 17478-88.

MARSDEN, P. A., SCHAPPERT, K. T., CHEN, H. S., FLOWERS, M., SUNDELL, C. L., WILCOX, J. N., LAMAS, S. & MICHEL, T. 1992. Molecular cloning and characterization of human endothelial nitric oxide synthase. *FEBS Lett,* 307**,** 287-93.

MARTENSSON, U. E., FENYO, E. M., OLDE, B. & OWMAN, C. 2006. Characterization of the human chemerin receptor--ChemR23/CMKLR1--as co-receptor for human and simian immunodeficiency virus infection, and identification of virus-binding receptor domains. *Virology,* 355**,** 6-17.

MEBRATU, Y. & TESFAIGZI, Y. 2009. How ERK1/2 activation controls cell proliferation and cell death: Is subcellular localization the answer? *Cell Cycle,* 8**,** 1168-75.

MEDER, W., WENDLAND, M., BUSMANN, A., KUTZLEB, C., SPODSBERG, N., JOHN, H., RICHTER, R., SCHLEUDER, D., MEYER, M. & FORSSMANN, W. G. 2003. Characterization of human circulating TIG2 as a ligand for the orphan receptor ChemR23. *FEBS Lett,* 555**,** 495-9.

MERRITT, C., ENSLEN, H., DIEHL, N., CONZE, D., DAVIS, R. J. & RINCON, M. 2000. Activation of p38 mitogen-activated protein kinase in vivo selectively induces apoptosis of CD8(+) but not CD4(+) T cells. *Mol Cell Biol,* 20**,** 936-46.

METHNER, A., HERMEY, G., SCHINKE, B. & HERMANS-BORGMEYER, I. 1997. A novel G protein-coupled receptor with homology to neuropeptide and chemoattractant receptors expressed during bone development. *Biochem Biophys Res Commun,* 233**,** 336-42.

MEYER, M. 2004a. Springtime for obstetrics and gynecology: will the specialty continue to blossom? *Obstet Gynecol,* 103**,** 199; author reply 200.

MEYER, M. A. 2004b. DKK1 in multiple myeloma. *N Engl J Med,* 350**,** 1464-6; author reply 1464-6.

MEYER, M. A. 2004c. Radiotherapeutic use of 2-deoxy-2-[18F]fluoro-D-glucose--a comment. *Breast Cancer Res,* 6**,** E2.

MEYER, M. H., LETSCHER-BRU, V., JAULHAC, B., WALLER, J. & CANDOLFI, E. 2004. Comparison of Mycosis IC/F and plus Aerobic/F media for diagnosis of fungemia by the bactec 9240 system. *J Clin Microbiol,* 42**,** 773-7.

MICHELL, B. J., GRIFFITHS, J. E., MITCHELHILL, K. I., RODRIGUEZ-CRESPO, I., TIGANIS, T., BOZINOVSKI, S., DE MONTELLANO, P. R., KEMP, B. E. & PEARSON, R. B. 1999. The Akt kinase signals directly to endothelial nitric oxide synthase. *Curr Biol,* 9**,** 845-8.

MIN, S. H., MACKENZIE, D. D., BREIER, B. H., MCCUTCHEON, S. N. & GLUCKMAN, P. D. 1996. Responses of young energy-restricted sheep to chronically administered insulin-like growth factor I (IGF-I): evidence that IGF-I suppresses the hepatic growth hormone receptor. *Endocrinology,* 137**,** 1129-37.

MINSHALL, R. D. & MALIK, A. B. 2006. Transport across the endothelium: regulation of endothelial permeability. *Handb Exp Pharmacol***,** 107-44.

MIRANDA, K. M., ESPEY, M. G. & WINK, D. A. 2001. A rapid, simple spectrophotometric method for simultaneous detection of nitrate and nitrite. *Nitric Oxide,* 5**,** 62-71.

MIURA, M., YAMAUCHI, H., ICHINOSE, M., OHUCHI, Y., KAGEYAMA, N., TOMAKI, M., ENDOH, N. & SHIRATO, K. 1997. Impairment of neural nitric oxide-mediated relaxation after antigen exposure in guinea pig airways in vitro. *Am J Respir Crit Care Med,* 156**,** 217-22.

MORRIS, S. M., JR. & BILLIAR, T. R. 1994. New insights into the regulation of inducible nitric oxide synthesis. *Am J Physiol,* 266**,** E829-39.

MUDGETT, J. S., DING, J., GUH-SIESEL, L., CHARTRAIN, N. A., YANG, L., GOPAL, S. & SHEN, M. M. 2000. Essential role for p38alpha mitogen-activated protein kinase in placental angiogenesis. *Proc Natl Acad Sci U S A,* 97**,** 10454-9.

MURPHY, P. M., BAGGIOLINI, M., CHARO, I. F., HEBERT, C. A., HORUK, R., MATSUSHIMA, K., MILLER, L. H., OPPENHEIM, J. J. & POWER, C. A. 2000. International union of pharmacology. XXII. Nomenclature for chemokine receptors. *Pharmacol Rev,* 52**,** 145-76.

NAGPAL, S., PATEL, S., JACOBE, H., DISEPIO, D., GHOSN, C., MALHOTRA, M., TENG, M., DUVIC, M. & CHANDRARATNA, R. A. 1997. Tazarotene-induced gene 2 (TIG2), a novel retinoid-responsive gene in skin. *J Invest Dermatol,* 109**,** 91-5.

NAKAMURA, K., OHUCHI, H., FUKUDA, I. & KOHNO, M. 1997. [Constrictive pericarditis complicated with hepatic coma--a case report]. *Nihon Kyobu Geka Gakkai Zasshi,* 45**,** 187-90.

NATHAN, C. & XIE, Q. W. 1994. Nitric oxide synthases: roles, tolls, and controls. *Cell,* 78**,** 915-8.

NEUFELD, G., COHEN, T., GENGRINOVITCH, S. & POLTORAK, Z. 1999. Vascular endothelial growth factor (VEGF) and its receptors. *FASEB J,* 13**,** 9-22.

NGUYEN, D. H., GANESAN, G. S., SUMFEST, J. M., LIGGITT, D. H., CARUSO, A., BURNS, M. W. & MITCHELL, M. E. 1993a. The use of the AMS800 artificial urinary sphincter in combination with the gastric tube for continence in the canine model. *J Urol,* 150**,** 737-41.

NGUYEN, M., FOLKMAN, J. & BISCHOFF, J. 1992. 1-Deoxymannojirimycin inhibits capillary tube formation in vitro. Analysis of N-linked oligosaccharides in bovine capillary endothelial cells. *J Biol Chem,* 267**,** 26157-65.

NGUYEN, M., STRUBEL, N. A. & BISCHOFF, J. 1993b. A role for sialyl Lewis-X/A glycoconjugates in capillary morphogenesis. *Nature,* 365**,** 267-9.

NISHIMOTO, S. & NISHIDA, E. 2006. MAPK signalling: ERK5 versus ERK1/2. *EMBO Rep,* 7**,** 782-6.

NITTOH, T., ARII, M., SUZUKI, R., KITOH, A., WATANABE, M., MUE, S. & OHUCHI, K. 1997a. Increase of eosinophilic cell population in bone marrow of rats by immunization with Ascaris suum antigen. *Immunol Invest,* 26**,** 439-51.

NITTOH, T., HIRAKATA, M., MUE, S. & OHUCHI, K. 1997b. Identification of cDNA encoding rat eosinophil cationic protein/eosinophil-associated ribonuclease. *Biochim Biophys Acta,* 1351**,** 42-6.

NOWAK, D. G., WOOLARD, J., AMIN, E. M., KONOPATSKAYA, O., SALEEM, M. A., CHURCHILL, A. J., LADOMERY, M. R., HARPER, S. J. & BATES, D. O. 2008. Expression of pro- and anti-angiogenic isoforms of VEGF is differentially regulated by splicing and growth factors. *J Cell Sci,* 121**,** 3487-95.

OHASHI, Y., KAWASHIMA, S., HIRATA, K., YAMASHITA, T., ISHIDA, T., INOUE, N., SAKODA, T., KURIHARA, H., YAZAKI, Y. & YOKOYAMA, M. 1998. Hypotension and reduced nitric oxide-elicited vasorelaxation in transgenic mice overexpressing endothelial nitric oxide synthase. *J Clin Invest,* 102**,** 2061-71.

OHUCHI, E., IMAI, K., FUJII, Y., SATO, H., SEIKI, M. & OKADA, Y. 1997a. Membrane type 1 matrix metalloproteinase digests interstitial collagens and other extracellular matrix macromolecules. *J Biol Chem,* 272**,** 2446-51.

OHUCHI, N., HARADA, Y., ISHIDA, T., KIYOHARA, H. & SATOMI, S. 1997b. Breast-Coserving Surgery for Primary Breast Cancer: Immediate Volume Replacement Using Lateral Tissue Flap. *Breast Cancer,* 4**,** 135-141.

OHUCHI, S., NAKAMURA, H., SLIGIURA, H., NARITA, M. & SODE, K. 1997c. An optical resolution of racemic organophosphorous esters by phosphotriesterase-catalyzing hydrolysis. *Appl Biochem Biotechnol,* 63-65**,** 659-65.

OKAMOTO, H., MORI, K., OHTSUKA, K., OHUCHI, H. & ISHII, H. 1997. Theory and computer programs for calculating solution pH, buffer formula, and buffer capacity for multiple component system at a given ionic strength and temperature. *Pharm Res,* 14**,** 299-302.

OLSON, J. M. & HALLAHAN, A. R. 2004. p38 MAP kinase: a convergence point in cancer therapy. *Trends Mol Med,* 10**,** 125-9.

PALFRAMAN, R. T., JUNG, S., CHENG, G., WENINGER, W., LUO, Y., DORF, M., LITTMAN, D. R., ROLLINS, B. J., ZWEERINK, H., ROT, A. & VON ANDRIAN, U. H. 2001. Inflammatory chemokine transport and presentation in HEV: a remote control mechanism for monocyte recruitment to lymph nodes in inflamed tissues. *J Exp Med,* 194**,** 1361-73.

PALMER, R. M., ASHTON, D. S. & MONCADA, S. 1988. Vascular endothelial cells synthesize nitric oxide from L-arginine. *Nature,* 333**,** 664-6.

PALMER, R. M., FERRIGE, A. G. & MONCADA, S. 1987. Nitric oxide release accounts for the biological activity of endothelium-derived relaxing factor. *Nature,* 327**,** 524-6.

PALMER, R. M. & MONCADA, S. 1989. A novel citrulline-forming enzyme implicated in the formation of nitric oxide by vascular endothelial cells. *Biochem Biophys Res Commun,* 158**,** 348-52.

PAPAPETROPOULOS, A., GARCIA-CARDENA, G., MADRI, J. A. & SESSA, W. C. 1997. Nitric oxide production contributes to the angiogenic properties of vascular endothelial growth factor in human endothelial cells. *J Clin Invest,* 100**,** 3131-9.

PERRIN, R. M., KONOPATSKAYA, O., QIU, Y., HARPER, S., BATES, D. O. & CHURCHILL, A. J. 2005. Diabetic retinopathy is associated with a switch in splicing from anti- to pro-angiogenic isoforms of vascular endothelial growth factor. *Diabetologia,* 48**,** 2422-7.

PIERCE, K. L., PREMONT, R. T. & LEFKOWITZ, R. J. 2002. Seven-transmembrane receptors. *Nat Rev Mol Cell Biol,* 3**,** 639-50.

PIETERSMA, A., TILLY, B. C., GAESTEL, M., DE JONG, N., LEE, J. C., KOSTER, J. F. & SLUITER, W. 1997. p38 mitogen activated protein kinase regulates endothelial VCAM-1 expression at the post-transcriptional level. *Biochem Biophys Res Commun,* 230**,** 44-8.

PLOUET, J., SCHILLING, J. & GOSPODAROWICZ, D. 1989. Isolation and characterization of a newly identified endothelial cell mitogen produced by AtT-20 cells. *EMBO J,* 8**,** 3801-6.

PONTICOS, M., LU, Q. L., MORGAN, J. E., HARDIE, D. G., PARTRIDGE, T. A. & CARLING, D. 1998. Dual regulation of the AMP-activated protein kinase provides a novel mechanism for the control of creatine kinase in skeletal muscle. *EMBO J,* 17**,** 1688-99.

PRIBYLOVA, H., DVORAKOVA, L., VONDRACEK, J., STROUFOVA, A. & MIKOVA, M. 1995. [Risk of diabetes mellitus, variations in glucose tolerance, insulin secretion and lipid parameters in offspring of diabetic mothers]. *Cas Lek Cesk,* 134**,** 203-6.

PRITCHARD-JONES, R. O., DUNN, D. B., QIU, Y., VAREY, A. H., ORLANDO, A., RIGBY, H., HARPER, S. J. & BATES, D. O. 2007. Expression of VEGF(xxx)b, the inhibitory isoforms of VEGF, in malignant melanoma. *Br J Cancer,* 97**,** 223-30.

QUNIBI, W. Y., HOOTKINS, R. E., MCDOWELL, L. L., MEYER, M. S., SIMON, M., GARZA, R. O., PELHAM, R. W., CLEVELAND, M. V., MUENZ, L. R., HE, D. Y. & NOLAN, C. R. 2004. Treatment of hyperphosphatemia in hemodialysis patients: The Calcium Acetate Renagel Evaluation (CARE Study). *Kidney Int,* 65**,** 1914-26.

RADOMSKI, M. W., PALMER, R. M. & MONCADA, S. 1987. The anti-aggregating properties of vascular endothelium: interactions between prostacyclin and nitric oxide. *Br J Pharmacol,* 92**,** 639-46.

RAMPAZZO, E., BONALDI, L., TRENTIN, L., VISCO, C., KEPPEL, S., GIUNCO, S., FREZZATO, F., FACCO, M., NOVELLA, E., GIARETTA, I., DEL BIANCO, P., SEMENZATO, G. & DE ROSSI, A. 2012. Telomere length and telomerase levels delineate subgroups of B-cell chronic lymphocytic leukemia with different biological characteristics and clinical outcomes. *Haematologica,* 97**,** 56-63.

RANDOLPH, G. J. & FURIE, M. B. 1995. A soluble gradient of endogenous monocyte chemoattractant protein-1 promotes the transendothelial migration of monocytes in vitro. *J Immunol,* 155**,** 3610-8.

RANGASAMY, T., SEMENZA, G. L. & GEORAS, S. N. 2011. What is hypoxia-inducible factor-1 doing in the allergic lung? *Allergy,* 66**,** 815-7.

RANU, B. C., HAJRA, A. & JANA, U. 2000. Indium(III) chloride-catalyzed one-pot synthesis of dihydropyrimidinones by a three-component coupling of 1,3-dicarbonyl compounds, aldehydes, and urea: an improved procedure for the Biginelli reaction. *J Org Chem,* 65**,** 6270-2.

READ, M. A., WHITLEY, M. Z., GUPTA, S., PIERCE, J. W., BEST, J., DAVIS, R. J. & COLLINS, T. 1997. Tumor necrosis factor alpha-induced E-selectin expression is activated by the nuclear factor-kappaB and c-JUN N-terminal kinase/p38 mitogen-activated protein kinase pathways. *J Biol Chem,* 272**,** 2753-61.

RECHEL, B., SUHRCKE, M., TSOLOVA, S., SUK, J. E., DESAI, M., MCKEE, M., STUCKLER, D., ABUBAKAR, I., HUNTER, P., SENEK, M. & SEMENZA, J. C. 2011. Economic crisis and communicable disease control in Europe: a scoping study among national experts. *Health Policy,* 103**,** 168-75.

REES, D. D., PALMER, R. M., HODSON, H. F. & MONCADA, S. 1989. A specific inhibitor of nitric oxide formation from L-arginine attenuates endothelium-dependent relaxation. *Br J Pharmacol,* 96**,** 418-24.

RIDKER, P. M., HENNEKENS, C. H., ROITMAN-JOHNSON, B., STAMPFER, M. J. & ALLEN, J. 1998. Plasma concentration of soluble intercellular adhesion molecule 1 and risks of future myocardial infarction in apparently healthy men. *Lancet,* 351**,** 88-92.

ROH, S. G., SONG, S. H., CHOI, K. C., KATOH, K., WITTAMER, V., PARMENTIER, M. & SASAKI, S. 2007. Chemerin--a new adipokine that modulates adipogenesis via its own receptor. *Biochem Biophys Res Commun,* 362**,** 1013-8.

ROTHBERG, K. G., HEUSER, J. E., DONZELL, W. C., YING, Y. S., GLENNEY, J. R. & ANDERSON, R. G. 1992. Caveolin, a protein component of caveolae membrane coats. *Cell,* 68**,** 673-82.

ROUSSEAU, S., HOULE, F., LANDRY, J. & HUOT, J. 1997. p38 MAP kinase activation by vascular endothelial growth factor mediates actin reorganization and cell migration in human endothelial cells. *Oncogene,* 15**,** 2169-77.

RYAN, E. T., ECKER, J. L., CHRISTAKIS, N. A. & FOLKMAN, J. 1992. Hirschsprung's disease: associated abnormalities and demography. *J Pediatr Surg,* 27**,** 76-81.

SAKATA, K., HAREYAMA, M., OHUCHI, A., SIDO, M., NAGAKURA, H., MORITA, K., HARABUCHI, Y. & KATAURA, A. 1997. Treatment of lethal midline granuloma type nasal T-cell lymphoma. *Acta Oncol,* 36**,** 307-11.

SAKURAI, Y., OHGIMOTO, K., KATAOKA, Y., YOSHIDA, N. & SHIBUYA, M. 2005. Essential role of Flk-1 (VEGF receptor 2) tyrosine residue 1173 in vasculogenesis in mice. *Proc Natl Acad Sci U S A,* 102**,** 1076-81.

SAMSON, M., EDINGER, A. L., STORDEUR, P., RUCKER, J., VERHASSELT, V., SHARRON, M., GOVAERTS, C., MOLLEREAU, C., VASSART, G., DOMS, R. W. & PARMENTIER, M. 1998. ChemR23, a putative chemoattractant receptor, is expressed in monocyte-derived dendritic cells and macrophages and is a coreceptor for SIV and some primary HIV-1 strains. *Eur J Immunol,* 28**,** 1689-700.

SAVOIA, C. & SCHIFFRIN, E. L. 2007. Vascular inflammation in hypertension and diabetes: molecular mechanisms and therapeutic interventions. *Clin Sci (Lond),* 112**,** 375-84.

SEMENZA, G. L. 2011. Regulation of metabolism by hypoxia-inducible factor 1. *Cold Spring Harb Symp Quant Biol,* 76**,** 347-53.

SEMENZA, G. L., ARTEMOV, D., BEDI, A., BHUJWALLA, Z., CHILES, K., FELDSER, D., LAUGHNER, E., RAVI, R., SIMONS, J., TAGHAVI, P. & ZHONG, H. 2001. 'The metabolism of tumours': 70 years later. *Novartis Found Symp,* 240**,** 251-60; discussion 260-4.

SEMENZA, J. C., PLOUBIDIS, G. B. & GEORGE, L. A. 2011. Climate change and climate variability: personal motivation for adaptation and mitigation. *Environ Health,* 10**,** 46.

SEMENZATO, G., MARINO, F. & ZAMBELLO, R. 2012. State of the art in natural killer cell malignancies. *Int J Lab Hematol,* 34**,** 117-28.

SELL, H., LAURENCIKIENE, J., TAUBE, A., ECKARDT, K., CRAMER, A., HORRIGHS, A., ARNER, P. & ECKEL, J. 2009. Chemerin is a novel adipocyte-derived factor inducing insulin resistance in primary human skeletal muscle cells. *Diabetes,* 58**,** 2731-40.(Sell et al., 2009)

SENGER, D. R., GALLI, S. J., DVORAK, A. M., PERRUZZI, C. A., HARVEY, V. S. & DVORAK, H. F. 1983. Tumor cells secrete a vascular permeability factor that promotes accumulation of ascites fluid. *Science,* 219**,** 983-5.

SEYMOUR, L. W., SHOAIBI, M. A., MARTIN, A., AHMED, A., ELVIN, P., KERR, D. J. & WAKELAM, M. J. 1996. Vascular endothelial growth factor stimulates protein kinase C-dependent phospholipase D activity in endothelial cells. *Lab Invest,* 75**,** 427-37.

SHIMAOKA, M., LU, C., PALFRAMAN, R. T., VON ANDRIAN, U. H., MCCORMACK, A., TAKAGI, J. & SPRINGER, T. A. 2001. Reversibly locking a protein fold in an active conformation with a disulfide bond: integrin alphaL I domains with high affinity and antagonist activity in vivo. *Proc Natl Acad Sci U S A,* 98**,** 6009-14.

SOHN, S. J., SARVIS, B. K., CADO, D. & WINOTO, A. 2002. ERK5 MAPK regulates embryonic angiogenesis and acts as a hypoxia-sensitive repressor of vascular endothelial growth factor expression. *J Biol Chem,* 277**,** 43344-51.

SORO-PAAVONEN, A., WESTERBACKA, J., EHNHOLM, C. & TASKINEN, M. R. 2006. Metabolic syndrome aggravates the increased endothelial activation and low-grade inflammation in subjects with familial low HDL. *Ann Med,* 38**,** 229-38.

TABUCHI, M., IWAIHARA, O., OHTANI, Y., OHUCHI, N., SAKURAI, J., MORITA, T., IWAHARA, S. & TAKEGAWA, K. 1997. Vacuolar protein sorting in fission yeast: cloning, biosynthesis, transport, and processing of carboxypeptidase Y from Schizosaccharomyces pombe. *J Bacteriol,* 179**,** 4179-89.

TAKAHASHI, T., YAMAGUCHI, S., CHIDA, K. & SHIBUYA, M. 2001. A single autophosphorylation site on KDR/Flk-1 is essential for VEGF-A-dependent activation of PLC-gamma and DNA synthesis in vascular endothelial cells. *EMBO J,* 20**,** 2768-78.

TAKENAKA, K., MORIGUCHI, T. & NISHIDA, E. 1998. Activation of the protein kinase p38 in the spindle assembly checkpoint and mitotic arrest. *Science,* 280**,** 599-602.

TARDIF, J. C., HEINONEN, T., ORLOFF, D. & LIBBY, P. 2006. Vascular biomarkers and surrogates in cardiovascular disease. *Circulation,* 113**,** 2936-42.

TEERLINK, T., LUO, Z., PALM, F. & WILCOX, C. S. 2009. Cellular ADMA: Regulation and action. *Pharmacol Res,* 60**,** 448-60.

TERMAN, B. I., DOUGHER-VERMAZEN, M., CARRION, M. E., DIMITROV, D., ARMELLINO, D. C., GOSPODAROWICZ, D. & BOHLEN, P. 1992. Identification of the KDR tyrosine kinase as a receptor for vascular endothelial cell growth factor. *Biochem Biophys Res Commun,* 187**,** 1579-86.

UIBO, O., METSKULA, K., KUKK, T., RAGO, T. & UIBO, R. 1996. Results of coeliac disease screening in Estonia in 1990-1994. *Acta Paediatr Suppl,* 412**,** 39-41.

VALLANCE, P., LEONE, A., CALVER, A., COLLIER, J. & MONCADA, S. 1992a. Accumulation of an endogenous inhibitor of nitric oxide synthesis in chronic renal failure. *Lancet,* 339**,** 572-5.

VALLANCE, P., LEONE, A., CALVER, A., COLLIER, J. & MONCADA, S. 1992b. Endogenous dimethylarginine as an inhibitor of nitric oxide synthesis. *J Cardiovasc Pharmacol,* 20 Suppl 12**,** S60-2.

VAN DER ZEE, R., MUROHARA, T., LUO, Z., ZOLLMANN, F., PASSERI, J., LEKUTAT, C. & ISNER, J. M. 1997. Vascular endothelial growth factor/vascular permeability factor augments nitric oxide release from quiescent rabbit and human vascular endothelium. *Circulation,* 95**,** 1030-7.

VAN HINSBERGH, V. W., ENGELSE, M. A. & QUAX, P. H. 2006. Pericellular proteases in angiogenesis and vasculogenesis. *Arterioscler Thromb Vasc Biol,* 26**,** 716-28.

VAPALAHTI, O., LUNDKVIST, A., KUKKONEN, S. K., CHENG, Y., GILLJAM, M., KANERVA, M., MANNI, T., PEJCOCH, M., NIEMIMAA, J., KAIKUSALO, A., HENTTONEN, H., VAHERI, A. & PLYUSNIN, A. 1996. Isolation and characterization of Tula virus, a distinct serotype in the genus Hantavirus, family Bunyaviridae. *J Gen Virol,* 77 (Pt 12)**,** 3063-7.

VAREY, A. H., RENNEL, E. S., QIU, Y., BEVAN, H. S., PERRIN, R. M., RAFFY, S., DIXON, A. R., PARASKEVA, C., ZACCHEO, O., HASSAN, A. B., HARPER, S. J. & BATES, D. O. 2008. VEGF 165 b, an antiangiogenic VEGF-A isoform, binds and inhibits bevacizumab treatment in experimental colorectal carcinoma: balance of pro- and antiangiogenic VEGF-A isoforms has implications for therapy. *Br J Cancer,* 98**,** 1366-79.

VASILE, E., QU, H., DVORAK, H. F. & DVORAK, A. M. 1999. Caveolae and vesiculo-vacuolar organelles in bovine capillary endothelial cells cultured with VPF/VEGF on floating Matrigel-collagen gels. *J Histochem Cytochem,* 47**,** 159-67.

VEREECKE, J. & CARMELIET, E. 2000. The effect of external pH on the delayed rectifying K+ current in cardiac ventricular myocytes. *Pflugers Arch,* 439**,** 739-51.

VERMI, W., RIBOLDI, E., WITTAMER, V., GENTILI, F., LUINI, W., MARRELLI, S., VECCHI, A., FRANSSEN, J. D., COMMUNI, D., MASSARDI, L., SIRONI, M., MANTOVANI, A., PARMENTIER, M., FACCHETTI, F. & SOZZANI, S. 2005. Role of ChemR23 in directing the migration of myeloid and plasmacytoid dendritic cells to lymphoid organs and inflamed skin. *J Exp Med,* 201**,** 509-15.

VODOVOTZ, Y., CHESLER, L., CHONG, H., KIM, S. J., SIMPSON, J. T., DEGRAFF, W., COX, G. W., ROBERTS, A. B., WINK, D. A. & BARCELLOS-HOFF, M. H. 1999. Regulation of transforming growth factor beta1 by nitric oxide. *Cancer Res,* 59**,** 2142-9.

WALTENBERGER, J., CLAESSON-WELSH, L., SIEGBAHN, A., SHIBUYA, M. & HELDIN, C. H. 1994. Different signal transduction properties of KDR and Flt1, two receptors for vascular endothelial growth factor. *J Biol Chem,* 269**,** 26988-95.

WARY, K. K., MARIOTTI, A., ZURZOLO, C. & GIANCOTTI, F. G. 1998. A requirement for caveolin-1 and associated kinase Fyn in integrin signaling and anchorage-dependent cell growth. *Cell,* 94**,** 625-34.

WATANABE, Y. & DVORAK, H. F. 1997. Vascular permeability factor/vascular endothelial growth factor inhibits anchorage-disruption-induced apoptosis in microvessel endothelial cells by inducing scaffold formation. *Exp Cell Res,* 233**,** 340-9.

WEIDNER, N., FOLKMAN, J., POZZA, F., BEVILACQUA, P., ALLRED, E. N., MOORE, D. H., MELI, S. & GASPARINI, G. 1992. Tumor angiogenesis: a new significant and independent prognostic indicator in early-stage breast carcinoma. *J Natl Cancer Inst,* 84**,** 1875-87.

WITTAMER, V., BONDUE, B., GUILLABERT, A., VASSART, G., PARMENTIER, M. & COMMUNI, D. 2005. Neutrophil-mediated maturation of chemerin: a link between innate and adaptive immunity. *J Immunol,* 175**,** 487-93.

WITTAMER, V., FRANSSEN, J. D., VULCANO, M., MIRJOLET, J. F., LE POUL, E., MIGEOTTE, I., BREZILLON, S., TYLDESLEY, R., BLANPAIN, C., DETHEUX, M., MANTOVANI, A., SOZZANI, S., VASSART, G., PARMENTIER, M. & COMMUNI, D. 2003. Specific recruitment of antigen-presenting cells by chemerin, a novel processed ligand from human inflammatory fluids. *J Exp Med,* 198**,** 977-85.

WITTAMER, V., GREGOIRE, F., ROBBERECHT, P., VASSART, G., COMMUNI, D. & PARMENTIER, M. 2004. The C-terminal nonapeptide of mature chemerin activates the chemerin receptor with low nanomolar potency. *J Biol Chem,* 279**,** 9956-62.

WONG, C. C., GILKES, D. M., ZHANG, H., CHEN, J., WEI, H., CHATURVEDI, P., FRALEY, S. I., WONG, C. M., KHOO, U. S., NG, I. O., WIRTZ, D. & SEMENZA, G. L. 2011. Hypoxia-inducible factor 1 is a master regulator of breast cancer metastatic niche formation. *Proc Natl Acad Sci U S A,* 108**,** 16369-74.

WOOLARD, J., WANG, W. Y., BEVAN, H. S., QIU, Y., MORBIDELLI, L., PRITCHARD-JONES, R. O., CUI, T. G., SUGIONO, M., WAINE, E., PERRIN, R., FOSTER, R., DIGBY-BELL, J., SHIELDS, J. D., WHITTLES, C. E., MUSHENS, R. E., GILLATT, D. A., ZICHE, M., HARPER, S. J. & BATES, D. O. 2004. VEGF165b, an inhibitory vascular endothelial growth factor splice variant: mechanism of action, in vivo effect on angiogenesis and endogenous protein expression. *Cancer Res,* 64**,** 7822-35.

XIA, Z., DICKENS, M., RAINGEAUD, J., DAVIS, R. J. & GREENBERG, M. E. 1995. Opposing effects of ERK and JNK-p38 MAP kinases on apoptosis. *Science,* 270**,** 1326-31.

YAMADA, E. 1955. The fine structure of the gall bladder epithelium of the mouse. *J Biophys Biochem Cytol,* 1**,** 445-58.

YAMANE, A., SEETHARAM, L., YAMAGUCHI, S., GOTOH, N., TAKAHASHI, T., NEUFELD, G. & SHIBUYA, M. 1994. A new communication system between hepatocytes and sinusoidal endothelial cells in liver through vascular endothelial growth factor and Flt tyrosine kinase receptor family (Flt-1 and KDR/Flk-1). *Oncogene,* 9**,** 2683-90.

YAO, Y., LI, W., WU, J., GERMANN, U. A., SU, M. S., KUIDA, K. & BOUCHER, D. M. 2003. Extracellular signal-regulated kinase 2 is necessary for mesoderm differentiation. *Proc Natl Acad Sci U S A,* 100**,** 12759-64.

ZABEL, B. A., ALLEN, S. J., KULIG, P., ALLEN, J. A., CICHY, J., HANDEL, T. M. & BUTCHER, E. C. 2005a. Chemerin activation by serine proteases of the coagulation, fibrinolytic, and inflammatory cascades. *J Biol Chem,* 280**,** 34661-6.

ZABEL, B. A., NAKAE, S., ZUNIGA, L., KIM, J. Y., OHYAMA, T., ALT, C., PAN, J., SUTO, H., SOLER, D., ALLEN, S. J., HANDEL, T. M., SONG, C. H., GALLI, S. J. & BUTCHER, E. C. 2008. Mast cell-expressed orphan receptor CCRL2 binds chemerin and is required for optimal induction of IgE-mediated passive cutaneous anaphylaxis. *J Exp Med,* 205**,** 2207-20.

ZABEL, B. A., OHYAMA, T., ZUNIGA, L., KIM, J. Y., JOHNSTON, B., ALLEN, S. J., GUIDO, D. G., HANDEL, T. M. & BUTCHER, E. C. 2006a. Chemokine-like receptor 1 expression by macrophages in vivo: regulation by TGF-beta and TLR ligands. *Exp Hematol,* 34**,** 1106-14.

ZABEL, B. A., SILVERIO, A. M. & BUTCHER, E. C. 2005b. Chemokine-like receptor 1 expression and chemerin-directed chemotaxis distinguish plasmacytoid from myeloid dendritic cells in human blood. *J Immunol,* 174**,** 244-51.

ZABEL, B. A., ZUNIGA, L., OHYAMA, T., ALLEN, S. J., CICHY, J., HANDEL, T. M. & BUTCHER, E. C. 2006b. Chemoattractants, extracellular proteases, and the integrated host defense response. *Exp Hematol,* 34**,** 1021-32.

ZHANG, H., WONG, C. C., WEI, H., GILKES, D. M., KORANGATH, P., CHATURVEDI, P., SCHITO, L., CHEN, J., KRISHNAMACHARY, B., WINNARD, P. T., JR., RAMAN, V., ZHEN, L., MITZNER, W. A., SUKUMAR, S. & SEMENZA, G. L. 2012. HIF-1-dependent expression of angiopoietin-like 4 and L1CAM mediates vascular metastasis of hypoxic breast cancer cells to the lungs. *Oncogene,* 31**,** 1757-70.

ZHANG, W. & LIU, H. T. 2002. MAPK signal pathways in the regulation of cell proliferation in mammalian cells. *Cell Res,* 12**,** 9-18.

ZHANG, X., SARKAR, K., REY, S., SEBASTIAN, R., ANDRIKOPOULOU, E., MARTI, G. P., FOX-TALBOT, K., SEMENZA, G. L. & HARMON, J. W. 2011. Aging impairs the mobilization and homing of bone marrow-derived angiogenic cells to burn wounds. *J Mol Med (Berl),* 89**,** 985-95.

ZICHE, M. & MORBIDELLI, L. 2000. Nitric oxide and angiogenesis. *J Neurooncol,* 50**,** 139-48.

ZICHE, M., MORBIDELLI, L., MASINI, E., AMERINI, S., GRANGER, H. J., MAGGI, C. A., GEPPETTI, P. & LEDDA, F. 1994. Nitric oxide mediates angiogenesis in vivo and endothelial cell growth and migration in vitro promoted by substance P. *J Clin Invest,* 94**,** 2036-44.